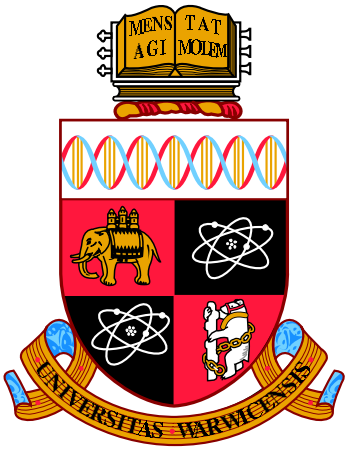

KIF1C CONTROL OF PODOSOME FORMATION IN VASCULAR SMOOTH MUSCLE CELLS

by

Alice Bachmann

Supervisors: Anne Straube and Irina Kaverina

Thesis

Submitted to the University of Warwick

for the degree of

Doctor of Philosophy

November 2016

TABLE OF CONTENT

Supplementary materials

Efimova, N., A. Grimaldi, A. Bachmann, K. Frye, X. Zhu, A. Feoktistov, A. Straube, and I. Kaverina. 2014. 'Podosome-regulating kinesin KIF1C translocates to the cell periphery in a CLASP-dependent manner', *J Cell Sci*, 127: 5179-88.

Bachmann, A., and A. Straube. 2015. 'Kinesins in cell migration', *Biochem Soc Trans*, 43: 79-83.

List of Tables

List of Figures

Acknowledgements

First, I would like to thank my supervisor Dr. Anne Straube for the opportunity to work and learn in her lab, for her dedication and her help during the course of this work. Thanks for never giving up on me and for always providing precious advice.
I would also like to thanks Dr. Irina Kaverina for co-supervising the project and for all the “podosomy” advice.

I would also thank all the present and past members of the Straube lab for making the lab such a good place to work. I owe special thanks to two very special lab members: Daniel and Nida.
To Daniel, the first person I met when I arrived. Thank you for your kindness, your support and your help. I’m truly sorry I never manage to clone things properly but let’s face it, if you are undeniably the master of cloning, I am the queen of madeleines and it probably is how things should be.
To Nida (or should I write Neeeedaaaaaaaaa?), what can I say? Thank you for everything, for your help, for your support, for the 3.45pm muffin sprints and for making the lab a very nice huggy place.
I also need to thank all the past and present members of the cake club, this “highlight of the week” venerable institution created to provide sugar, fun and an extended baking knowledge to all its members.
I would also thank those with whom I shared coffee and tea breaks at various times of the day. Thank you for making these moments ‘little islands of quietness’ in the middle of the PhD maelstrom.

I think I didn’t forget anybody from this side of the English Channel, so it’s time for me to thank those who make the other half of my life.

J’aimerais remercier tout ceux qui, d’une façon ou d’une autre, ont rendu cette aventure possible.
A la magie des rencontres et aux copains qui m’ont accompagné plus ou moins longtemps sur ce chemin.
A Benjamin. Merci d’avoir été là. Ton amitié aura été d’un grand réconfort pendant ces années difficiles.

A Quentin. Merci d'avoir apporté une distraction plus que bienvenue lors de cette dernière année de thèse. Merci pour les excursions "gadoue/ah c'est froid/j'ai les pieds mouillés" dans le Peak District, les soirées tartiflette/saucisson/bières (on ne se refait pas), les ateliers patisserie parfois un peu foireux et tout le reste. On se sera quand même bien marré copain et je ne pense pas qu'on puisse vraiment en demander plus.

A ma famille, et particulièrement à mes grand-parents, merci de votre soutien sans faille. Particulièrement à Mémé. Merci d'y avoir cru quand personne d'autre n'y croyait.

A Maman. Merci d'avoir tout mis entre parenthèses pour nous et de toujours nous avoir fait passer avant tout le reste. Nous ne t'en remercierons jamais assez. Merci aussi de m'avoir laissé partir. Je sais que ça n'a pas été facile.

A Papa. Merci pour les week-ends à Lisbonne et Copenhague. Merci aussi d'avoir été ce puits de science qui a contribué à m'ouvrir l'esprit sur autre chose. On se retrouve autour d'une petite bétonnière Chef?

Enfin, à Adrien et Camille, mes deux compagnons de toujours. Je suis très fière de vous avoir pour frère et soeur et d'avoir grandi à vos côtés. Je dédierai donc ce travail aux enfants que nous étions et aux adultes que nous sommes devenus.

Tu y crois, toi? La magie des rencontres
D.Saez

Adieu, dit le Renard. Voici mon secret. Il est très simple: on ne voit bien qu'avec le coeur. L'essentiel est invisible pour les yeux.
Le Petit Prince – Antoine de Saint-Exupery

Declaration

This thesis is submitted to the University of Warwick in support of my application for the degree of Doctor of Philosophy. It has been composed by myself and has not been submitted in any previous application for any degree.

The work presented (including data generated and data analysis) was carried out by the author except in the cases outlined below:

- pKIF1C-RIP-1_950, pKIF1C-RIP-Δ623_679-GFP and pKIF1C-708_822-GFP were cloned by Nida Siddiqui.
- pHA-PTPD1-RIP-WT and pHAPTPD1-RIP-C1108S were cloned by Daniel Roth.

Parts of this thesis have been published by the author:

- Efimova, N., A. Grimaldi, A. Bachmann, K. Frye, X. Zhu, A. Feoktistov, A. Straube, and I. Kaverina. 2014. 'Podosome-regulating kinesin KIF1C translocates to the cell periphery in a CLASP-dependent manner', *J Cell Sci*, 127: 5179-88.
- Bachmann, A., and A. Straube. 2015. 'Kinesins in cell migration', *Biochem Soc Trans*, 43: 79-83.

Abstract

Podosomes are adhesion structures formed at the ventral side of cells whose physiological functions require an efficient cell migration across tissues. In addition to their adhesive properties, podosomes display a protrusive activity responsible for the local degradation of matrix components that helps cells to migrate across basement membranes. Because of their ability to degrade matrix components, podosome formation, activity and turnover need to be tightly regulated to avoid an uncontrolled protrusive activity that could damage tissues.

The kinesin-3 KIF1C was shown to contribute to the regulation of podosome dynamics in macrophages and here, we used depletion-rescue and dominant negative approaches to show that KIF1C activity is required for podosome formation in A7r5 cells. Little is known about the mechanism regulating KIF1C activity. To better understand the molecular mechanism underlying the KIF1C-control of podosome formation in A7r5 cells, we generated different truncations of the KIF1C tail, tested the ability of each construct to mediate podosome formation in these cells and identified a ~150 amino acid long region between KIF1C third and fourth coiled-coil domains that is required for podosome formation in A7r5 cells, suggesting that this ~150 amino acid long region of KIF1C tail participates in the regulation of KIF1C activity during the podosome formation process. This region of KIF1C tail is known to interact with two proteins that were both described for their involvement in the regulation of cellular adhesion: the non-muscle Myosin IIA and the Protein Tyrosine Phosphatase PTPD1.

We addressed the involvement of the non-muscle Myosin IIA in podosome formation in A7r5 cells using two Myosin inhibitor: Blebbistatin and the Y27632 ROCK inhibitor. The treatment of A7r5 cells with one or the other Myosin IIA inhibitor had no effect on the ability of these cells to form podosomes, suggesting that the non-muscle Myosin IIA is not required for the formation of podosomes in A7r5 cells. We therefore ruled out its involvement in the regulation of KIF1C activity during the podosome formation process to focus our work on PTPD1.

PTPD1 is a scaffolding tyrosine phosphatase known to regulate focal adhesion and stress fibre stability. Using a depletion-rescue approach, we showed that PTPD1 expression is absolutely required for podosome formation in A7r5 cells.

As PTPD1 displays both a scaffolding and a phosphatase activity, we used the catalytic inactive mutant of the phosphatase PTPD1-C1108S to discriminate between these two activities and show that PTPD1 ability to mediate podosome formation in A7r5 cells does not require its catalytic activity.

Because PTPD1 and KIF1C depletions performed independently of each other both led to a decrease of the ability of A7r5 cells to form podosomes and because these two proteins interact with each other, we tested the ability of PTPD1 and KIF1C to cooperate with each other to mediate podosome formation and showed that PTPD1-C1108S over-expression in KIF1C-depleted cells restored the ability of A7r5 cells to efficiently form podosomes. Taken together, results obtained suggested that the interaction of PTPD1 with KIF1C could stimulate the activity of the remaining pool of KIF1C motors.

To test this hypothesis, we used a pre-established α5-integrin transport assay, as KIF1C is a known α5-integrin transporter and its motor activity can therefore be assessed by following its ability to transport GFP-tagged α5-integrin cargoes to the tail of migratory RPE-1 cells. Using this assay in KIF1C-depleted RPE-1 cells stably expressing GFP-α5-integrin, we showed that PTPD1 over-expression restores the transport of α5-integrin to the tail of RPE-1 cells, therefore stimulating the activity of the remaining pool of KIF1C motors.

Results obtained in this study and *in vitro* data generated during the course of this work allowed us to establish the following model for KIF1C activation: in the absence of PTPD1, KIF1C is in its auto-inhibitory state and can't ensure its cellular function. In presence of PTPD1, the phosphatase binds to KIF1C tail, inducing the activation of the motor that can thus mediate podosome formation and transport α5-integrins to the tail of RPE-1 cells.

List of abbreviations

ADP	Adenosine Di-Phosphate
AKAP	A-kinase Anchor Protein
AMP	Adenosine Mono-Phosphate
ATP	Adenosine Tri-Phosphate
CLASP	Clip-170 Associated Protein
EGF	Epithelial Growth Factor
EGFR	Epithelial Growth Factor Receptor
FAK	Focal Adhesion Kinase
FERM	4.1 protein Ezrin Radixin Moesin-like domain
FHA	Forkhead-associated domain
MAPs	Microtubule-associated Proteins
mRNA	Messenger RNA
MT	Microtubules
MTOC	Microtubule Organizing Center
PCR	Poly-chain Reaction
PDBu	Phorbol-12,13-Dibutyrate
PBS	Phosphate-buffered Saline
PBST	Phosphate-buffered Saline 0.1% Tween 20
PtdIns	Phosphinositides
PTPD1	Protein Tyrosine Phosphatase D1
RNA	Ribonucleic acid
RT-PCR	Reverse Transcriptase Poly-chain Reaction
siRNA	Small-interfering RNA
VSMCs	Vascular Smooth Muscle Cells

Amino acids abbreviations

Alanine	A
Arginine	R
Asparagine	N
Aspartic acid	D
Cysteine	C
Glutamine	Q
Glutamic acid	E
Glycine	G
Histidine	H
Isoleucine	I
Leucine	L
Lysine	K
Methionine	M
Phenylalanine	F
Proline	P
Serine	S
Threonine	T
Tryptophan	W
Tyrosine	Y
Valine	V

Chapter 1: Introduction

1-1: Overview of the microtubule cytoskeleton and the kinesin family of molecular motors

Cellular architecture and many cellular functions rely on the cytoskeleton, a dynamic structure made of four types of polymers: actin filaments, microtubules, intermediate filaments and septin filaments. Each type of cytoskeletal element displays a specific composition and ensures a specific range of function. Actin filaments mainly ensure cellular adhesion to the substratum and support cellular architecture (Revenu et al., 2004; Blanchoin et al., 2014) while microtubules are mainly used as tracks for the transport of cargoes to specific areas of the cell during interphase and form the mitotic spindle during cell division. Intermediate filaments mainly ensure the positioning of the nucleus in the cell and septin filaments act as scaffolding structures ensuring the interaction of proteins with each other (Mostowy & Cossart, 2012). Despite these features that are specific for each cytoskeletal element, the four types of filaments work together to ensure cellular functions.

In this study, we are interested in microtubules (MTs), polar polymers of α and β-tubulin heterodimers that have a slow growing minus-end anchored in the Microtubule Organizing Centre (MTOC) they grow from and a fast growing plus-end. MTs are characterized by their ability to rapidly alternate between phases of growth and shrinkage, a phenomenon called dynamic instability (Mitchison & Kirschner, 1984). In many cells, the majority of MTs are anchored with their minus-end at the MTOC close the nucleus and with their plus-end extending towards the cell periphery. MTs are decorated by various microtubule-associated proteins (MAPs) that regulate their growth, stability, 3-dimensional organisation or use them as tracks to ensure the trafficking of cargoes throughout the cell. Two classes of microtubule-based molecular motors ensure the transport of proteins or organelles throughout the cell: kinesins, most of them mediating plus end-directed transport and dyneins responsible for the minus end-directed traffic. These MT-based motors ensure the long-range cargo transport from one point of the cell to the other.

The first kinesin was identified in the middle of the 1980's in the axon of the giant squid (Vale et al., 1985) and in sea urchin eggs (Scholey et al., 1985). The characterization of this first kinesin opened the way to the identification of a growing number of kinesins or kinesin-like proteins (KLPs) in the following years. Today, the human genome is known to contain at least 45 kinesin genes but alternative mRNA splicing might generate more than 45 distinct proteins (Miki et al., 2001). These have been classified in 14 subfamilies based on the position of their motor domain and the sequence homology of their tails (Lawrence et al., 2004) (Figure 1.1 A).

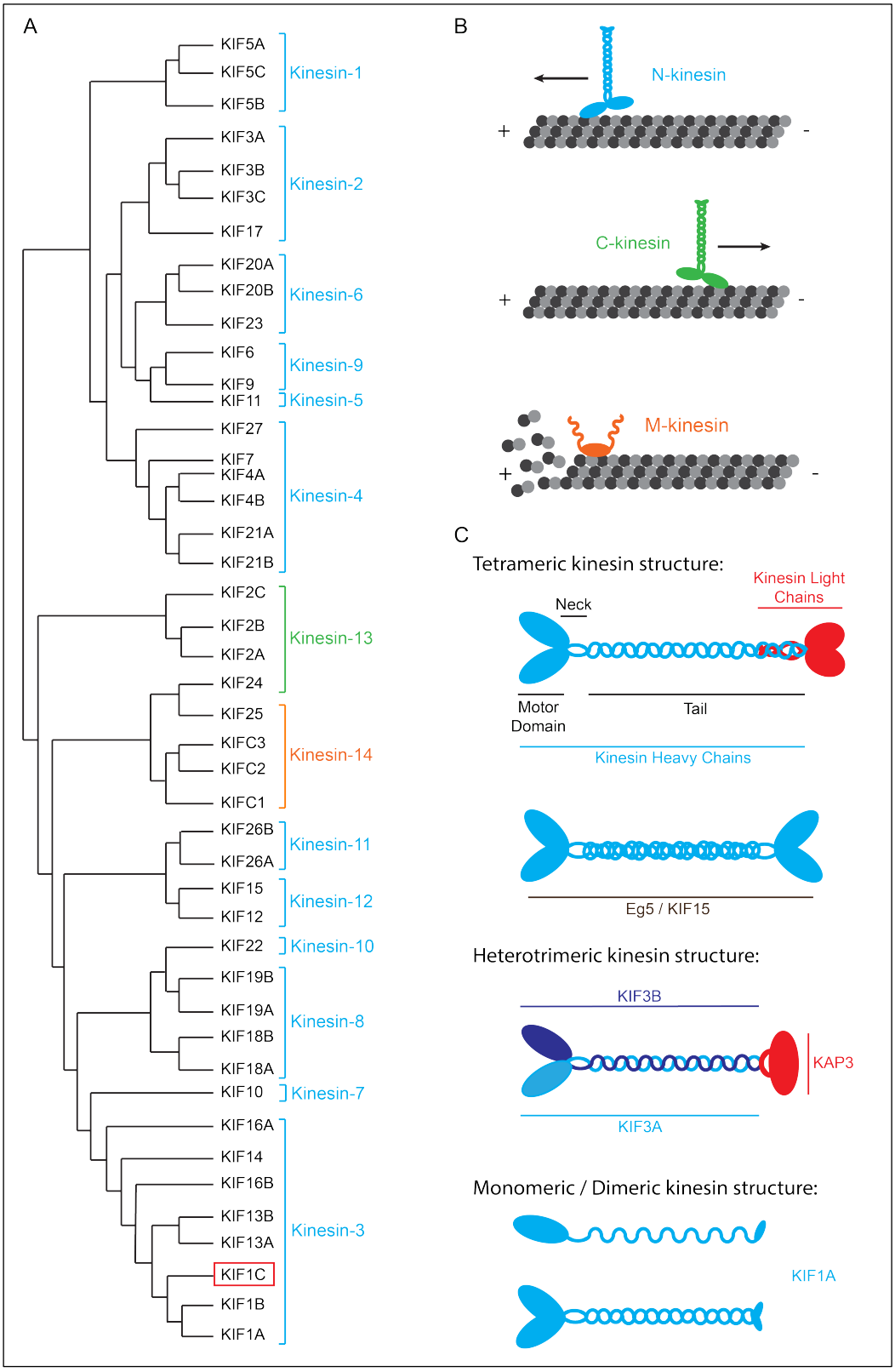

Figure 1.1: Kinesin families and structures.
(A) Phylogenic tree of the 14 kinesin families. Blue: N-kinesins, Green: C-kinesins, Orange: M-kinesins. (B) N-kinesins move towards MT plus-end while C-kinesins move towards MT minus-end. M-kinesins induce the depolymerization of the MT they interact with. (C) Schematic representation of tetrameric, dimeric and monomeric kinesin structures.
Based on Hirokawa et al., 2009.

1-2: Kinesin structure

All kinesins share the same basic structure made of a conserved ~350 amino acid long motor domain and a tail responsible for cargo binding, kinesin regulation and protein oligomerization. The position of the motor domain relative to the tail determines the directionality of the kinesin movement along MTs. Kinesins displaying an amino-terminal motor domain are MT plus-end-directed motors (N-kinesins; kinesin-1 to 12), while C-kinesins (kinesin-14), whose motor domain is positioned at their carboxy-terminal end move towards the minus-end of MTs. A third group of kinesins containing a central motor domain (M-kinesins; Kinesin-13) has been identified. On the contrary to N- and C-kinesins, M-kinesins are not involved in cargo transport but are responsible for the destabilization and the depolymerization of MTs they interact with (Figure 1.1B; Hirokawa et al., 2009).

The motor domain contains a MT-binding site (Woehlke et al., 1997) and a nucleotide-binding site (P-loop) while kinesin tail contains a various number of coiled-coil domains suspected to mediate kinesin oligomerization. The tail can also contain other structural domains specific of a kinesin subfamily (Hirokawa et al., 2009), such as light chain binding sites (Diefenbach et al., 1998), Forkhead homology-associated (FHA) domains (Miki et al., 2005) or additional MT-binding sites (Straube et al., 2006).

Kinesin quaternary structure can vary from one kinesin subfamily to the other (Figure 1.1C). Some kinesins, as conventional kinesin-1 are tetramers made of two Kinesin Heavy Chains (KHCs) bearing the motor activity and two Kinesin Light Chains (KLCs) that mediate cargo binding and regulate KHC motor activity (Kuznetsov et al., 1988). Other kinesins, such as kinesin-2s, are heterotrimers made of two different but complementary motor chains (KIF3A and KIF3B) associated to a non-motor regulatory chain (KAP3) (Yamazaki et al., 1996). Lastly, some kinesins are thought to be monomeric, as the kinesin-3 KIF1A (Okada et al., 1995) and KIF1B (Nangaku et al., 1994). Despite these structural differences, all kinesins use MTs as tracks to move within the cell, although the establishment of a canonical model to describe kinesin mechanical movement and its regulation is difficult because of this structural variability.

1-3: Kinesin function and regulation

All kinesins use the chemical energy produced by ATP hydrolysis to move along MTs. The kinesin motor domain binds an ATP nucleotide in its P-loop and hydrolyzes it to ADP-Pi. The chemical energy released by this ATPase activity is then converted into a mechanical force that promotes kinesin stepping on the MT track (Endow, 1999; Vale et al., 2000). Thus, kinesins oscillate between two states depending on the nucleotide bound in their motor domain. ATP binding in the P-loop makes the MT-binding domain of the kinesin accessible for tubulin interaction and hence, confers a high MT affinity to the motor domain. ATP hydrolysis induces a conformational change in the motor domain structure that impairs the kinesin interaction with tubulin (Naber et al., 2003). Kinesin movement along MTs comes from the repetition of the cycling between the two states over time.

Kinesin activity needs to be accurately regulated to ensure its efficiency and several levels of regulation have been described. The conventional kinesin-1 has been extensively studied to understand the conformational change that occurs upon kinesin activation by cargo binding. Inactive kinesin-1 adopts a “closed” conformation, its tail interacting with the motor domain and covering its MT-binding domain, hence abolishing kinesin interaction with MTs and futile ATP hydrolysis. Upon cargo binding, the tail detaches from the motor domain that can then interact with and move along the MT (Coy et al., 1999).
Kinesin activity can also be regulated by reversible post-translational modifications of specific residues of the motor domain or the kinesin tail. The phosphorylation of specific serine residues of the kinesin motor domain was shown to stabilize kinesins “closed” conformation to negatively regulate kinesin motor activity (DeBerg et al., 2013; Morfini et al., 2009). The phosphorylation of tail residues can also modulate kinesin activity by promoting (Ichimura et al., 2002) or inhibiting (Guillaud et al., 2008; Vagnoni et al., 2011) cargo binding.

Kinesin regulation is complex due to the diversity of cargoes these motors transport within the cell. It is understood that cargo selection relies on adaptor proteins that link a cargo to the motor that transports it. Nonetheless, mechanisms governing the timing of cargo loading onto kinesins and controlling the delivery to specific cellular locations remain unclear. The timing of cargo

loading could be controlled by phosphorylation of the adaptor protein linking the cargo to its motor (Horiuchi et al., 2007). However, the control of cargo loading on a kinesin could be more complex as more than one adaptor protein may be required to ensure the cargo linkage to the kinesin that transports it (Blasius et al., 2007; Franker & Hoogenraad, 2013).

As for the selection of cargo delivery site, it could rely on the MT track itself as tubulin can be post-translationally modified and these tubulin modifications were shown to have an influence on kinesin movement along MTs. For instance, KIF1C and KIF16B traffic to the cellular periphery is impaired upon MT acetylation (Bhuwania et al., 2014). Moreover, MTs are decorated with numerous MAPs that can modulate MT dynamics and kinesin affinity for the MT track (Trinczek et al., 1999; Sung et al., 2008; Lipka et al., 2016).

1-4: The kinesin-3 family

Kinesin-3s form a subfamily of N-kinesins whose founding member (Unc-104) was identified in the nematode *Caenorhabditis elegans* as an axonal synaptic vesicle transporter (Hall & Hedgecock, 1991; Otsuka et al., 1991). The first Unc-104 mammal ortholog was identified later as the murine KIF1A (Okada et al., 1995) and since then, the kinesin-3 family expended to also include KIF1B, KIF1C, KIF13A, KIF13B, KIF14, KIF16A and KIF16B (Lawrence et al., 2004; Figure 1.1A).

Kinesin-3s share the overall N-kinesin structure made of a N-terminal motor domain followed by a cargo binding tail. In addition to this common basic structure, kinesin-3s display two more characteristics: a K-loop insertion in their motor domain (Marx et al., 2009) and the presence of a Forkhead homology-associated (FHA) domain in their tail (Miki et al., 2005).

K-loops are clusters of lysine residues in the MT-binding site of the kinesin-3 motor domain (Marx et al., 2009). This positively charged motif is thought to interact with the negatively charged glutamate-rich tubulin C-terminal tail (E-Hook) to facilitate kinesin interaction with MTs, retain the motor in close proximity to the MT track and avoid its release from the surface of the MT during the nucleotide exchange step of the ATP hydrolysis cycle (Soppina & Verhey, 2014).

The second kinesin-3 specific feature is the presence of a structural FHA domain in the kinesin tail. This motif is found in a broad variety of proteins, such as transcription factors, phosphatases and kinesins (Hofmann & Bucher, 1995; Li et al., 2000). In addition to their structural properties, FHA domains specifically recognize and bind phosphoserine and phosphothreonine motive to mediate protein interactions (Li et al., 2000).

Kinesin-3 oligomeric status as well as its regulation have been the area of great debates and investigations. First studies conducted on KIF1A concluded on its monomeric status and its processive movement along MTs explained by the interaction of the kinesin K-loop with the tubulin E-hook during its MT low-affinity state (Okada & Hirokawa, 2000). However, several studies later on contradicted this unconventional monomeric status of kinesin-3s both *in vitro* and *in vivo* as kinesin-3 oligomeric status seems to be regulated by the local concentration of the motor (Al-Bassam et al., 2003; Lee et al., 2004; Hammond et al., 2009; Huckaba et al., 2011). At low local concentration, KIF1A adopts a closed conformation due to intra-molecular interactions (Al-Bassam et al., 2003; Lee et al., 2004) and is found as a monomer in cells. However, a local increase of the kinesin-3 concentration, at the membrane of cargoes for instance, destabilizes the intra-molecular interactions, enabling kinesin-3s to dimerize and move along MTs processively (Soppina et al., 2014; Huo et al., 2012).

Kinesin-3s were shown to transport various types of cargo, including synaptic vesicles (KIF1A and KIF1C; Hall & Hedgecock, 1991; Okada et al., 1995), mitochondria (KIF1B; Nangaku et al., 1994) or proteins involved in the regulation of cellular adhesion (KIF1C; Theisen et al., 2012). Some kinesin-3s were also shown to participate to the regulation of the cell cycle. The drosophila kinesin-3 Khc73 (Siegrist & Doe, 2005) has been shown to participate to the polarization of *Drosophila* neuroblasts, a phenomenon that is essential for neuroblast assymetric division (Siegrist and Doe, 2005) and the kinesin-3 KIF14 was shown to regulate chromosome congression, alignment and segregation during mitosis (Zhu et al., 2005; Carleton et al., 2006)

1-5: The kinesin-3 KIF1C

The kinesin-3 KIF1C has been identified in a yeast two-hybrid screen for its interaction with the FERM (4.1 Ezrin Radixin Moesin) domain of the Tyrosine phosphatase PTPD1 (Protein Tyrosine Phosphatase D1) and named after KIF1A and KIF1B because of the high degree of sequence homology in their motor domain (Dorner et al., 1998). KIF1C is a 1.103 amino acid long fast non-processive molecular motor (Rogers et al., 2001) sharing the two kinesin-3 specific features: it contains a K-loop in its motor domain (Rogers et al., 2001) and a FHA domain (amino acids 523 to 590) in its tail. KIF1C FHA domain is flanked by four coiled-coil domains and a proline-rich domain at the very carboxy-terminal end (Figure 1.2).

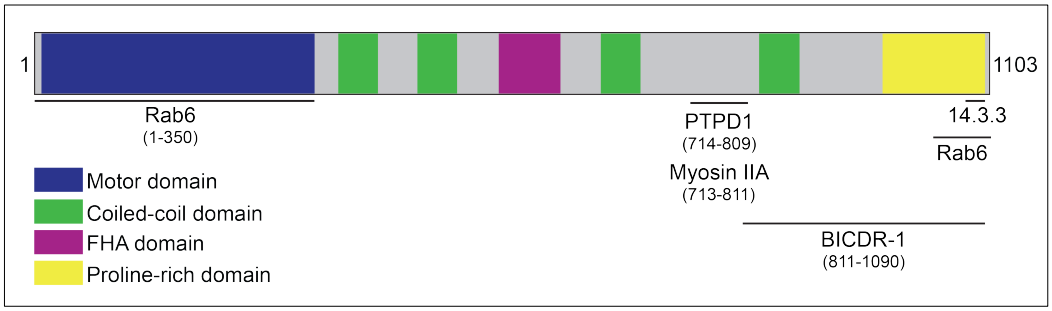

Figure 1.2: KIF1C domain structure and identified binding sites of its known interactors.

KIF1C is ubiquitously expressed and preferentially accumulates in the pericentrosomal region of the cell, in close proximity to the Golgi apparatus (Dorner et al., 1998; Nakajima et al., 2002; Kopp et al., 2006; Efimova et al., 2014), a localization that is in agreement with its cargo transport activity. Indeed, the Golgi apparatus acts as a hub for protein maturation, loading of molecular motors and distribution to the cellular periphery. Some proteins need to be re-routed from the Golgi apparatus to the Endoplasmic Reticulum (ER) because they are ER-residing proteins or because they are misfolded. Cell treatment with the Golgi disrupting agent Brefeldin-A (BFA) highlighted the involvement of KIF1C in the retrograde transport of Golgi vesicles to the ER (Figure 1.3; Dorner et al., 1998). Nonetheless, KIF1C might not be the only molecular motor involved in this retrograde transport as its knockout has no significant effect on this Golgi to ER retrograde transport (Nakajima et al., 2002).

In addition to a potential role in Golgi to ER retrograde transport activity, KIF1C is also required for the maintenance of the Golgi structure, a function that seems to be independent of its motor activity (Simpson et al., 2012; Lee et al., 2015). A first clue to explain the involvement of KIF1C in the maintenance of the Golgi apparatus structure was provided recently when Rab6 was identified as new interactor for KIF1C (Lee et al., 2015). Rab6 is a cargo adaptor protein that mainly localizes to the *trans*-Golgi network (Antony et al, 1992) where it controls the trafficking of proteins to and from it (Storrie et al, 2012). Both KIF1C and Rab6 depletions performed independently from each other lead to the same phenotype of Golgi fragmentation, suggesting that they cooperate to ensure the maintenance of the Golgi structure (Storrie et al., 2012; Lee et al., 2015).

To a lesser extent, KIF1C also localizes at the cell periphery where it participates to the regulation of cellular adhesion. In macrophages, KIF1C has been shown to accumulate at the plus-end of a subset of MTs responsible for the targeting of peripheral podosomes (Figure 1.3; Chapter 1-9). The repeated targeting of these peripheral podosomes by KIF1C-decorated MTs induces their fission or their dissolution (Kopp et al., 2006). KIF1C seems to participate in the control of podosome targeting by MTs. Indeed, it decorates the plus-end of a subset of MTs and only these KIF1C-decorated MTs seem to be able to contact peripheral podosomes to induce their fission or dissolution whereas non-decorated MTs do not target peripheral podosomes (Kopp et al., 2006). Moreover, as mentioned above, only peripheral podosomes are targeted by KIF1C-decorated MTs, suggesting an unknown guidance mechanism. It has been suggested that KIF1C's interaction with the non-muscle Myosin IIA could guide targeting MTs to podosome sites as Myosin IIA is known to localize to podosomes (Kopp et al., 2006; Bhuwania et al., 2012; van den Dries et al., 2013) and Myosin IIA has been co-precipitated with KIF1C from cell extracts, suggesting a physical interaction (Kopp et al., 2006).

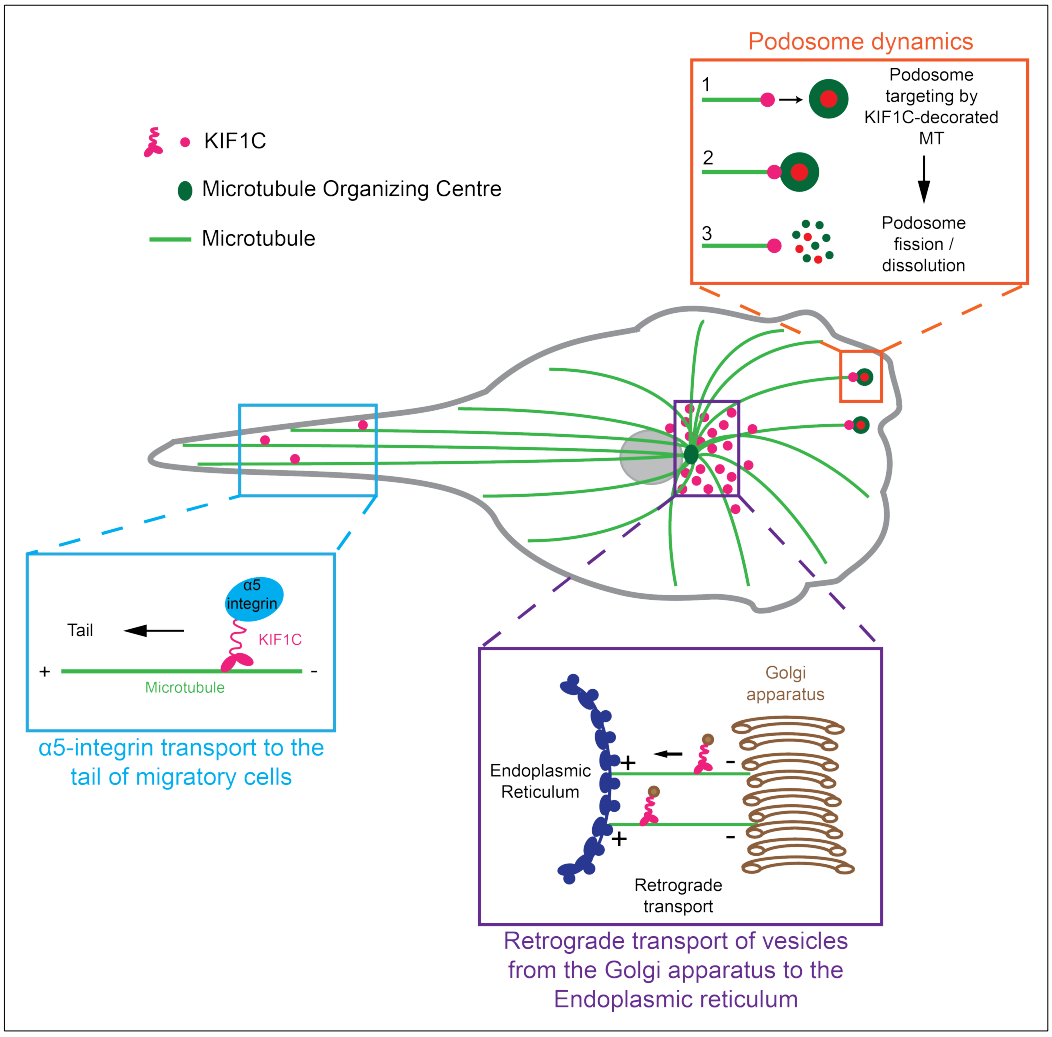

Figure 1.3: Schematic representation of motor-based KIF1C functions in cells.
KIF1C mainly localizes at the perinuclear region to ensure the retrograde transport of vesicles from the Golgi to the Endoplasmic Reticulum. At the cell periphery, KIF1C accumulates at the plus-end of a subset of MTs that target peripheral podosomes, inducing their fission or their dissolution. KIF1C also mediates the transport of α5-integrin to the tail formed at the rear of migratory cells to ensure the maturation of rear adhesions and facilitate directional persistence of cell migration.
Based on Kopp et al., 2006; Theisen et al., 2012; Dorner et al., 1998; Nakajima et al., 2002.

The involvement of KIF1C in the regulation of cellular adhesion has clearly been demonstrated in migratory RPE-1 cells. Indeed, KIF1C has been shown to transport the α5-integrin fibronectin receptor to the tail formed at the rear of migratory RPE-1 cells (Figure 1.3; Theisen et al., 2012). This KIF1C-mediated α5-integrin transport activity is required for the maturation of rear adhesions and the stability of the tail. Impairing KIF1C-mediated α5-integrin trafficking to the cell rear weakens the tail stability and impairs the directionality

of the cell migration (Theisen et al., 2012), reinforcing the importance of KIF1C for the regulation of cellular adhesion.

The molecular mechanisms controlling KIF1C movement along MTs have not been unraveled yet but KIF1C interacts with various proteins that could regulate its activity. KIF1C was first described to interact with 14-3-3 proteins through its C-terminal proline-rich domain in a phosphoserine-dependent manner (Figure 1.2; Dorner et al., 1999).

14-3-3 proteins are a family of highly conserved small acidic proteins named after their characteristic migration pattern on scratch gel electrophoresis (Moore & McGregor, 1965). The 14-3-3 protein family contains at least seven isoforms that are ubiquitously expressed and that are able to form homo- or hetero-dimers interacting with a broad range of proteins (Liu et al., 1995; Xiao et al., 1995) in a phosphoserine or phosphothreonine dependent manner (Muslin et al., 1996). Because 14-3-3 proteins are able to dimerize, each dimer can interact with two proteins in the same time to regulate their activity. Indeed, 14-3-3 protein interaction with their binding partners can either bring these interactors in close proximity to one another to stabilize their interaction and favor their activation; 14-3-3 protein dimers can also inhibit the activity of bound proteins by sequestering them or by competing for the binding of an activator of these interactors (Mrowiec & Schwappach, 2006). Because of their ability to interact with numerous proteins, 14-3-3 proteins participate in the regulation of a broad spectrum of cellular functions such as cellular adhesion, cell signaling, cell metabolism, protein biogenesis or mitosis (Mhawech, 2005).

14-3-3 proteins are known to participate in the regulation of kinesin-mediated cargo transport (Geiger et al., 2014; Ichimura et al., 2002). Indeed, in addition to their ability to directly bind kinesin tails (Dorner et al., 1999; Ichimura et al., 2002), 14-3-3 proteins can interact with cargo adaptors to regulate cargo loading onto kinesin tails. For instance, 14-3-3 proteins can interact with the cargo adaptor GRIP1 (Glutamate Receptor Interacting Protein 1) in a phospho-dependent manner to impair its interaction with the conventional kinesin KIF5 and therefore inhibit the transport of GRIP1-associated vesicles to the cell periphery (Geiger et al., 2014).

14-3-3 proteins are also known to regulate kinesin clustering. Indeed, 14-3-3 proteins were shown to interact with MKLP1 (KIF23) in a phosphodependent manner to regulate its MT bundling activity (Douglas et al., 2010).

The relevance of 14-3-3 protein interaction with KIF1C tail has not been addressed yet but it could either regulate the binding of KIF1C cargo to the kinesin tail or regulate KIF1C folding or dimerization.

KIF1C is known to interact with the dynein adaptor and Rab6 interactor Bicaudal D-related protein 1 (BICDR-1) (Schlager et al., 2010) and during the course of this work, KIF1C has been shown to directly interact with Rab6 (Lee et al., 2015). Rab6 is a cargo adaptor that interacts in a very unusual manner with KIF1C as it can interact with both the KIF1C motor domain and a 40 amino acid long sequence in the kinesin tail (Figure 1.2). Rab6 interaction with KIF1C tail is thought to mediate cargo binding whereas Rab6 interaction with KIF1C motor domain inhibits the interaction of the kinesin with MTs and impairs its movement along them (Lee et al., 2015).

BICDR-1 interacts with KIF1C, Rab6 and the dynein/dynactin complex and is suspected to bring together these proteins to form a molecular complex that regulates the bidirectional trafficking of Rab6-associated vesicles during neuronal development (Schlager et al., 2010). Indeed, during early neuronal development, BICDR-1 is highly expressed and retains Rab6-associated vesicles in the pericentrosomal region due to its ability to bind and activate the MT minus end-directed motor dynein. Later, when the neuronal system matures, BICDR-1 expression decreases, and the reduction of its expression correlates with the gradual scattering of Rab6-associated vesicles towards the cell periphery (Figure 1.4; Schlager et al., 2010).
Hence, a high expression level of BICDR-1 seems to favor the dynein-mediated retrograde transport of Rab6-associated vesicles to the detriment of KIF1C transport activity. The gradual decrease of BICDR-1 expression with neuronal development is suspected to destabilize the balance between dynein and KIF1C activities in favor of KIF1C, leading to the transport of Rab6-associated vesicles to the cell periphery. Hence, BICDR-1 could act as a molecular switch controlling the balance between anterograde and retrograde transport during neuronal development (Figure 1.4).

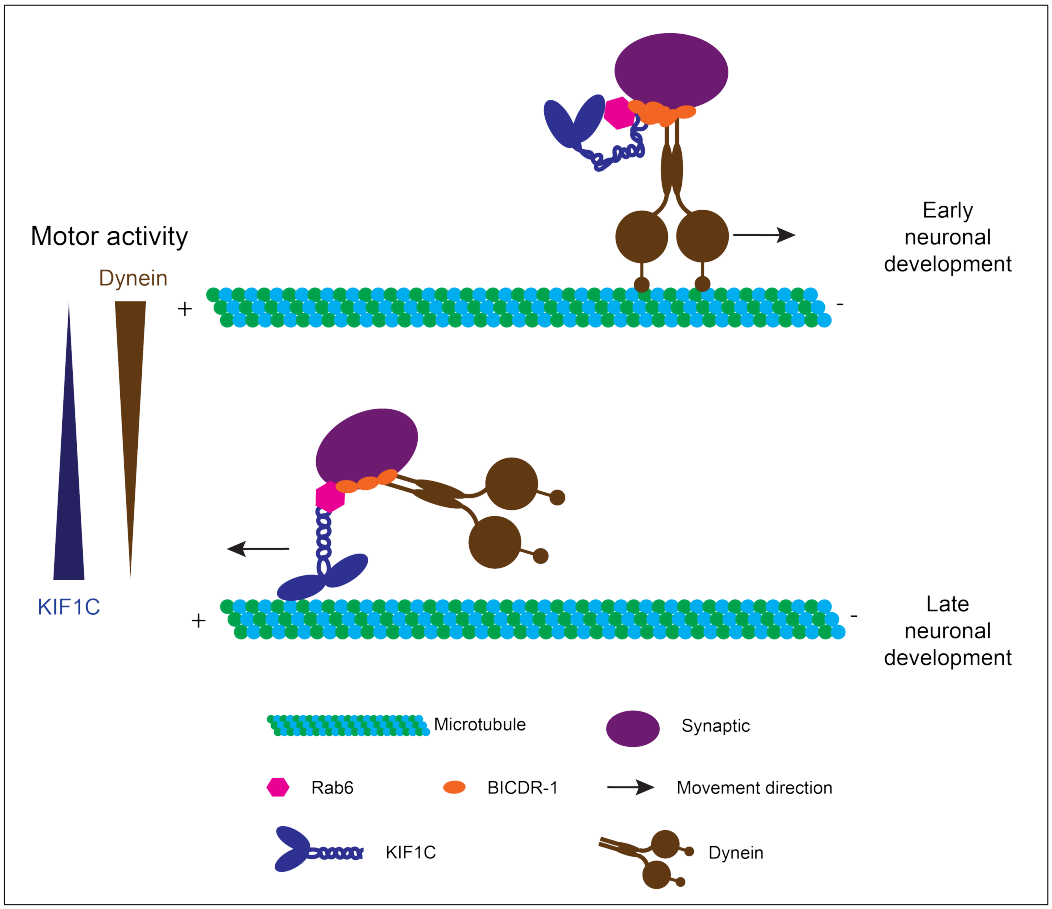

Figure 1.4: Model of BICDR-1 control of dynein and KIF1C activities during neuronal development.
BICDR-1, dynein, KIF1C and Rab6 form a complex at the surface of neuronal secretory vesicles. At early stages of neuronal development, the high expression of BICDR-1 favors the Dynein motor activity to the detriment of the KIF1C one leading to the retention of Rab6-associated vesicles at the pericentrosomal region. During neuronal development, BICDR-1 expression level gradually decreases, destabilizing the balance between dynein and KIF1C activities in favor of KIF1C. KIF1C then mediates Rab6-associated vesicle transport toward the plus-end of MTs.
Based on Schlager et al., 2010; Lee et al., 2015.

The regulation of this balance between plus end-directed and minus end-directed transports could be of major importance for neuronal development and function as the impairment of KIF1C activity leads to serious neuronal defects. Indeed, a point mutation introducing a premature STOP codon in the exon 22 of KIF1C gene has been shown to be responsible for the development of cerebellar dysfunction and spastic paraparesis in patients carrying this mutation, a syndrome caused by nerve dysfunction or defects (Dor et al., 2014; Caballero Oteyza et al., 2014).

1-6: Overview of the cellular adhesion system

Cell matrix adhesions are actin-based structures that were first described in 1964 in embryonic chick fibroblasts using Interference Reflection Microscopy (Curtis, 1964) and since then, the study of the structure, the composition and the dynamics of cell matrix adhesions is the area of active investigations. Despite the great progresses that have been made in the field, the study of cellular adhesions remain challenging as more than 150 proteins have been identified as being involved in the formation and the regulation of cellular adhesion (Zaidel-Bar et al., 2007; Byron et al., 2011). Cell matrix adhesions are usually classified in four main subfamilies and the current view is that each adhesion subtype derives from the maturation of another one: nascent adhesions maturate in focal complexes than can evolve in focal adhesions and later on, in fibrillar adhesions (Hanein & Horwitz, 2012).

Nascent adhesions are small (<0.25µm) short-lived adhesions (~1 minute) formed in the lamellipodium of migratory cells. At the very leading edge of migratory cells, signaling events induced by the interaction of transmembranous integrin receptors and matrix components induce the local polymerization of actin filaments and the recruitment of talin at these sites (Izzard, 1988; Parsons et al., 2010). These initial contacts can rapidly (60 to 90 seconds) maturate into small (<1µm^2) dot-like adhesions called focal complexes that last for at least several minutes and characterized by their enrichment in the tension-sensitive protein vinculin that brings the ventral cell side in close proximity to the underlying matrix to locally secure cellular adhesion (DePasquale & Izzard, 1987; Izzard, 1988). Whilst nascent adhesions formation and maturation is Myosin II-independent, the maturation of focal complexes depends on traction forces exerted by the contractile activity of the non-muscle Myosin II on these adhesion structures (Parsons et al., 2010; Galbraith et al., 2002).

Focal adhesions are stable and elongated adhesions (up to several microns) evolving from focal complexes (Zamir et al., 2000; Parsons et al., 2010) and bridging membrane-substratum adhesion sites to actin stress fibers. Focal adhesions are characterized by their enrichment in zyxin (Hanein & Horwitz, 2012), a phospho-protein localizing at both focal adhesions and stress

fibers to enhance actin polymerization at these sites (Hirata et al., 2008). Because of their size (3-10µm long) and their stability, focal adhesions provide strong attachment sites for the cell to the substratum (Block et al., 2008; Dumbauld et al., 2013). Focal adhesions usually last for 10 to 20 minutes and can evolve in fibrillar adhesions when cells are plated on fibronectin and when focal adhesions are enriched in the fibronectin α5β1-integrin receptor (Zamir et al., 2000; Pankov et al, 2000). Fibrillar adhesions are more elongated and more stable than focal adhesions and they are usually associated with larger actin bundles and are involved in the assembly and the reorganization of fibronectin matrix (Parsons et al., 2010)

These cell matrix adhesion described above have been extensively studied during cell spreading and migration on a 2-Dimensional substratum and for a long time, they were thought to form only when cells were plated on a 2-Dimensional surface as they could not be distinguished in 3D migration assays. However, recent progress in microscopy resolution allowed the visualization of focal-like adhesions in invasive cells (Kubow & Horwitz, 2011; Kubow et al., 2013), suggesting that these adhesions structures are not artifact of 2-Dimensional cell culture but may actually be formed *in vivo*.

A fifth type of cell matrix adhesions called invadosomes has been described in invasive cells. The term invadosomes designate dot-like adhesion structures called podosomes when formed by normal cells and invadopodia when formed by cancer cells. Invadosomes differ from cell matrix adhesions described above though their columnar-like organization and their ability to protrude into the underlying matrix to degrade it and facilitate cell migration across basement membranes (Burgstaller & Gimona, 2005; Linder, 2007).

1-7: Podosomes

Podosomes are adhesion structures that were first described in cultured osteoclasts (Marchisio et al., 1984) and in Rous Sarcoma Virus-transformed fibroblasts, where they were defined as “short protrusions of the ventral cell surface that contact the substratum at their apical portion […] which may represent cellular feet” (Tarone et al., 1985). Podosomes were then described in various cell types such as macrophages (Linder et al., 1999), dendritic cells

(Burns et al., 2001), endothelial cells (Moreau et al., 2003) and Vascular Smooth Muscle Cells (VSMCs) (Hai et al., 2002) where they appear as light-dense structures in phase contrast microscopy (Hai et al., 2002; Kaverina et al., 2003).
Hence, podosomes are not specific adhesion features of one cell type but rather an adhesion structure commonly formed by different cell types whose functions require an efficient 3-Dimensional migration (Schachtner et al., 2013). Cell migration is also commonly observed during cancer progression and podosome pathological counterparts, called invadopodia (Chen, 1989) are often observed in and used by transformed cells to exit from the primary tumor and spread throughout the organism (Seano & Primo, 2015).

If podosomes and invadopodia are often indifferently called invadosomes, slight differences between podosomes and invadopodia should be noted. First, normal cells usually tend to form numerous podosomes (>100) whereas cancer cells form only a few invadopodia (Linder, 2007). To compensate for the low number of protrusive structures they form compared to normal cells, transformed cells form invadopodia that are much bigger in size than podosomes (Buccione et al., 2004). While podosome diameters typically range from 0.3 to 0.4µm and their height from 0.5 to 0.6µm (Marchisio et al., 1988; Gavazzi et al., 1989; Destaing et al., 2003; Gawden-Bone et al., 2010), invadopodia diameters can reach 8µm and their depth several micrometers (Buccione et al., 2004), giving individual invadopodia a stronger capacity to penetrate the matrix to degrade it compared to single podosomes.

One of the main functions of invadosomes is to locally degrade matrix components to facilitate cell migration across basement membranes (Linder, 2007; Schachtner et al., 2013) and the second notable difference between podosomes and invadopodia relates to their matrix-degrading capacity and how it affects their structural organization. Invadopodia were shown to be protrusive structures by nature whereas the protrusive activity of podosomes seems to require its activation. At a structural level, this difference in the regulation of podosomes and invadopodia protrusive activity results in the presence of an adhesive ring in podosomes (Linder & Aepfelbacher, 2003; Murphy and Courtneidge, 2011; van den Dries et al., 2013b) mainly made of transmembranous adhesion receptors (Gaidano et al., 1990; Linder & Aepfelbacher, 2003) and surrounding the actin-rich core that is absent in

invadopodia (Linder et al., 2011). The adhesive ring of podosomes physically connect the podosome structure to the plasma membrane and the underlying matrix, sense the matrix properties and transduce signals modulating podosome protrusive activity depending on the molecular properties and the stiffness of the substratum (Collin et al., 2008; Labernadie et al., 2014). The adhesive ring could be dispensable for invadopodia protruding activity as they extend for several micrometers into the matrix to mediate their protruding activity (Gimona et al., 2008; Artym et al., 2011; Buccione et al., 2004; Linder, 2007; Linder et al., 2011).

At a molecular level, invadosomes share most of their components with focal adhesions but the relative amount and the organization of each component differ between the different types of adhesions (Block et al., 2008). The core of invadosomes is made of densely packed branched-actin filaments associated with actin nucleation promoting factors such as the Arp2/3 complex, cortactin or the Wiskott-Aldrich syndrome protein WASP (Figure 1.5; Kaverina et al, 2003; Burgstaller and Gimona, 2004; Linder et al., 1999; Garcia et al., 2012). These proteins mainly localize at the base of the actin column, in close proximity to the plasma membrane where actin polymerization takes place (Pfaff & Jurdic, 2001). Electron microscopy studies conducted in VSMC podosomes also highlighted the presence of short loosely arranged actin filaments with no apparent organization in the podosome core (Gimona et al., 2003) whose role remains unknown. Two types of adhesion proteins were identified to localize at the podosome core: the integrin β1 (Marchisio et al., 1988) and the hyaluronan receptor CD44 (Chabadel et al., 2007). These adhesion proteins are most likely involved in the anchoring of the podosome core structure to the underlying matrix (Figure 1.5). So far, reports showing a clear accumulation of adhesive proteins at the actin-rich core of invadopodia are scarce (Deryugina et al., 2001; Mueller et al., 1991; Linder et al., 2011), suggesting that invadopodia adhesive properties may only be limited (Linder et al., 2011).

A protein cap made of the formin FMNL-1 (Mersich et al., 2010) and Supervillin, a member of the villin and gelsolin family (Bhuwania et al., 2012) sits on top of the core (Figure 1.5). The role of this cap remains elusive but it is suspected to serve as a hub for vesicle trafficking and to be involved in the regulation of the size and the growth of the core (Linder & Wiesner, 2015).

The core of podosomes is surrounded by an adhesive ring mainly made of transmembranous integrin receptors anchoring the adhesive ring to the underlying matrix (Pfaff & Jurdic, 2001; Chabadel et al., 2007) and associated with plaque proteins such as vinculin, paxillin and talin (Figure 1.5; Pfaff & Jurdic, 2001; Zambonin-Zallone et al., 1989). Recent ultrastructural studies revealed that the apparent ring homogeneity that was described initially was actually an artifact caused by the diffraction limit of light microscopy. Proteins of the ring form clusters sitting next to each other rather than forming a homogenous continuum of adhesion proteins, suggesting these islets could work as local sensors of the cell-matrix interface (van den Dries et al., 2013b; Walde et al., 2014).

These recent structural studies also highlighted the presence of actin filaments radiating from the core toward the ring that physically link core and ring together (Figure 1.5; Gawden-Bone et al., 2010; van den Dries et al., 2013b). This network of radiating actin filaments is of major importance for the maintenance of the adhesive ring composition. For instance, vinculin is not evenly distributed in the adhesive ring but peaks in close proximity to the actin core and its intensity decreases with distance to it. The disruption of its binding to the radiating actin network results in its dispersion in the adhesive ring (van den Dries et al., 2013b).

The non-muscle Myosin IIA, known to localize to the adhesive ring while being strictly excluded from the core (Burgstaller & Gimona, 2004; Gawden-Bone et al., 2010) associates with these radiating actin filaments. Hence, the Myosin IIA is not part of the adhesive ring but rather sits on top of it (Figure 1.5) to pull on radiating actin filaments and ensure the maintenance of the podosomal structural integrity as well as generating forces for its protruding activity (Gawden-Bone et al., 2010; van den Dries et al., 2013).

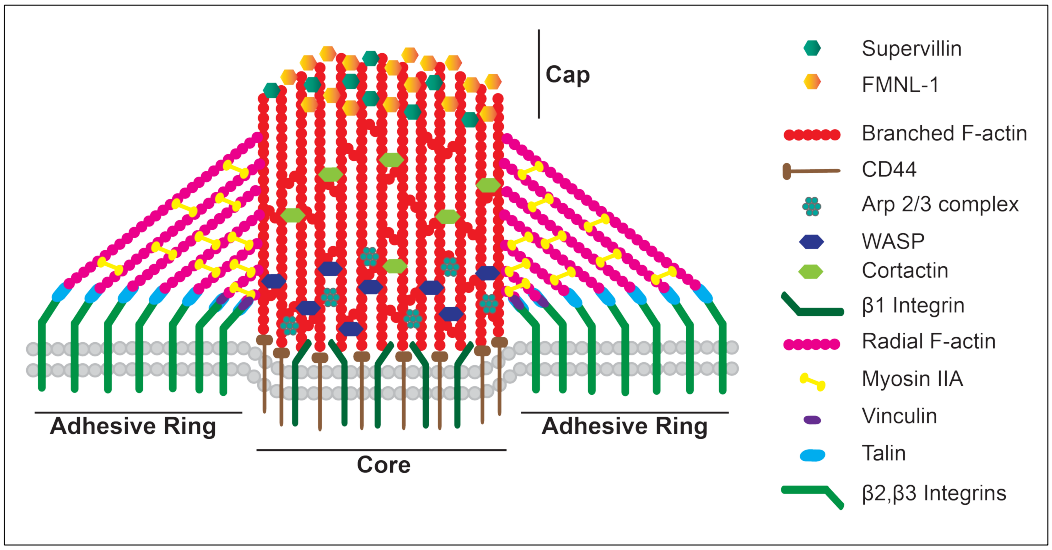

Figure 1.5: Schematic representation of the structure of an individual podosome. Podosomes are bipartite structures made of a central actin-rich core surrounded by an adhesive ring. The core is made of densely packed branched actin filaments associated with actin nucleation promoting factors such as cortactin and ARP2/3 complex. The core is anchored in the matrix by CD44 and β1-integrin receptors and a cap of supervillin and formin sits on top of it. The adhesive ring is made of β2- and β3-integrins associated with plaque proteins (Vinculin, Talin). Radiating actin filaments associated with the non-muscle Myosin IIA connect the structure of the core to the adhesive ring.
Based on Gawden-Bone et al., 2010; Marchisio et al., 1988; Kaverina et al., 2003; Pfaff & Jurdic, 2001, Mersich et al., 2010; Bhuwania et al., 2012.

In contrast to focal adhesions, which are found as single entities dispersed throughout the cell, podosomes can either be found as single scattered adhesion structures or re-arranged as clusters and rings, allowing them to cooperate and coordinate their activity (Figure 1.6). To do so, podosomes are physically connected to each other through a heterogeneous actin filament network extending from each podosome core toward neighbouring ones, meaning that virtually, all the podosomes of a cluster are connected to each other (Destaing et al., 2003; Saltel et al., 2008). Concomitantly, the adhesive ring surrounding each core fuses with the ring of neighbouring podosomes, creating a carpet of adhesion proteins rather than individual well-defined rings sitting next to each other to secure the adhesion of the cluster to the substrate (van den Dries et al., 2013b) (Figure 1.6). This higher organization of podosomes is particularly important in mature osteoclasts. Indeed, mature osteoclasts display a podosome belt that surrounds their cytoplasm and allow them to tightly adhere to the bone matrix (Saltel et al., 2008). This podosome belt, called the sealing zone, is the site of local degradation of bone matrix and impairing its formation impairs osteoclast's ability to degrade the bone matrix (Destaing et al., 2005).

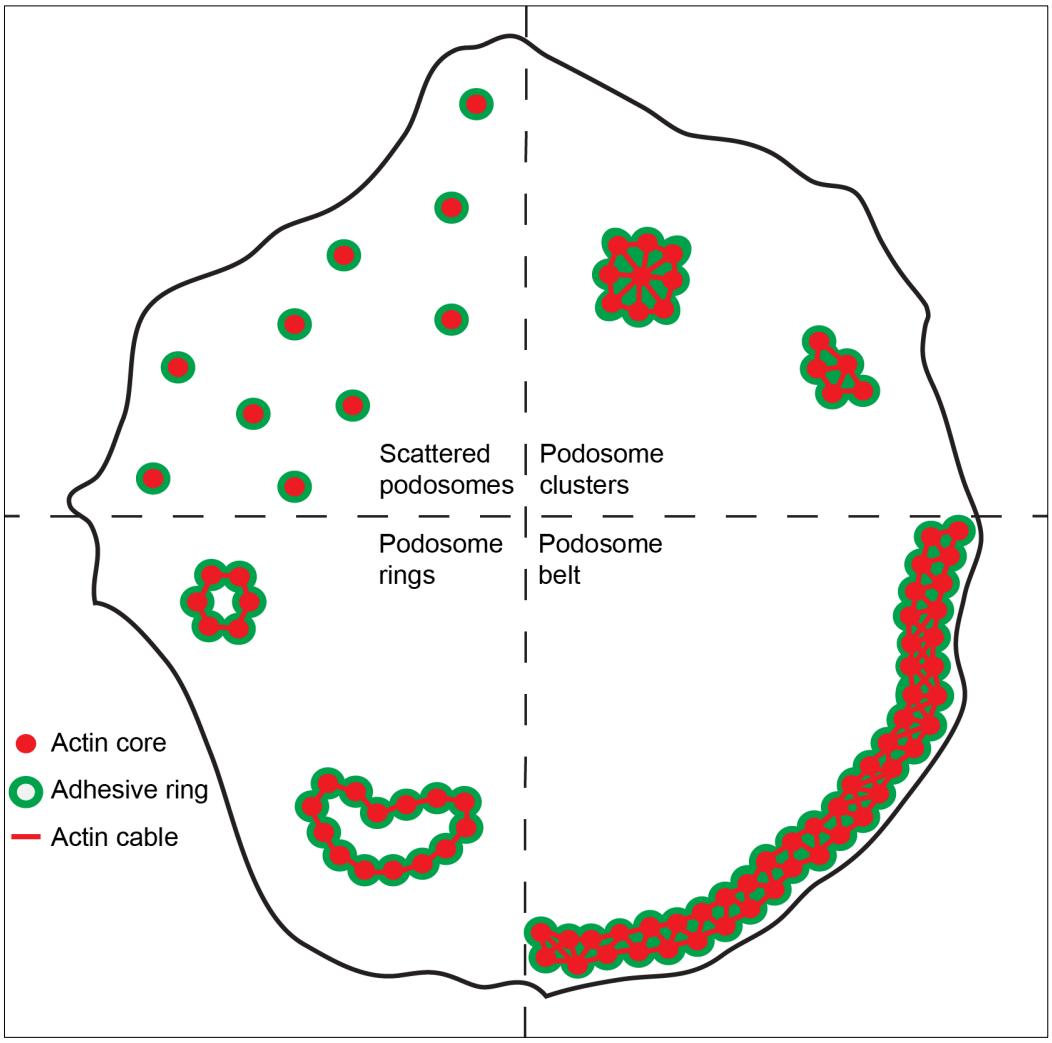

Figure 1.6: Schematic representation of the different types of podosome organization. Podosomes can be found scattered throughout the cell, form clusters or rings. Mature osteoclasts display a very peculiar organization of podosomes in a belt that surround the cell periphery.

1-8: Mechanism of podosome formation and dynamics

The molecular mechanism regulating podosome formation and turnover has to be tightly regulated to avoid an inappropriate podosome protrusive activity that could damage tissues (Rudijanto, 2007; Georgess et al., 2014). Cells forming podosomes can be divided in two subfamilies: cells forming podosomes without the requirement of any additional signals than those provided by their adhesion to the substratum (cells deriving from the monocytic lineage mainly e.g. macrophages, dendritic cells, osteoclasts; Marchisio et al., 1984; Marchisio et al., 1988; Kopp et al., 2006) and cells requiring external

signals in addition to those provided by the substratum they adhere on to trigger podosome formation (VSMCs, endothelial cells; Hai et al., 2002; Brandt et al., 2002; Moreau et al., 2003). Additional signals can either be growth factors (Quintavalle et al., 2010), the expression of the constitutively active v-Src kinase (Tarone et al., 1985) or chemical compounds such as phorbol esters (Hai et al., 2002; Brandt et al., 2002). It is therefore difficult to establish a canonical signaling pathway triggering the induction of podosome formation as different kind of signals can induce their formation. Moreover, it is unclear how the site of emergence of a podosome is chosen in most podosome-forming cell types (Gimona et al., 2008).

However, several studies point at the same general molecular mechanism for podosome formation in all podosome-forming cell types. This mechanism can be divided in 3 main phases that occur in a very short period of time as podosome lifespan ranges from 2 to 10 minutes (Kaverina et al., 2003; Destaing et al., 2003; Gimona et al., 2008):

1) polymerization of the actin core,
2) recruitment of adhesion and plaque proteins at the ring,
3) local accumulation and release of proteases responsible for the degradation of the matrix at podosome sites.

The recruitment of the actin polymerizing machinery at the future site of podosome emergence is likely to start before the induction of podosome formation. Indeed, studies conducted in VSMCs highlighted the local accumulation of the two actin nucleation promoting factors Arp2/3 complex (Kaverina et al., 2003) and cortactin (Burgstaller & Gimona, 2004) at the interface between focal adhesions and stress fibers in resting conditions (Figure 1.7). The induction of podosome formation by phorbol esters induces some of these accumulation foci to grow in size and to be used as platforms for the assembly of the podosome structure (Kaverina et al., 2003). Within minutes, other actin regulatory proteins and scaffolding proteins, such as α-actinin (Luxenburg et al., 2012) or Tks5 (Crimaldi et al., 2009) are recruited to the core of the newly forming podosome to facilitate its assembly (Figure 1.7).

Likewise, studies conducted in cells of the monocytic lineage highlighted the requirement of the Wiskott-Aldrich syndrome protein WASP, a well-known Arp2/3 activator, for podosome formation in macrophages (Linder et al., 1999) and dendritic cells (Burns et al., 2001), suggesting that the polymerization of

branched-actin at the core is a fundamental step for podosome formation in all podosome-forming cell types.

Once a basic core is assembled, adhesion and adaptor proteins such as integrins and talin are recruited to the podosome formation site to form the ring (Figure 1.7; Luxenburg et al., 2012; van den Dries et al., 2013). Some adhesion plaque proteins, paxillin for instance, are recruited to the ring during early stages of core assembly, most likely to stabilize its polymerization and facilitate the recruitment of other podosome components recruited at later stages of podosome formation (Luxenburg et al., 2012).

Mature podosomes are sites of local accumulation and exocytosis of matrix metalloproteases as MMP2, MMP9 and the transmembranous MT-MMP1 (Tatin et al., 2006; Gawden-Bone et al., 2010; Xiao et al., 2010). These MMPs locally degrade matrix components and mediate, at least partially, podosome protrusive activity (Tatin et al., 2006; Wiesner et al., 2010; Gawden-Bone et al., 2010; Xiao et al., 2010). Interestingly, matrix-degrading enzymes also participate in the endocytosis of the matrix components they degrade (Gawden-Bone et al., 2010) as well as in the regulation of podosome turnover (West et al., 2008; Goto et al., 2002). Thus, the recruitment of matrix-degrading enzymes to podosomes is of major importance for podosome homeostasis and function. The involvement of these proteases in these processes could be explained by their ability to modify the matrix podosomes are in contact with. As mechanosensors, podosomes are able to detect modifications in the organization, stiffness or molecular composition of the matrix, leading in turn to modifications of their size, stiffness or turnover rate (Collin et al., 2008; Labernadie et al., 2010; Labernadie et al., 2014).

Finally, individual podosomes can organized in higher structures to potentiate their activity. The best example of podosome reorganization is probably provided by the dynamic rearrangement of podosomes in maturing osteoclasts. Immature osteoclasts form single podosomes that rearrange into clusters and rings while the cell matures. Podosome rings gradually expand and fuse with each other to finally form the bone matrix-resorbing podosome belt characteristic of mature osteoclasts (Destaing et al., 2003). The same kind of dynamic podosome reorganization has been described in Rous-Sarcoma Virus transformed Baby Hamster Kidney cells (RSV-BHK cells; Badowski et al.,

2008), suggesting that molecular mechanisms regulating podosome reorganization may be shared by various cell types.

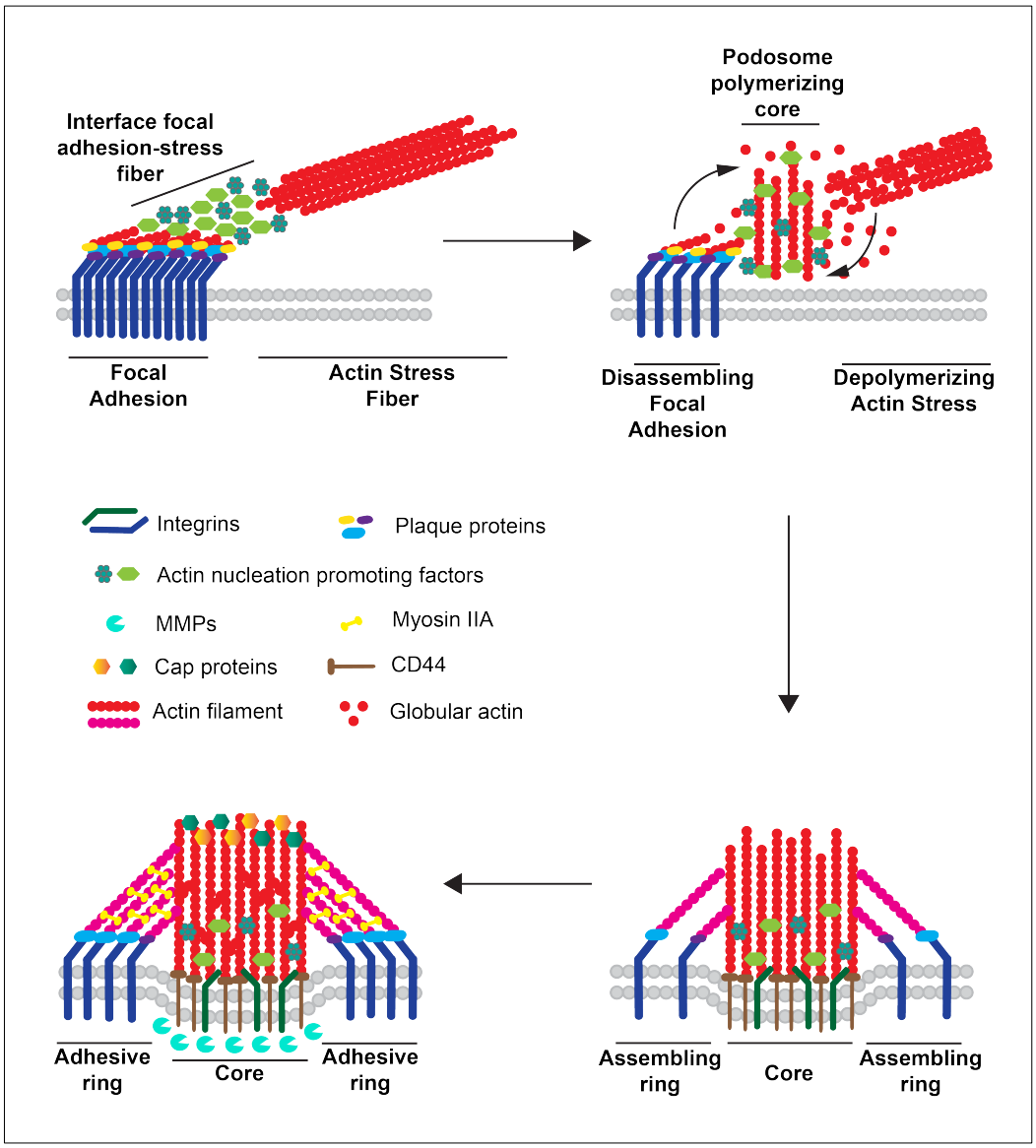

Figure 1.7: General mechanism of podosome formation.
In resting conditions, the interface between a focal adhesion and a stress fiber is the site of local accumulation of actin nucleation promoting factors. Upon podosome induction, the podosome core polymerizes thanks to the local recycling of components released by disassembling focal adhesions and stress fibers. Once a basic core is polymerized, the adhesive ring forms around the core. Mature podosomes are sites of local release of matrix degrading enzymes.
Based on Kaverina et al., 2003; Luxenburg et al., 2012; van den Dries, 2013.

The regulation of podosome formation is tightly linked to the internal podosome dynamics that has been reported in numerous studies to occur over time. Podosomes undergo small and rapid oscillations generated by actin turnover in the podosome core (Labernadie et al., 2010). Indeed, actin filaments

forming the core are constantly polymerizing and depolymerizing and FRAP experiments conducted in osteoclasts showed that during the 2 to 3 minutes average lifespan of a podosome, the amount of actin a core contains is renewed about 2.5 times (Destaing et al., 2003). In the core, actin polymerization occurs at the base of the structure, in close proximity to the plasma membrane where actin filament barbed-ends localize and where actin nucleation promoting factors accumulate (Pfaff & Jurdic, 2001). The addition of actin monomers at the base of pre-existing actin filaments pushes the plasma membrane towards the underlying substrate, while monomers are removed at the top of the actin core (van den Dries et al., 2013).

In addition to these small oscillations of the core, podosomes are submitted to larger oscillations of their whole structure (Labernadie et al., 2010). This second type of oscillations seems to be mediated by the Myosin IIA contractile activity as cell treatment with the Blebbistatin Myosin IIA inhibitor abolishes them in dendritic cells (Labernadie et al., 2010; van den Dries et al., 2013). The Myosin IIA localizes at radiating actin filaments linking the core and the adhesive ring together (Gawden-Bone et al, 2010). Its contractile activity pulls onto these radiating actin filaments, bringing the whole podosome structure in closer proximity to the underlying matrix and hence, creating large vertical oscillations of the entire podosome structure (Labernadie et al., 2010).
These two types of oscillations are thought to mediate, in association with the local release and activation of matrix proteases, the protrusive activity of podosomes (Labernadie et al., 2010).

1-9: Podosome regulation by MTs and MAPs

The existence of an interplay between MTs and the adhesion system was first suggested in the end of the 1980's when the growing end of some MTs were found to enter the lamellipodium formed at the leading edge of migratory fibroblasts to co-localize with focal contact sites (Rinnerthaler et al., 1988). Later on, several studies highlighted the influence of MTs on the adhesion system and *vice versa*, showing that the interaction of adhesions and MTs is not fortuitous as it modulates the dynamics of both structures.

Indeed, MT disruption was shown to stimulate the formation of stress fibers and focal adhesions (Bershadsky et al., 1996; Enomoto, 1996; Krylyshkina et al., 2002), most likely because it induces an increase of Rho activation and actomyosin contractility (Danowski, 1989; Enomoto, 1996; Pletjushkina et al., 1998; Liu et al., 1998). Contemporary, MTs were shown to target focal adhesions, sometimes repeatedly (Kaverina et al., 1998), inducing the turnover of the targeted adhesions (Kaverina et al., 1999). This phenomenon is most likely due to the cargo transport activity of kinesins that use MTs as tracks to deliver cargoes at precise cellular locations. Indeed, inhibition of the activity of the kinesin-1 MT-based motor has been shown to induce an increase in focal adhesion size but no modification of the average number of contact sites formed in cell could be detected, suggesting that kinesin-1 motor activity is required for focal adhesion turnover (Kaverina et al., 1997; Krylyshkina et al., 2002).

The long-term hypothesis for the regulation this phenomenon relies on the ability of kinesin-1 to transport relaxing factors to focal adhesions. Little is known about these factors kinesin-1 could transport to regulate focal adhesion turnover but a recent study suggested a possible involvement of IQGAP1 in this mechanism. Indeed, kinesin-1 was suggested to transport IQGAP1 at the leading edge of migratory cells (Schiefermeier et al., 2014), where it interacts with Rac1 and Cdc42 to stimulate the dynamic actin polymerization required for cell migration (Noritake et al., 2005). The impairment of kinesin-1-mediated IQGAP1 transport in migratory cells leads to its accumulation at focal adhesions rather than at the leading edge of the cell and this accumulation of IQGAP1 correlates with a twofold increase in focal adhesion size (Schiefermeier et al., 2014). In addition to its ability to activate Rac1 and Cdc42, IQGAP1 is also known to enhance RhoA activity (Goode & Eck, 2007) through its interaction with the RhoA effector Dia1 (Brandt & Grosse, 2007). The local accumulation of IQGAP1 at focal adhesions upon kinesin-1 impairment could increase RhoA activity and therefore stabilize focal adhesions. This result is in agreement with previous reports showing an increase in RhoA activity upon MT depolymerization (Ren et al., 1999; Ory et al., 2002).

Another explanation for MT-induced focal adhesion turnover relies on the ability of MTs to stimulate the dynamin- and clathrin-mediated endocytosis of adhesion components (Ezratty et al., 2009; Ezratty et al., 2005). Given that

MTs repeatedly target focal adhesions (Kaverina et al., 1998; Kaverina et al., 1999), one may think that each targeting stimulates the endocytosis of focal adhesion components such as integrins (Ezratty et al., 2009; Ezratty et al., 2005), destabilizing the structure of the targeted adhesion and inducing its disassembly over time.

The crosstalk between MTs and cellular adhesions is reciprocal and also involves a modulation of MT dynamics by the adhesion system. Adhesion sites targeted by MTs were first shown to capture and transiently stabilize targeting MTs against the MT depolymerizing agent nocodazole (Kaverina et al., 1998), suggesting that focal adhesions may have a stabilizing effect on MTs. This hypothesis was reinforced by the ability of focal adhesions to nucleate MTs during the recovery phase after nocodazole treatment and the observation that MTs are more stable in cells displaying a high number of focal adhesions than in cells forming only few adhesions (Kaverina et al., 1998; Small et al., 2002 Nat Rev Mol Cell Biol). The ability of focal adhesions to stabilize MTs seems to be the result of the accumulation of many cycles of shrinkage and rescue of the MT plus-end, as MTs were shown to be more dynamic in close proximity to focal adhesions than in cell regions devoid of adhesion sites (Efimov et al., 2008). The overall stabilizing effect of adhesions on MTs is thought to rely on the interaction of tubulin with paxillin (Herreros et al., 2000) in close proximity to adhesion sites that has been shown to stabilize the MT plus-end by inhibiting catastrophe events (Efimov et al., 2008).

Similarly to regulating focal adhesions, MTs and MAPs decorating them were shown to regulate podosome formation and dynamics. Cell treatment with the MT depolymerizing agent Nocodazole highlighted the requirement of an intact microtubular system for proper podosome formation (Linder et al., 2000; Efimova et al., 2014) and patterning (Babb et al., 1997; Destaing et al., 2003; Zhu et al., 2016). MTs were shown to target podosomes, sometimes repeatedly to induce their fission or dissolution (Kopp et al., 2006; Cornfine et al., 2011). Indeed, podosomes formed in cells can be divided in two distinct populations: dynamic podosomes undergoing frequent fission or fusion events at the periphery and static podosomes in the inner region of the cell. Podosomes of the two populations can be targeted by MTs (Kopp et al., 2006; Cornfine et al., 2011; Bhuwania et al., 2012), however, the plus-ends of MTs targeting each podosome population were shown to be differently decorated with MAPs. MTs

targeting the peripheral population of podosomes are characterized by the accumulation of KIF1C motors at their plus-end (Kopp et al., 2006) whereas the growing-end of MTs targeting central static podosomes is decorated by KIF9 kinesins (Cornfine et al., 2011). In both cases, MT-targeting induces the fission or the dissolution of the contacted podosomes but this molecular bias suggests that these motors function in the selection of the podosome to target.

The molecular mechanism controlling the fission or the dissolution of the targeted podosome has not been addressed yet but given the nature of identified MAPs accumulating at the plus-end of targeting MTs, MT contact with podosomes could induce the uptake of podosome components by the accumulated kinesins, inducing the destabilization of the podosome structure. This hypothesis is reinforced by data showing that some MT-associated molecular motors transport podosomes components (Weisner et al., 2010). Hence, the dynein minus end-directed motor as well as KIF3A/KIF3B and KIF5B plus end-directed kinesins were shown to coordinate the delivery and surface exposure of MT-MMP1 at podosomes, a cargo trafficking activity that is crucial for podosomes to be able to degrade the matrix they protrude into (Wiesner et al., 2010).

Some MAPs were shown to interact with podosome components, providing a physical link between podosomes and MTs targeting them. For instance, KIF1C motors decorating the plus-end of podosome targeting MTs interact with the non-muscle Myosin IIA, an interaction proposed to coordinate the delivery of KIF1C motors to podosomes (Kopp et al., 2006). Another example is the Cdc42-interacting protein 4 CIP4 that interacts with the actin nucleation-promoting factor WASP and this interaction seems to be required for podosome formation in macrophages (Linder et al, 2000). A third example is the MT end-binding protein EB1 that is known to interact with two podosome components: cortactin and vinculin (Biosse-Duplan et al., 2014). EB1 interaction with cortactin is thought to guide MT plus-ends to podosomes in osteoclasts (Biosse-Duplan et al., 2014). EB1 is known to modulate MT dynamic instability (Manna et al., 2008) to control cortactin interaction with and phosphorylation by the Src kinase, a phenomenon known to regulate cortactin activity, including its ability to nucleate actin filaments (Tehrani et al., 2007) and to regulate the formation of the podosome belt in osteoclasts (Luxenburg et al., 2006).

Finally, MT stability was shown to participate in the regulation of podosome organization in cells. Podosome patterning in maturing osteoclasts relies on an intact microtubular system as osteoclast treatment with the MT-depolymerizing agent nocodazole impairs their ability to reorganize and maintain their podosomes into a belt surrounding the cell (Destaing et al., 2003; Destaing et al., 2005). The stability of MTs relies on post-translational modifications of tubulin (Garnham & Roll-Mecak, 2012) and MT acetylation has been shown to be involved in the regulation of podosome patterning in osteoclasts. Indeed, MT acetylation increases during osteoclast maturation (Destaing et al., 2005; Jurdic et al., 2006; Akisaka et al., 2011) and the impairment of MT acetylation results in the collapse of the podosome belt in mature osteoclasts (Destaing et al., 2005; Gil-Henn et al., 2007), suggesting that MT acetylation stabilizes podosome belts in osteoclasts (Akisaka et al., 2011). However, the molecular mechanism regulating the stability of the podosome belt by acetylated MTs remains unknown, as no physical interaction between MTs and podosomes of the belt has ever been proven.

1-10: VSMCs and podosomes

Vascular Smooth Muscle Cells are contractile cells surrounding blood vessels and acting to regulate blood pressure (Davis-Dusenbery et al., 2011). After an injury, cytokines and growth factors secreted during the inflammatory response induce VSMCs to switch from the contractile to a synthetic phenotype characterized by cell proliferation, migration and matrix remodeling due to their ability to form podosomes and secrete matrix components (Rudijanto, 2007). VSMCs were shown to form podosomes *in vivo* (Quintavalle et al., 2010) and the molecular mechanism triggering podosome formation has been extensively studied *in vitro*. In resting conditions, VSMCs display a very well developed actin stress fiber network (Fultz et al., 2000). VSMC treatment with Phorbol 12,13-dibutyrate (PDBu) activates the PKC pathway and induces the reorganization of the actin cytoskeleton characterized by the gradual depolymerization of the pre-existing system of stress fibers and focal adhesions and the formation of podosomes (Hai et al., 2002).

In VSMCs, podosomes form at the interface between stress fibers and focal adhesions, a region that is enriched in actin nucleation promoting factors,

such as the Arp2/3 complex (Kaverina et al., 2003) and cortactin (Burgstaller & Gimona, 2004). Podosomes formed in VSMCs display the same characteristics as podosomes formed in other cell types, with a central actin-rich core surrounded by an adhesive ring, a 3 to 10 minutes average lifespan and a fully functional matrix protruding activity (Hai et al., 2002; Kaverina et al., 2003; Burgstaller & Gimona, 2005).

Podosome formation in VSMCs needs to be tightly regulated *in vivo* as a non-regulated podosomal activity can lead to pathological lesions of artery walls (Rudijanto, 2007; Lacolley et al., 2012). Indeed, after an injury and once the artery wall remodeling mediated by activated VSMCs is completed, synthetic VSMCs need to reacquire their contractile phenotype to avoid their podosomal protruding activity damaging blood vessel walls. If cells fail to switch back to this inactive state, the accumulation of active VSMCs, the local secretion of ECM proteins by these cells and the extensive ECM remodeling activity they mediate can lead to the gradual thickening of the artery wall and the development of hypertension and atherosclerosis (Rudijanto, 2007). Hence, control of podosome formation and turnover is of major importance to maintain the arterial system integrity.

1-11: Outline of this work

Prior to this work, KIF1C was suggested to be involved in the formation and the regulation of podosome dynamics in macrophages (Kopp et al., 2006). Here we confirm a role for KIF1C in podosome formation in VSMCs (Chapter 3-1). We then use structure-function analysis to identify the domains of KIF1C required for this process (Chapter 3-2). Finally, we identify PTPD1 as a KIF1C activator that is essential for podosome formation (Chapter 3-2) and we show that catalytically inactive PTPD1 stimulates KIF1C trafficking in human cells (Chapter 3-3).

Chapter 2: Materials and Methods

2-1: Cell Biology

2-1-1: Cell maintenance

A7r5 rat Vascular Smooth Muscle Cells were a kind gift from Dr. Irina Kaverina (Vanderbilt University, Nashville, USA). A7r5 cells were grown in VSMC growth medium (low glucose Dulbecco's modified Eagle's Medium (DMEM, Sigma) supplemented with 10% Fetal Bovine Serum (FBS; Sigma), 2mM L-Glutamine (Sigma), 100 U/ml Penicillin (Sigma) and 100µg/ml Streptomycin (Sigma)) in a humidified incubator at 37°C and 5% CO2. For maintenance, A7r5 cells were grown to 90% confluency, washed with PBS and incubated with 0.05% Trypsin and 0.02% EDTA (w/v) solution (Sigma). Cell detachment was assessed using an inverted microscope and split 1 in 5 in fresh pre-warmed VSMC growth medium.

The GFP-α5-integrin RPE-1 stable cell line was established by Dr Anne Straube as followed: hTERT RPE-1 cells (Clonetech) were transfected with GFP-α5-integrin (kind gift from Benjamin Geiger) followed by selection with 500µg/ml Geneticin (Gibco). GFP-α5-integrin RPE-1 stable cell line was grown in RPE-1 growth medium (DMEM/Nutrient F-12 Ham (Sigma) supplemented with 10% FBS (Sigma), 2mM L-Glutamine (Sigma), 100 U/ml Penicillin (Sigma), 100µg/ml Streptomycin (Sigma) and 2.3g/l Sodium Bicarbonate (Sigma)) supplemented with 500µg/ml Geneticin (Gibco). For maintenance, GFP-α5-integrin RPE-1 cells were grown to 70% confluency, washed with PBS and incubated with 0.05% Trypsin and 0.02% EDTA (w/v) solution (Sigma). Cell detachment was assessed using an inverted microscope and split 1 in 10 in fresh pre-warmed RPE-1 growth medium supplemented with 500µg/ml Geneticin.

Normal Rat Kidney epithelial cells (NRK) were a kind gift from Dr. Steven Royle (Centre for Mechanochemical Cell Biology, University of Warwick) and were grown in Dulbecco's Modified Eagle's Medium (DMEM, Sigma) supplemented with 10% Fetal Bovine Serum (FBS; Sigma), 2mM L-Glutamine (Sigma), 100 U/ml Penicillin (Sigma) and 100µg/ml Streptomycin (Sigma)) in a

humidified incubator at 37°C and 5% CO2. For maintenance, NRK cells were grown to 90% confluency, washed with PBS and incubated with 0.05% Trypsin and 0.02% EDTA (w/v) solution (Sigma). Cell detachment was assessed using an inverted microscope and split 1 in 5 in fresh pre-warmed growth medium.

2-1-2: siRNA-mediated protein depletion and rescue experiments

Protein expression depletion was carried out using small interfering RNA (siRNA) as indicated in Table 1. siRNA oligonucleotides were delivered into A7r5 cells using HiPerfect transfection reagent (Qiagen) as followed: 4.5µl of the 20µM siRNA oligonucleotide stock solution (see Table 2 for siRNA sequence) were resuspended in 150µl Opti-MEM (Gibco) before the addition of 12µl of HiPerfect Transfection reagent (Qiagen). The transfection solution was vigorously mixed and incubated for 15 minutes at room temperature. In the mean time, 100 000 A7r5 cells were seeded in individual wells of a 6-well plate (6x3.5mm) in 1.5ml of VSMC growth medium. The transfection mix was then added to freshly seeded A7r5 cells. For efficient protein depletion, experiments were conducted 72 hours after siRNA transfection.
When a rescue experiment was required, plasmid transfection occurred 24 to 36 hours before the experiment was conducted as indicated in section 2-1-3.

Oligofectamine (Invitrogen) was used for the delivery of siRNA into GFP-α5-integrin RPE-1 cells. GFP-α5-integrin RPE-1 cells were seeded 24 hours prior siRNA transfection in individual wells of a 6-well plate (6x3.5mm) and RPE-1 growth medium was replaced by 1.5ml of fresh pre-warmed RPE-1 growth medium before transfection. siRNA transfection solutions were prepared as indicated in Table 1: 4.5µl of the 20µM stock solution of siRNA oligonucleotide were resuspended in 150µl of Opti-MEM in a first 1.5ml Eppendorf tube. In a second tube, 9µl of the Oligofectamine transfection reagent were resuspended in 36µl Opti-MEM. Tubes were incubated 8 minutes at room temperature and mixed together. The transfection mix was incubated for an additional 25 minutes at room temperature before addition to cells. RPE-1 growth medium was replaced 24 hours after siRNA transfection by 2ml of fresh pre-warmed RPE-1 growth medium.

Transfection using HiPerfect Transfection Reagent			
Opti-MEM (Gibco)		150µl	
siRNA Oligo (20µM stock)		4.5µl	
HiPerfect Transfection Reagent		12µl	
Incubation Time		15 minutes	
Transfection using Oligofectamine			
Tube 1		Tube 2	
Opti-MEM	150µl	Opti-MEM	36
siRNA Oligo (20µM stock)	4.5µl	Oligofectamine	9µl
Incubation time prior Tube 1 and Tube 2 mixing		8 minutes	
Incubation time prior addition to cells		25 minutes	

Table 1: siRNA component volumes mixed per individual well of a 6-well plate.

siRNA name	siRNA sequence	Target mRNA	Source
siControl	GGACCUGGAGGUCUGCUGU-[dT]-[dT] ACAGCAGACCUCCAGGUCC-[dT]-[dT]	None	Sigma
siKIF1C	GUGAGCUAUAUGGAGAUCU-[dA]-[dT] AGAUCUCCAUAUAGCUCAC-[dA]-[dT]	KIF1C	Sigma
siPTPD1	UUCAGCCUCUGGUACUACA-[dT]-[dT] UGUAGUACCAGAGGCUGAA-[dT]-[dT]	PTPD1	Sigma

Table 2: Sequences of siRNA oligonucleotides used in this study.

2-1-3: DNA transfection

Fugene6 (Promega) was used for plasmid transfection as described in Table 3. Cells were seeded 24 hours before DNA transfection and medium was replaced with fresh pre-warmed growth medium prior DNA transfection. DNA was resuspended in Opti-MEM (Gibco) before Fugene6 addition. The DNA transfection mix was vigorously shaken and incubated 15 minutes at room temperature before addition to cells.

Vessel size	Individual wells of 6-well plate (6x3.5mm)	Individual well of 4 quadrant fluorodish
Opti-MEM	150µl	37.5µl
DNA	1.5µg	0.375µg
Fugene6	4.5µl	1.125µl

Table 3: Volumes of components used for DNA transfection.

2-1-4: Drug treatments

All the drugs used in this study were resuspended in fresh pre-warm growth medium. Growth medium cells were grown in was then replaced by growth medium supplemented with the drug of interest. Podosome formation was induced in A7r5 cells using 5µM PDBu (Phorbol 12,13-dibutyrate; Sigma). Myosin IIA contractile activity inhibition was performed using different working concentration of the Y27632 Rock inhibitor (5, 10 and 15µM; Sigma) or Blebbistatin (10, 20 and 30µM; Sigma). To do so, Myosin IIA inhibitors were diluted in the pre-warmed VSMC growth medium supplemented with 5µM PDBu before its addition to cells. The myosin IIA inhibition was hence carried out during the whole time course of podosome induction. When required, DMSO (Sigma) was used a negative control.

2-2: Podosome formation assay

24 hours before experiment, ~ 5000 A7r5 cells were seeded on 16mm glass coverslips coated for 24 hours with 10µg/ml Fibronectin. Podosome formation was induced replacing growth medium with fresh pre-warmed medium supplemented with 5µM PDBu (Phorbol 12,13-dibutyrate; Sigma). The duration of podosome induction is indicated for each experiment in the result section. Cells were then fixed for 15 minutes with 4% Paraformaldehyde (Electron Microscopy Sciences) diluted in Cytoskeleton Buffer (10mM MES pH6.1, 138mM KCl, 3mM $MgCl_2$, 2mM EGTA, 0.32M Sucrose). Fixed cells were incubated for 2 minutes with 0.1% TritonX100 (Fisher Scientific) diluted in PBS. Coverslips were then washed for at least an hour with PBS and incubated for 30 minutes with 0.5% Bovine Serum Albumin (BSA; Sigma) diluted in PBS-0.1%Tween (PBST). Cells were then stained for an hour at room temperature or overnight at 4°C with primary antibodies (see Table 4) diluted in 0.5% BSA-PBST solution. Coverslips were washed 10 minutes with PBS and three time 10 minutes with PBST and incubated for 45 minutes at room temperature with secondary antibodies and Phalloidin or Acti-stain diluted in 0.5% BSA-PBST solution. Nuclei were stained with DAPI for 1 minute and coverslips washed for 10 minutes with PBS and three times 10 minutes with PBST prior mounting on glass slides with Vectashield (Vector Laboratories).

Cells were imaged using a Deltavision Elite Wide-field microscope and Z-stack of individual cells were acquired using a 40x objective and a Z-spacing of 0.2µm. To determine the number of podosome formed in each cell, Z-stack images of the cortactin channel were first transformed in a Z-projection. Cortactin Z-projection images were then analyzed using the ImageProAnalyzer 7 software as indicated in Figure 2.1: images were thresholded and every object with a size larger than 16 pixels (0.259μm^2, corresponding to the minimal size of the core, Chapter 1-7) was automatically identified. Individual objects identified in cortactin Z-projection images were then visually compared to the actin channel to confirm they are podosomes, removed if the cortactin staining didn't coincide with the actin one and podosome clusters were split into individual podosomes.

Antibody Name	Manufacturer	Specie	Primary / secondary antibody	Dilution	Usage
Cortactin	Millipore	Mouse	Primary	1/100	IF
Phalloidin	Sigma	-	-	1/1000	IF
Acti-stain 555	Cytoskeleton	-	-	1/1000	IF
Anti-mouse IgG 647 conjugate	Molecular Probes	Donkey	Secondary	1/300	IF
KIF1C	Abcam	Rabbit	Primary	1/2000	WB
Tubulin DM1A	Sigma	Mouse	Primary	1/10 000	WB
Anti-mouse IgG HRP conjugate	Promega	Goat	Secondary	1/4000	WB
Anti-rabbit IgG HRP conjugate	Promega	Goat	Secondary	1/4000	WB
IF: Immunofluorescence; WB; Western Blot					

Table 4: List of antibodies used in this study.

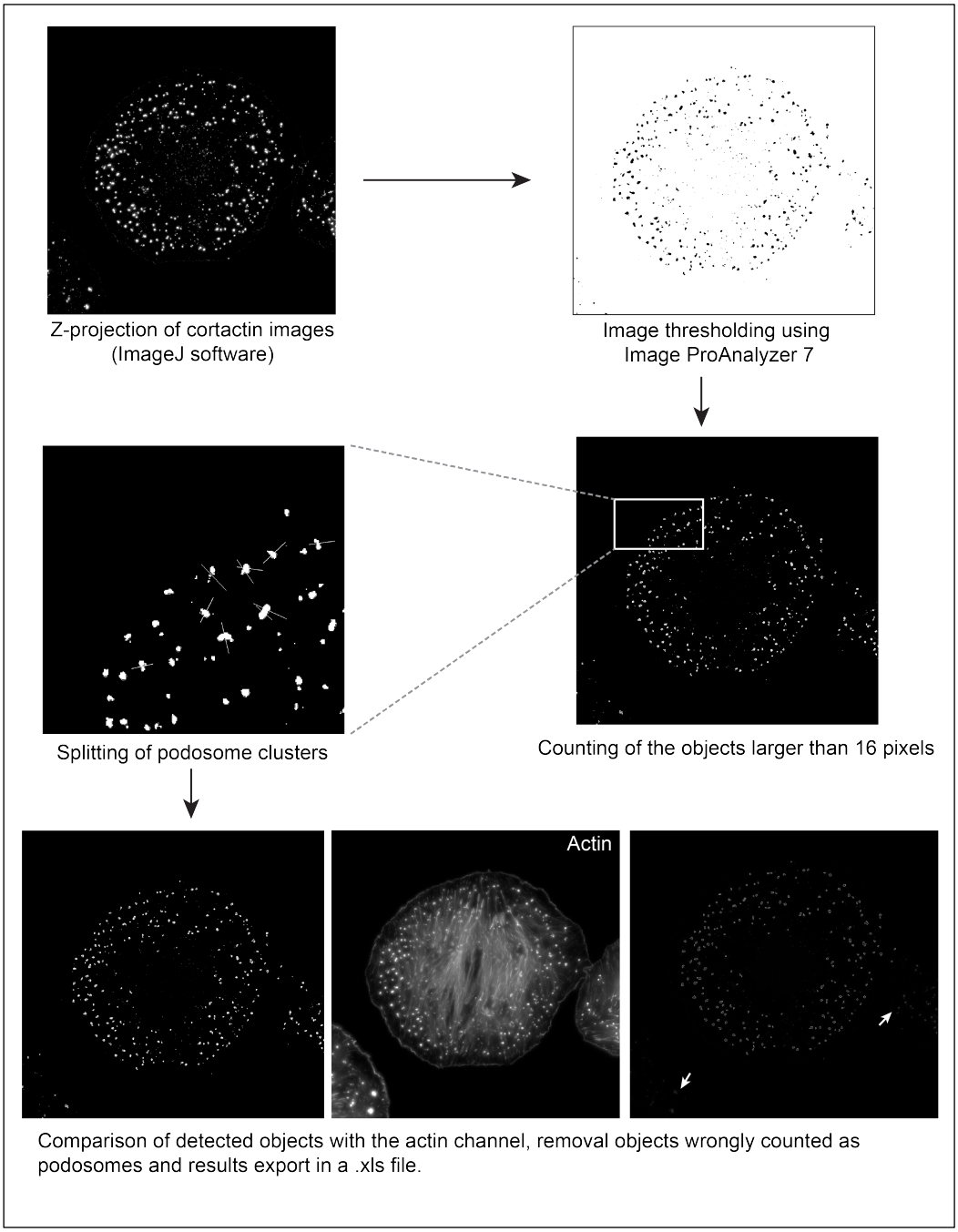

Figure 2.1: Podosome counting method.
Z-stack (spacing=0.2µm) of the actin and cortactin channels were acquired and images from the cortactin channel were transformed in Z-projection (Maximum Z projection) in ImageJ. Z-projections were loaded in Image-Pro Analyzer 7 and podosomes counted as following. Z-projections were thresholded and every object larger than 16 pixels were automatically detected. Podosome clusters were split in individual podosomes. The image was then compared with the actin channel and the colocalization of automatically detected podosomes in Image-Pro Analyzer 7 with the actin channel was visually addressed. Objects counted as podosomes in the cortactin channel that do not colocalize with spots detected in the actin channel were manually removed using the toggle function of the software (arrows). Results were then exported and compiled in an excel file.

2-3: α5-integrin transport assay

GFP-α5-integrin RPE-1 cells were split 24 hours before imaging in a 4 quadrants fluorodish coated for 24 hours with 10μg/ml Fibronectin. Photobleaching and imaging were conducted on a Deltavision Elite Wide-field microscope. Cell tail was imaged once prior photobleaching with a 488nm laser and every 0.5second for 2 minutes after photobleaching to detect GFP-α5-integrin trafficking in the photobleached area.

GFP-α5-integrin trafficking was analyzed using ImageJ image analysis software. 21 pixels width kymographs were drawn in the photobleached area and the movement of each vesicle detected in each kymograph was tracked. Vesicles movement was then classified as previously reported (Theisen et al., 2012) in stationary vesicle if the total displacement of the vesicle does not exceed 1μm and in moving vesicle if the total displacement of the vesicle exceeds 1μm. As PTPD1 overexpression could have an effect on the directional persistence of KIF1C-mediated GFP-α5-integrin transport, moving vesicles were then classified in 3 subcategories: jiggling vesicles if vesicles show a repeated forward and backward movement and if the distance between directional changes does not exceed 3μm; uni-directional movement if the vesicle moves towards one direction and if its total displacement is larger than 1μm; bi-directional movement was defined as vesicles moving in both directions with a distance range larger than 3μm between each directional change. A cutoff of 3μm to distinguish jiggling vesicles from bi-directionally moving vesicles was chosen based on personal observations as the distance between directional changes usually did not exceed 3μm for the majority of jiggling vesicles.

2-4: Molecular Biology

2-4-1: RT-PCR

Cells were harvested, washed in PBS and kept at -80°C in 1.5ml Eppendorf tubes until mRNA extraction. Cells harvested from an individual well of a 6-well plate (6x3.5mm) at 75% confluency were resuspended in 400µl Trizol (Ambion Life Technologies) and incubated 5 minutes at room temperature before the addition of 300µl Chloroform. Tube content was vigorously shaken for 15 seconds and incubated 5 minutes at room temperature prior centrifugation for 10 minutes at maximum speed. The upper layer was transferred into a new 1.5ml Eppendorf tube before the addition of 350µl Isopropanol. After gentle mixing, tubes were incubated 10 minutes at room temperature and centrifuged for 10 minutes at maximum speed. The supernatant was removed and pelleted mRNA resuspended in 70% Ethanol prior centrifugation for 5 minutes at maximum speed. Supernatant was removed and pelleted mRNA allowed to dry before resuspension in 20µl ddH_2O. mRNA concentration was measured using a NanoDrop 2000.

For RT-PCR, 2µg total mRNA were mixed with 0.2µg random hexamers and the volume adjusted to 12.5µl with ddH_20. The mix was incubated 5 minutes at 70°C and chilled on ice before addition of 4µl 5X Reaction buffer, 0.8µl 25mM dNTP mix (NEB) and 0.5µl RNase inhibitor (NEB). After 5 minutes incubation at 25°C, 1µl of H-minus Reverse Transcriptase (NEB) was added and the mix was incubated 10 minutes at 25°C and 60 minutes at 42°C. The reaction was stopped by heating the mix 10 minutes at 70°C and the cDNA obtained stored at -20°C.

2-4-2: PCR

PCR mixes were prepared in PCR tubes in a total volume of 50µl and reactions performed as indicated in Table 5. PCR product amplification was confirmed running 5µl of PCR reaction mixed with 1µl 6X Orange G loading buffer on agarose gel. PCR product size was compared to the GeneRuler 1kb ladder (Fermentas). When needed, PCR products were purified using PureLink Quick PCR Purification Kit as per manufacturers guidelines (Invitrogen) and resuspended in 50µl ddH_2O. Primers used for PCR are listed in Table 6.

To confirm PTPD1 depletion, primers AS380 and AS416 were used to amplify a 350bp fragment of PTPD1 cDNA and AS453 and AS454 to amplify a 500bp fragment of GAPDH cDNA.

PCR Mix		PCR Reaction		
10ng/µl DNA	1µl	Step	Temp.	Time
100µM Forward Primer	1µl	1	98°	2 min.
100µM Reverse Primer	1µl	2	60°	30 sec.
25mM dNTP mix	0.4µl	3	72°	30 sec./kb
25mM $MgCl_2$	2µl	4	98°C	10 sec.
10X Reaction Buffer	5µl	Step 2 to 4 repeated 34 times		
Taq Polymerase (5U/µL; Sigma)	1µl	5	72°	10 min.
ddH_2O	38.6 µl	6	4°C	∞

Table 5: PCR mix and reaction.

Name	Direction	5' to 3' sequence	Target
AS83	Reverse	GCCGTTTACGTCGCCGTC	GFP
AS264	Forward	CGCAAATGGGCGGTAGGCGTG	CMV
AS362	Forward	CTGTGGAGGTGtctTAcATGGAaATCTACT GTGAGCG	Human KIF1C
AS358	Reverse	GAAGGGATCCACAGTTCCCCCATCCTC	Human KIF1C
AS359	Reverse	GGGGATCCCCTCGTTCCCGTTCC	Human KIF1C
AS360	Reverse	GCTGGATCCTCACTGCCACCACCAC	Human KIF1C
AS370	Forward	CGGGGTCGACTCTGACAAGCGCTCTTG	Human KIF1C
AS371	Forward	GGAGGTCGACCGAGGGGCGGAGGTGG	Human KIF1C
AS379	Reverse	GTTGTAGTACCAtAatgaaAAGTAAGTGACC	Rat PTPD1
AS380	Reverse	GAGCCCTCTGTATTTCTGATG	Rat PTPD1
AS416	Forward	TTGGAGTGGTGTTTTATGTGC	Rat PTPD1
AS453	Forward	CTGAGAATGGGAAGCTGGTCA	Rat GAPDH
AS454	Reverse	GCCAGTGAGCTTCCCGTTC	Rat GAPDH
AS495	Reverse	TGCGGATCCTGCAGCCGTAGCTGCTC	Human KIF1C
AS588	Forward	GAAGTGCAGTCCAAGATTGAG	Rat Transgelin
AS589	Reverse	GGTCGCCCATAGCCTGTC	Rat Transgelin
UT01	Forward	GGAATTCTGGAGCTATGGCTGGTG	Human KIF1C
UT05	Forward	CAACACGGAGTCCCAGATTG	Human KIF1C
UT170	Reverse	ACTGACCTTCTCCGAGTCC	Human KIF1C

Table 6: Primers used in this study.
AS362 and AS379 were used to generate RNAi-protected KIF1C and PTPD1 respectively. Lower cases indicate silent point mutations.

2-4-3: Mutagenesis PCR

Mutagenesis PCR was used to generate RNAi-protected plasmids using the High-fidelity Phusion Polymerase (NEB). The PCR mix was set up mixing in a PCR tube 10ng of template DNA with 1µl of 10µM upstream primer, 1µl of 10µM mutagenesis primer (AS362 to generate KIF1C-RIP; AS379 to generate PTPD1-RIP), 10µl of 5X High-Fidelity PhusionBuffer, 1µl of Physion polymerase and 0.4µl of 25mM dNTP mix. The final volume was adjusted to 50µl using ddH_2O. The PCR was then carried out as indicated in Table 7. PCR product amplification was confirmed loading 5µl of the PCR product diluted in 6X Orange G loading buffer on an agarose gel. PCR product was purified using PureLink Quick PCR Purification Kit as per manufacturers guidelines (Invitrogen) and resuspended in 50µl ddH_2O.

Mutagenesis PCR program		
Step	Temperature	Duration
1	98°C	2 min.
2	98°C	10 sec.
3	60°C	30 sec.
4	72°C	10 sec.
Step 2 to 4 repeated 9 times		
5	72°C	Pause
Addition of 0.5µl of 100µM downstream primer		
6	98°C	10 sec.
7	60°C	30 sec.
8	72°C	20 sec.
Step 6 to 8 repeated 9 times		
9	72°C	Pause
Addition of 0.5µl of 100µM upstream primer		
10	98°C	10 sec.
11	60°C	30 sec.
12	72°C	20 sec.
Step 10 to 12 repeated 9 times		
13	72°C	10 min.
14	4°C	∞

Table 7: PCR Mutagenesis steps

2-4-4: Cloning

Restriction enzymes used to digest plasmids and PCR products were purchased from New England Biolab and used as per manufacturers instructions. Digested plasmids were loaded on agarose gel, DNA band of interest cut out from the gel and purified using PureLink Quick Gel Extraction Kit as per manufacturer instructions (Invitrogen) while digested PCR products were purified using PureLink Quick PCR Purification kit as per manufacturers instructions (Invitrogen). Ligation was carried out for an hour at room temperature in a total volume of 10µl mixing 6µl insert with 1µl plasmid, 2µl 5X Fast Ligation Buffer (Fermentas) and 1µl T4 DNA ligase (Thermo Scientific).
Ligation mix was incubated for 30 minutes with TOP10 competent cells on ice. Transformation was carried out incubating TOP10 competent cells mixed with the ligation product for 45 seconds at 42°C. Transformed cells were chilled on ice for 2 minutes and resuspended in 700µl SOC. Cells were allowed to recover at 37°C with shacking for at least 30 minutes prior seeding on LB plates containing the required selection antibiotic and plates were incubated at 37°C overnight.
Colonies that grew on the plate were picked in 3ml DYT containing the correct selection antibiotic and kept in culture overnight at 37°C with shaking. Plasmids were purified using UltraClean 6 minutes Mini Plasmid Prep Kit (Cambio) and resuspended in 50µl ddH_2O. Purified plasmids were subjected to test digestion and/or sent for sequencing (ATCC). Plasmids expressed in mammal cells were purified from 50ml culture using the PureLink HiPure Plasmid Midiprep Kit (Invitrogen) as per manufacturer instructions and resuspended in 200µl TE. Details of primers, enzymes and plasmids used for cloning are indicated in Table 8.

pKIF1C-RIP-GFP was cloned by PCR mutagenesis using pKan-CMV-hsKIF1C-GFP (cloned by Ulrike Theisen) as a template, UT01 as the upstream primer, AS362 as the mutagenesis primer and UT170 as the downstream primer. The PCR product and the template plasmid were both digested with EcoRI and BsiWI and the digested PCR product was cloned into to the digested pKan-CMV-hsKIF1C-GFP.

pKIF1C-RIP-1_490-GFP was cloned by amplification of KIF1C region of interest using pKIF1C-RIP-GFP as a template, UT01 as the forward primer and AS358

as the reverse primer. The PCR product and the template were digested with BsiWI and BamHI and the digested PCR product ligated in the digested pKIF1C-RIP-GFP.

pKIF1C-RIP-1_610-GFP was cloned by amplification of KIF1C region of interest using pKIF1C-RIP-GFP as a template, UT05 as the forward primer and AS359 as the reverse primer. The PCR product and the template were digested with BspEI and BamHI and the digested PCR product ligated in the digested pKIF1C-RIP-GFP.

pKIF1C-RIP-1_822-GFP was cloned by amplification of KIF1C region of interest using pKIF1C-RIP-GFP as a template, UT05 as the forward primer and AS360 as the reverse primer. The PCR product and the template were digested with BspEI and BamHI and the digested PCR product ligated in the digested pKIF1C-RIP-GFP.

pKIF1C-RIP-1_950-GFP was cloned by Nida Siddiqui by amplification of KIF1C region of interest using pKIF1C-RIP-GFP as a template, UT05 as the forward primer and AS459 as the reverse primer. The PCR product and the template were digested with BspEI and BamHI and the digested PCR product ligated in the digested pKIF1C-RIP-GFP.

pKIF1C-RIP-Δ623_679-GFP was cloned by Nida Siddiqui by amplification of KIF1C C-terminal region using pKIF1C-RIP-GFP as a template, AS370 as the forward primer and AS83 as the reverse primer. The PCR product and the template were digested with SalI and BamHI and the PCR product was ligated into the digested vector.

pKIF1C-RIP-Δ623_825-GFP was cloned by amplification of KIF1C C-terminal region using pKIF1C-RIP-GFP as a template, AS371 as the forward primer and AS83 as the reverse primer. The PCR product and the template were digested with SalI and BamHI and the PCR product was ligated into the digested vector.

pKIF1C-RIP-CHK2-GFP was cloned digesting both pKIF1C-RIP-GFP and pKan-CMV-KIF1C-rescue(1-500)-CHK2(501-623)-KIF1C-rescue(624-end)-2XFlag (cloned by Ulrike Theisen) plasmids with BsiWI and BamHI. The DNA fragment

excised from pKan-CMV-KIF1C-rescue(1-500)-CHK2(501-623)-KIF1C-rescue(624-end)-2XFlag and corresponding to the CHK2 FHA domain was then transferred in the digested pKIF1C-RIP-GFP.

pHA-PTPD1-RIP-WT was cloned by Daniel Roth by mutagenesis PCR using pHA-PTPD1-WT as a template (kind gift from A. Feliciello; Cardone et al., 2004), AS380 as the upstream primer, AS379 as the mutagenesis primer and AS264 as the downstream primer. The PCR product and pHA-PTPD1-WT were both digested with NheI and the digested PCR product ligated in the digested plasmid.

pHA-PTPD1-RIP-C1108S was cloned digesting pHA-PTPD1-RIP-WT and pHA-PTPD1-C1108S (kind gift from A. Feliciello; Cardone et al., 2004) with BsgI. The fragment excised from pHA-PTPD1-C1108S was then cloned into the digested pHA-PTPD1-RIP-WT.

2-4-5: Western Blotting

Samples were prepared harvesting and resuspending cells in 50µl PBS before addition of 10µl 6X Laemmeli containing β-Mercaptoethanol. Samples were boiled for 10 minutes at 95°C and stored at -20°C. For protein size reference, 5 µl of the Color Plus Pre-stained Protein Ladder Broad range (10-230kDa) (NEB) was loaded on the first well of each gel. After protein transfer on nitrocellulose membrane (GE healthcare), membranes were incubated for 30 minutes in 5% Milk (Sigma) diluted in PBS and probed with primary antibodies overnight at 4°C or an hour at room temperature. After extensive washes with PBS and TBS-0.1%Tween (TBST), membranes were incubated with HRP-coupled secondary antibodies for 45 minutes at room temperature (see Table 4 for the list of antibodies and dilutions used in this study). After extensive washes, revelation was carried out with SuperSignal West Pico Chemiluminescent Substrate (Thermo Scientific).

Plasmid name	Backbone	Primers	Restriction enzymes	Comments
pKIF1C-RIP-GFP	pKan-CMV-hsKIF1C-GFP	UT01 (forward) AS362 (mutagenesis) UT170 (reverse)	EcoRI, BsiWI	
pKIF1C-RIP-1_490	pKIF1C-RIP-GFP	UT01 (forward) AS358 (reverse)	BsiWI, BamHI	
pKIF1C-RIP-1_610	pKIF1C-RIP-GFP	UT05 (forward) AS359 (reverse)	BspEI, BamHI	
pKIF1C-RIP-1_822	pKIF1C-RIP-GFP	UT05 (forward) AS360 (reverse)	BspEI, BamHI	
pKIF1C-RIP-1_950	pKIF1C-RIP-GFP	UT05 (forward) AS459 (reverse)	BspEI, BamHI	Cloned by Nida Siddiqui
pKIF1C-RIP-Δ623_679-GFP	pKIF1C-RIP-GFP	AS370 (forward) AS83 (reverse)	SalI, BamHI	Cloned by Nida Siddiqui
pKIF1C-RIP-Δ623_825-GFP	pKIF1C-RIP-GFP	AS371 (forward) AS83 (reverse)	SalI, BamHI	
pKIF1C-RIP-CHK2-GFP	pKIF1C-RIP-GFP		BsiWI, BamHI	FHA domain from 8728 cloned by Ulrike Theisen
pKIF1C-Headless	pKan-CMV			Cloned by Ulrike Theisen *Efimova et al., 2014*
pKIF1C-G102E	pKan-CMV			Cloned by Ulrike Theisen *Efimova et al., 2014*
pHA-PTPD1-WT	pcDNA3.1			Gift from A. Feliciello *Cardone et al., 2004*
pHA-PTPD1-C1108S	pcDNA3.1			Gift from A. Feliciello *Cardone et al., 2004*
pHA-PTPD1-RIP-WT	pHA-PTPD1-WT	AS264 (forward) AS379 (mutagenesis) AS380 (reverse)	NheI	Cloned by Daniel Roth
pHA-PTPD1-RIP-C1108S	pHA-PTPD1-WT		BsgI	Cloned by Daniel Roth
pFlag	pKan-CMV			Cloned by Ulrike Theisen
pTks5-GFP				Gift from T. Oikawa *Oikawa et al., 2008*
pGFP-Vinculin				Gift from B. Geiger
pEGFP-N1	pKan-CMV			Clonetech
8728: pKan-CMV-KIF1C-rescue(1-500)-CHK2(501-623)-KIF1C-rescue(624-end)-2XFlag				

Table 8: List of plasmids used in this study.

2-5: Statistical analysis and figure preparation

The significance of the results was tested using a Mann-Whitney *U*-test using Origin Pro 8 software. Results were considered significant for $p<0.05$.

Graphs were made using Origin Pro 8 software. Box plots show 10-90 range Whisker.

Figures were made using Adobe Illustrator.

Cortactin and actin stainings inserted in figures show inverted images of Z stack.

Chapter 3: Results

3-1: Podosome formation in VSMCs requires a functional KIF1C

3-1-1: PDBu induction of podosome formation in VSMCs

In physiological conditions, Vascular Smooth Muscle Cells (VSMCs) surround blood vessel to regulate blood flow pressure through their contractile activity (Davis-Dusenbery et al., 2011). The inflammatory response caused by an injury or some specific pathological conditions (such as atherosclerosis) causes the release of pro-inflammatory factors (cytokines, chemokines, growth factors) in the circulation that activates the de-differentiation of VSMCs from a static contractile to an active synthetic phenotype characterized by cell proliferation, cell migration and podosome formation (Rudijanto, 2007; Chistiakov et al., 2015).

In vitro, VSMCs sporadically form very few podosomes. VSMC podosome formation can be induced by the overexpression of the constitutively active form of Src (v-Src) (Zhu et al., 2016) or the incubation of cells with growth factors (Quintavalle et al., 2010) or specific chemical compounds (Hai et al., 2002; Brandt et al., 2002). One of the most widely used chemical agent to induce podosome formation in VSMCs is the Phorbol-12,13-dibutyrate ester (PDBu). PDBu activates the PKCα signaling pathway to induce a global remodeling of the actin cytoskeleton and podosome formation (Hai et al., 2002).

To confirm that the rat Vascular Smooth Muscle Cell line used in this study behaves as previously described (Hai et al., 2002), A7r5 cell phenotype was characterized before and after podosome induction with 5μM PDBu. We first confirmed that the A7r5 cell line used in this study retained its smooth muscle characteristics even after growing it for several years in culture. To test this, we confirmed by RT-PCR the expression of the smooth muscle myosin heavy chain or transgelin by A7r5 cells, a specific marker for smooth muscle cells (Figure 3.1; Miano et al., 1994). We compared the level of expression of transgelin in A7r5 cells used in podosome formation assays (A7r5 synthetic) to

the expression level of transgelin in A7r5 cells freshly isolated from the aorta of embryonic rat and obtained from ATCC (A7r5 contractile). No significant difference in the expression level of transgelin could be detected between the two A7r5 cell lines tested (Figure 3.1), confirming that the A7r5 cells used during the course of this work actually were VSMCs. To confirm the specificity of the transgelin primers we designed, we tested their ability to amplify cDNA obtained from the retro-transcription of total mRNA purified from NRK cells. NRK cells are epithelial-like cells; they therefore do not express smooth muscle myosin heavy chain (Figure 3.1), providing a good negative control for transgelin expression in rat cells. A fragment of the GAPDH (Glyceraldheyde 3-phosphate dehydrogenase) cDNA of similar size (~500bp) was amplified in parallel and used as a loading control (Figure 3.1).

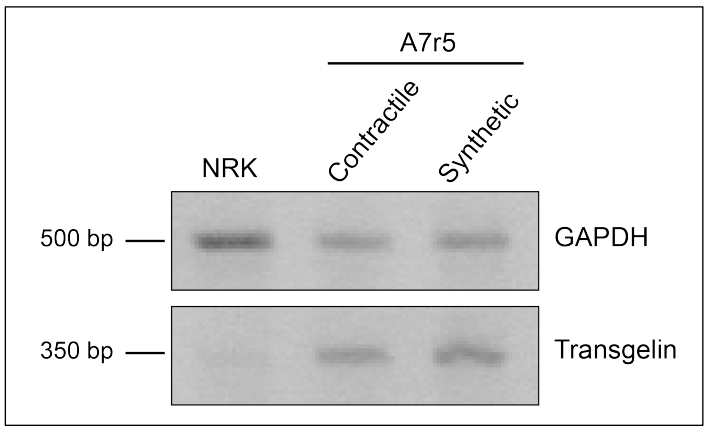

Figure 3.1: A7r5 cells used in this study express the transgelin smooth muscle cell specific marker.
Total mRNA of fresh A7r5 cells (Contractile A7r5 cells), A7r5 cells kept in culture for several years (Synthetic A7r5 cells) or epithelial like cells (NRK cells) were extracted and reverse transcribe using random hexamers primers. Transgelin and GAPDH cDNA were amplified with specific primers

A7r5 cells were then tested for their ability to form podosomes in response to treatment with the phorbol ester PDBu. Podosomes were immuno-stained using cortactin as a marker for the podosome core (Figure 3.2). Actin was also stained and observed in parallel to the cortactin staining to confirm its podosomal specificity.

In unstimulated cells, the actin cytoskeleton was well developed with stress fibers forming a strong well-organized network throughout the cytoplasm and the cortactin showed a diffuse distribution in the cytoplasm and accumulating at the cell cortex (Figure 3.2). As early as 10 minutes after PDBu addition, modifications of the actin cytoskeleton and podosome formation could be

detected. The actin network density was reduced in the cell body and an increase of the peripheral membrane ruffling activity was observed. Newly forming podosomes appeared as cortactin- and actin-enriched punctae at the very periphery of the cell (Figure 3.2).

After 30 minutes of PDBu treatment, the number of podosomes detected in cells was greatly increased and a modification in the general distribution of podosomes was observed. Cortactin-enriched punctae were not confined to the cell periphery as observed after only 10 minutes of PDBu treatment but podosomes covered a cellular area extending towards the cell centre. This phenomenon is most likely due to the centripetal relocation of material from old depolymerizing podosomes into more central newly forming ones (Zhu et al., 2016).

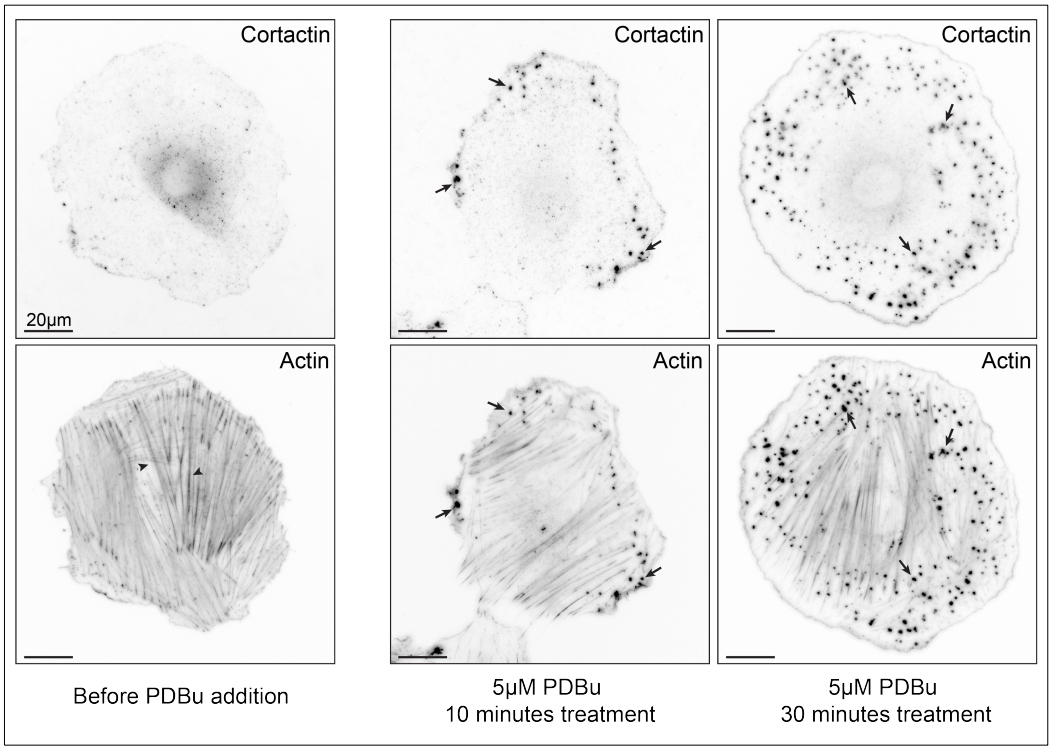

Figure 3.2: Phenotypical characterization of unstimulated and PDBu-treated A7r5 cells. A7r5 cells were stained for cortactin and actin in resting condition (left panel), after 10 minutes (middle panel) or 30 minutes (right panel) of stimulation with 5µM PDBu. Unstimulated cells show a well-developed actin stress fiber network (arrowheads) and the cortactin staining is dispersed throughout the cytoplasm. After 10 minutes of stimulation with 5µM PDBu, podosomes (arrows) are visualized as cortactin-dense spots formed at the very periphery of the cell. After 30 minutes of PDBu treatment, cells display an increased number of podosomes (arrow) scattered throughout the cytoplasm.

To confirm the podosomal specificity of the cortactin immuno-staining used, another specific marker of podosome core was used: the adaptor protein

Tks5. Tks5 has been shown to localize at the podosome core in Src-transformed fibroblasts (Abram et al., 2003) where it participates in the regulation of podosome formation and function (Seals et al., 2005) through its scaffolding activity, and is responsible for the recruitment of podosome components such as cortactin (Crimaldi et al., 2009). A GFP-fusion of Tks5 was expressed in A7r5 cells and its localization determined after podosome induction by PDBu treatment. Endogenous actin and cortactin were concomitantly stained and signals detected for each of these channels compared to Tks5-GFP localization (Figure 3.3).

Tks5-GFP was enriched at membrane ruffles and at podosome cores. Comparison of the GFP signal to cortactin and actin channels showed a very high degree of co-localization of cortactin and actin signals with GFP accumulations at podosome cores, proving the reliability of the cortactin staining as a podosome core specific marker for future experiments.

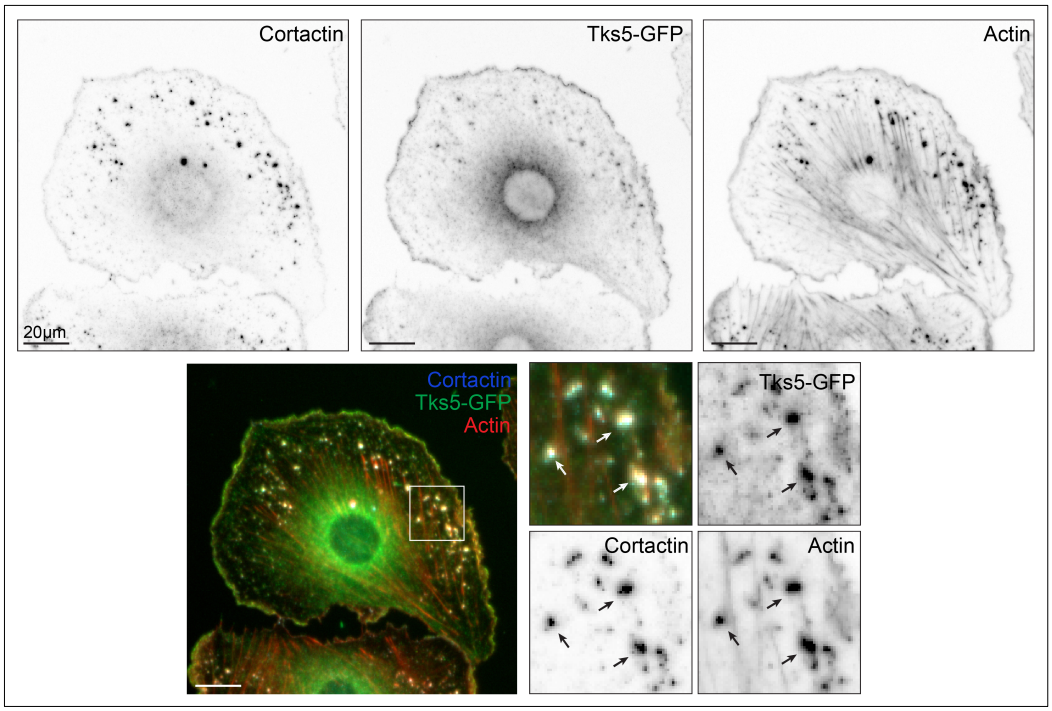

Figure 3.3: Cortactin, Actin and Tks5 colocalize at podosomes in VSMCs.
A7r5 cells expressing Tks5-GFP were treated for 30 minutes with 5µM PDBu prior fixation. Cortactin and actin stainings show a very high degree of colocalization with Tks5-GFP at the podosome core.

The cortactin staining used to detect podosomes in stimulated A7r5 cells only stains the podosome core. However, podosomes are considered as functional structures if they are able to assemble the adhesive ring around the

actin-rich core (Linder et al., 2011). To make sure podosomes formed in our A7r5 cell line were mature adhesion structures, GFP-vinculin was expressed in A7r5 cells and podosome formation induced for 30 minutes with 5µM PDBu. Podosome cores were stained with cortactin and the localization of vinculin-GFP at podosomes was determined (Figure 3.4).

Vinculin-GFP was enriched at elongated structures scattered throughout the cell and looking like focal adhesions. Podosome cores visualized by cortactin accumulations were often localized in close proximity to focal adhesions and vinculin-GFP formed a ring around the podosome core (Figure 3.4), confirming that A7r5 cells are able to form mature podosomes.

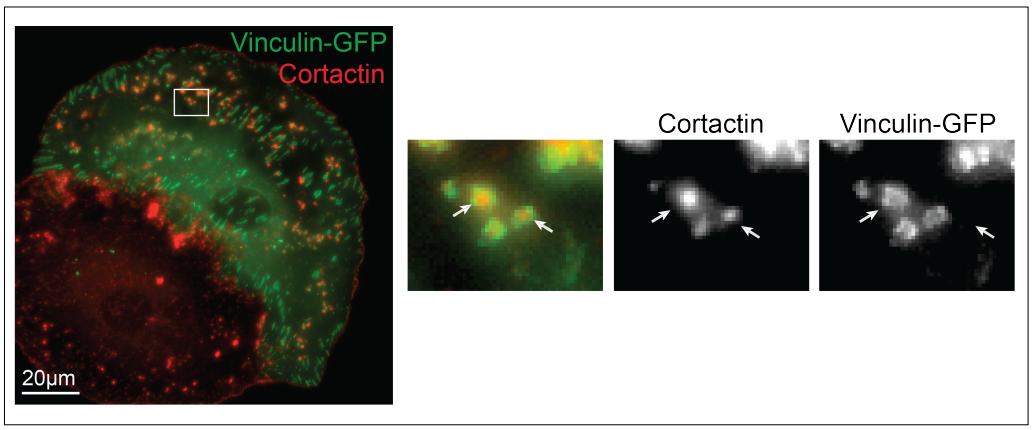

Figure 3.4: Vinculin-GFP forms a ring around the podosome core in A7r5 cells.
A7r5 cells expressing vinculin-GFP were treated for 30 minutes with 5µM PDBu prior fixation. Vinculin-GFP stains elongated structures scattered throughout the cells and resembling focal adhesions and forms a ring around the core of podosomes visualized with the cortactin staining.

3-1-2: Functional KIF1C is required for podosome formation in VSMCs

Prior to this work, KIF1C had been shown to participate in podosome dynamics in macrophages (Kopp et al., 2006). The macrophagic model differs from the VSMC one because it does not require extra-cellular signaling to trigger podosome formation as signals provided by their adhesion on a surface are sufficient to induce podosome formation. In VSMCs, podosome formation can be triggered subsequently to adhesion and these cells are thus a good model to study podosome formation mechanisms.

To test the requirement of KIF1C for podosome formation in VSMCs, a depletion-rescue approach was used. The expression of endogenous KIF1C

was reduced using a small-interfering RNA (siRNA) designed to specifically target KIF1C transcripts (Figure 3.5A) and the protein expression was restored using a RNAi-protected (RIP) version of KIF1C. To generate the RNAi-protected version of KIF1C, silent point mutations were introduced in the sequence of KIF1C cDNA to generate a transcript that cannot be recognized by the siRNA targeting KIF1C, and thus restores KIF1C protein expression in cells depleted for the endogenous protein without changing its amino acid sequence (Figure 3.5A).

The depletion of endogenous KIF1C and its re-expression with KIF1C-RIP were confirmed by Western-blot of cellular lysates. An antibody specifically recognizing KIF1C (region between amino acids 850 and 900) was used to detect KIF1C protein level in each condition and tubulin was used as a loading control. Two bands were detected for KIF1C: one around 130kDa and another one around 170kDa. The 130kDa band corresponds to the endogenous protein and the higher one to KIF1C-GFP. The shift observed between the two KIF1C forms comes from the GFP tag (Figure 3.5B).

Western-blot showed that the expression level of the endogenous KIF1C was strongly reduced after 72 hours of KIF1C siRNA treatment compared to control cells, confirming the efficiency of the siRNA used to target KIF1C transcript. It also showed that KIF1C was efficiently re-expressed with the RNAi-protected version of it (Figure 3.5B). The GFP-tagged protein is expressed at similar level as the endogenous protein and at the same level in control and KIF1C-depletion conditions, allowing the podosome formation assay to be performed.

For each condition, cells were seeded on fibronectin-coated glass coverslips 24 hours prior to the induction of podosome formation with 5µM PDBu to give cells enough time to adhere and spread on the substratum. After podosome induction for 30 minutes, cells were fixed, the endogenous cortactin was immuno-stained and the average number of podosomes formed in each condition was determined and compared to the average number of podosomes formed in control cells. To confirm the podosomal specificity of cortactin punctae observed, actin was stained and the colocalization of actin and cortactin stainings at podosome core was checked for each podosome detected in the cortactin channel (Figure 2.1).

A significant decrease of the average number of podosomes formed in KIF1C-depleted cells compared to the control condition was observed (p=0.02 using a Mann-Whitney U-test). KIF1C-depleted cells formed 33±3 podosomes on

average when control cells formed 47±5 podosomes (results indicate mean ± SEM; Figure 3.6), indicating that podosome formation is impaired in KIF1C-depleted cells and that KIF1C is required for podosome formation in VSMCs.
KIF1C-depleted cells expressing KIF1C-RIP formed an average number of podosomes that was very close to that formed in control cells (48±5 against 47±5 in control cells; Figure 3.6) and significantly different from KIF1C-depleted cells (33±3 podosomes formed per cell on average; p = 0.02 using a Mann-Whitney *U*-test). This result indicates that KIF1C re-expression after its depletion restores podosome formation in A7r5 cells and proves that the KIF1C depletion phenotype previously observed was specific to KIF1C depletion and not the result of the unspecific targeting of another transcript by the siRNA the cells were treated with.

We took advantage of the GFP tag fused to KIF1C-RIP to determine the localization of KIF1C at podosome in fixed cells. The GFP signal formed a ring around the cortactin core and seemed to be excluded from it (Figure 3.7), indicating that KIF1C most likely localizes at the podosome adhesive ring.

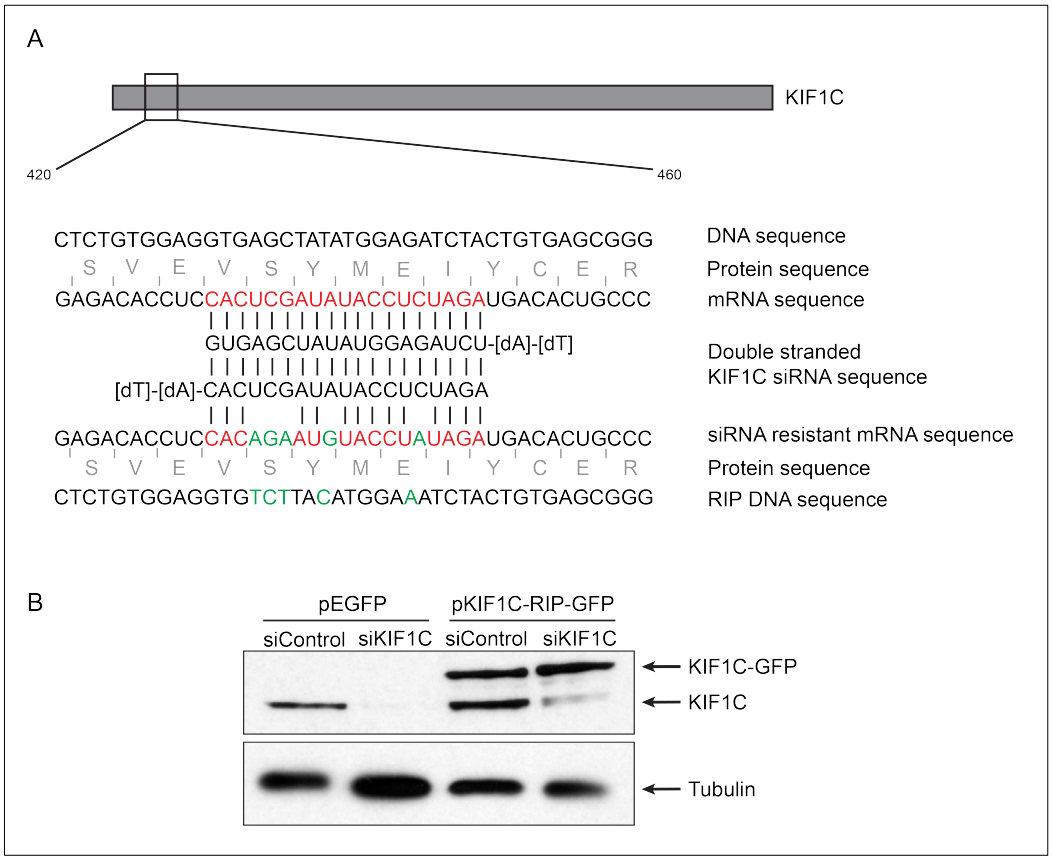

Figure 3.5: KIF1C depletion is efficient in A7r5 cells.
A: Principle of KIF1C depletion. A siRNA oligonucleotide (KIF1C siRNA sequence) was designed to target a sequence of the KIF1C transcript (mRNA sequence; red nucleotides) to induce its degradation. Silent point mutations (green nucleotides) were introduced in KIF1C cDNA sequence (RIP DNA sequence) to generate a transcript (siRNA resistant mRNA sequence) that cannot hybridize to the siRNA and thus, resistant to its degrading effect. B: Western-Blot showing the efficient KIF1C depletion after 72 hours of cell treatment with siKIF1C and the re-expression of a RNAi-protected version of the protein.

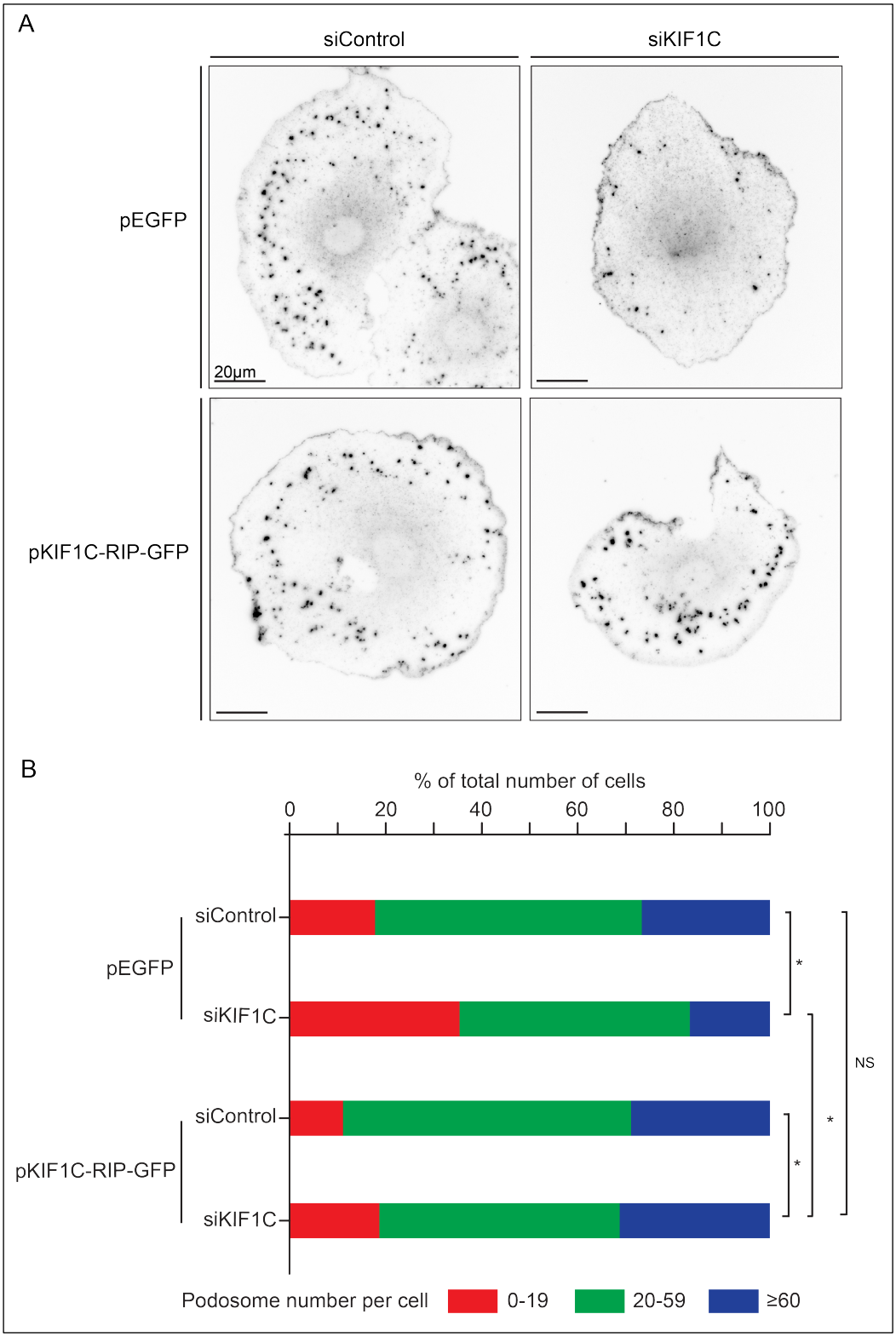

Figure 3.6: PDBu-induced podosome formation relies on KIF1C in VSMCs.
A7r5 cells depleted for KIF1C expression for 72 hours and transfected with a control (pEGFP) or the RNAi-protected version of KIF1C (pKIF1C-RIP-GFP) were treated with 5µM PDBu for 30 minutes prior fixation and cortactin immunostaining (A). Podosome number formed per cell was counted for each condition and compared to the control condition (B). n=60 cells pooled from 3 independent experiments; * $p<0.05$ using a Mann-Whitney *U*-test.

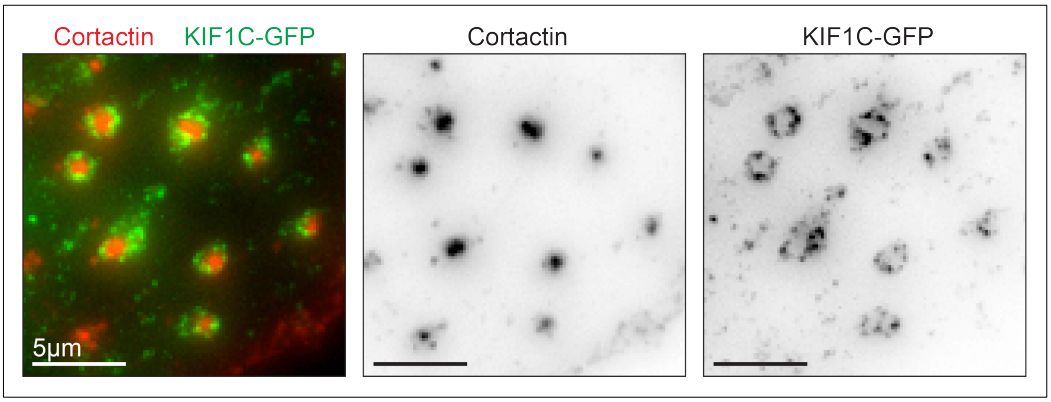

Figure 3.7: KIF1C forms a ring around the podosome core.
GFP-fusion of KIF1C was over-expressed in A7r5 cells. Cells were treated with 5µm PDBu for 30 minutes prior fixation. Podosome core was stained with cortactin. KIF1C-GFP forms a ring around the core of podosomes and seems to be excluded from it.

Results obtained so far suggested that KIF1C is required for the formation of a normal podosome number in VSMCs. As a member of the kinesin superfamily, KIF1C displays a motor activity to move along MTs and transport cargoes within the cell. To test if KIF1C involvement in podosome formation in VSMCs was motor-dependent, KIF1C motor activity was impaired using two different dominant negative forms of the kinesin: a KIF1C Headless mutant and a KIF1C rigor mutant (KIF1C-G102E). The Headless mutant contains only KIF1C tail and lacks its MT-interacting motor domain. The truncated protein can then bind its cargoes but it cannot interact with MTs anymore to ensure its cargo transport activity.

A rigor mutant is a catalytically inactive version of the kinesin (Nakata & Hirokawa, 1995). Point mutations inserted in the motor domain P-loop generate a kinesin that retains its ability to bind ATP but that had lost its ability to hydrolyze it, making it unable to generate the force required for its movement along MTs. However, kinesin rigor mutant capacity to bind microtubules stays intact as well as its cargo binding ability.

KIF1C dominant negative constructs were expressed in A7r5 cells and the ability of cells to form podosomes after 30 minutes of 5µM PDBu treatment was determined and compared to a control expressing pFlag. In both cases, a significant decrease in podosome formation was observed compared to control cells (Figure 3.8A). While control cells formed an average of 38±3 podosomes, cells transfected with the Headless construct formed 27±4 podosomes on average and cells expressing the rigor mutant only 21±3 podosomes (Figure

3.8A). It is noteworthy that the decrease of podosome formation after the over-expression of dominant negative mutants is stronger than the phenotype observed after KIF1C knockdown (Figure 3.6). As the endogenous KIF1C has not been depleted before the over-expression of the dominant negative constructs, it is suspected that these KIF1C mutants impair the activity of the endogenous motor, most likely through their ability to dimerize with the endogenous KIF1C.

Looking more closely at the cortactin staining of control cells and cells expressing KIF1C dominant negative constructs, an intriguing difference in podosome localization and distribution was observed. Podosomes formed in control cells were scattered throughout the cell cytoplasm with the exception of the perinuclear region whereas podosomes seemed to be preferentially localized to the cell periphery in cells expressing KIF1C dominant negative constructs (Figure 3.8B).

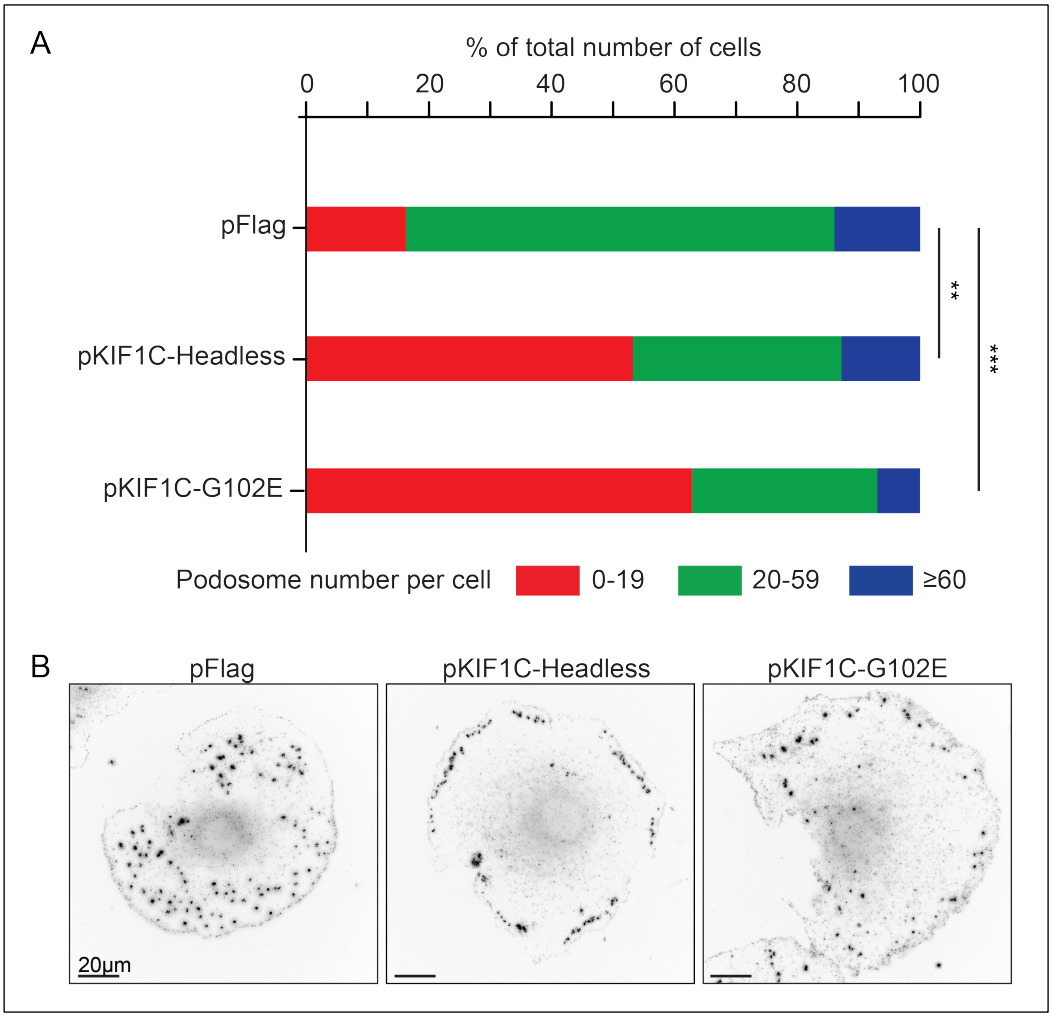

Figure 3.8: KIF1C motor activity is required for podosome formation in VSMCs.
A7r5 cells expressing a control plasmid (pFlag), a KIF1C mutant lacking its motor domain (pKIF1C-Headless) or a KIF1C rigor mutant (pKIF1C-G102E) were treated with 5µM PDBu for 30 minutes prior fixation and cortactin staining (B). Podosome number formed in each condition was determined and compared to the control condition (pFlag) to test the requirement of KIF1C motor activity for podosome formation (A).
n=60 cells pooled from 3 independent experiments, $**p<0.005$; $***p<0.0005$ using a Mann-Whitney *U*-test.

3-1-3: KIF1C-dependent timing of podosome formation in VSMCs

Podosome formation capacity of rat VSMCs was determined after 30 minutes of PDBu treatment in the first set of experiments of this work. However, podosome patterns observed at 10 and 30 minutes of podosome induction as well as in KIF1C dominant negative expressing cells suggested that KIF1C might be required for the relocation of podosomes from the cell periphery to the cell centre. The formation of the first batch of podosomes occurs at the cell periphery in VSMCs, at the interface between focal adhesions and stress fibers

to be more precise (Kaverina et al., 2003; Burgstaller & Gimona, 2004). Centrally located podosomes appear later on following the transfer of proteins from peripheral depolymerizing podosomes to newly forming ones at the cell centre. KIF1C involvement in this phenomenon as well as its requirement for podosome formation throughout time was thus tested. Podosome formation was induced with 5µM PDBu for 10, 20, 30, 40, 50, 60, 75 and 90 minutes in control and KIF1C-depleted A7r5 cells in parallel and the average number of podosomes formed in KIF1C-depleted cells was compared to the control condition for each time point (Figure 3.9A).

The results of this time course experiment suggested that podosome formation in control and KIF1C-depleted cells could be divided into 2 phases. During the early phase of podosome formation (first 20 to 30 minutes of podosome formation), the average podosome number formed in control and KIF1C-depleted cells increased at the same rate (Figure 3.9A). However, from 40 minutes after podosome induction, the average number of podosomes formed in KIF1C-depleted cells stagnated at ~ 30 podosomes per cell while the average number of podosomes formed in control cells continued to gradually increase and stabilized around 40 podosomes per cell after 60 minutes of PDBu treatment. At 90 minutes of PDBu treatment, a decrease in the number of podosomes formed per cells was detected in both conditions that may be due to the degradation of the phorbol ester and a decrease of the signals it mediates.

Taken together, results obtained so far highlight the importance of KIF1C for podosome formation in VSMCs. We showed here that KIF1C involvement in podosome formation is not cell-type specific as the same kind of results were previously obtained in macrophages (Kopp et al., 2006). KIF1C ability to form podosomes relies on its motor activity, as the over-expression of catalytically inactive forms of KIF1C impairs podosome formation (Figure 3.8). The main function of kinesin motor activity is to mediate cargo transport throughout the cell. The observation of cortactin stainings and podosome patterning at different time points of podosome induction revealed that impairing KIF1C motor activity results in the retention of podosomes at the cell periphery, most likely because of KIF1C inability to transport podosome components in a centripetal way.

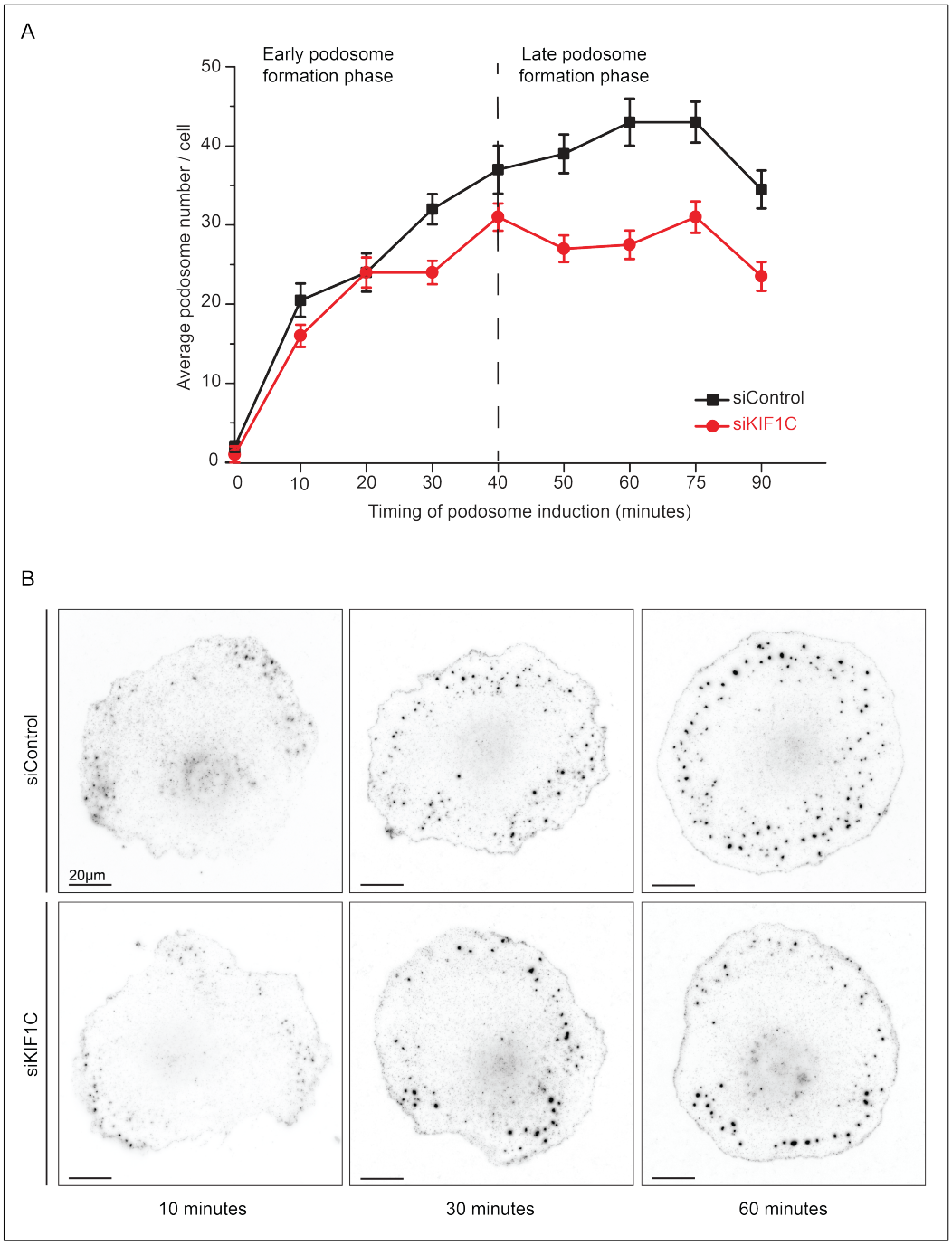

Figure 3.9: Kinetic of podosome formation in control and KIF1C-depleted VSMCs.
A7r5 cells treated for 72 hours with a control (siControl) or a KIF1C-targeting siRNA (siKIF1C) were treated with 5µM PDBu for various periods of time prior to fixation and cortactin staining. The number of podosomes formed was then determined for each time point (A). Data show mean ± SEM. n=90 cells pooled form 3 independent experiments. (B) Examples of cortactin staining of cells treated for 10, 30 or 60 minutes with 5µM PDBu.

3-2: KIF1C and PTPD1 cooperate to form podosomes in VSMCs

3-2-1: The Myosin IIA / PTPD1-binding domain of KIF1C is required for podosome formation in VSMCs.

Results produced in the first part of this study highlighted the requirement of a functional KIF1C motor activity for podosome formation in VSMCs. Apart from the recent discovery of Rab6-mediated control of KIF1C activity during synaptic vesicle transport (Lee et al., 2015), little is known about mechanism(s) controlling KIF1C transport activity. As I described in the introduction (Chapter 1-1), kinesin tails are known to participate in the regulation of kinesin motor activity. Depending on its cargo binding status, the tail can interact with or release the motor domain, leading to kinesin inactivation or activation respectively. Moreover, kinesin tails can mediate the oligomerization of the motor, allowing it to move along microtubules.

The KIF1C tail contains various structural domains separated from each other by regions without apparent structural characteristics. It is known to interact with a number of proteins whose functional role remains poorly understood but which could influence KIF1C transport activity. In order to identify regions in the KIF1C tail that are important for podosome formation in VSMCs and hereby the activation of its motor activity, KIF1C truncation constructs were tested for their ability to mediate podosome formation. To do so, the RNAi-protected KIF1C construct (pKIF1C-RIP-GFP) previously generated to restore KIF1C expression after its depletion was used as a template for the design of various KIF1C mutants lacking a specific region or domain of its tail (Figure 3.10). Truncation sites were chosen in unstructured regions of the protein to preserve the structural integrity of any folded domains as much as possible. Known binding domains for KIF1C interactors were also preserved as protein interactions may regulate KIF1C activity during the podosome formation process. Each construct was then expressed in KIF1C-depleted A7r5 cells and the ability of these cells to efficiently form podosomes in the absence of the endogenous protein was tested. Cells were treated with 5μM PDBu for an hour and not 30 minutes as previously as the time course

experiments conducted in the first part of this study (Figure 3.9) suggested that a stronger phenotype could be observed after an hour of podosome induction.

Four C-terminal truncations were initially generated to determine the minimal length of KIF1C tail required to mediate podosome formation in VSMCs. To do so, the motor domain and the two first coiled-coil domains were preserved to form a minimal construct (pKIF1C-RIP-1_490). The tail length was then gradually increased to include the FHA domain (pKIF1C-RIP-1_610), the FHA domain plus the third coiled-coil domain (pKIF1C-RIP-1_822) and finally the fourth coiled-coil domain (pKIF1C-RIP-1_950). The full length KIF1C-RIP construct (pKIF1C-RIP) was used as a control to compare podosome formation in each condition with and determine the ability of each truncation to mediate podosome formation in the absence of the endogenous motor (Figure 3.10).

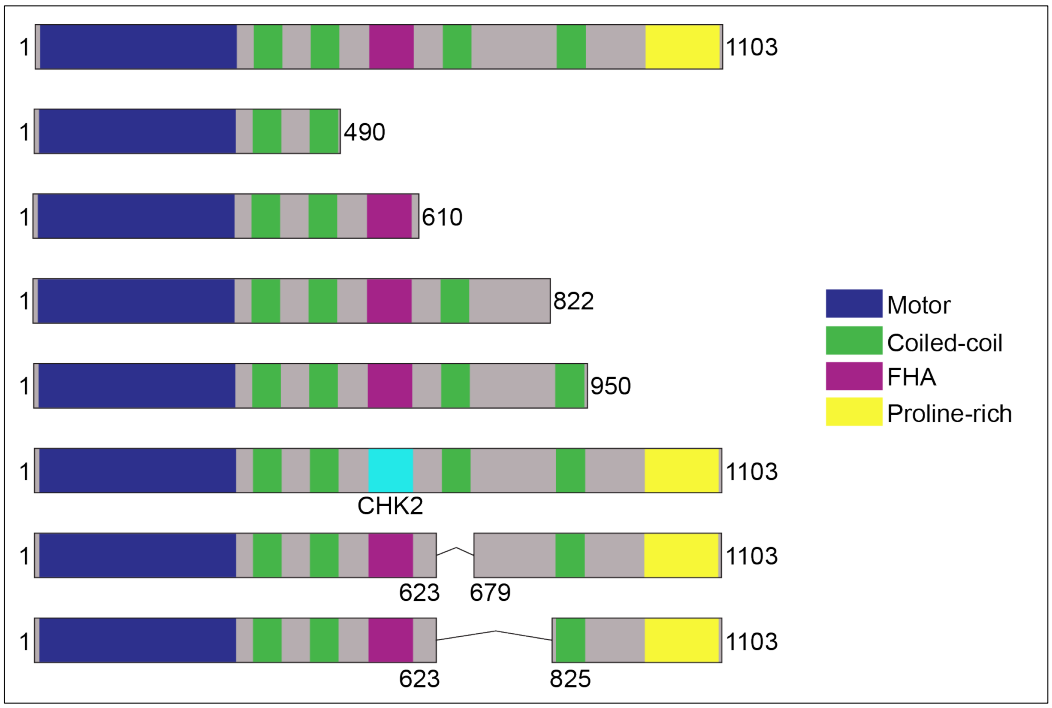

Figure 3.10: Schematic representation of KIF1C mutants used to identify the region of the kinesin that is important for podosome formation in VSMCs.

KIF1C-depleted cells (siKIF1C pEGFP) formed 43±3 podosomes on average (Figure 3.11), a result that is significantly different from the 84±5 podosomes formed in control cell (siControl pEGFP) (p<0.00001 using Mann-Whitney *U*-test). In these experiments, cells formed a higher number of podosomes than those used in the previous experiments (Chapter 3.1). This

difference can be explained by the gradual decrease of VSMC contractility with time when cells are kept in culture that favors podosome formation. To confirm the ability of the RNAi-protected version of KIF1C full-length to restore podosome formation after 60 minutes of podosome induction, KIF1C-depleted cells were transfected with pKIF1C-RIP-GFP (siKIF1C KIF1C-FL condition) and their ability to form podosomes was tested after 60 minutes of PDBu treatment. These cells formed 75±4 podosomes on average. This result is significantly different from that obtained in the KIF1C depletion condition (siKIF1C pEGFP cells; $p<0.00001$ using Mann-Whitney *U*-test) and not significantly different from the control condition (siControl pEGFP cells; $p=0.31$ using a Mann-Whitney *U*-test). Hence, podosome formation can be restored after 60 minutes of PDBu treatment in KIF1C-depleted cells using the RNAi-protected version of KIF1C and these results provided baselines to compare podosome formation with in the different conditions tested below.

The first truncation that has been tested for its ability to mediate podosome formation in KIF1C-depleted cells was the KIF1C minimal construct described above. After an hour of PDBu treatment, KIF1C-depleted cells expressing the KIF1C-RIP-1_490 truncation (siKIF1C KIF1C1_490 condition) formed only 40±4 podosomes on average, a number that is significantly different from the 75±4 podosomes formed in the rescue condition (siKIF1C KIF1C-FL condition; $p=0.0015$ using Mann-Whitney *U*-test). However, this result is not different from the KIF1C depletion condition (siKIF1C pEGFP; $p=0.85$ using Mann-Whitney *U*-test), showing that this KIF1C minimal truncation is not able to mediate podosome formation in VSMCs.

KIF1C tail was then extended to include the FHA domain (pKIF1C-RIP-1_610), a specific feature of kinesin-3s. Again, KIF1C-depleted cells expressing this construct were not able to restore podosome formation as cells of the siKIF1C KIF1C-1_610 condition formed an average number of only 48±5 podosomes (Figure 3.11), a number that is significantly different from the 75±4 podosomes formed with the full length construct ($p=0.02$ using Mann-Whitney *U*-test).

The longer truncation containing the third coiled-coil domain and truncated just before the fourth coiled-coil domain was then tested for its ability to restore podosome formation in the absence of the endogenous KIF1C motor.

KIF1C-depleted cells expressing this construct (siKIF1C KIF1C-1_822 condition) formed a number of podosomes that is not significantly different from the full-length rescue condition (63±4 compared to 75±4; p=0.25 using Mann-Whitney U-test), meaning that this truncation is able to support KIF1C podosome-forming activity (Figure 3.11).

Likewise, the longest truncation lacking only the carboxy-terminal Proline-rich domain formed a normal number of 85±7 podosomes on average (Figure 3.11).

Results obtained using these KIF1C truncations suggest that KIF1C full length is not absolutely required for podosome formation in VSMCs as the KIF1C-1_822 truncation can efficiently mediate podosome formation in the absence of the endogenous kinesin. The shortest truncation (KIF1C-1_610) is unable to efficiently mediate podosome formation, suggesting that the KIF1C-610_822 region is required for podosome formation in VSMCs.

FHA domains are structural domains that were first identified in transcription factors and kinases (Hofmann & Bucher, 1995) and that have since been identified in many other types of proteins such as phosphatases, glycoproteins and kinesins (Li et al., 2000). In addition to their structural properties, FHA domains also recognize and interact with phospho-serine and phospho-threonine epitopes exposed at the protein surface (Li et al., 2000).
FHA domains were shown to regulate kinesin-3 activity through their ability to interact with kinesin coiled-coil domains. Indeed, KIF1A FHA domain can interact with the coiled-coil domain that immediately follows it in the protein sequence to negatively regulate KIF1A motor activity (Lee et al., 2004). The same FHA domain can also work in tandem with KIF1A first coiled-coil domain to mediate kinesin dimerization and thus facilitate KIF1A motor activity (Huo et al., 2012). Therefore, the FHA domain appears to be crucial for the regulation of KIF1A activity and as a specific feature of the kinesin-3 family, it might regulate the activity of the other members of the family.

	siControl pEGFP	siKIF1C pEGFP	siKIF1C KIF1C-FL	siKIF1C KIF1C-1_490	siKIF1C KIF1C-1_610	siKIF1C KIF1C-1_822	siKIF1C KIF1C-1_950	siKIF1C KIF1C-CHK2	siKIF1C KIF1C-Δ623-679	siKIF1C KIF1C-Δ623-825
siControl pEGFP		*p*<0.00001	*p*=0.31	*p*=0.0007	*p*=0.01	*p*=0.54	*p*=0.73	*p*=0.52	*p*=0.72	*p*<0.00001
siKIF1C pEGFP	*p*<0.00001		*p*<0.00001	*p*=0.85	*p*=0.41	*p*=0.00004	*p*<0.00001	*p*<0.00001	*p*=0.00008	*p*=0.04
siKIF1C KIF1C-FL	*p*=0.31	*p*<0.00001		*p*=0.0015	*p*=0.02	*p*=0.25	*p*=0.79	*p*=0.84	*p*=0.44	*p*<0.00001

Figure 3.11: KIF1C truncations revealed the crucial importance of a ~ 150 amino acid long domain to mediate its podosome forming activity.
A7r5 cells depleted for the endogenous KIF1C were transfected with tail truncations as indicated and their ability to form podosomes determined after 60 minutes of treatment with 5µM PDBu. Each condition tested was compared to a control condition (siControl pEGFP) and to the rescue condition (siKIF1C KIF1C-FL). Results colored in green are not significantly different from the rescue condition; results colored in red are significantly different from the rescue condition. The table indicates *U*-test *p* values. n=90 pooled form 3 different experiments.

To determine the requirement of the FHA domain for KIF1C function and without interfering with the structural role of the FHA domain, KIF1C FHA domain was replaced by an FHA domain from an unrelated protein, the CHK2 kinase (pKIF1C-RIP-CHK2). This KIF1C mutant was able to restore podosome

formation in cells depleted for the endogenous protein (siKIF1C KIF1C-CHK2 FHA domain condition). Indeed, these cells formed 86±5 podosomes on average, which is not significantly different from the 75±4 podosomes formed in cells expressing KIF1C full-length (Figure 3.11; p=0.84 using Mann-Whitney U-test). This result suggests that if KIF1C FHA domain is important for KIF1C podosome-forming activity, it's most likely due to its structural function rather than to its phospho-specific interactions with proteins.

As mentioned above, the KIF1A FHA domain can modulate the kinesin folding and hence its activity through its interaction with the coiled-coil domain that immediately follows it (Lee et al., 2004). To test if the coiled-coil domain that follows KIF1C FHA domain is involved in the regulation of KIF1C activity, a deletion mutant lacking KIF1C third coiled-coil domain (pKIF1C-RIP-Δ623-679) was generated and its ability to restore podosome formation tested in KIF1C-depleted cells. These cells formed an average number of podosomes of 62±4 after 60 minutes of PDBu treatment, a number that is not significantly different from the rescue with the full length construct (Figure 3.11; p=0.44 using Mann-Whitney U-test), thus indicating that the third coiled-coil domain of KIF1C is not absolutely required to mediate its podosome-forming activity.

The region of interest identified with the four initial KIF1C truncations highlighted the importance of the region between amino acids 610 and 822 for podosome formation in VSMCs. As deleting the third coiled-coil domain that falls within that region had no effect on KIF1C ability to mediate podosome formation, an additional deletion mutant lacking the third coiled-coil and the following unstructured domains was generated (pKIF1C-RIP-Δ623-825) and its ability to mediate podosome formation tested. KIF1C-depleted cells expressing this construct (siKIF1C KIF1C-Δ623-825 cells) formed a strikingly low number of podosomes compared to all of the other conditions tested. Indeed, these cells formed only 26±3 podosomes on average, a number that is even lower than the one formed in KIF1C-depleted cells only (Figure 3.11). This result suggests that this region comprised between the third and fourth coiled-coil domain is of major importance to mediate KIF1C podosome-forming activity.

Rescue experiments using these seven KIF1C mutants allowed the identification of a region of about 150 amino acids in the tail of KIF1C that seems to be crucial to mediate its podosome forming activity. This region

between the third and fourth coiled-coil domain is known to interact with the non-muscle Myosin IIA (Kopp et al., 2006) and the tyrosine phosphatase PTPD1 (Dorner et al., 1998). Interestingly, these two proteins were shown to participate to the regulation of the cellular adhesion (Conti et al., 2004; Carlucci et al., 2008) and are thus good candidate to investigate to understand the mechanism ruling KIF1C-mediated podosome formation in VSMCs.

3-2-2: The non-muscle Myosin IIA is not required for podosome formation in VSMCs.

The non-muscle Myosin IIA is a well-known podosome component that localizes on top of the adhesive ring where it crosslinks radial actin filaments to maintain podosome structural integrity and mediate podosome oscillations (Gawden-Bone et al., 2010; van den Dries et al., 2013). Myosin IIA interaction with KIF1C has previously been suggested to be important for podosome formation in macrophages (Kopp et al., 2006). Indeed, the microinjection of a truncated version of KIF1C containing only KIF1C Myosin IIA/PTPD1 binding domain impairs podosomes reformation in macrophages after their disruption with the PP2 Src inhibitor (Kopp et al, 2006). A similar GFP-tagged construct was tested (pKIF1C-708_822-GFP) and appeared to localize to the nucleus in A7r5 cells (Figure 3.12) and the published effect on podosome formation could not be confirmed. To address the requirement of the Myosin IIA contractile activity for podosome formation in VSMCs, an inhibitory approach was chosen.

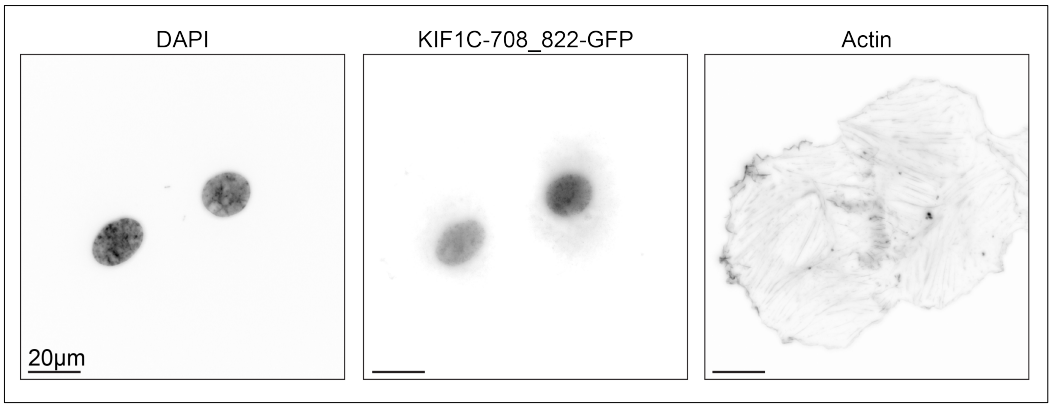

Figure 3.12: KIF1C-708_822 localizes to the nucleus of A7r5 cells.
A7r5 cells were transfected with the pKIF1C-708_822-GFP construct, fixed and stained with DAPI and Acti-staining. The GFP signal colocalizes with the DAPI staining, proving the nuclear localization of the KIF1C-708_822 construct.

Cells were first treated with Blebbistatin, a Myosin II inhibitor that binds to the Myosin-ADP-Pi complex with high affinity and impairs the release of the hydrolyzed nucleotide. Hence, Blebbistatin-bound Myosin IIA is blocked in its low actin affinity state and cannot bind actin filaments after the first cycle of ATP hydrolysis (Kovács et al, 2004). Podosome formation was induced for 60 minutes with 5μM PDBu and in the same moment, Myosin IIA contractile activity was inhibited using different concentration of Blebbistatin (0, 10, 20 and 30μM). The efficiency of the Blebbistatin inhibitor was confirmed comparing the actin stress fiber network in control cells (0μM Blebbistatin) and cells treated with the Myosin IIA inhibitor. Indeed, the loss of the actin stress fiber network has previously been associated with an efficient Blebbistatin-mediated decrease of Myosin IIA contractile activity (Even-Ram et al., 2007). While DMSO-treated cells (0μM Blebbistatin) retain a well-developed actin stress fiber network at the cell center, Blebbistatin treated cells lost most, if not completely, their actin stress fibers (Figure 3.13B), proving the efficiency of the Blebbistatin inhibitor.

The number of podosomes formed in each condition was then determined and compared to the number of podosomes formed in DMSO-treated cells (0μM Blebbistatin; Figure 3.13A). For every inhibitor concentration tested, no significant difference between DMSO-treated cells and Blebbistatin-treated cells could be detected (Figure 3.13A), suggesting that inhibiting Myosin IIA contractile activity has no effect on podosome formation in VSMCs.

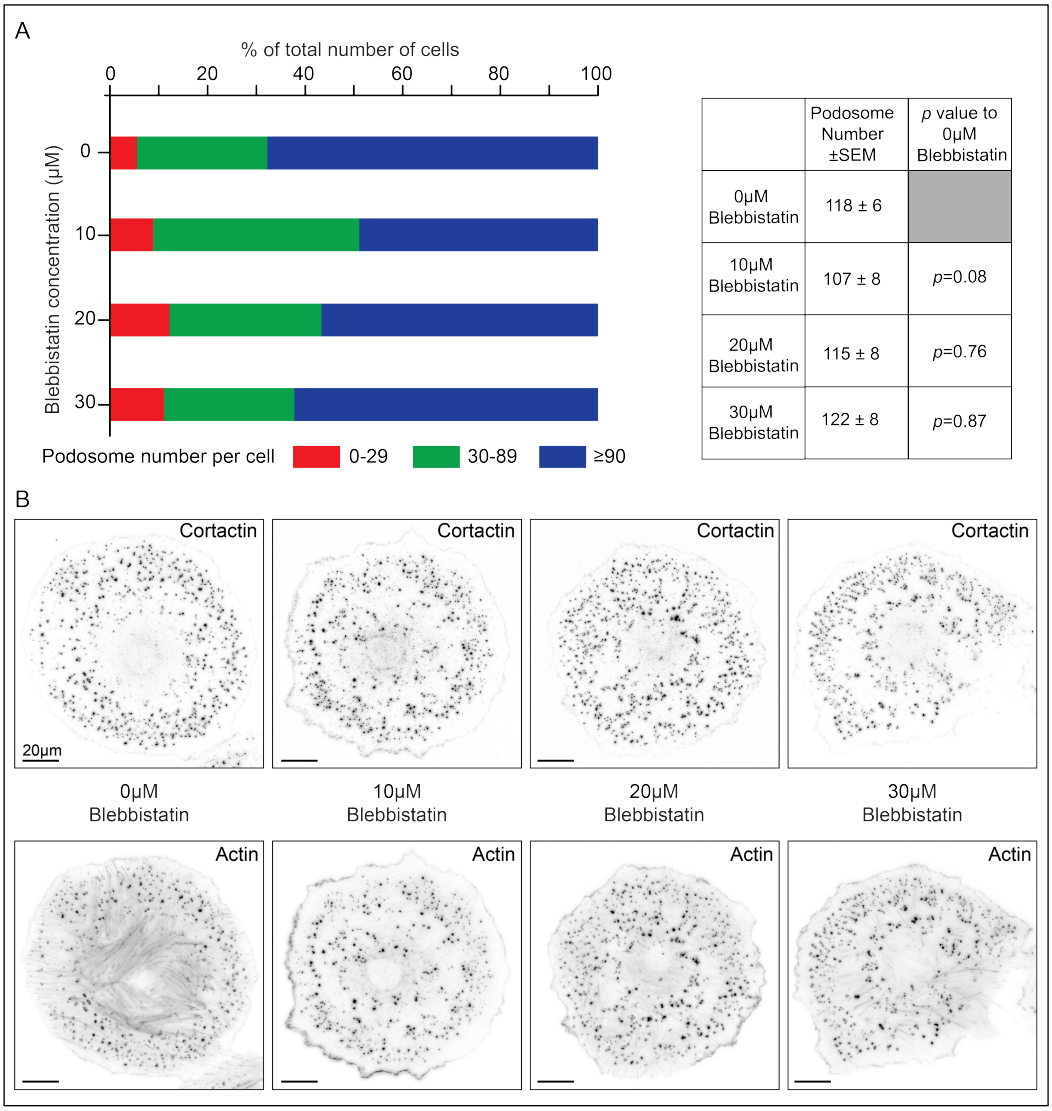

	Podosome Number ±SEM	*p* value to 0µM Blebbistatin
0µM Blebbistatin	118 ± 6	
10µM Blebbistatin	107 ± 8	*p*=0.08
20µM Blebbistatin	115 ± 8	*p*=0.76
30µM Blebbistatin	122 ± 8	*p*=0.87

Figure 3.13: Myosin IIA inhibition with Blebbistatin has no effect on podosome formation in VSMCs.
A7r5 cells treated for 60 minutes with 5µM PDBu were concomitantly treated with different concentrations (0, 10, 30 or 30µM) of the Myosin IIA inhibitor Blebbistatin. Cells were fixed and stained with actin and cortactin (B). The number of podosomes formed in each condition was determined and compared to the DMSO-treated control condition (0µM Blebbistatin) using Mann-Whitney *U*-test (A). No significant difference could be observed between control cells (0µM Blebbistatin) and cells treated with the inhibitor. n=90 pooled from 3 independent experiments.

To confirm this result, we used an alternative method to reduce Myosin IIA activity: the Y27632 Rho-associated Coiled-coil containing protein Kinase (ROCK) inhibitor. This chemical compound competes with ATP for the binding of the ROCK catalytic site and impairs the activation of its downstream effectors, including the non-muscle Myosin IIA-regulating kinase MLCK (Myosin Light Chain Kinase). Hence, treatment with Y27632 impairs Myosin IIA contractile

activity but in contrast to Blebbistatin, it doesn't compromise its ability to bind and crosslink actin filaments.

Three different concentrations of the ROCK inhibitor were tested (5μM, 10μM and 15μM) while podosome formation was induced with PDBu and the average number of podosomes formed in cells treated with Y27632 was determined and compared to a DMSO-treated control condition (0μM Y27632). Y27632 efficiency was confirmed using the actin staining. While control cells (0μM Y27632) displayed a well-developed actin stress fiber network throughout their cytoplasm, the actin network was weakened in Y27632-treated cells (Figure 3.14B), proving the efficiency of the Myosin IIA contractile activity inhibition. No significant difference in the average number of podosomes formed per cell was detectable when the Myosin IIA contractile activity was inhibited with 5 and 10μM of the ROCK inhibitor (Figure 3.14A). Cells treated with 15μM displayed a significant increase of the average number of podosomes they formed (130±7 on average) compared to control cells (109±6 podosomes formed on average; p=0.009 using a Mann-Whitney U-test; Figure 3.14A).

These results suggest that the inhibition of the Myosin IIA contractile activity using two different methods has no dramatic effect on the ability of cells to form podosomes. Moreover, in contrast to the Y27632 ROCK inhibitor, the Blebbistatin inhibitor not only impairs Myosin IIA contractile activity but also abolishes its ability to bind and crosslink actin filaments. Thus, Myosin IIA appears to be dispensable for podosome formation in VSMCs and in light of these results, it was ruled out as the relevant KIF1C interactor to explain KIF1C-mediating podosome formation in VSMCs.

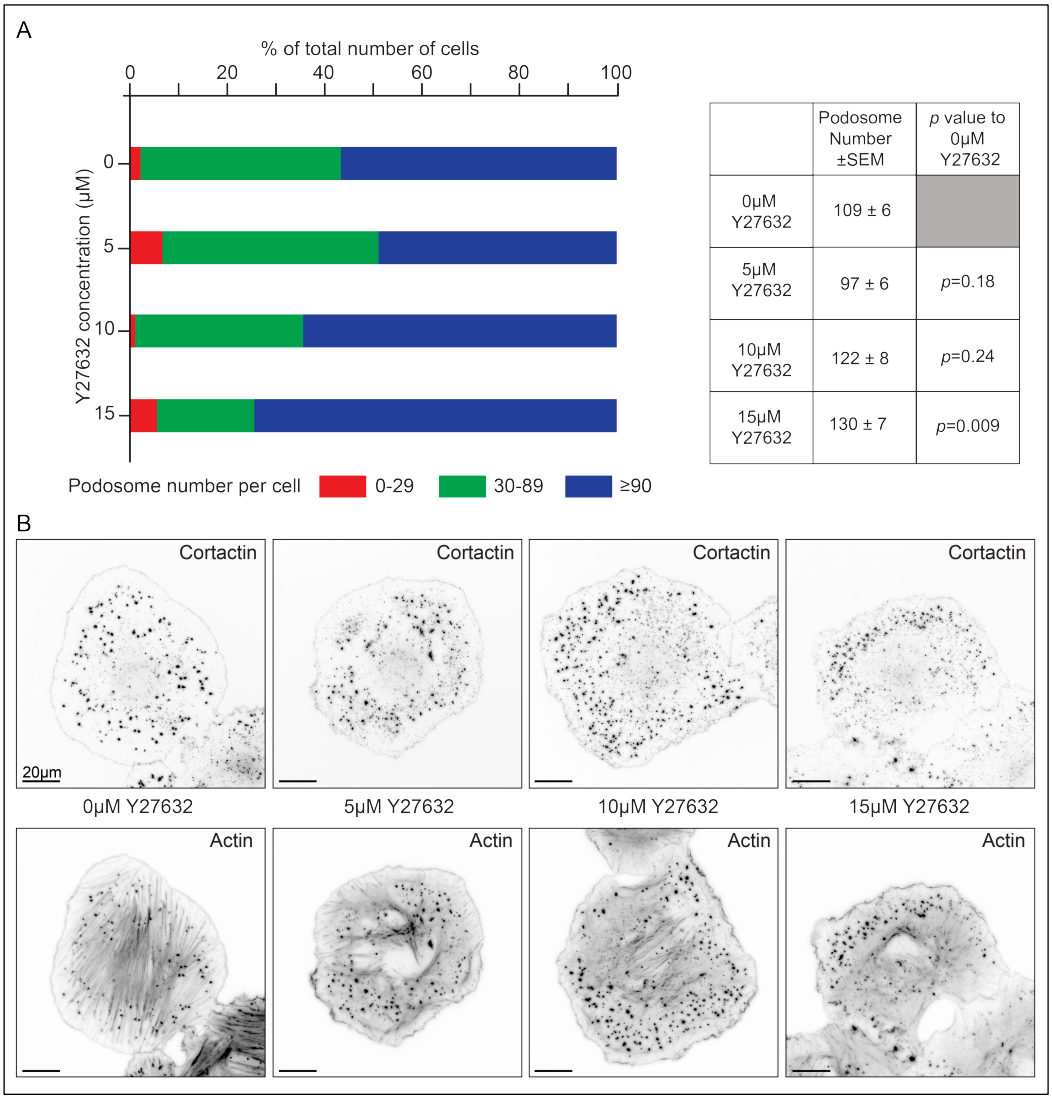

	Podosome Number ±SEM	*p* value to 0µM Y27632
0µM Y27632	109 ± 6	
5µM Y27632	97 ± 6	*p*=0.18
10µM Y27632	122 ± 8	*p*=0.24
15µM Y27632	130 ± 7	*p*=0.009

Figure 3.14: Myosin IIA inhibition with the Y27632 ROCK inhibitor has no dramatic effect on podosome formation in VSMCs.
A7r5 cells treated for 60 minutes with 5µM PDBu were concomitantly treated with different concentrations (5, 10 and 15µM) of the ROCK inhibitor Y27632. Cells were fixed, stained with actin and cortactin (B) and the average number of podosomes formed in each condition determined (A). No significant difference could be observed between DMSO-treated control cells (0µM Y27632) and cells treated with 5 and 10µM of the inhibitor. n=90 pooled from 3 independent experiments.

3-2-3: PTPD1 is necessary for podosome formation in VSMCs.

The important region of KIF1C tail for podosome formation in VSMCs is known to interact with two proteins: the non-muscle Myosin IIA (Kopp et al., 2006) and the non-receptor Protein Tyrosine Phosphatase PTPD1 (Dorner et al., 1998). The involvement of the Myosin IIA for KIF1C-mediated podosome formation had been ruled out using Myosin II inhibitors, leaving PTPD1 as a

potential candidate to explain KIF1C involvement in podosome formation in VSMCs.

PTPD1 is known to participate in the regulation of focal adhesion and stress fiber formation and stability (Carlucci et al., 2008) but its possible involvement in the regulation of podosome formation has not been addressed yet. To test it, PTPD1 expression was depleted in A7r5 cells using a siRNA oligonucleotide that specifically targets PTPD1 transcript (Figure 3.17). As we were unable to detect PTPD1 with commercial antibodies, depletion efficiency was assessed by RT-PCR. Total cellular RNAs was extracted and random primed cDNA synthesized. Then, a 300bp fragment of PTPD1 cDNA was amplified using specific primers to address the relative amount of mRNA still present after 72 hours of siRNA treatment compared to control cells. A fragment of the GAPDH (Glyceraldehyde 3-phosphate dehydrogenase) cDNA of similar size (500bp) was amplified in parallel and used as a loading control. PTPD1 mRNA reduction was very efficient after 72 hours of siRNA treatment, proving the efficiency of the siRNA designed to depleted PTPD1 expression in rat VSMCs (Figure 3.15).

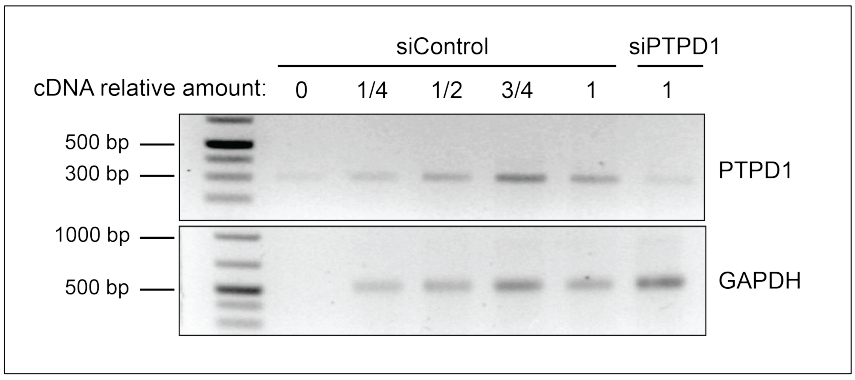

Figure 3.15: PTPD1 siRNA efficiently reduces PTPD1 expression in VSMCs.
Total RNA of A7r5 cells treated for 72 hours with a control or a PTPD1-targeting siRNA were extracted and reverse transcribe using random hexamer primers. PTPD1 and GAPDH cDNA were amplified with specific primers.

Next, PTPD1-depleted cells were tested for their ability to form podosomes. Control and PTPD1-depleted cells seeded on fibronectin-coated glass coverslips were treated with 5µM PDBu for 60 minutes prior fixation and cortactin immuno-staining. While control cells (siControl pFlag condition) formed 46±3 podosomes on average, barely any podosomes were detected in PTPD1-depleted cells (average podosome number formed per cell in the siPTPD1

pFlag condition: 6±1; $p<0.00001$ using a Mann-Whitney *U*-test; Figure 3.16), suggesting that the presence of PTPD1 is absolutely required for podosome formation in VSMCs.

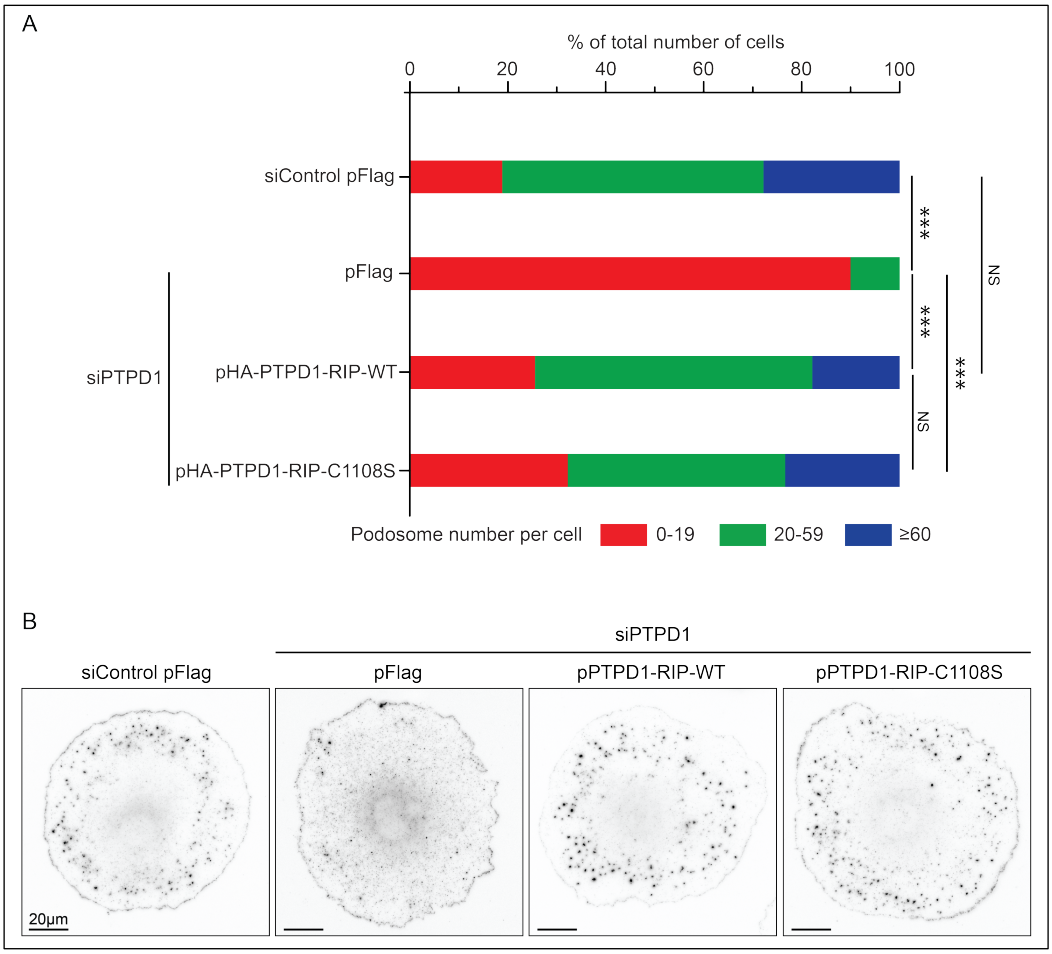

Figure 3.16: PTPD1 is required for podosome formation in VSMCs.
Control or PTPD1-depleted A7r5 cells transfected with a control plasmid (pFlag) or a RNAi-protected version of PTPD1 (pHA-PTPD1-RIP) were treated for 60 minutes with 5µM PDBu prior fixation and cortactin immunostaining (B). The number of podosomes formed in cells was quantified for each condition (A) and compared to that formed in control cells (siControl pFlag). n=90 pooled from 3 independent experiments; NS=non significant; * $p<0.05$; *** $p<0.0005$ using a Mann-Whitney *U*-test.

To prove the specificity of the PTPD1 depletion phenotype observed, silent point mutations were introduced in the PTPD1 cDNA sequence to generate a RNAi-protected (RIP) version of PTPD1 without changing its amino acid sequence (pHA-PTPD1-RIP; Figure 3.17). PTPD1 was then re-expressed in PTPD1-depleted cells and cellular ability to form podosomes was tested. PTPD1-depleted cells expressing the RNAi-protected version of the phosphatase (siPTPD1 pHA-PTPD1-RIP-WT) formed 38±3 podosomes on

average after 60 minutes of PDBu treatment (Figure 3.16), a number that is not significantly different from the 46±3 podosomes formed in control cells (p=0.07 using a Mann-Whitney U-test). This result confirms the specificity of the phenotype observed after cell treatment with the siRNA targeting PTPD1.

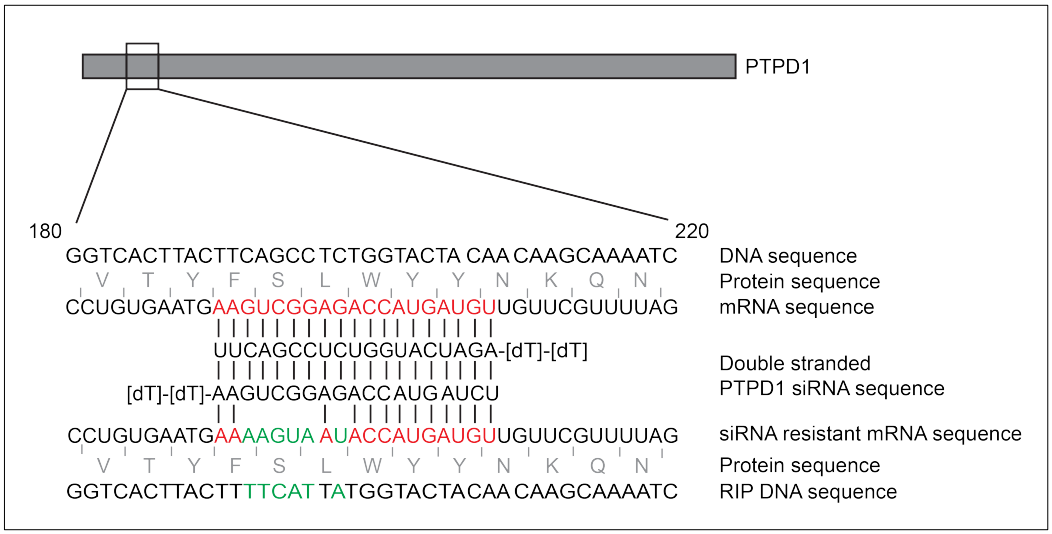

Figure 3.17: Principle of PTPD1 depletion and re-expression.
A double stranded siRNA oligonucleotide was designed to specifically target a sequence of PTPD1 transcript (mRNA sequence, red nucleotides) to induce its degradation. Silent point mutations (green nucleotides) were introduced in PTPD1 cDNA sequence (RIP DNA sequence) to generate a RNAi-resistant PTPD1 transcript (siRNA resistant mRNA sequence) that can't be recognized by the siRNA and, thus that can't be degraded.

In addition to its phosphatase activity, PTPD1 is known to act as a scaffold protein that brings two proteins together to potentiate their activities (Jui et al., 2000; Carlucci et al., 2008). Results previously obtained highlighted the absolute requirement of PTPD1 for podosome formation in VSMCs (Figure 3.16). We took advantage of our ability to restore PTPD1 expression after its depletion with a RNAi-protected version of the phosphatase to test the requirement of its catalytic activity for podosome formation. To do so, a RNAi-protected version of a catalytically inactive mutant of PTPD1 was re-expressed in PTPD1-depleted cells (siPTPD1 pHA-PTPD1-RIP-C1108S) and their ability to form podosomes was tested and compared to the ability of cells re-expressing the active phosphatase to form podosomes. Cells re-expressing the catalytically inactive form of PTPD1 formed 38±4 podosomes on average, a number that is significantly different from the 6±1 podosomes formed in PTPD1 depleted cells (siPTPD1 pFlag; p<0.00001 using a Mann-Whitney U-test) but not from the 38±3 podosomes formed by cells rescued with the active form of the

phosphatase (siPTPD1 pHA-PTPD1-RIP-C1008S; p=0.39 using a Mann-Whitney *U*-test) (Figure 3.16).
Taken together, these results suggest that PTPD1 is absolutely required for podosome formation in VSMCs and that its catalytic activity is dispensable to mediate podosome formation in these cells.

3-2-4: KIF1C and PTPD1 cooperate to form podosomes in VSMCs

Results obtained so far highlighted some important information to understand podosome formation in VSMCs. First, efficient podosome formation relies on the kinesin-3 KIF1C as its knockdown impairs it. Moreover, KIF1C podosome forming activity is most likely due to its cargo carrier function as impairing its motor activity impairs podosome formation in a similar way than reducing its expression level.
Then, rescue experiments with truncations of the KIF1C tail highlighted the importance of a ~150 amino acid long domain between its third and fourth coiled-coil domain, a region that interacts with two proteins involved in the regulation of cellular adhesion: the non-muscle Myosin IIA and the Tyrosine phosphatase PTPD1. However, the inhibition of the Myosin IIA contractile activity with Blebbistatin or the Y27632 ROCK inhibitor ruled out its involvement in podosome formation in A7r5 cells, as it has no apparent effect on this phenomenon.
Finally, PTPD1 deletion highlighted its absolute requirement for podosome formation in A7r5 cells. Given that PTPD1 depletion generated a more severe phenotype than impairing KIF1C, one hypothesis is that KIF1C transports PTPD1 to reach podosomes more efficiently.

To test this hypothesis, PTPD1 was over-expressed in KIF1C-depleted cells and the ability of these cells to form podosomes was determined after 60 minutes of PDBu treatment. KIF1C depletion efficiency was first addressed comparing the number of podosomes formed in control cells (siControl pFlag) to that formed in KIF1C-depleted cells (siKIF1C pFlag). KIF1C-depleted cells formed 50±4 podosomes on average, a number that is significantly different from the 86±5 podosomes formed in control cells (p<0.00001 using a Mann-Whitney *U*-test; Figure 3.18). PTPD1 was then over-expressed in control and KIF1C-depleted cells to test its ability to stimulate podosome formation. The

over-expression of the active phosphatase in KIF1C-depleted cells (siKIF1C pHA-PTPD1-WT) couldn't restore the ability of these cells to form podosomes as they formed only 57±5 podosomes on average, a number that is not significantly different from the KIF1C depletion condition (p=0.25 using a Mann-Whitney U-test; Figure 3.18). Interestingly, the over-expression of the catalytically active PTPD1 significantly reduced the ability of VSMCs to form podosomes. Indeed, cells over-expressing the active form of PTPD1 (siControl pHA-PTPD1-WT) formed 65±4 podosomes on average, which is significantly different to the 86±5 podosomes formed in the control condition (p=0.006 using a Mann-Whitney U-test; Figure 3.18).

Given this dominant negative effect of the over-expression of the active form of PTPD1 on podosome formation, we couldn't conclude with certainty on the inability of the phosphatase to restore podosome formation in KIF1C-depleted VSMCs. However, results previously obtained showed that the catalytically inactive form of PTPD1 was able to restore podosome formation in cells depleted for the endogenous phosphatase (Figure 3.16). The ability of the inactive phosphatase to restore podosome formation in KIF1C-depleted cells was thus tested. We first over-expressed PTPD1-C1108S in control cells to address its effect on podosome formation. Inactive PTPD1 overexpression in control cells has no effect on podosome formation as these cells (siControl pHA-PTPD1-C1108S) formed a normal number of 86±5 podosomes on average (Figure 3.18). This result suggests that the dominant negative effect on podosome formation observed when the active PTPD1 was over-expressed in control cells is due to its catalytic activity.

KIF1C-depleted cells over-expressing the inactive form of PTPD1 were then tested for their ability to form podosomes. These cells efficiently formed 70±4 podosomes on average after 60 minutes of PDBu treatment, a number that is not significantly different from the 86±5 podosomes formed in control cells (p=0.56 using a Mann-Whitney U-test; Figure 3.18). This result suggests that PTPD1 scaffolding activity is sufficient to restore podosome formation in VSMCs depleted for KIF1C expression.

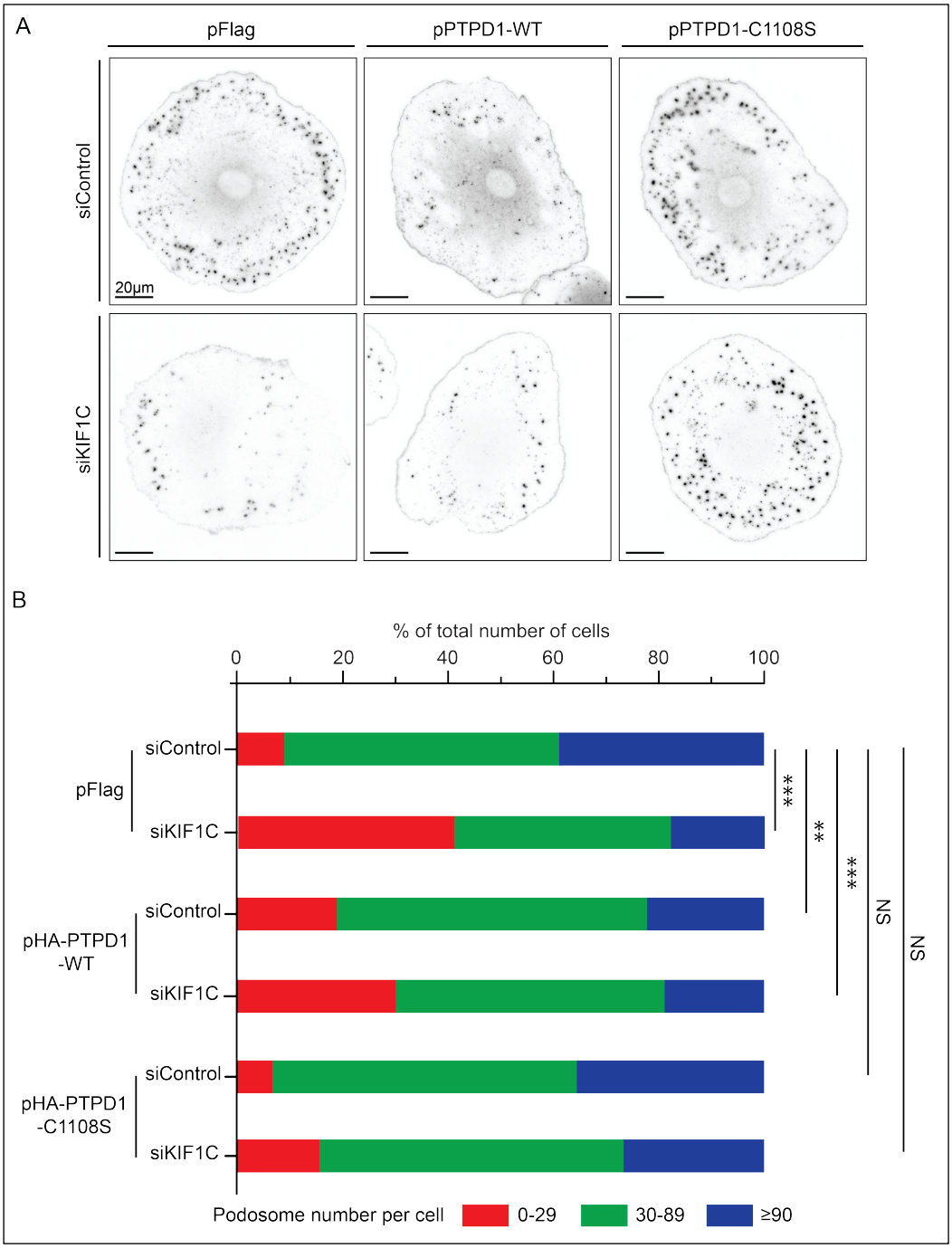

Figure 3.18: Catalytically inactive PTPD1 restores podosome formation in KIF1C-depleted VSMCs.

A7r5 cells treated for 72 hours with siControl or siKIF1C and expressing a control plasmid (pFlag), the active PTPD1 (pHA-PTPD1-WT) or the catalytically inactive PTPD1 (pHA-PTPD1-C1108S) were treated 60 minutes with 5µM PDBu prior to fixation and cortactin staining (A). The number of podosomes formed in each condition was determined (B) and compared to the control condition (siControl pFlag). NS: non significant; ** p<0.005; *** p<0.0005; n=90 pooled from 3 independent experiments.

3-3: PTPD1 activates KIF1C transport activity

Results obtained using the podosome-forming assay highlighted the absolute requirement of the Tyrosine Phosphatase PTPD1 for podosome formation in VSMCs. Interestingly, its catalytic activity is dispensable for podosome formation as re-expressing the catalytically inactive form of PTPD1 (PTPD1-C1108S) in cells depleted for the endogenous protein restores podosome formation in A7r5 cells. In addition to its phosphatase activity, PTPD1 displays a scaffolding activity that brings two proteins together to potentiate their activities (Jui et al., 2000; Carlucci et al., 2008) and this additional function is suspected to mediate podosome formation in VSMCs. More importantly, experiments performed using the podosome-forming assay pointed at cooperation between PTPD1 and the kinesin-3 KIF1C to mediate podosome formation in VSMCs.

As PTPD1 restores podosome formation in KIF1C-depleted A7r5 cells and is known to directly interact with KIF1C (Dorner et al., 1998), we hypothesized that PTPD1 could activate KIF1C transport activity. Indeed, the knockdown of a protein doesn't induce its complete depletion (Figure 3.5B) and we thought that the over-expression of PTPD1 could activate the remaining pool of KIF1C motors, facilitate its cargo transport activity and hence, help KIF1C-mediated podosome formation in VSMCs.

Previous work conducted in the lab identified α5-integrin as one of KIF1C cargoes and we have at our disposal a α5-integrin transport assay to test the ability of KIF1C motors to transport a GFP-fusion of α5-integrin in RPE-1 cells (Theisen et al., 2012). Indeed, migratory RPE-1 cells form a tail at their rear, whose stability relies on the formation of stable focal adhesions and that is required for the directional persistence of the migration (Theisen et al., 2012). One of the major components of focal adhesions is the α5β1 integrin heterodimer and KIF1C has been shown to be of crucial importance for α5-integrin transport to the tail of migratory RPE-1 cells (Theisen et al., 2012). Hence, the trafficking of GFP-fusion α5-integrins in the tail of RPE-1 cells depends on KIF1C and the α5-integrin transport assay can be used to address the activation of KIF1C transport activity.

The trafficking of GFP-α5-integrin receptors in the tail of RPE-1 cells can easily be detected using a FRAP (Fluorescence Recovery After Photobleaching) approach. To do so, a selected area of the tail is photobleached using a 488nm laser and the trafficking of GFP vesicles within the photobleached area is tracked over a 2 minutes period of time (Figure 3.19).

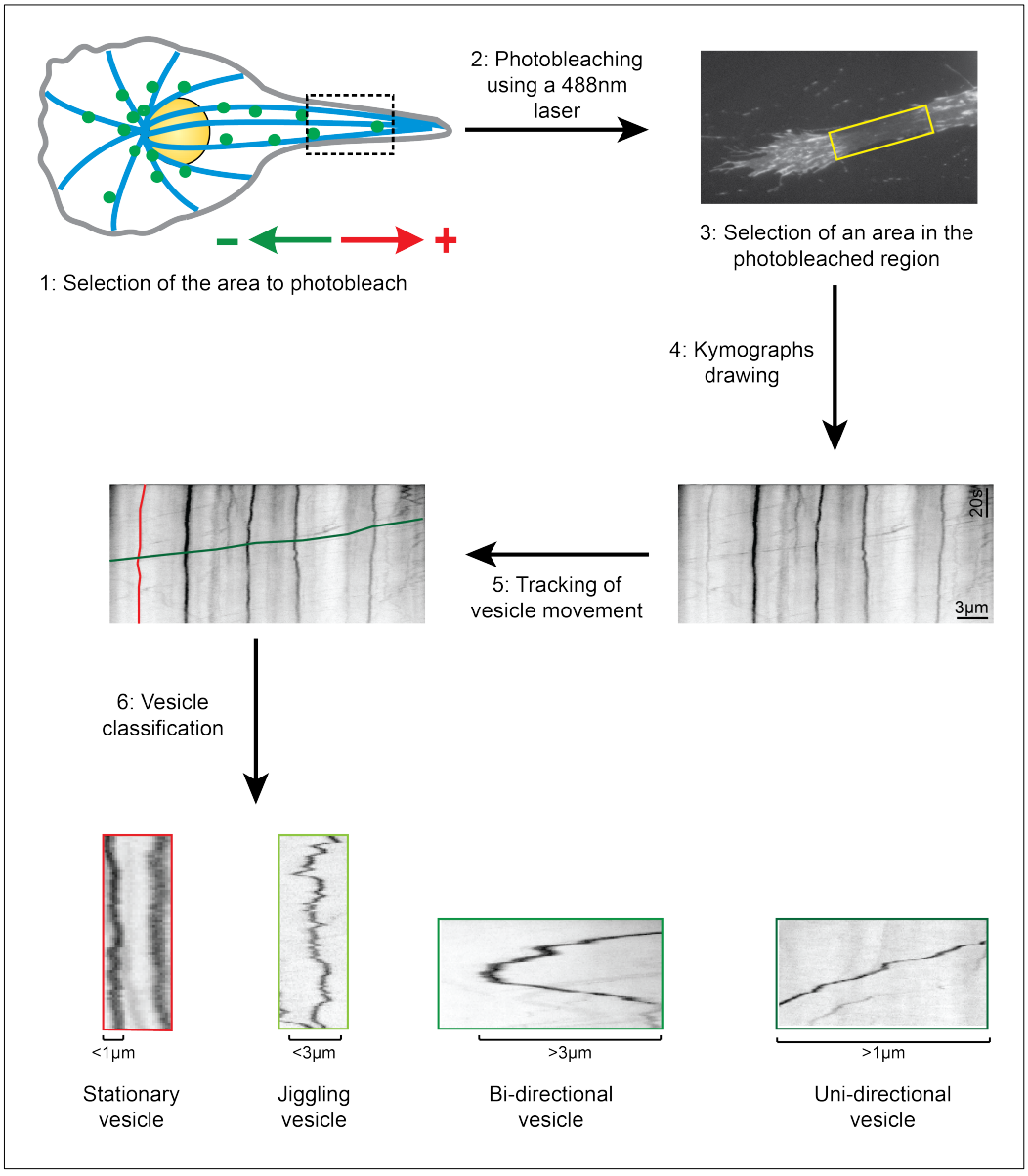

Figure 3.19: α5-integrin transport assay principle.
An area of the cell tail is selected (1) and photobleached using a 488nm laser (2). The trafficking of GFP-α5-integrin in the photobleached area is then recorded for 2 minutes (3). Kymographs are drawn to cover the photobleached area (4) and the movement of vesicles is tracked over time (5). Vesicle movement is then classified (6). Stationary vesicles don't show a displacement bigger than1µm. Jiggling vesicles show frequent directional changes and their movement doesn't exceed 3µm between starting and ending points. Bi-directional vesicles show long runs with at least one directional change. Uni-directional vesicles move in one direction and their total displacement is bigger than 1µm.

Using this approach, we were able to identify two main populations of vesicles: stationary vesicles, whose displacement doesn't exceed 1µm in any direction and motile vesicles, whose movement is larger than 1µm. Three categories of motile vesicles could be distinguished: jiggling vesicles, vesicles moving in one direction and vesicles moving in two directions. Jiggling vesicles display repeated forward and backward movements within a 3µm distance range whereas bi-directional vesicles display longer runs (>3µm) intersperse with at least one direction change. Uni-directional vesicles show persistent movement in one direction and their total displacement is larger than 1µm.

23.4±2.5% of vesicles were stationary in control cells (siControl pFlag; n=623 pooled from 105 cells of 7 independent experiments), a fraction that increases to 44.6±4.1% in KIF1C-depleted cells (siKIF1C pFlag; n=346 pooled from 45 cells of 5 independent experiments) (Figure 3.20A,D). It is noteworthy that we deliberately performed a partial knockdown of KIF1C expression in GFP-α5-integrin RPE-1 cells as a too efficient KIF1C depletion impaired the ability of cells to form tails. Despite this partial KIF1C depletion, results we obtained were in agreement with results previously described (Theisen et al., 2012), proving the reliability of the assay. The ability of PTPD1 to activate KIF1C transport activity was then addressed. To do so, control and KIF1C-depleted cells were transfected with PTPD1-WT and PTPD1-C1108S to over-express both the active and inactive phosphatase respectively and the ability of GFP-α5-integrin vesicles to be transported within the cell tail in each condition was tested.

The effect of PTPD1 over-expression on GFP-α5-integrin vesicle transport was first addressed in control cells. Control cells expressing the active phosphatase (siControl pPTPD1-WT) displayed 26.1±6.1% stationary vesicles (n=328 pooled from 68 cells of 4 independent experiments; Figure 3.20B), which is not significantly different from the 23.4±2.5% stationary vesicles measured in control cells (siControl pFlag). The over-expression of the inactive phosphatase (siControl pPTPD1-C1108S) resulted in 25.6±3.8% GFP-α5-integrin vesicles (n=197 pooled from 63 cells of 3 independent experiments; Figure 3.20C) were stationary, which is also very similar to results obtained in control cells. No significant differences in the occurrence of the three different types of motile vesicles could be observed between these three conditions (siControl pFlag; siControl pPTPD1-WT; siControl pPTPD1-C1108S; Figure

3.20A-C). These results suggest that the over-expression of the active or inactive form of PTPD1 does not impair KIF1C transport activity of GFP-α5-integrin vesicles within the tail of RPE-1 cells, but also does not significantly increase it.

The ability of PTPD1 to restore KIF1C-mediated GFP-α5-integrin transport in RPE-1 tail was then tested. RPE-1 cells stably expressing GFP- α5-integrin and depleted for KIF1C expression were transfected with the active (siKIF1C pHA-PTPD1-WT) or inactive phosphatase (siKIF1C pHA-PTPD1-C1108S) and submitted to the α5-integrin transport assay.

Whereas KIF1C-depleted cells displayed 44.6±4.1% stationary vesicles, this number was decreased to that observed in control cells in KIF1C-depleted cells over-expressing either form of PTPD1 (Figure 3.20E,F). Indeed, KIF1C-depleted cells over-expressing the active phosphatase (siKIF1C pHA-PTPD1-WT) displayed 20.5±0.5% stationary vesicles (n=87 pooled from 18 cells of 3 independent experiments) and KIF1C-depleted cells over-expressing the inactive form of PTPD1 (siKIF1C pPTPD1-C1108S) showed 26±2.2% stationary vesicles (n=449 pooled from 126 cells of 3 independent experiments).

Taken together, results obtained using the α5-integrin transport assay suggest that PTPD1 activates KIF1C transport activity. Indeed, the significant increase of stationary vesicles observed in KIF1C-depleted cells is brought back to its basal level (23.4±2.5% in siControl pFlag cells) when PTPD1 is over-expressed in KIF1C-depleted cells. More importantly, it appears that PTPD1 catalytic activity is dispensable to stimulate KIF1C motor activity. Indeed, the inactive phosphatase is able to activate remaining KIF1C motors after their depletion to the same extent the active phosphatase does, possibly due to its scaffolding activity.

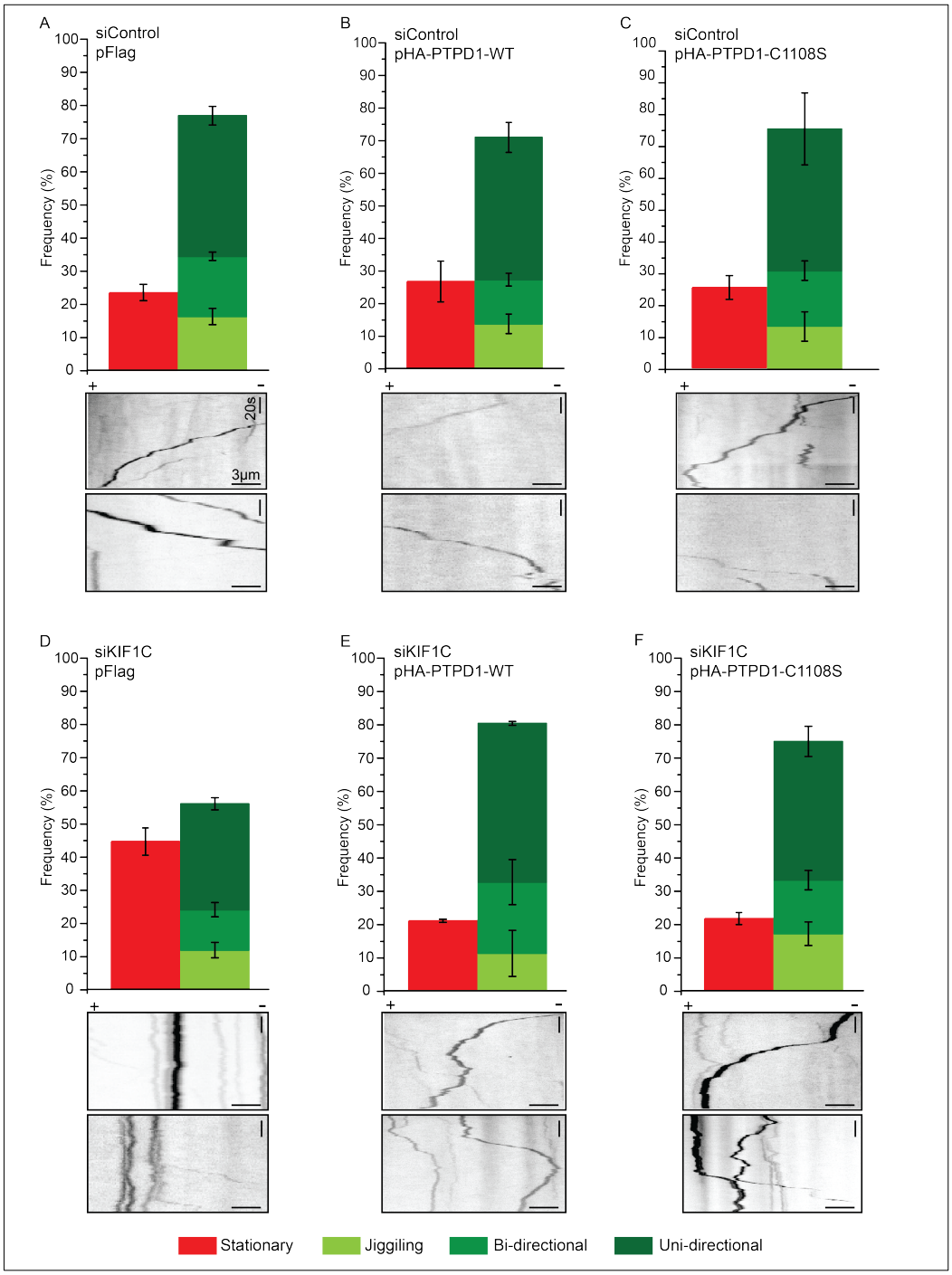

Figure 3.20: PTPD1 activates KIF1C transport of α5-integrins in the tail of RPE-1 cells. RPE-1 cells stably expressing GFP-α5-integrin treated with a control siRNA (siControl) or a siRNA targeting KIF1C (siKIF1C) were transfected with a control plasmid (pFlag) or a plasmid coding for the active (pHA-PTPD1-WT) or inactive PTPD1 (pHA-PTPD1-C1108S). A selected area of the cell tail was photobleached using a 488nm laser and the trafficking of α5-integrins within the photobleached area was recorded for 2 minutes. Vesicle movement was tracked and classified for each condition. Two representative kymograph examples are shown for each condition. A: n=623 pooled from 105 cells of 7 independent experiments. B: n=328 pooled from 68 cells of 4 independent experiments. C: n=197 pooled from 63 cells of 3 independent experiments. D: n=346 pooled from 45 cells of 5 independent experiments. E: n=87 pooled from 18 cells of 3 independent experiments. F: n=449 pooled from 126 cells of 7 independent experiments.

4: Discussion

4-1: KIF1C and the transport of podosome components in VSMCs

Prior to this work, the kinesin-3 KIF1C had been shown to be involved in the regulation of podosome formation and dynamics in macrophages (Kopp et al., 2006). Here we showed that KIF1C contributes to podosome formation in VSMCs (Figures 3.6, 3.8, 3.9).

VSMC are characterized by a very well developed actin cytoskeleton (Fultz et al., 2000) and their treatment with PDBu induces a general remodeling of this actin cytoskeleton that is characterized by the gradual disassembly of pre-existing focal adhesions and stress fibers and the rapid formation of podosomes (Hai et al., 2002). Podosome formation in VSMCs has been divided in two phases: a first phase starting within 2 minutes following the addition of PDBu to cells and characterized by the polymerization of unstable podosomes at the interface between focal adhesions and stress fibers and a later phase occurring after 30 to 70 minutes of PDBu treatment characterized by the weakening or the complete disappearance of focal adhesions and stress fibers and the formation of more stable podosomes (Kaverina et al., 2003).
In this study, we addressed the possible involvement of the kinesin-3 KIF1C for podosome formation in A7r5 cells and results obtained highlighted its requirement for the proper formation of these structures in VSMCs. At the beginning of this study, experiments were conducted after 30 minutes of PDBu treatment and although results were significant, the phenotype observed in KIF1C-impaired cells was only mild (Figure 3.6; Figure 3.8). Time course experiments (Figure 3.9) revealed that a stronger KIF1C depletion phenotype could be observed after 40-60 minutes of podosome induction, suggesting that the requirement of KIF1C activity could be more crucial during the late phase of podosome formation in VSMCs.

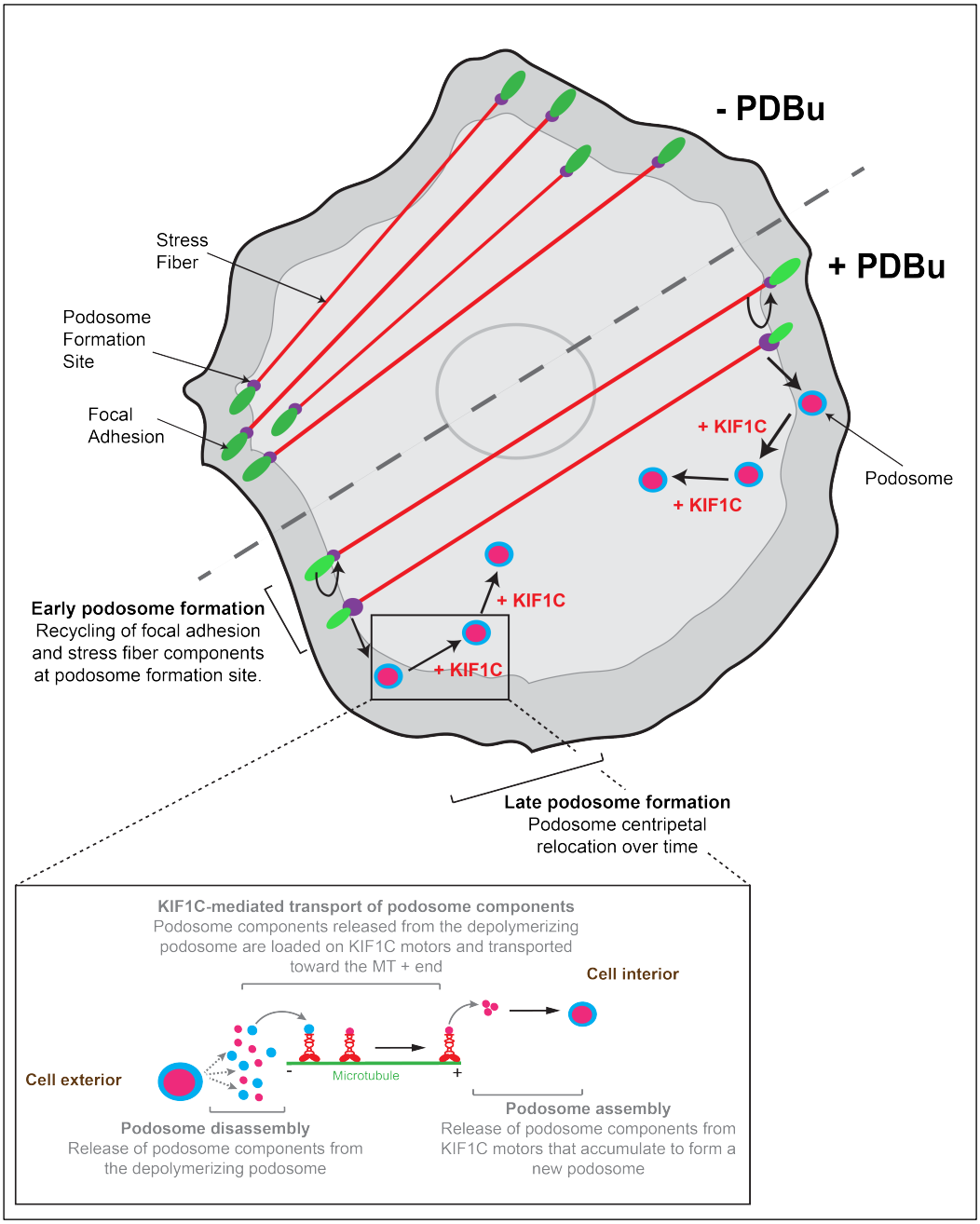

Figure 4.1: Model for KIF1C-mediated centripetal relocation of podosomes in VSMCs. Unstimulated VSMCs (-PDBu) display a well-developed actin stress fiber network with actin stress fiber bundles anchored on focal adhesions. Upon PDBu treatment, focal adhesions and stress fibers depolymerize and their components are recycled at the podosome formation site located at the interface between the two depolymerizing structures. Later, podosomes are relocated to the cell centre, most likely thanks to KIF1C motor activity.
Adapted from Kaverina et al., 2003.

Upon PDBu addition, VSMCs rapidly form podosomes at the cell periphery and at the interface between focal adhesions and stress fibers to be more precise (Kaverina et al., 2003; Burgstaller & Gimona, 2004). In unstimulated cells, these micro-domains are enriched in actin nucleation

promoting factors such as cortactin and Arp2/3 complex (Burgstaller & Gimona, 2004; Kaverina et al., 2003) and they were shown to be the initial site of podosome formation in VSMCs (Kaverina et al., 2003; Burgstaller & Gimona, 2004). Upon PDBu treatment, these micro-domains grow in size due to the Arp2/3-mediated actin *de novo* polymerization to form unstable podosomes that are rapidly replaced by new ones formed in their immediate vicinity but slightly proximally to the stress fiber (Kaverina et al., 2003). During the late phase of podosome formation, these unstable podosomes are replaced by more stable ones enriched in plaque proteins as vinculin and zyxin most likely recycled from depolymerizing focal adhesions located in close proximity (Kaverina et al., 2003). As podosomes are mainly made of actin and share most of their components with focal adhesions, one might assume that proteins released by focal adhesions and stress fibers during their disassembly are incorporated in nascent podosomes polymerizing at the interface between the two disassembling structures (Kaverina et al., 2003; Dorfleutner et al., 2008). Thus, the formation of the first batches of podosomes might not require the transport of podosomes components to the future site of podosome formation as the components are released there upon induction of podosome formation, explaining the mild phenotype observed after 30 minutes of podosome induction in KIF1C-impaired A7r5 cells.

Podosome lifespan ranges from 3 to 10 minutes in VSMCs (Kaverina et al., 2003), and the successive cycles of podosome assembly and disassembly that occur over time were shown to result in the relocation of podosomes formed at the cell periphery towards the cell centre (Kaverina et al., 2003; Zhu et al., 2016). Podosome centripetal relocation requires the translocation of podosome components from a peripheral depolymerizing podosome to a more centrally located newly forming one and the hypothesis of the involvement of KIF1C in this phenomenon is reinforced by several clues. First, podosome relocation relies on MTs as VSMC treatment with the MT-depolymerizing agent Nocodazole impairs this phenomenon and leads to the reformation of podosomes at the exact same place than depolymerizing podosomes were located (Zhu et al., 2016). This observation strongly suggests that podosome relocation could be mediated by MT-based transport and given its requirement for podosome formation (Figure 3.6 and 3.8; Efimova et al., 2014) and its affiliation to the MT-based molecular motor, KIF1C is a good candidate to mediate the centripetal relocation of podosome components.

Cortactin stainings provided in the 3-1 section of this thesis reinforce this hypothesis. Indeed, cells that efficiently form podosomes often display a podosome distribution extending toward the cell centre (Figure 3.8B pFlag cortactin staining example; Figure 3.9B siControl cortactin staining examples) on the contrary to cells impaired for KIF1C motor activity, which often display peripheral podosomes and a cell centre almost devoid of any podosomes (Figure 3.8B pKIF1C-Headless and pKIF1C-G102E cortactin staining examples; Figure 3.9B siKIF1C cortactin staining examples).

The assumption of a KIF1C involvement in podosome centripetal relocation was indirectly reinforced by recent observations incriminating the requirement of the MT plus end-associated proteins CLASPs (Akhmanova et al., 2001) for podosome centripetal relocation in A7r5 cells (Zhu et al., 2016). Upon PDBu treatment, a fraction of the pool of KIF1C motors that are initially located in the pericentrosomal region of unstimulated cells translocates to the cell periphery in a CLASP-dependent manner (Efimova et al., 2014). Indeed, PDBu treatment induces the recruitment of KIF1C motors at MTs by CLASPs that are then able to move along CLASP-associated MTs (Efimova et al., 2014). CLASP depletion has been shown to impair podosome formation (Efimova et al., 2014) as well as their centripetal relocation in A7r5 cells (Zhu et al., 2016), reinforcing the hypothesis of an involvement of KIF1C in podosome translocation toward the cell centre.

Finally, podosome centripetal relocation has recently been shown to correlate with KIF1C movement within cells (Zhu et al., 2016). As previously mentioned, upon PDBu treatment, KIF1C motors translocate from the pericentrosomal region to the cell periphery where they locally accumulate (Efimova et al., 2014; Zhu et al., 2016) and the appearance of these KIF1C-rich punctae often precedes the local appearance of podosomes (Zhu et al., 2016). Once podosomes are formed at KIF1C accumulation sites, KIF1C rearranges to form a ring around the cortactin core (Figure 3.7; Efimova et al., 2014; Zhu et al., 2016). Upon removal from the ring, KIF1C often moves towards the cell centre to form another accumulation point whose location correlates with the appearance of a new podosome (Zhu et al., 2016). Taken together, all these results strongly reinforce the assumption of an active involvement of KIF1C in podosome translocation from the cell periphery to the cell centre.

KIF1C is a N-kinesin and one can object that as a MT plus end-directed motor, it shouldn't be able to actively move toward the cell centre and hence, shouldn't be able to mediate podosome centripetal relocation. However, KIF1C movement toward the centre of VSMCs can be explained by the modification of MT organization and orientation at the cell periphery induced by PDBu treatment. Indeed, VSMCs treatment with PDBu induces the bundling of MTs in the cell body and their bending once they reached the cell periphery (Figure 4.2; Zhu et al., 2016). Upon bending, MT plus-ends point and grow toward the cell centre, resulting in KIF1C motors to move towards the cell centre. KIF1C movement towards the plus-end of these reversed MTs could then mediate the centripetal relocation of VSMC podosomes.

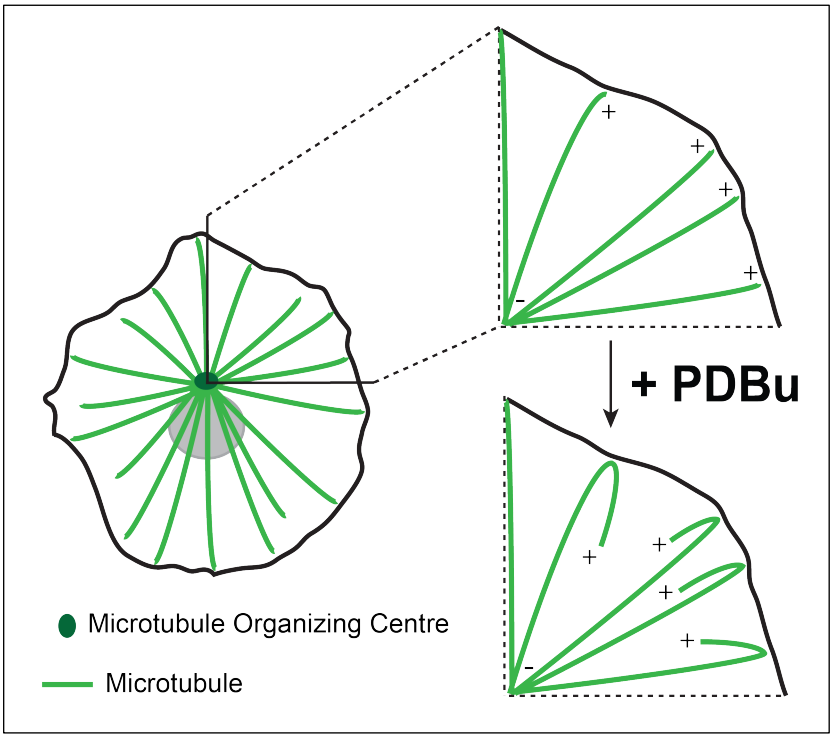

Figure 4.2: Schematic representation of the bending of microtubules upon PDBu treatment in VSMCs.
In resting VSMCs, MTs grow from the Microtubule Organizing Centre with their plus end oriented toward the cell periphery (left and upper right panels). Upon PDBu treatment, the growing ends of MTs bend when they reach the cell cortex and MTs keep growing with their plus end oriented toward the cell centre.
Adapted from Zhu et al., 2016

While there is good evidence for the involvement of KIF1C in podosome centripetal relocation, nothing is known about the nature of cargoes it transports to mediate podosome formation and relocation. KIF1C is known to transport α5-integrin receptors (Theisen et al., 2012) but so far, the podosomal localization of

this precise integrin subunit hasn't been described. However, integrin β1 subunit, known to dimerize with α5 to form the major fibronectin receptor (Pytela et al., 1985) has been shown to localize at the podosome core (Marchisio et al., 1988). Other integrin receptors have been shown to localize to the adhesive ring of podosomes, such as αvβ3 dimers (Marchisio et al., 1988; Pfaff & Jurdic, 2001; Chabadel et al., 2007; Myers et al., 2014) or αMβ2 receptors (van den Dries et al., 2013b). KIF1C itself localizes to the adhesive ring (Figure 3.7; Efimova et al., 2014; Zhu et al., 2016) and it might transport integrins or other cargoes from one podosome to the other.

Indeed, KIF1C accumulates at podosome forming sites before the appearance of the core (Zhu et al., 2016) and as described in the introduction (Chapter 1-8), the ring is assembled after the polymerization of the core. Two hypotheses can be formulated based on current knowledge: KIF1C-mediated transport and local accumulation of α5β1 integrins might form micro-domains to initiate the podosome polymerization or KIF1C might transport other components of the core that control the initial steps of the podosome core polymerization, maybe actin nucleation promoting factors (Kaverina et al., 2003; Luxenburg et al., 2012). It is noteworthy that these two hypotheses are not mutually exclusive.

4-2: KIF1C, Myosin IIA and podosome formation in VSMCs

Using different truncations of KIF1C (Chapter 3-2-1), we identified a ~150 amino acid long region between the third and fourth coiled-coil domain of KIF1C tail that is of major importance for podosome formation. Two proteins that were both described for their involvement in the regulation of cellular adhesion are known to interact with this region: the non-muscle Myosin IIA (Kopp et al., 2006) and the Tyrosine phosphatase PTPD1 (Dorner et al., 1998).

The non-muscle Myosin IIA is known to localize at podosomes (Kopp et al., 2006; Gawden-Bone et al., 2010) where it surrounds the core and sits on top of the adhesive ring, associated to actin filaments radiating from the core toward the ring (Gawden-Bone et al., 2010; van den Dries et al., 2013). Prior to this work, Kopp *et al* reported that Myosin IIA contractile activity was required for podosome formation in macrophages (Kopp et al., 2006). We therefore tested

the requirement of Myosin IIA contractile activity for podosome formation in VSMCs using two different methods and showed that none of them impaired podosome formation in VSMCs (Figures 3.13 and 3.14). Our results are in agreements with a study published during the course of this work showing that the treatment of VSMCs with 10μM Blebbistatin doesn't impair their ability to form podosomes (Tanaka et al., 2015) and the same kind of results was earlier reported in immature dendritic cells (Gawden-Bone et al., 2010; van den Dries et al., 2013).

The difference of results obtained in macrophages and VSMCs or dendritic cells could be explained by the type of adhesions these different cell-types are able to form. Indeed, VSMCs and immature dendritic cells are able to form both podosomes and mature focal adhesions (Kaverina et al., 2003; van den Dries et al., 2013), while macrophages only form podosomes and immature focal complexes (Pixley, 2012). Hence, Myosin IIA contractile activity could be more important for podosome formation in macrophages than in VSMCs or immature dendritic cells because podosomes are the only type of mature adhesion structures macrophages are able to form.

Another hypothesis one can formulate to explain the difference of phenotype observed in macrophages and VSMCs upon Myosin IIA inhibition relies on the types of Myosin these cell-types express. Indeed, in contrast to macrophages and in addition to the non-muscle Myosin IIA, VSMCs express smooth muscle myosin (Gimona et al., 2003). As the non-muscle Myosin IIA, the smooth muscle myosin localizes at podosomes (Gimona et al., 2003) and is able to bundle actin filaments (Han et al., 2009). However, in contrast to the non-muscle Myosin IIA, the smooth muscle myosin is only poorly inhibited by Blebbistatin (Kovács et al., 2004), suggesting that it could, at least partially, compensate for the loss of Myosin IIA contractile activity upon Blebbistatin treatment and ensure podosome formation in VSMCs.

VSMC treatment with Blebbistatin disrupts the actin stress fiber network (Figure 3.13). Consequently, one can object that it also seems to impair the smooth muscle myosin contractile activity. However, it appears that the smooth muscle myosin could be locally activated at podosome sites and not along stress fibers, explaining the efficiency of podosome formation while stress fibers are disrupted upon Blebbistatin treatment. Indeed, the smooth muscle myosin light chain kinase has been shown to be activated by the Ca^{++}/calmodulin complex (Van

Lierop et al., 2002) and even though calmodulin localization at podosomes has not been addressed yet, its interaction with the actin-associated factor caldesmon has been shown to be required for caldesmon translocation from stress fibers to podosomes in VSMC treated with PDBu, suggesting that calmodulin could also localize to podosomes upon PDBu treatment (Eves et al., 2006).

VSMC treatment with PDBu has been shown to induce a sensitization of these cells to Ca^{++} (Woodsome et al., 2001) and an increase of the intracellular Ca^{++} concentration had been shown to correlate with an increase of calmodulin activity (Vogel, 1994; Chin & Means, 2000). Taken together, these observations suggest that the smooth muscle myosin could be locally activated at podosome site, explaining the non-requirement of the non-muscle Myosin IIA contractile activity for podosome formation in VSMCs.

In addition to the decrease of the fraction of macrophages able to form podosomes upon Blebbistatin treatment, Kopp *et al* also reported a modification of the cellular distribution of podosomes in cells impaired for Myosin IIA contractile activity. Indeed, Blebbistatin-treated macrophages that still form podosomes display a loss of peripheral podosomes compared to control cells (Kopp et al., 2006). In the same study, they also showed that KIF1C accumulates at the plus end of a subset of MTs and that these KIF1C-decorated MT plus-ends specifically target peripheral podosomes to induce their fission or dissolution and they identified the non-muscle Myosin IIA as a KIF1C interactor (Kopp et al., 2006). Based on these results, they hypothesized that KIF1C interaction with Myosin IIA may couple actin and tubulin cytoskeletons and proposed a molecular model suggesting that the Myosin IIA present at podosomes may guide KIF1C to podosome sites. However, direct evidence for that model has not been provided in that study (Kopp et al., 2006).

Based on results obtained during the course of this work and the general mechanism of podosome formation in VSMCs that has previously been described, it is unlikely that this molecular model applies to the VSMC model. First, results presented in this thesis don't confirm obvious modification of podosome distribution upon Myosin IIA inhibition in VSMCs (Figures 3.13 and 3.14).

Second, Blebbistatin interacts with Myosin IIA and blocks its binding to actin filaments (Kovács et al., 2004). The molecular model established by Kopp and

co-workers suggests that the Blebbistatin-induced removal of Myosin IIA from podosome actin filaments leads to the loss of peripheral podosomes due to the inability of KIF1C to be guided to these peripheral podosomes by the Myosin IIA (Kopp et al., 2006). We showed in this study that KIF1C is required for podosome formation in VSMCs and that Blebbistatin treatment doesn't impair podosome formation in these cells. If the molecular model presented by Kopp and co-workers would apply to VSMCs, one would expect to detect a similar phenotype to that observed in A7r5 cells impaired for KIF1C activity in Blebbistatin-treated cells, e.g. a decrease of the number of podosome formed by Blebbistatin-treated cells or at least a modification of the podosome distribution, with podosomes restricted to the cell periphery. However, none of these phenotypical modifications have been observed in VSMCs treated with Blebbistatin.

Finally, podosome formation in VSMCs has been correlated with the local inhibition of contractility at podosome formation sites (Burgstaller & Gimona, 2004). Indeed, VSMCs display a very well developed actin stress fiber network whose contractility is locally modulated by PDBu treatment to allow its remodeling and the concomitant formation of peripheral podosomes (Fultz et al., 2000; Hai et al., 2002; Burgstaller & Gimona, 2004). PDBu treatment induces the contraction of the central region of the cell (Fultz et al., 2000) while at the cell periphery, the Myosin IIA contractile activity is inhibited at podosome formation sites by the local accumulation of p190RhoGAP (Burgstaller & Gimona, 2004).

As the local inhibition of the Myosin IIA at podosome sites is a prerequisite for the formation of these structures and podosomes are primarily formed at the periphery of VSMCs, it is not surprising that we could not observed in VSMCs the loss of peripheral podosomes that has been reported in macrophages.

Finally, we addressed the effect of Myosin IIA inhibition on podosome formation in A7r5 cells using fixed samples. By doing so, we made sure that the timing of podosome induction was consistent between the different conditions tested but it also meant missing information relative to podosome dynamics, such as the timing of arrival of podosome components, podosome lifespan or podosome oscillations. The average number of podosomes formed in A7r5 cells whose Myosin IIA contractile activity has been inhibited remains similar to what is observed in control cells (Figures 3.13 and 3.14). In fact, we observed a slight increase in podosome number formed by cells treated with the Y2732 ROCK

inhibitor (Figure 3.14), suggesting that podosome dissolution could actually be impaired upon Myosin IIA inhibition. More investigations need to be conducted on the involvement of Myosin IIA in podosome formation and turnover because apart from its role in podosome oscillations (van den Dries et al., 2013) and its localization at radiating actin filaments linking the podosome core to the adhesion ring (Gawden-Bone et al., 2010), little is known about its role in these processes.

4-3: PTPD1 and podosome formation in VSMCs

Instead of Myosin IIA, we show here that PTPD1 is required to activate KIF1C transport and for its role in podosome formation in VSMCs.

It is noteworthy that PTPD1 depletion induces a stronger phenotype than that observed in KIF1C knockdown cells and this may be due to two main reasons: the direct involvement of PTPD1 in the regulation of cellular adhesion and its involvement in the regulation of other cellular processes.

PTPD1 has been shown to be a major regulator of Src and FAK kinases in fibroblasts (Cardone et al., 2004; Carlucci et al., 2008). Indeed, in response to fibroblast stimulation with EGF (Epithelial Growth Factor), PTPD1 has been shown to interact with and dephosphorylate Src Y527, inducing a conformational change in Src structure that releases its catalytic domain and activates its kinase activity (Cardone et al., 2004). Concomitantly, EGF stimulation induces FAK to auto-phosphorylate its Tyrosine 397 residue, creating a docking site for the active Src to bind to (Carlucci et al., 2008). PTPD1 has been shown to facilitate the interaction of active Src with Y397-phosphorylated FAK to enhance FAK activity (Carlucci et al., 2008).

Src and FAK are mainly known for their ability to regulate cellular adhesion (Webb et al., 2004). However, these two kinases were also described for their involvement in the local enrichment of the plasma membrane in specific phosphoinositides (PtdIns(3,4)P2 and PtdIns(3,4,5)P3 to a lesser extend), creating micro-domains in close proximity to focal adhesions and whose localizations were shown to correlate with the site of emergence of podosomes (Oikawa et al., 2008; Yu et al., 2013).

As it interacts with both kinases to enhance their activity (Carlucci et al., 2008; Cardone et al., 2004), PTPD1 could facilitate the formation of these PtdIns-

enriched micro-domains and the subsequent podosome formation at these sites. PTPD1 depletion could impair the formation of these micro-domains and the subsequent assembly of podosomes at these sites.

Podosome formation in VSMCs has been described to initially occur in close proximity to focal adhesions (Kaverina et al., 2003; Burgstaller & Gimona, 2004), a localization that is in agreement with that described in v-Src-transformed fibroblasts (Oikawa et al., 2008). However, no bias in the composition of the plasma membrane at podosome site has yet been reported in VSMCs. Given that PTPD1 depletion in VSMCs induces a dramatic decrease of the ability of these cells to form podosomes, it would be interesting to address this in these cells. Indeed, in addition to test PTPD1 involvement in the appearance of PtdIns-enriched micro-domains at the plasma membrane, it could help to better understand the mechanism controlling the determination of the precise location podosome grow from during the late phase of podosome formation.

In addition to its interaction with Src (Møller et al., 1994; Carlucci et al., 2008), FAK (Carlucci et al., 2008) and KIF1C (Dorner et al., 1998), PTPD1 has been shown to interact with proteins of the Tec kinase family (Jui et al., 2000), two mitochondrial A-kinase anchor protein (AKAP), AKAP121/AKAP84 (Cardone et al., 2004) and the kinesin-3 KIF16B (Carlucci et al., 2010) (Figure 4.3).

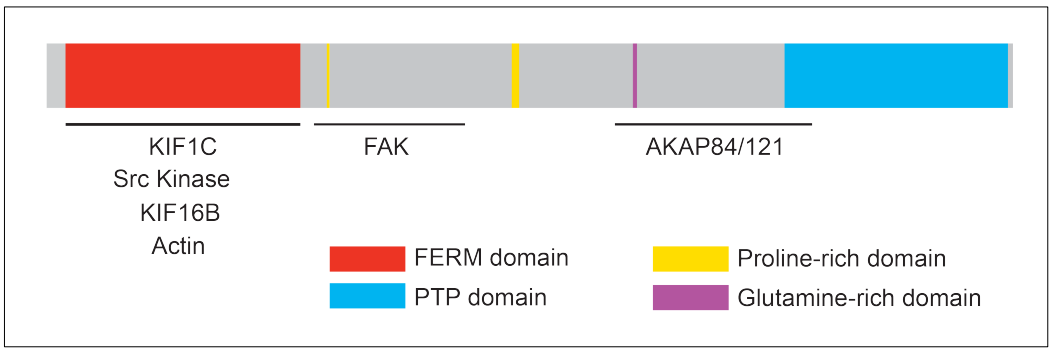

Figure 4.3: PTPD1 domain structure and known interactors.

Together with Src, PTPD1 can form a molecular complex with AKAP121/AKAP84 that can be targeted at the mitochondria membrane to participate in the regulation of the cyclic AMP production (Cardone et al., 2004;

Livigni et al., 2006) and PTPD1 interaction with the kinesin-3 KIF16B targets the phosphatase at the membrane of endosomes to regulate the recycling of the Epithelial Growth Factor Receptor (Carlucci et al., 2010).
The dramatic phenotype observed in PTPD1-depleted A7r5 cells upon PDBu treatment could be explain by the numerous molecular interactions PTPD1 is able to establish at different cellular localization. All these interactions could dilute the remaining pool of PTPD1 throughout the cell, making it less likely to be available for podosome formation.

Because it enhances Src and FAK activities, PTPD1 catalytic activity has been described to modulate the formation and the stability of focal adhesions and stress fibers in fibroblasts (Carlucci et al., 2008).
As podosomes are formed at the interface between focal adhesions and stress fibers in VSMCs (Kaverina et al., 2003; Burgstaller & Gimona, 2004), one could suspect that PTPD1 knockdown abolishes podosome formation in A7r5 cells because it impairs Src and FAK activities, the subsequent formation of focal adhesions and stress fibers and consequently the formation of the micro-domains formed at their interface and that are the sites of emergence of podosomes in VSMCs. However, the catalytically inactive PTPD1 mutant (PTPD1-C1108S) was able to restore podosome formation in VSMCs depleted for the endogenous phosphatase to the same level as the active phosphatase does (Figure 3.16), suggesting that PTPD1 phosphatase activity is dispensable for podosome formation in VSMCs and pointing at the involvement of its scaffolding activity as the important activity of PTPD1 for podosome formation in VSMCs.

However, the involvement of PTPD1 catalytic activity in the regulation of the cellular adhesion of VSMCs can't be ruled out as the over-expression of the active form of PTPD1 in control A7r5 cells impaired ability of these cells to form podosomes in response to PDBu treatment (Figure 3.18). As mentioned above, PTPD1 phosphatase activity stabilizes focal adhesions and stress fibers in fibroblasts (Carlucci et al., 2008) and given that the formation of podosomes in VSMCs depends on the incorporation in growing podosomes of proteins locally released by the depolymerization of focal adhesions and stress fibers, one might speculate that the impairment of podosome formation in VSMCs over-expressing active PTPD1 is due to the stabilization of the pre-existing adhesion system. Indeed, if PTPD1 catalytic activity reinforces focal adhesions and stress

fibers in VSMCs the same way it does in fibroblasts, these structures may be less likely to disassemble upon PDBu treatment. They would then sequester their components and make them unavailable for podosome formation. This suggests that PTPD1 activity needs to be finely tuned to support the podosome formation process.

In this study, we showed that the PTPD1 phosphatase activity is dispensable for podosome formation in VSMCs (Figure 3.16) and that the over-expression of the catalytically inactive PTPD1 (PTPD1-C1108S) had no apparent effect on the ability of control A7r5 cells to form podosomes (Figure 3.18).

The catalytic domain of Protein Tyrosine Phosphatases (PTPs) is conserved and contains a characteristic PTP signature motif or “P-loop” (Andersen et al., 2001 Mol Cell Biol). This motif displays a conserved Cysteine residue whose mutation in Serine or Alanine abrogates all enzymatic activity without abrogating PTP affinity for its substrate (Guan & Dixon, 1991; Andersen et al., 2001).

The PTPD1 catalytically inactive mutant used in this study was generated replacing this conserved Cysteine residue in a Serine amino acid (PTPD1-C1108S) and was since used as a catalytically inactive form of PTPD1 (Cardone et al., 2004; Carlucci et al., 2008; Carlucci et al., 2010). No direct evidence for the actual abolishment of PTPD1 phosphatase activity has been published yet, most likely because all PTPD1 known substrates are enzymes that can auto-phosphorylate one of their residues to initiate their own activation and their interaction with PTPD1 acts as a support to enhance their activation (Jui et al., 2000; Carlucci et al., 2008). However, the level of activation of PTPD1 substrates had been shown to decrease in presence of the inactive phosphatase and phenotypes observed were consistent with the level of activation of these substrates (Jui et al., 2000; Carlucci et al., 2008), suggesting that PTPD1-C1108S is indeed catalytically inactive.

4-4: PTPD1 and the activation of KIF1C motor activity

PTPD1-C1108S over-expression in KIF1C-depleted A7r5 cells restored their ability to efficiently form podosomes in response to PDBu treatment (Figure 3.18), suggesting that catalytically inactive PTPD1 can compensate for KIF1C

depletion and that PTPD1 and KIF1C cooperate to mediate podosome formation in VSMCs.

As PTPD1 directly binds the tail of KIF1C (Dorner et al., 1998) and given that the interaction of proteins with kinesin tails can modulate their motor activity (Coy et al., 1999), we hypothesized that PTPD1 could activate KIF1C motor activity. We tested this hypothesis using a α5-integrin transport assay established in the lab (Theisen et al., 2012) and showed that PTPD1 over-expression in cells partially depleted for KIF1C expression restores KIF1C-mediated α5-integrin transport in the tail of RPE-1 cells (Figure 3.20). While we cannot exclude that PTPD1 activates other motors to compensate for the reduction of KIF1C levels in these experiments, there are good indications for PTPD1 to regulate KIF1C transport non-catalytically.

PTPD1-mediated activation of KIF1C activity does n0t require PTPD1 catalytic activity, as both the active and inactive forms of the phosphatase are able to restore KIF1C-mediated α5-integrin transport to the tail of RPE-1 cells (Figure 3.20). KIF1C has been identified for its ability to interact with the N-terminal FERM domain of PTPD1 (Dorner et al., 1998). Single molecule assays conducted *in vitro* with purified KIF1C and PTPD1 FERM domain suggest an increase of the number of activated KIF1C motors in presence of PTPD1 FERM domain (Siddiqui and Straube, unpublished). As the catalytically inactive form of PTPD1 seems to activate KIF1C motor activity, it would be interesting to test the ability of PTPD1 FERM domain only to compensate for KIF1C depletion in cells. If this construct would be able to restore podosome formation and α5-integrin transport in KIF1C-depleted A7r5 and RPE-1 cells respectively to the same level as PTPD1-C1108S does, this would confirm that this domain is sufficient to stimulate KIF1C motor activity and rule out the involvement in KIF1C activation of any PTPD1 interactors that does not bind to its FERM domain.

In addition to KIF1C (Dorner et al., 1998), PTPD1 FERM domain has also been shown to interact with the kinesin-3 KIF16B (Carlucci et al., 2010). KIF16B is known to regulate the trafficking of early endosomes (Hoepfner et al., 2005; Blatner et al., 2007) and mediate the recycling of EGFR at the plasma membrane (Hoepfner et al., 2005). KIF16B has been shown to anchor PTPD1 at the membrane of early endosomes and PTPD1 depletion impairs the recycling of EGFR receptor to the plasma membrane (Carlucci et al., 2010), suggesting PTPD1 and KIF16B work together to regulate EGFR recycling to the

membrane. Based on our results and this information, it would be interesting to test the ability of PTPD1 to activate KIF16B to determine if PTPD1-mediated KIF1C activation is specific of KIF1C motors or if it can be extended to other members of the kinesin-3 family.

PTPD1 FERM domain is also known to interact with the Src kinase (Carlucci et al., 2008) and the interaction of KIF1C and Src with the same domain of PTPD1 is interesting for two reasons: first, independently of its catalytic activity, PTPD1 is known to act as a scaffolding protein bringing together two proteins and helping them to functionally work together (Jui et al., 2000; Carlucci et al., 2008). Then, Src has been shown to phosphorylate KIF1C (Dorner et al, 1998). The direct interaction of Src and KIF1C has not been addressed yet but because they both interact with the same domain of PTPD1, one would suspect that PTPD1 FERM domain brings Src and KIF1C together to facilitate the phosphorylation of the kinesin by Src.

Kinesin phosphorylations of Serine and Threonine residues have been shown to participate in the regulation of the motor activity (DeBerg et al., 2013; Morfini et al., 2009; Cahu et al., 2008). However, Src is a Tyrosine kinase and so far, the effect of kinesin tyrosine phosphorylations has only been addressed in the *Drosophila* kinesin-5 KLP61F (Garcia et al., 2009). Phosphorylation of some Tyrosine residues of the KLP61F motor domain had been shown to be required for the kinesin-5 to ensure its mitotic spindle maintenance activity, suggesting these Tyrosine phosphorylation stimulate the kinesin-5 activity (Garcia et al., 2009).

Src kinase phosphorylates KIF1C but the position(s) it occurs remain unknown, but based on results published by Garcia *et al*, one could speculate that the Tyrosine phosphorylation of KIF1C by Src may activate the motor. As no binding site for Src has been identified in KIF1C yet, it is suspected that PTPD1 would only ensure a scaffolding activity bringing KIF1C and Src together. This hypothesis is reinforced by the ability of the inactive phosphatase to stimulate KIF1C motor activity in cells.

Single molecule assay conducted *in vitro* with purified KIF1C and PTPD1 FERM domain showed an increase of the fraction of KIF1C motors moving along MTs upon the addition of PTPD1 FERM domain (Siddiqui and Straube, unpublished). However, most motors still remained stationary after the addition of PTPD1 FERM domain, suggesting that PTPD1 could help the activation of the motor but

might not be sufficient to allow the full activation of KIF1C motors. It would then be interesting to see if the fraction of motors moving along MTs can be increased upon the addition of Src to KIF1C and PTPD1 FERM domain in the single molecule assay.

PTPD1 binds KIF1C between its third and fourth coiled-coil domain (Dorner et al., 1998). Using cross-linking agents, Dorner *et al* showed that KIF1C could be found as a dimer in cells and computational analysis suggested that the region surrounding the fourth coiled-coil domain of KIF1C could mediate the dimerization of the motor (Dorner et al., 1999). One could then suspect that PTPD1 binding to KIF1C between its third and fourth coiled-coil domain could help the dimerization of the motor and facilitate its activation. However, full length KIF1C is a dimer at physiological salt concentrations, suggesting an interaction should not be required to stabilize the dimerization (Siddiqui and Straube, unpublished).

One last explanation for PTPD1-mediated KIF1C activation would then rely on the ability of PTPD1 to bind KIF1C tail and induce a conformational change in the structure of the kinesin that would activate it. When inactive, conventional kinesins adopt a “close” conformation with their tail interacting with their motor domain to abolish their interaction with MTs. Cargo binding to Kinesin-1 tail induces a conformational change that releases the motor domain, allowing it to interact with and move along MTs (Coy et al., 1999).
A slightly different model for KIF1A, KIF13A, KIF13B and KIF16B Kinesin-3s activation has recently been suggested (Soppina et al., 2014). In this model, Kinesin-3s are present as soluble monomers in the cell cytoplasm and display a “closed” conformation due to intra-molecular interactions (Al-Bassam et al., 2003; Lee et al., 2004) Cargo binding induces a disruption of these intra-molecular interactions, allowing the motor to dimerize, interact with and move processively along MTs (Soppina et al., 2014).
Because full-length KIF1C forms a dimer at physiological salt conditions without the requirement of cargo binding (Siddiqui and Straube, unpublished), we suspect that the same kind of mechanism could regulate KIF1C activity. In our model (Figure 4.4), KIF1C dimers would adopt a “closed” conformation in the absence of PTPD1, its tail covering its motor domain or impairing its interaction with MTs to inhibit its motor activity. PTPD1 binding to KIF1C tail would

destabilize KIF1C auto-inhibitory “closed” conformation, releasing the motor domain that would then be able to efficiently interact with and move along MTs.

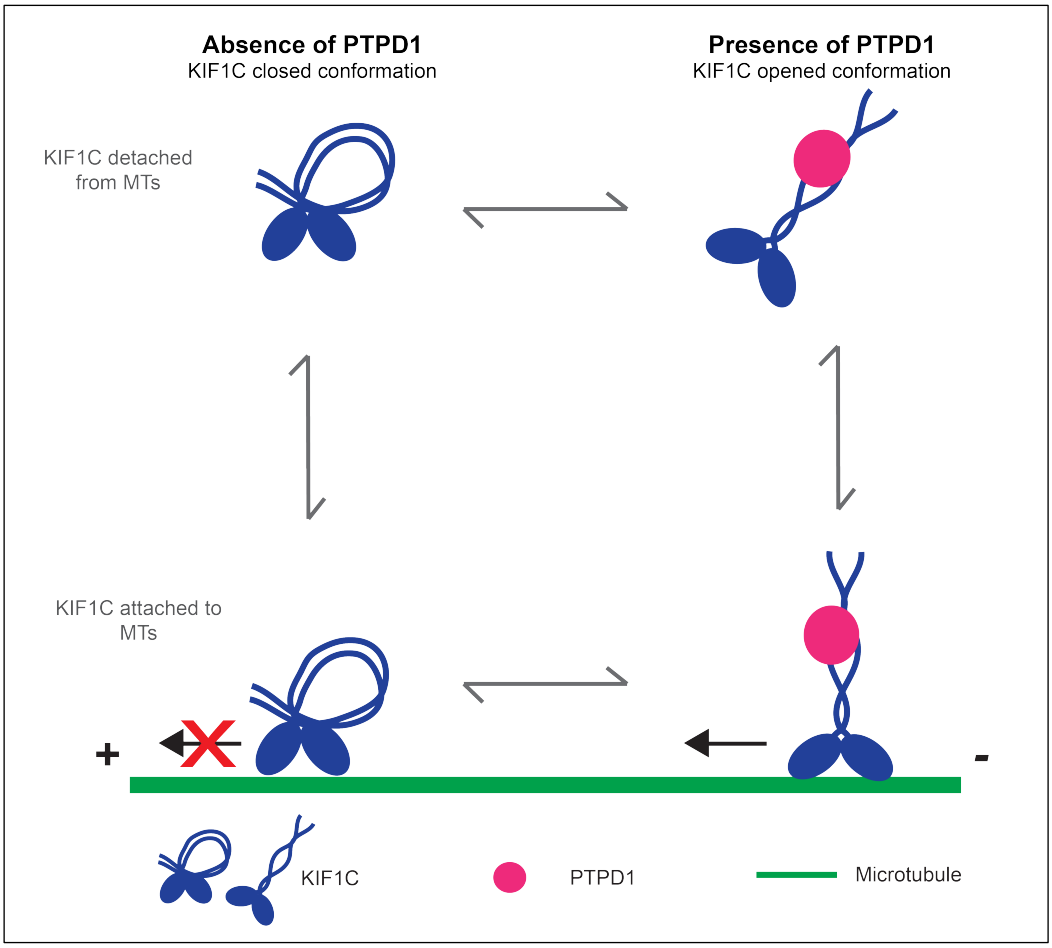

Figure 4.4: Model for PTPD1-mediated KIF1C activation.
In absence of PTPD1, KIF1C adopts a close conformation, its tail covering its motor domain and impairing its ability to interact with MTs (upper left) or to move along them (lower left). PTPD1 binding to KIF1C destabilizes KIF1C tail interaction with the kinesin motor domain, uncovering it (upper right) and making it able to interact with and move along MTs (lower right). The arrow indicates the direction of KIF1C movement.

In this study, we proposed a model explaining how PTPD1 binding to KIF1C tail could activate KIF1C motor activity. However, a model for the regulation of the trafficking of KIF1C-associated vesicles has already been proposed in developing neurons (Chapter 1-4, Figure 1.7; Schlager et al., 2010; Lee et al., 2015). In this model, BICDR-1 anchors both KIF1C and dynein motors at the cargo surface and acts as a molecular switch controlling the balance between KIF1C-mediated anterograde and dynein-mediated retrograde transport in favour of the latter (Schlager et al., 2010). The Rab6 adaptor protein

participates in the regulation of KIF1C-mediated cargo transport as it modulates KIF1C folding through its interaction with both its tail and motor domain (Lee et al., 2015).

As PTPD1 seems to activate KIF1C transport activity, it would be interesting to test if its presence can disrupt the inhibitory interaction of Rab6 with KIF1C motor domain and destabilize the balance between KIF1C- and dynein-mediated transports in favour of KIF1C in developing neurons. These experiments could allow the extension of our proposed model of PTPD1-mediated activation of KIF1C to a third cell type, show that it is not restricted to the regulation of cellular adhesion as KIF1C is known to transport the neuropeptide Y in neurons (Schlager et al., 2010) and help to better understand how the balance between KIF1C- and dynein-mediated transport is regulated in cells.

5: Bibliography

Abram, C. L., D. F. Seals, I. Pass, D. Salinsky, L. Maurer, T. M. Roth, and S. A. Courtneidge. 2003. 'The adaptor protein fish associates with members of the ADAMs family and localizes to podosomes of Src-transformed cells', *J Biol Chem*, 278: 16844-51.

Akhmanova, A., C. C. Hoogenraad, K. Drabek, T. Stepanova, B. Dortland, T. Verkerk, W. Vermeulen, B. M. Burgering, C. I. De Zeeuw, F. Grosveld, and N. Galjart. 2001. 'Clasps are CLIP-115 and -170 associating proteins involved in the regional regulation of microtubule dynamics in motile fibroblasts', *Cell*, 104: 923-35.

Akisaka, T., H. Yoshida, and T. Takigawa. 2011. 'Differential distribution of posttranslationally modified microtubules in osteoclasts', *J Histochem Cytochem*, 59: 630-8.

Al-Bassam, J., Y. Cui, D. Klopfenstein, B. O. Carragher, R. D. Vale, and R. A. Milligan. 2003. 'Distinct conformations of the kinesin Unc104 neck regulate a monomer to dimer motor transition', *J Cell Biol*, 163: 743-53.

Andersen, J. N., O. H. Mortensen, G. H. Peters, P. G. Drake, L. F. Iversen, O. H. Olsen, P. G. Jansen, H. S. Andersen, N. K. Tonks, and N. P. Moller. 2001. 'Structural and evolutionary relationships among protein tyrosine phosphatase domains', *Mol Cell Biol*, 21: 7117-36.

Antony, C., C. Cibert, G. Geraud, A. Santa Maria, B. Maro, V. Mayau, and B. Goud. 1992. 'The small GTP-binding protein rab6p is distributed from medial Golgi to the trans-Golgi network as determined by a confocal microscopic approach', *J Cell Sci*, 103 (Pt 3): 785-96.

Artym, V. V., K. Matsumoto, S. C. Mueller, and K. M. Yamada. 2011. 'Dynamic membrane remodeling at invadopodia differentiates invadopodia from podosomes', *Eur J Cell Biol*, 90: 172-80.

Babb, S. G., P. Matsudaira, M. Sato, I. Correia, and S. S. Lim. 1997. 'Fimbrin in podosomes of monocyte-derived osteoclasts', *Cell Motil Cytoskeleton*, 37: 308-25.

Badowski, C., G. Pawlak, A. Grichine, A. Chabadel, C. Oddou, P. Jurdic, M. Pfaff, C. Albiges-Rizo, and M. R. Block. 2008. 'Paxillin phosphorylation controls invadopodia/podosomes spatiotemporal organization', *Mol Biol Cell*, 19: 633-45.

Bershadsky, A., A. Chausovsky, E. Becker, A. Lyubimova, and B. Geiger. 1996. 'Involvement of microtubules in the control of adhesion-dependent signal transduction', *Curr Biol*, 6: 1279-89.

Bhuwania, R., A. Castro-Castro, and S. Linder. 2014. 'Microtubule acetylation regulates dynamics of KIF1C-powered vesicles and contact of microtubule plus ends with podosomes', *Eur J Cell Biol*, 93: 424-37.

Bhuwania, R., S. Cornfine, Z. Fang, M. Kruger, E. J. Luna, and S. Linder. 2012. 'Supervillin couples myosin-dependent contractility to podosomes and enables their turnover', *J Cell Sci*, 125: 2300-14.

Biosse Duplan, M., D. Zalli, S. Stephens, S. Zenger, L. Neff, J. M. Oelkers, F. P. Lai, W. Horne, K. Rottner, and R. Baron. 2014. 'Microtubule dynamic instability controls podosome patterning in osteoclasts through EB1, cortactin, and Src', *Mol Cell Biol*, 34: 16-29.

Blanchoin, L., R. Boujemaa-Paterski, C. Sykes, and J. Plastino. 2014. 'Actin dynamics, architecture, and mechanics in cell motility', *Physiol Rev*, 94: 235-63.

Blasius, T. L., D. Cai, G. T. Jih, C. P. Toret, and K. J. Verhey. 2007. 'Two binding partners cooperate to activate the molecular motor Kinesin-1', *J Cell Biol*, 176: 11-7.

Blatner, N. R., M. I. Wilson, C. Lei, W. Hong, D. Murray, R. L. Williams, and W. Cho. 2007. 'The structural basis of novel endosome anchoring activity of KIF16B kinesin', *EMBO J*, 26: 3709-19.

Block, M. R., C. Badowski, A. Millon-Fremillon, D. Bouvard, A. P. Bouin, E. Faurobert, D. Gerber-Scokaert, E. Planus, and C. Albiges-Rizo. 2008. 'Podosome-type adhesions and focal adhesions, so alike yet so different', *Eur J Cell Biol*, 87: 491-506.

Brandt, D., M. Gimona, M. Hillmann, H. Haller, and H. Mischak. 2002. 'Protein kinase C induces actin reorganization via a Src- and Rho-dependent pathway', *J Biol Chem*, 277: 20903-10.

Brandt, D. T., and R. Grosse. 2007. 'Get to grips: steering local actin dynamics with IQGAPs', *EMBO Rep*, 8: 1019-23.

Buccione, R., J. D. Orth, and M. A. McNiven. 2004. 'Foot and mouth: podosomes, invadopodia and circular dorsal ruffles', *Nat Rev Mol Cell Biol*, 5: 647-57.

Burgstaller, G., and M. Gimona. 2004. 'Actin cytoskeleton remodelling via local inhibition of contractility at discrete microdomains', *J Cell Sci*, 117: 223-31.

Burgstaller, G., and M. Gimona. 2005. 'Podosome-mediated matrix resorption and cell motility in vascular smooth muscle cells', *Am J Physiol Heart Circ Physiol*, 288: H3001-5.

Burns, S., A. J. Thrasher, M. P. Blundell, L. Machesky, and G. E. Jones. 2001. 'Configuration of human dendritic cell cytoskeleton by Rho GTPases, the WAS protein, and differentiation', *Blood*, 98: 1142-9.

Byron, A., J. D. Humphries, M. D. Bass, D. Knight, and M. J. Humphries. 2011. 'Proteomic analysis of integrin adhesion complexes', *Sci Signal*, 4: pt2.

Caballero Oteyza, A., E. Battaloglu, L. Ocek, T. Lindig, J. Reichbauer, A. P. Rebelo, M. A. Gonzalez, Y. Zorlu, B. Ozes, D. Timmann, B. Bender, G. Woehlke, S. Zuchner, L. Schols, and R. Schule. 2014. 'Motor protein mutations cause a new form of hereditary spastic paraplegia', *Neurology*, 82: 2007-16.

Cahu, J., A. Olichon, C. Hentrich, H. Schek, J. Drinjakovic, C. Zhang, A. Doherty-Kirby, G. Lajoie, and T. Surrey. 2008. 'Phosphorylation by Cdk1 increases the binding of Eg5 to microtubules in vitro and in Xenopus egg extract spindles', *PLoS One*, 3: e3936.

Cardone, L., A. Carlucci, A. Affaitati, A. Livigni, T. DeCristofaro, C. Garbi, S. Varrone, A. Ullrich, M. E. Gottesman, E. V. Avvedimento, and A. Feliciello. 2004. 'Mitochondrial AKAP121 binds and targets protein tyrosine phosphatase D1, a novel positive regulator of src signaling', *Mol Cell Biol*, 24: 4613-26.

Carleton, M., M. Mao, M. Biery, P. Warrener, S. Kim, C. Buser, C. G. Marshall, C. Fernandes, J. Annis, and P. S. Linsley. 2006. 'RNA interference-mediated silencing of mitotic kinesin KIF14 disrupts cell cycle progression and induces cytokinesis failure', *Mol Cell Biol*, 26: 3853-63.

Carlucci, A., C. Gedressi, L. Lignitto, L. Nezi, E. Villa-Moruzzi, E. V. Avvedimento, M. Gottesman, C. Garbi, and A. Feliciello. 2008. 'Protein-tyrosine phosphatase PTPD1 regulates focal adhesion kinase autophosphorylation and cell migration', *J Biol Chem*, 283: 10919-29.

Carlucci, A., M. Porpora, C. Garbi, M. Galgani, M. Santoriello, M. Mascolo, D. di Lorenzo, V. Altieri, M. Quarto, L. Terracciano, M. E. Gottesman, L. Insabato, and A. Feliciello. 2010. 'PTPD1 supports receptor stability and mitogenic signaling in bladder cancer cells', *J Biol Chem*, 285: 39260-70.

Chabadel, A., I. Banon-Rodriguez, D. Cluet, B. B. Rudkin, B. Wehrle-Haller, E. Genot, P. Jurdic, I. M. Anton, and F. Saltel. 2007. 'CD44 and beta3 integrin organize two functionally distinct actin-based domains in osteoclasts', *Mol Biol Cell*, 18: 4899-910.

Chen, W. T. 1989. 'Proteolytic activity of specialized surface protrusions formed at rosette contact sites of transformed cells', *J Exp Zool*, 251: 167-85.

Chin, D., and A. R. Means. 2000. 'Calmodulin: a prototypical calcium sensor', *Trends Cell Biol*, 10: 322-8.

Chistiakov, D. A., A. N. Orekhov, and Y. V. Bobryshev. 2015. 'Vascular smooth muscle cell in atherosclerosis', *Acta Physiol (Oxf)*, 214: 33-50.

Collin, O., S. Na, F. Chowdhury, M. Hong, M. E. Shin, F. Wang, and N. Wang. 2008. 'Self-organized podosomes are dynamic mechanosensors', *Curr Biol*, 18: 1288-94.

Conti, M. A., S. Even-Ram, C. Liu, K. M. Yamada, and R. S. Adelstein. 2004. 'Defects in cell adhesion and the visceral endoderm following ablation of nonmuscle myosin heavy chain II-A in mice', *J Biol Chem*, 279: 41263-6.

Cornfine, S., M. Himmel, P. Kopp, K. El Azzouzi, C. Wiesner, M. Kruger, T. Rudel, and S. Linder. 2011. 'The kinesin KIF9 and reggie/flotillin proteins regulate matrix degradation by macrophage podosomes', *Mol Biol Cell*, 22: 202-15.

Coy, D. L., W. O. Hancock, M. Wagenbach, and J. Howard. 1999. 'Kinesin's tail domain is an inhibitory regulator of the motor domain', *Nat Cell Biol*, 1: 288-92.

Crimaldi, L., S. A. Courtneidge, and M. Gimona. 2009. 'Tks5 recruits AFAP-110, p190RhoGAP, and cortactin for podosome formation', *Exp Cell Res*, 315: 2581-92.

Curtis, A. S. 1964. 'The Mechanism of Adhesion of Cells to Glass. A Study by Interference Reflection Microscopy', *J Cell Biol*, 20: 199-215.

Danowski, B. A. 1989. 'Fibroblast contractility and actin organization are stimulated by microtubule inhibitors', *J Cell Sci*, 93 (Pt 2): 255-66.

Davis-Dusenbery, B. N., C. Wu, and A. Hata. 2011. 'Micromanaging vascular smooth muscle cell differentiation and phenotypic modulation', *Arterioscler Thromb Vasc Biol*, 31: 2370-7.

DeBerg, H. A., B. H. Blehm, J. Sheung, A. R. Thompson, C. S. Bookwalter, S. F. Torabi, T. A. Schroer, C. L. Berger, Y. Lu, K. M. Trybus, and P. R. Selvin. 2013. 'Motor domain phosphorylation modulates kinesin-1 transport', *J Biol Chem*, 288: 32612-21.

DePasquale, J. A., and C. S. Izzard. 1987. 'Evidence for an actin-containing cytoplasmic precursor of the focal contact and the timing of incorporation of vinculin at the focal contact', *J Cell Biol*, 105: 2803-9.

Deryugina, E. I., B. Ratnikov, E. Monosov, T. I. Postnova, R. DiScipio, J. W. Smith, and A. Y. Strongin. 2001. 'MT1-MMP initiates activation of pro-MMP-2 and integrin alphavbeta3 promotes maturation of MMP-2 in breast carcinoma cells', *Exp Cell Res*, 263: 209-23.

Destaing, O., F. Saltel, J. C. Geminard, P. Jurdic, and F. Bard. 2003. 'Podosomes display actin turnover and dynamic self-organization in osteoclasts expressing actin-green fluorescent protein', *Mol Biol Cell*, 14: 407-16.

Destaing, O., F. Saltel, B. Gilquin, A. Chabadel, S. Khochbin, S. Ory, and P. Jurdic. 2005. 'A novel Rho-mDia2-HDAC6 pathway controls podosome patterning through microtubule acetylation in osteoclasts', *J Cell Sci*, 118: 2901-11.

Diefenbach, R. J., J. P. Mackay, P. J. Armati, and A. L. Cunningham. 1998. 'The C-terminal region of the stalk domain of ubiquitous human kinesin heavy chain contains the binding site for kinesin light chain', *Biochemistry*, 37: 16663-70.

Dor, T., Y. Cinnamon, L. Raymond, A. Shaag, N. Bouslam, A. Bouhouche, M. Gaussen, V. Meyer, A. Durr, A. Brice, A. Benomar, G. Stevanin, M. Schuelke, and S. Edvardson. 2014. 'KIF1C mutations in two families with hereditary spastic paraparesis and cerebellar dysfunction', *J Med Genet*, 51: 137-42.

Dorfleutner, A., Y. Cho, D. Vincent, J. Cunnick, H. Lin, S. A. Weed, C. Stehlik, and D. C. Flynn. 2008. 'Phosphorylation of AFAP-110 affects podosome lifespan in A7r5 cells', *J Cell Sci*, 121: 2394-405.

Dorner, C., T. Ciossek, S. Muller, P. H. Moller, A. Ullrich, and R. Lammers. 1998. 'Characterization of KIF1C, a new kinesin-like protein involved in vesicle transport from the Golgi apparatus to the endoplasmic reticulum', *J Biol Chem*, 273: 20267-75.

Dorner, C., A. Ullrich, H. U. Haring, and R. Lammers. 1999. 'The kinesin-like motor protein KIF1C occurs in intact cells as a dimer and associates with proteins of the 14-3-3 family', *J Biol Chem*, 274: 33654-60.

Douglas, M. E., T. Davies, N. Joseph, and M. Mishima. 2010. 'Aurora B and 14-3-3 coordinately regulate clustering of centralspindlin during cytokinesis', *Curr Biol*, 20: 927-33.

Dumbauld, D. W., T. T. Lee, A. Singh, J. Scrimgeour, C. A. Gersbach, E. A. Zamir, J. Fu, C. S. Chen, J. E. Curtis, S. W. Craig, and A. J. Garcia. 2013. 'How vinculin regulates force transmission', *Proc Natl Acad Sci U S A*, 110: 9788-93.

Efimov, A., N. Schiefermeier, I. Grigoriev, R. Ohi, M. C. Brown, C. E. Turner, J. V. Small, and I. Kaverina. 2008. 'Paxillin-dependent stimulation of microtubule catastrophes at focal adhesion sites', *J Cell Sci*, 121: 196-204.

Efimova, N., A. Grimaldi, A. Bachmann, K. Frye, X. Zhu, A. Feoktistov, A. Straube, and I. Kaverina. 2014. 'Podosome-regulating kinesin KIF1C translocates to the cell periphery in a CLASP-dependent manner', *J Cell Sci*, 127: 5179-88.

Endow, S. A. 1999. 'Determinants of molecular motor directionality', *Nat Cell Biol*, 1: E163-7.

Enomoto, T. 1996. 'Microtubule disruption induces the formation of actin stress fibers and focal adhesions in cultured cells: possible involvement of the rho signal cascade', *Cell Struct Funct*, 21: 317-26.

Even-Ram, S., A. D. Doyle, M. A. Conti, K. Matsumoto, R. S. Adelstein, and K. M. Yamada. 2007. 'Myosin IIA regulates cell motility and actomyosin-microtubule crosstalk', *Nat Cell Biol*, 9: 299-309.

Eves, R., B. A. Webb, S. Zhou, and A. S. Mak. 2006. 'Caldesmon is an integral component of podosomes in smooth muscle cells', *J Cell Sci*, 119: 1691-702.

Ezratty, E. J., C. Bertaux, E. E. Marcantonio, and G. G. Gundersen. 2009. 'Clathrin mediates integrin endocytosis for focal adhesion disassembly in migrating cells', *J Cell Biol*, 187: 733-47.

Ezratty, E. J., M. A. Partridge, and G. G. Gundersen. 2005. 'Microtubule-induced focal adhesion disassembly is mediated by dynamin and focal adhesion kinase', *Nat Cell Biol*, 7: 581-90.

Franker, M. A., and C. C. Hoogenraad. 2013. 'Microtubule-based transport - basic mechanisms, traffic rules and role in neurological pathogenesis', *J Cell Sci*, 126: 2319-29.

Fultz, M. E., C. Li, W. Geng, and G. L. Wright. 2000. 'Remodeling of the actin cytoskeleton in the contracting A7r5 smooth muscle cell', *J Muscle Res Cell Motil*, 21: 775-87.

Gaidano, G., L. Bergui, M. Schena, M. Gaboli, O. Cremona, P. C. Marchisio, and F. Caligaris-Cappio. 1990. 'Integrin distribution and cytoskeleton organization in normal and malignant monocytes', *Leukemia*, 4: 682-7.

Galbraith, C. G., K. M. Yamada, and M. P. Sheetz. 2002. 'The relationship between force and focal complex development', *J Cell Biol*, 159: 695-705.

Garcia, E., G. E. Jones, L. M. Machesky, and I. M. Anton. 2012. 'WIP: WASP-interacting proteins at invadopodia and podosomes', *Eur J Cell Biol*, 91: 869-77.

Garcia, K., J. Stumpff, T. Duncan, and T. T. Su. 2009. 'Tyrosines in the kinesin-5 head domain are necessary for phosphorylation by Wee1 and for mitotic spindle integrity', *Curr Biol*, 19: 1670-6.

Garnham, C. P., and A. Roll-Mecak. 2012. 'The chemical complexity of cellular microtubules: tubulin post-translational modification enzymes and their roles in tuning microtubule functions', *Cytoskeleton (Hoboken)*, 69: 442-63.

Gavazzi, I., M. V. Nermut, and P. C. Marchisio. 1989. 'Ultrastructure and gold-immunolabelling of cell-substratum adhesions (podosomes) in RSV-transformed BHK cells', *J Cell Sci*, 94 (Pt 1): 85-99.

Gawden-Bone, C., Z. Zhou, E. King, A. Prescott, C. Watts, and J. Lucocq. 2010. 'Dendritic cell podosomes are protrusive and invade the extracellular matrix using metalloproteinase MMP-14', *J Cell Sci*, 123: 1427-37.

Geiger, J. C., J. Lipka, I. Segura, S. Hoyer, M. A. Schlager, P. S. Wulf, S. Weinges, J. Demmers, C. C. Hoogenraad, and A. Acker-Palmer. 2014. 'The GRIP1/14-3-3 pathway coordinates cargo trafficking and dendrite development', *Dev Cell*, 28: 381-93.

Georgess, D., I. Machuca-Gayet, A. Blangy, and P. Jurdic. 2014. 'Podosome organization drives osteoclast-mediated bone resorption', *Cell Adh Migr*, 8: 191-204.

Gil-Henn, H., O. Destaing, N. A. Sims, K. Aoki, N. Alles, L. Neff, A. Sanjay, A. Bruzzaniti, P. De Camilli, R. Baron, and J. Schlessinger. 2007. 'Defective microtubule-dependent podosome organization in osteoclasts leads to increased bone density in Pyk2(-/-) mice', *J Cell Biol*, 178: 1053-64.

Gimona, M., R. Buccione, S. A. Courtneidge, and S. Linder. 2008. 'Assembly and biological role of podosomes and invadopodia', *Curr Opin Cell Biol*, 20: 235-41.

Gimona, M., I. Kaverina, G. P. Resch, E. Vignal, and G. Burgstaller. 2003. 'Calponin repeats regulate actin filament stability and formation of podosomes in smooth muscle cells', *Mol Biol Cell*, 14: 2482-91.

Goode, B. L., and M. J. Eck. 2007. 'Mechanism and function of formins in the control of actin assembly', *Annu Rev Biochem*, 76: 593-627.

Goto, T., H. Maeda, and T. Tanaka. 2002. 'A selective inhibitor of matrix metalloproteinases inhibits the migration of isolated osteoclasts by increasing the life span of podosomes', *J Bone Miner Metab*, 20: 98-105.

Guan, K. L., and J. E. Dixon. 1991. 'Evidence for protein-tyrosine-phosphatase catalysis proceeding via a cysteine-phosphate intermediate', *J Biol Chem*, 266: 17026-30.

Guillaud, L., R. Wong, and N. Hirokawa. 2008. 'Disruption of KIF17-Mint1 interaction by CaMKII-dependent phosphorylation: a molecular model of kinesin-cargo release', *Nat Cell Biol*, 10: 19-29.

Hai, C. M., P. Hahne, E. O. Harrington, and M. Gimona. 2002. 'Conventional protein kinase C mediates phorbol-dibutyrate-induced cytoskeletal remodeling in a7r5 smooth muscle cells', *Exp Cell Res*, 280: 64-74.

Hall, D. H., and E. M. Hedgecock. 1991. 'Kinesin-related gene unc-104 is required for axonal transport of synaptic vesicles in C. elegans', *Cell*, 65: 837-47.

Hammond, J. W., D. Cai, T. L. Blasius, Z. Li, Y. Jiang, G. T. Jih, E. Meyhofer, and K. J. Verhey. 2009. 'Mammalian Kinesin-3 motors are dimeric in vivo and move by processive motility upon release of autoinhibition', *PLoS Biol*, 7: e72.

Han, M., L. H. Dong, B. Zheng, J. H. Shi, J. K. Wen, and Y. Cheng. 2009. 'Smooth muscle 22 alpha maintains the differentiated phenotype of vascular smooth muscle cells by inducing filamentous actin bundling', *Life Sci*, 84: 394-401.

Hanein, D., and A. R. Horwitz. 2012. 'The structure of cell-matrix adhesions: the new frontier', *Curr Opin Cell Biol*, 24: 134-40.

Herreros, L., J. L. Rodriguez-Fernandez, M. C. Brown, J. L. Alonso-Lebrero, C. Cabanas, F. Sanchez-Madrid, N. Longo, C. E. Turner, and P. Sanchez-Mateos. 2000. 'Paxillin localizes to the lymphocyte microtubule organizing center and associates with the microtubule cytoskeleton', *J Biol Chem*, 275: 26436-40.

Hirata, H., H. Tatsumi, and M. Sokabe. 2008. 'Mechanical forces facilitate actin polymerization at focal adhesions in a zyxin-dependent manner', *J Cell Sci*, 121: 2795-804.

Hirokawa, N., Y. Noda, Y. Tanaka, and S. Niwa. 2009. 'Kinesin superfamily motor proteins and intracellular transport', *Nat Rev Mol Cell Biol*, 10: 682-96.

Hoepfner, S., F. Severin, A. Cabezas, B. Habermann, A. Runge, D. Gillooly, H. Stenmark, and M. Zerial. 2005. 'Modulation of receptor recycling and degradation by the endosomal kinesin KIF16B', *Cell*, 121: 437-50.

Hofmann, K., and P. Bucher. 1995. 'The FHA domain: a putative nuclear signalling domain found in protein kinases and transcription factors', *Trends Biochem Sci*, 20: 347-9.

Horiuchi, D., C. A. Collins, P. Bhat, R. V. Barkus, A. Diantonio, and W. M. Saxton. 2007. 'Control of a kinesin-cargo linkage mechanism by JNK pathway kinases', *Curr Biol*, 17: 1313-7.

Huckaba, T. M., A. Gennerich, J. E. Wilhelm, A. H. Chishti, and R. D. Vale. 2011. 'Kinesin-73 is a processive motor that localizes to Rab5-containing organelles', *J Biol Chem*, 286: 7457-67.

Huo, L., Y. Yue, J. Ren, J. Yu, J. Liu, Y. Yu, F. Ye, T. Xu, M. Zhang, and W. Feng. 2012. 'The CC1-FHA tandem as a central hub for controlling the dimerization and activation of kinesin-3 KIF1A', *Structure*, 20: 1550-61.

Ichimura, T., A. Wakamiya-Tsuruta, C. Itagaki, M. Taoka, T. Hayano, T. Natsume, and T. Isobe. 2002. 'Phosphorylation-dependent interaction of kinesin light chain 2 and the 14-3-3 protein', *Biochemistry*, 41: 5566-72.

Izzard, C. S. 1988. 'A precursor of the focal contact in cultured fibroblasts', *Cell Motil Cytoskeleton*, 10: 137-42.

Jui, H. Y., R. J. Tseng, X. Wen, H. I. Fang, L. M. Huang, K. Y. Chen, H. J. Kung, D. K. Ann, and H. M. Shih. 2000. 'Protein-tyrosine phosphatase D1, a potential regulator and effector for Tec family kinases', *J Biol Chem*, 275: 41124-32.

Jurdic, P., F. Saltel, A. Chabadel, and O. Destaing. 2006. 'Podosome and sealing zone: specificity of the osteoclast model', *Eur J Cell Biol*, 85: 195-202.

Kaverina, I., O. Krylyshkina, and J. V. Small. 1999. 'Microtubule targeting of substrate contacts promotes their relaxation and dissociation', *J Cell Biol*, 146: 1033-44.

Kaverina, I., K. Rottner, and J. V. Small. 1998. 'Targeting, capture, and stabilization of microtubules at early focal adhesions', *J Cell Biol*, 142: 181-90.

Kaverina, I., T. E. Stradal, and M. Gimona. 2003. 'Podosome formation in cultured A7r5 vascular smooth muscle cells requires Arp2/3-dependent de-novo actin polymerization at discrete microdomains', *J Cell Sci*, 116: 4915-24.

Kaverina, I. N., A. A. Minin, F. K. Gyoeva, and J. M. Vasiliev. 1997. 'Kinesin-associated transport is involved in the regulation of cell adhesion', *Cell Biol Int*, 21: 229-36.

Kopp, P., R. Lammers, M. Aepfelbacher, G. Woehlke, T. Rudel, N. Machuy, W. Steffen, and S. Linder. 2006. 'The kinesin KIF1C and microtubule plus ends regulate podosome dynamics in macrophages', *Mol Biol Cell*, 17: 2811-23.

Kovacs, M., J. Toth, C. Hetenyi, A. Malnasi-Csizmadia, and J. R. Sellers. 2004. 'Mechanism of blebbistatin inhibition of myosin II', *J Biol Chem*, 279: 35557-63.

Krylyshkina, O., I. Kaverina, W. Kranewitter, W. Steffen, M. C. Alonso, R. A. Cross, and J. V. Small. 2002. 'Modulation of substrate adhesion dynamics via microtubule targeting requires kinesin-1', *J Cell Biol*, 156: 349-59.

Kubow, K. E., S. K. Conrad, and A. R. Horwitz. 2013. 'Matrix microarchitecture and myosin II determine adhesion in 3D matrices', *Curr Biol*, 23: 1607-19.

Kubow, K. E., and A. R. Horwitz. 2011. 'Reducing background fluorescence reveals adhesions in 3D matrices', *Nat Cell Biol*, 13: 3-5; author reply 5-7.

Kuznetsov, S. A., E. A. Vaisberg, N. A. Shanina, N. N. Magretova, V. Y. Chernyak, and V. I. Gelfand. 1988. 'The quaternary structure of bovine brain kinesin', *EMBO J*, 7: 353-6.

Labernadie, A., A. Bouissou, P. Delobelle, S. Balor, R. Voituriez, A. Proag, I. Fourquaux, C. Thibault, C. Vieu, R. Poincloux, G. M. Charriere, and I. Maridonneau-Parini. 2014. 'Protrusion force microscopy reveals oscillatory force generation and mechanosensing activity of human macrophage podosomes', *Nat Commun*, 5: 5343.

Labernadie, A., C. Thibault, C. Vieu, I. Maridonneau-Parini, and G. M. Charriere. 2010. 'Dynamics of podosome stiffness revealed by atomic force microscopy', *Proc Natl Acad Sci U S A*, 107: 21016-21.

Lacolley, P., V. Regnault, A. Nicoletti, Z. Li, and J. B. Michel. 2012. 'The vascular smooth muscle cell in arterial pathology: a cell that can take on multiple roles', *Cardiovasc Res*, 95: 194-204.

Lawrence, C. J., R. K. Dawe, K. R. Christie, D. W. Cleveland, S. C. Dawson, S. A. Endow, L. S. Goldstein, H. V. Goodson, N. Hirokawa, J. Howard, R. L. Malmberg, J. R. McIntosh, H. Miki, T. J. Mitchison, Y. Okada, A. S. Reddy, W. M. Saxton, M. Schliwa, J. M. Scholey, R. D. Vale, C. E. Walczak, and L. Wordeman. 2004. 'A standardized kinesin nomenclature', *J Cell Biol*, 167: 19-22.

Lee, J. R., H. Shin, J. Choi, J. Ko, S. Kim, H. W. Lee, K. Kim, S. H. Rho, J. H. Lee, H. E. Song, S. H. Eom, and E. Kim. 2004. 'An intramolecular interaction between the FHA domain and a coiled coil negatively regulates the kinesin motor KIF1A', *EMBO J*, 23: 1506-15.

Lee, P. L., M. B. Ohlson, and S. R. Pfeffer. 2015. 'Rab6 regulation of the kinesin family KIF1C motor domain contributes to Golgi tethering', *Elife*, 4.

Li, J., G. I. Lee, S. R. Van Doren, and J. C. Walker. 2000. 'The FHA domain mediates phosphoprotein interactions', *J Cell Sci*, 113 Pt 23: 4143-9.

Linder, S. 2007. 'The matrix corroded: podosomes and invadopodia in extracellular matrix degradation', *Trends Cell Biol*, 17: 107-17.

Linder, S., and M. Aepfelbacher. 2003. 'Podosomes: adhesion hot-spots of invasive cells', *Trends Cell Biol*, 13: 376-85.

Linder, S., K. Hufner, U. Wintergerst, and M. Aepfelbacher. 2000. 'Microtubule-dependent formation of podosomal adhesion structures in primary human macrophages', *J Cell Sci*, 113 Pt 23: 4165-76.

Linder, S., D. Nelson, M. Weiss, and M. Aepfelbacher. 1999. 'Wiskott-Aldrich syndrome protein regulates podosomes in primary human macrophages', *Proc Natl Acad Sci U S A*, 96: 9648-53.

Linder, S., and C. Wiesner. 2015. 'Tools of the trade: podosomes as multipurpose organelles of monocytic cells', *Cell Mol Life Sci*, 72: 121-35.

Linder, S., C. Wiesner, and M. Himmel. 2011. 'Degrading devices: invadosomes in proteolytic cell invasion', *Annu Rev Cell Dev Biol*, 27: 185-211.

Lipka, J., L. C. Kapitein, J. Jaworski, and C. C. Hoogenraad. 2016. 'Microtubule-binding protein doublecortin-like kinase 1 (DCLK1) guides kinesin-3-mediated cargo transport to dendrites', *EMBO J*, 35: 302-18.

Liu, B. P., M. Chrzanowska-Wodnicka, and K. Burridge. 1998. 'Microtubule depolymerization induces stress fibers, focal adhesions, and DNA synthesis via the GTP-binding protein Rho', *Cell Adhes Commun*, 5: 249-55.

Liu, D., J. Bienkowska, C. Petosa, R. J. Collier, H. Fu, and R. Liddington. 1995. 'Crystal structure of the zeta isoform of the 14-3-3 protein', *Nature*, 376: 191-4.

Livigni, A., A. Scorziello, S. Agnese, A. Adornetto, A. Carlucci, C. Garbi, I. Castaldo, L. Annunziato, E. V. Avvedimento, and A. Feliciello. 2006. 'Mitochondrial AKAP121 links cAMP and src signaling to oxidative metabolism', *Mol Biol Cell*, 17: 263-71.

Luxenburg, C., J. T. Parsons, L. Addadi, and B. Geiger. 2006. 'Involvement of the Src-cortactin pathway in podosome formation and turnover during polarization of cultured osteoclasts', *J Cell Sci*, 119: 4878-88.

Luxenburg, C., S. Winograd-Katz, L. Addadi, and B. Geiger. 2012. 'Involvement of actin polymerization in podosome dynamics', *J Cell Sci*, 125: 1666-72.

Manna, T., S. Honnappa, M. O. Steinmetz, and L. Wilson. 2008. 'Suppression of microtubule dynamic instability by the +TIP protein EB1 and its modulation by the CAP-Gly domain of p150glued', *Biochemistry*, 47: 779-86.

Marchisio, P. C., L. Bergui, G. C. Corbascio, O. Cremona, N. D'Urso, M. Schena, L. Tesio, and F. Caligaris-Cappio. 1988. 'Vinculin, talin, and integrins are localized at specific adhesion sites of malignant B lymphocytes', *Blood*, 72: 830-3.

Marchisio, P. C., D. Cirillo, L. Naldini, M. V. Primavera, A. Teti, and A. Zambonin-Zallone. 1984. 'Cell-substratum interaction of cultured avian osteoclasts is mediated by specific adhesion structures', *J Cell Biol*, 99: 1696-705.

Marx, A., A. Hoenger, and E. Mandelkow. 2009. 'Structures of kinesin motor proteins', *Cell Motil Cytoskeleton*, 66: 958-66.

Mersich, A. T., M. R. Miller, H. Chkourko, and S. D. Blystone. 2010. 'The formin FRL1 (FMNL1) is an essential component of macrophage podosomes', *Cytoskeleton (Hoboken)*, 67: 573-85.

Mhawech, P. 2005. '14-3-3 proteins--an update', *Cell Res*, 15: 228-36.

Miano, J. M., P. Cserjesi, K. L. Ligon, M. Periasamy, and E. N. Olson. 1994. 'Smooth muscle myosin heavy chain exclusively marks the smooth muscle lineage during mouse embryogenesis', *Circ Res*, 75: 803-12.

Miki, H., Y. Okada, and N. Hirokawa. 2005. 'Analysis of the kinesin superfamily: insights into structure and function', *Trends Cell Biol*, 15: 467-76.

Miki, H., M. Setou, K. Kaneshiro, and N. Hirokawa. 2001. 'All kinesin superfamily protein, KIF, genes in mouse and human', *Proc Natl Acad Sci U S A*, 98: 7004-11.

Mitchison, T., and M. Kirschner. 1984. 'Dynamic instability of microtubule growth', *Nature*, 312: 237-42.

Moller, N. P., K. B. Moller, R. Lammers, A. Kharitonenkov, I. Sures, and A. Ullrich. 1994. 'Src kinase associates with a member of a distinct subfamily of protein-tyrosine phosphatases containing an ezrin-like domain', *Proc Natl Acad Sci U S A*, 91: 7477-81.

Moore, B. W., and D. McGregor. 1965. 'Chromatographic and Electrophoretic Fractionation of Soluble Proteins of Brain and Liver', *J Biol Chem*, 240: 1647-53.

Moreau, V., F. Tatin, C. Varon, and E. Genot. 2003. 'Actin can reorganize into podosomes in aortic endothelial cells, a process controlled by Cdc42 and RhoA', *Mol Cell Biol*, 23: 6809-22.

Morfini, G. A., Y. M. You, S. L. Pollema, A. Kaminska, K. Liu, K. Yoshioka, B. Bjorkblom, E. T. Coffey, C. Bagnato, D. Han, C. F. Huang, G. Banker, G. Pigino, and S. T. Brady. 2009. 'Pathogenic huntingtin inhibits fast axonal transport by activating JNK3 and phosphorylating kinesin', *Nat Neurosci*, 12: 864-71.

Mostowy, S., and P. Cossart. 2012. 'Septins: the fourth component of the cytoskeleton', *Nat Rev Mol Cell Biol*, 13: 183-94.

Mrowiec, T., and B. Schwappach. 2006. '14-3-3 proteins in membrane protein transport', *Biol Chem*, 387: 1227-36.

Mueller, S. C., G. Ghersi, S. K. Akiyama, Q. X. Sang, L. Howard, M. Pineiro-Sanchez, H. Nakahara, Y. Yeh, and W. T. Chen. 1999. 'A novel protease-docking function of integrin at invadopodia', *J Biol Chem*, 274: 24947-52.

Murphy, D. A., and S. A. Courtneidge. 2011. 'The 'ins' and 'outs' of podosomes and invadopodia: characteristics, formation and function', *Nat Rev Mol Cell Biol*, 12: 413-26.

Muslin, A. J., J. W. Tanner, P. M. Allen, and A. S. Shaw. 1996. 'Interaction of 14-3-3 with signaling proteins is mediated by the recognition of phosphoserine', *Cell*, 84: 889-97.

Myers, R. B., L. Wei, and J. J. Castellot, Jr. 2014. 'The matricellular protein CCN5 regulates podosome function via interaction with integrin alphavbeta 3', *J Cell Commun Signal*, 8: 135-46.

Naber, N., T. J. Minehardt, S. Rice, X. Chen, J. Grammer, M. Matuska, R. D. Vale, P. A. Kollman, R. Car, R. G. Yount, R. Cooke, and E. Pate. 2003. 'Closing of the nucleotide pocket of kinesin-family motors upon binding to microtubules', *Science*, 300: 798-801.

Nakajima, K., Y. Takei, Y. Tanaka, T. Nakagawa, T. Nakata, Y. Noda, M. Setou, and N. Hirokawa. 2002. 'Molecular motor KIF1C is not essential for mouse survival and motor-dependent retrograde Golgi apparatus-to-endoplasmic reticulum transport', *Mol Cell Biol*, 22: 866-73.

Nakata, T., and N. Hirokawa. 1995. 'Point mutation of adenosine triphosphate-binding motif generated rigor kinesin that selectively blocks anterograde lysosome membrane transport', *J Cell Biol*, 131: 1039-53.

Nangaku, M., R. Sato-Yoshitake, Y. Okada, Y. Noda, R. Takemura, H. Yamazaki, and N. Hirokawa. 1994. 'KIF1B, a novel microtubule plus end-directed monomeric motor protein for transport of mitochondria', *Cell*, 79: 1209-20.

Noritake, J., T. Watanabe, K. Sato, S. Wang, and K. Kaibuchi. 2005. 'IQGAP1: a key regulator of adhesion and migration', *J Cell Sci*, 118: 2085-92.

Oikawa, T., T. Itoh, and T. Takenawa. 2008. 'Sequential signals toward podosome formation in NIH-src cells', *J Cell Biol*, 182: 157-69.

Okada, Y., and N. Hirokawa. 2000. 'Mechanism of the single-headed processivity: diffusional anchoring between the K-loop of kinesin and the C terminus of tubulin', *Proc Natl Acad Sci U S A*, 97: 640-5.

Okada, Y., H. Yamazaki, Y. Sekine-Aizawa, and N. Hirokawa. 1995. 'The neuron-specific kinesin superfamily protein KIF1A is a unique monomeric motor for anterograde axonal transport of synaptic vesicle precursors', *Cell*, 81: 769-80.

Ory, S., O. Destaing, and P. Jurdic. 2002. 'Microtubule dynamics differentially regulates Rho and Rac activity and triggers Rho-independent stress fiber formation in macrophage polykaryons', *Eur J Cell Biol*, 81: 351-62.

Otsuka, A. J., A. Jeyaprakash, J. Garcia-Anoveros, L. Z. Tang, G. Fisk, T. Hartshorne, R. Franco, and T. Born. 1991. 'The C. elegans unc-104 gene encodes a putative kinesin heavy chain-like protein', *Neuron*, 6: 113-22.

Pankov, R., E. Cukierman, B. Z. Katz, K. Matsumoto, D. C. Lin, S. Lin, C. Hahn, and K. M. Yamada. 2000. 'Integrin dynamics and matrix assembly: tensin-dependent translocation of alpha(5)beta(1) integrins promotes early fibronectin

fibrillogenesis', *J Cell Biol*, 148: 1075-90.
Parsons, J. T., A. R. Horwitz, and M. A. Schwartz. 2010. 'Cell adhesion: integrating cytoskeletal dynamics and cellular tension', *Nat Rev Mol Cell Biol*, 11: 633-43.

Pfaff, M., and P. Jurdic. 2001. 'Podosomes in osteoclast-like cells: structural analysis and cooperative roles of paxillin, proline-rich tyrosine kinase 2 (Pyk2) and integrin alphaVbeta3', *J Cell Sci*, 114: 2775-86.

Pixley, F. J. 2012. 'Macrophage Migration and Its Regulation by CSF-1', *Int J Cell Biol*, 2012: 501962.

Pletjushkina, O. J., A. M. Belkin, O. J. Ivanova, T. Oliver, J. M. Vasiliev, and K. Jacobson. 1998. 'Maturation of cell-substratum focal adhesions induced by depolymerization of microtubules is mediated by increased cortical tension', *Cell Adhes Commun*, 5: 121-35.

Pytela, R., M. D. Pierschbacher, and E. Ruoslahti. 1985. 'A 125/115-kDa cell surface receptor specific for vitronectin interacts with the arginine-glycine-aspartic acid adhesion sequence derived from fibronectin', *Proc Natl Acad Sci U S A*, 82: 5766-70.

Quintavalle, M., L. Elia, G. Condorelli, and S. A. Courtneidge. 2010. 'MicroRNA control of podosome formation in vascular smooth muscle cells in vivo and in vitro', *J Cell Biol*, 189: 13-22.

Ren, X. D., W. B. Kiosses, and M. A. Schwartz. 1999. 'Regulation of the small GTP-binding protein Rho by cell adhesion and the cytoskeleton', *EMBO J*, 18: 578-85.

Revenu, C., R. Athman, S. Robine, and D. Louvard. 2004. 'The co-workers of actin filaments: from cell structures to signals', *Nat Rev Mol Cell Biol*, 5: 635-46.

Rinnerthaler, G., B. Geiger, and J. V. Small. 1988. 'Contact formation during fibroblast locomotion: involvement of membrane ruffles and microtubules', *J Cell Biol*, 106: 747-60.

Rogers, K. R., S. Weiss, I. Crevel, P. J. Brophy, M. Geeves, and R. Cross. 2001. 'KIF1D is a fast non-processive kinesin that demonstrates novel K-loop-dependent mechanochemistry', *EMBO J*, 20: 5101-13.

Rudijanto, A. 2007. 'The role of vascular smooth muscle cells on the pathogenesis of atherosclerosis', *Acta Med Indones*, 39: 86-93.

Saltel, F., A. Chabadel, E. Bonnelye, and P. Jurdic. 2008. 'Actin cytoskeletal organisation in osteoclasts: a model to decipher transmigration and matrix degradation', *Eur J Cell Biol*, 87: 459-68.

Schachtner, H., S. D. Calaminus, S. G. Thomas, and L. M. Machesky. 2013. 'Podosomes in adhesion, migration, mechanosensing and matrix remodeling', *Cytoskeleton (Hoboken)*, 70: 572-89.

Schiefermeier, N., J. M. Scheffler, M. E. de Araujo, T. Stasyk, T. Yordanov, H. L. Ebner, M. Offterdinger, S. Munck, M. W. Hess, S. A. Wickstrom, A. Lange, W. Wunderlich, R. Fassler, D. Teis, and L. A. Huber. 2014. 'The late endosomal p14-MP1 (LAMTOR2/3) complex regulates focal adhesion dynamics during cell migration', *J Cell Biol*, 205: 525-40.

Schlager, M. A., L. C. Kapitein, I. Grigoriev, G. M. Burzynski, P. S. Wulf, N. Keijzer, E. de Graaff, M. Fukuda, I. T. Shepherd, A. Akhmanova, and C. C. Hoogenraad. 2010. 'Pericentrosomal targeting of Rab6 secretory vesicles by Bicaudal-D-related protein 1 (BICDR-1) regulates neuritogenesis', *EMBO J*, 29: 1637-51.

Scholey, J. M., M. E. Porter, P. M. Grissom, and J. R. McIntosh. 1985. 'Identification of kinesin in sea urchin eggs, and evidence for its localization in the mitotic spindle', *Nature*, 318: 483-6.

Seals, D. F., E. F. Azucena, Jr., I. Pass, L. Tesfay, R. Gordon, M. Woodrow, J. H. Resau, and S. A. Courtneidge. 2005. 'The adaptor protein Tks5/Fish is required for podosome formation and function, and for the protease-driven invasion of cancer cells', *Cancer Cell*, 7: 155-65.

Seano, G., and L. Primo. 2015. 'Podosomes and invadopodia: tools to breach vascular basement membrane', *Cell Cycle*, 14: 1370-4.

Siegrist, S. E., and C. Q. Doe. 2005. 'Microtubule-induced Pins/Galphai cortical polarity in Drosophila neuroblasts', *Cell*, 123: 1323-35.

Simpson, J. C., B. Joggerst, V. Laketa, F. Verissimo, C. Cetin, H. Erfle, M. G. Bexiga, V. R. Singan, J. K. Heriche, B. Neumann, A. Mateos, J. Blake, S. Bechtel, V. Benes, S. Wiemann, J. Ellenberg, and R. Pepperkok. 2012. 'Genome-wide RNAi screening identifies human proteins with a regulatory function in the early secretory pathway', *Nat Cell Biol*, 14: 764-74.

Small, J. V., B. Geiger, I. Kaverina, and A. Bershadsky. 2002. 'How do microtubules guide migrating cells?', *Nat Rev Mol Cell Biol*, 3: 957-64.

Soppina, V., S. R. Norris, A. S. Dizaji, M. Kortus, S. Veatch, M. Peckham, and K. J. Verhey. 2014. 'Dimerization of mammalian kinesin-3 motors results in superprocessive motion', *Proc Natl Acad Sci U S A*, 111: 5562-7.

Soppina, V., and K. J. Verhey. 2014. 'The family-specific K-loop influences the microtubule on-rate but not the superprocessivity of kinesin-3 motors', *Mol Biol Cell*, 25: 2161-70.

Storrie, B., M. Micaroni, G. P. Morgan, N. Jones, J. A. Kamykowski, N. Wilkins, T. H. Pan, and B. J. Marsh. 2012. 'Electron tomography reveals Rab6 is essential to the trafficking of trans-Golgi clathrin and COPI-coated vesicles and the maintenance of Golgi cisternal number', *Traffic*, 13: 727-44.

Straube, A., G. Hause, G. Fink, and G. Steinberg. 2006. 'Conventional kinesin mediates microtubule-microtubule interactions in vivo', *Mol Biol Cell*, 17: 907-16.

Sung, H. H., I. A. Telley, P. Papadaki, A. Ephrussi, T. Surrey, and P. Rorth. 2008. 'Drosophila ensconsin promotes productive recruitment of Kinesin-1 to microtubules', *Dev Cell*, 15: 866-76.

Tanaka, H., H. H. Wang, S. E. Thatcher, H. Hagiwara, H. Takano-Ohmuro, and K. Kohama. 2015. 'Electron microscopic examination of podosomes induced by phorbol 12, 13 dibutyrate on the surface of A7r5 cells', *J Pharmacol Sci*, 128: 78-82.

Tarone, G., D. Cirillo, F. G. Giancotti, P. M. Comoglio, and P. C. Marchisio. 1985. 'Rous sarcoma virus-transformed fibroblasts adhere primarily at discrete protrusions of the ventral membrane called podosomes', *Exp Cell Res*, 159: 141-57.

Tatin, F., C. Varon, E. Genot, and V. Moreau. 2006. 'A signalling cascade involving PKC, Src and Cdc42 regulates podosome assembly in cultured endothelial cells in response to phorbol ester', *J Cell Sci*, 119: 769-81.

Tehrani, S., N. Tomasevic, S. Weed, R. Sakowicz, and J. A. Cooper. 2007. 'Src phosphorylation of cortactin enhances actin assembly', *Proc Natl Acad Sci U S A*, 104: 11933-8.

Theisen, U., E. Straube, and A. Straube. 2012. 'Directional persistence of migrating cells requires Kif1C-mediated stabilization of trailing adhesions', *Dev Cell*, 23: 1153-66.

Trinczek, B., A. Ebneth, E. M. Mandelkow, and E. Mandelkow. 1999. 'Tau regulates the attachment/detachment but not the speed of motors in microtubule-dependent transport of single vesicles and organelles', *J Cell Sci*, 112 (Pt 14): 2355-67.

Vagnoni, A., L. Rodriguez, C. Manser, K. J. De Vos, and C. C. Miller. 2011. 'Phosphorylation of kinesin light chain 1 at serine 460 modulates binding and trafficking of calsyntenin-1', *J Cell Sci*, 124: 1032-42.

Vale, R. D., R. Case, E. Sablin, C. Hart, and R. Fletterick. 2000. 'Searching for kinesin's mechanical amplifier', *Philos Trans R Soc Lond B Biol Sci*, 355: 449-57.

Vale, R. D., T. S. Reese, and M. P. Sheetz. 1985. 'Identification of a novel force-generating protein, kinesin, involved in microtubule-based motility', *Cell*, 42: 39-50.

van den Dries, K., M. B. Meddens, S. de Keijzer, S. Shekhar, V. Subramaniam, C. G. Figdor, and A. Cambi. 2013. 'Interplay between myosin IIA-mediated contractility and actin network integrity orchestrates podosome composition and oscillations', *Nat Commun*, 4: 1412.

van den Dries, K., S. L. Schwartz, J. Byars, M. B. Meddens, M. Bolomini-Vittori, D. S. Lidke, C. G. Figdor, K. A. Lidke, and A. Cambi. 2013b. 'Dual-color superresolution microscopy reveals nanoscale organization of mechanosensory podosomes', *Mol Biol Cell*, 24: 2112-23.

Van Lierop, J. E., D. P. Wilson, J. P. Davis, S. Tikunova, C. Sutherland, M. P. Walsh, and J. D. Johnson. 2002. 'Activation of smooth muscle myosin light chain kinase by calmodulin. Role of LYS(30) and GLY(40)', *J Biol Chem*, 277: 6550-8.

Vogel, H. J. 1994. 'The Merck Frosst Award Lecture 1994. Calmodulin: a versatile calcium mediator protein', *Biochem Cell Biol*, 72: 357-76.

Walde, M., J. Monypenny, R. Heintzmann, G. E. Jones, and S. Cox. 2014. 'Vinculin binding angle in podosomes revealed by high resolution microscopy', *PLoS One*, 9: e88251.

Webb, D. J., K. Donais, L. A. Whitmore, S. M. Thomas, C. E. Turner, J. T. Parsons, and A. F. Horwitz. 2004. 'FAK-Src signalling through paxillin, ERK and MLCK regulates adhesion disassembly', *Nat Cell Biol*, 6: 154-61.

West, M. A., A. R. Prescott, K. M. Chan, Z. Zhou, S. Rose-John, J. Scheller, and C. Watts. 2008. 'TLR ligand-induced podosome disassembly in dendritic cells is ADAM17 dependent', *J Cell Biol*, 182: 993-1005.

Wiesner, C., J. Faix, M. Himmel, F. Bentzien, and S. Linder. 2010. 'KIF5B and KIF3A/KIF3B kinesins drive MT1-MMP surface exposure, CD44 shedding, and extracellular matrix degradation in primary macrophages', *Blood*, 116: 1559-69.

Woehlke, G., A. K. Ruby, C. L. Hart, B. Ly, N. Hom-Booher, and R. D. Vale. 1997. 'Microtubule interaction site of the kinesin motor', *Cell*, 90: 207-16.

Woodsome, T. P., M. Eto, A. Everett, D. L. Brautigan, and T. Kitazawa. 2001. 'Expression of CPI-17 and myosin phosphatase correlates with Ca(2+) sensitivity of protein kinase C-induced contraction in rabbit smooth muscle', *J Physiol*, 535: 553-64.

Xiao, B., S. J. Smerdon, D. H. Jones, G. G. Dodson, Y. Soneji, A. Aitken, and S. J. Gamblin. 1995. 'Structure of a 14-3-3 protein and implications for coordination of multiple signalling pathways', *Nature*, 376: 188-91.

Xiao, H., X. H. Bai, A. Kapus, W. Y. Lu, A. S. Mak, and M. Liu. 2010. 'The protein kinase C cascade regulates recruitment of matrix metalloprotease 9 to podosomes and its release and activation', *Mol Cell Biol*, 30: 5545-61.

Yamazaki, H., T. Nakata, Y. Okada, and N. Hirokawa. 1996. 'Cloning and characterization of KAP3: a novel kinesin superfamily-associated protein of KIF3A/3B', *Proc Natl Acad Sci U S A*, 93: 8443-8.

Yu, C. H., N. B. Rafiq, A. Krishnasamy, K. L. Hartman, G. E. Jones, A. D. Bershadsky, and M. P. Sheetz. 2013. 'Integrin-matrix clusters form podosome-like adhesions in the absence of traction forces', *Cell Rep*, 5: 1456-68.

Zaidel-Bar, R., S. Itzkovitz, A. Ma'ayan, R. Iyengar, and B. Geiger. 2007. 'Functional atlas of the integrin adhesome', *Nat Cell Biol*, 9: 858-67.

Zambonin-Zallone, A., A. Teti, M. Grano, A. Rubinacci, M. Abbadini, M. Gaboli, and P. C. Marchisio. 1989. 'Immunocytochemical distribution of extracellular matrix receptors in human osteoclasts: a beta 3 integrin is colocalized with vinculin and talin in the podosomes of osteoclastoma giant cells', *Exp Cell Res*, 182: 645-52.

Zamir, E., M. Katz, Y. Posen, N. Erez, K. M. Yamada, B. Z. Katz, S. Lin, D. C. Lin, A. Bershadsky, Z. Kam, and B. Geiger. 2000. 'Dynamics and segregation of cell-matrix adhesions in cultured fibroblasts', *Nat Cell Biol*, 2: 191-6.

Zhu, C., J. Zhao, M. Bibikova, J. D. Leverson, E. Bossy-Wetzel, J. B. Fan, R. T. Abraham, and W. Jiang. 2005. 'Functional analysis of human microtubule-based motor proteins, the kinesins and dyneins, in mitosis/cytokinesis using RNA interference', *Mol Biol Cell*, 16: 3187-99.

Zhu, X., N. Efimova, C. Arnette, S. K. Hanks, and I. Kaverina. 2016. 'Podosome dynamics and location in vascular smooth muscle cells require CLASP-dependent microtubule bending', *Cytoskeleton (Hoboken)*, 73: 300-15.

© 2014. Published by The Company of Biologists Ltd | Journal of Cell Science (2014) 127, 5179–5188 doi:10.1242/jcs.149633

RESEARCH ARTICLE

Podosome-regulating kinesin KIF1C translocates to the cell periphery in a CLASP-dependent manner

Nadia Efimova[1,*], Ashley Grimaldi[1], Alice Bachmann[2], Keyada Frye[1], Xiaodong Zhu[1], Alexander Feoktistov[1], Anne Straube[2] and Irina Kaverina[1,‡]

ABSTRACT

The kinesin KIF1C is known to regulate podosomes, actin-rich adhesion structures that remodel the extracellular matrix during physiological processes. Here, we show that KIF1C is a player in the podosome-inducing signaling cascade. Upon induction of podosome formation by protein kinase C (PKC), KIF1C translocation to the cell periphery intensifies and KIF1C accumulates both in the proximity of peripheral microtubules that show enrichment for the plus-tip-associated proteins CLASPs and around podosomes. Importantly, without CLASPs, both KIF1C trafficking and podosome formation are suppressed. Moreover, chimeric mitochondrially targeted CLASP2 recruits KIF1C, suggesting a transient CLASP–KIF1C association. We propose that CLASPs create preferred microtubule tracks for KIF1C to promote podosome induction downstream of PKC.

KEY WORDS: CLASP, KIF1C, Podosome, Kinesin, Microtubule, Trafficking

INTRODUCTION

Microtubules (MTs) serve to deliver and position molecular complexes and organelles within a cell, thereby defining its architecture. An important part of this function is locating the sites of actin cytoskeleton assembly and remodeling (Hoogenraad and Akhmanova, 2010; Kaverina and Straube, 2011; Etienne-Manneville, 2013). Amongst other actin-based structures, MTs regulate invasive protrusions, termed podosomes (Babb et al., 1997; Linder et al., 2000; Destaing et al., 2003; Evans et al., 2003; Destaing et al., 2005; Jurdic et al., 2006; Kopp et al., 2006; Gil-Henn et al., 2007; Purev et al., 2009; McMichael et al., 2010; Biosse Duplan et al., 2014), and their cancer counterparts, invadopodia (Schoumacher et al., 2010; Quintavalle et al., 2011).

Podosomes consist of a core of constantly polymerizing actin filaments and an outer adhesive ring. These structures serve as exocytosis sites for matrix metalloproteases (MMPs) (Lener et al., 2006; Gimona et al., 2008; Linder et al., 2011; Murphy and Courtneidge, 2011). Podosomes are found in multiple extracellular matrix (ECM)-remodeling cells, such as osteoclasts, macrophages and synthetic vascular smooth muscle cells (VSMCs). In these cell types, efficient ECM remodeling does not occur if podosomes are not present. A growing body of evidence implicates podosome-dependent ECM remodeling in cell migration and invasion during morphogenesis (Teti et al., 1991; Lener et al., 2006; Gil-Henn et al., 2007; Proszynski et al., 2009; Rottiers et al., 2009; Quintavalle et al., 2010; Linder et al., 2011; Saltel et al., 2011). For example, the ECM-remodeling capacity of synthetic VSMCs is important for angiogenesis and vascular repair (Lener et al., 2006; Quintavalle et al., 2010; Chen et al., 2013). Also, the migration and invasion potentials of VSMCs have a direct impact on atherosclerotic plaque formation and stability (Quintavalle et al., 2010; Lacolley et al., 2012; Chen et al., 2013).

Podosomes are dynamic structures and are induced or disassembled in response to physiological signals (Chambers and Fuller, 2011; Dovas and Cox, 2011; van Helden and Hordijk, 2011; Hoshino et al., 2013). Podosome dynamics are strongly regulated by MTs (Babb et al., 1997; Linder et al., 2000; Destaing et al., 2003; Evans et al., 2003; Destaing et al., 2005; Jurdic et al., 2006; Kopp et al., 2006; Gil-Henn et al., 2007; Purev et al., 2009; McMichael et al., 2010; Biosse Duplan et al., 2014). It has become clear from a number of recent studies that MT–podosome relationships are multifaceted – both stable (acetylated; Destaing et al., 2005; Purev et al., 2009; Biosse Duplan et al., 2014) and dynamic (Kopp et al., 2006; Biosse Duplan et al., 2014) MT subpopulations are essential for podosome regulation. Moreover, several independent molecular machineries structurally and/or functionally link MTs to podosomes, including tubulin acetylation enzymes (Destaing et al., 2005; Purev et al., 2009; Biosse Duplan et al., 2014), MT plus-end-associated protein complexes (EB1; Biosse Duplan et al., 2014), actin-dependent molecular motors (myosin-X; McMichael et al., 2010) and several MT-dependent molecular motors (Kopp et al., 2006; Wiesner et al., 2010; Cornfine et al., 2011). Within the last group, podosome function in ECM remodeling crucially depends on the kinesins KIF5B, the KIF3A–KIF3B complex and KIF9, which deliver MMPs to podosomes (Wiesner et al., 2010; Cornfine et al., 2011). More intriguingly, the kinesin KIF1C regulates the dynamics of podosomes themselves (Kopp et al., 2006), possibly owing to the capacity of this motor to transport essential podosome components, such as integrins (Theisen et al., 2012). In principle, such transportation could be either constitutive or triggered downstream of physiological signals that induce podosome formation. Activation of KIF1C trafficking would be a suitable regulatory step in the signaling cascade leading to ECM remodeling. However, whether KIF1C transport is regulated by podosome-inducing signals has not been addressed.

In this study, we show that protein kinase C (PKC) activation strongly facilitates KIF1C transport to the cell periphery to initiate podosome formation. Moreover, our results reveal that the

[1]Department of Cell and Developmental Biology, Vanderbilt University Medical Center, Nashville 37232, TN, USA. [2]Centre for Mechanochemical Cell Biology, Warwick Medical School, University of Warwick, Coventry CV4 7AL, UK.
*Present address: Department of Biology, University of Pennsylvania, PA 19104, USA.

‡Author for correspondence (irina.kaverina@vanderbilt.edu)

Received 13 January 2014; Accepted 14 October 2014

Journal of Cell Science (2014) 127, 5179–5188 doi:10.1242/jcs.149633

MT-associated proteins CLASPs are necessary for efficient translocation of KIF1C along MTs and are crucial components of podosome-induction signaling. Taken together, these findings reveal a new pathway within the multifaceted MT-dependent podosome regulation.

RESULTS

Podosome formation in VSMCs requires MTs

In the rat aortic VSMC line A7r5, multiple small podosomes can be rapidly induced by PKC activation by phorbol ester phorbol 12,13-dibutyrate (PDBu) treatment (Hai et al., 2002). Podosomes in VSMCs contain specific podosome markers, such as Tks5 (also known as SH3PXD2A) (Fig. 1A), include accumulations of F-actin with a characteristic morphology (Fig. 1A,C) and are enriched in proteins involved in actin polymerization (Hai et al., 2002; Kaverina et al., 2003; Lener et al., 2006), such as cortactin (Fig. 1A,F).

We took advantage of the PDBu-inducible podosome model to address the regulation of *de novo* podosome formation by MTs. To test whether MTs are essential for podosome formation, we completely depolymerized MTs in A7r5 cells by treatment with nocodazole (supplementary material Fig. S1A–C) and applied PDBu. We found that the number of podosomes formed was significantly decreased under these conditions (Fig. 1D,G,H) to levels comparable to those of non-induced cells (Fig. 1B,E). This indicates that MTs are required for podosome formation in VSMCs, as was described previously for macrophages and osteoclasts (Babb et al., 1997; Linder et al., 2000; Destaing et al., 2003; Evans et al., 2003; Destaing et al., 2005; Jurdic et al., 2006; Kopp et al., 2006; Gil-Henn et al., 2007; Purev et al., 2009; McMichael et al., 2010; Biosse Duplan et al., 2014).

Podosome formation in VSMCs requires KIF1C

It has been proposed that MTs exert their control on podosomes by delivering regulatory and structural molecules to podosome sites by MT-dependent transport. Indeed, one of the few identified molecular players that is essential for podosome turnover is the kinesin KIF1C (Kopp et al., 2006). Interestingly, we found that KIF1C was enriched at podosome sites in A7r5 cells (Fig. 1I). By performing small interfering (si)RNA-mediated depletion of KIF1C in A7r5 cells (Fig. 2I,J), we found that the number and size of PDBu-induced podosomes were significantly decreased in the absence of this kinesin (Fig. 2A–H). This phenotype was rescued by re-expression of RNA interference (RNAi)-resistant KIF1C–GFP (Fig. 2K–N), indicating the specificity of the depletion phenotype. In agreement with this result, the expression of dominant-negative mutants of KIF1C [either a truncated cargo-binding tail domain (Fig. 2P) or motor-dead rigor mutant (Fig. 2Q)] mimicked the effect of KIF1C depletion (Fig. 2O–R). The effects of KIF1C loss of function were very significant but milder than the effect of complete MT depolymerization (Fig. 1), suggesting that KIF1C is an essential, although not the only, factor in MT-dependent podosome regulation. These data indicate that KIF1C is required for efficient podosome formation in VSMCs.

The PKC pathway facilitates MT-dependent transport of KIF1C to the cell periphery

Next, we questioned whether KIF1C-dependent trafficking is regulated as part of the podosome induction pathway downstream of PKC. Using A7r5 cells stably expressing low levels of KIF1C–GFP (supplementary material Fig. S1E), we found that PDBu treatment strongly stimulated KIF1C–GFP translocation to the cell periphery (Fig. 3A–C; supplementary material Movies 1, 2). In contrast to cell-center localization in control cells, KIF1C accumulated at the cell edge and at the ventral surface of the lamellae in PDBu-treated cells (Fig. 3D,E). This localization was abolished by nocodazole treatment (Fig. 3F–H; supplementary material Fig. S1A,B), indicating that KIF1C targeting to the cell periphery was MT-dependent. This result indicates that KIF1C

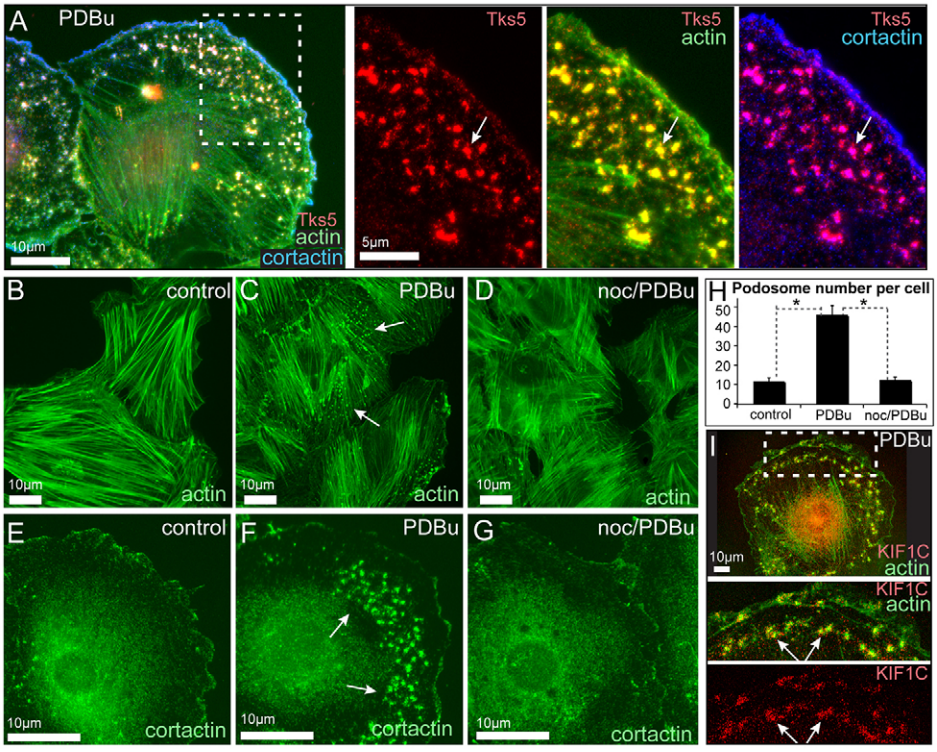

Fig. 1. Podosome formation in A7r5 cells requires MTs. (A) Visualization of podosomes in a PDBu-treated A7r5 cell by expression of Tks5–GFP (red) and immunofluorescence detection of actin (phalloidin, green) and cortactin (blue). The boxed region from the overview (left) is enlarged on the right and shows Tks5-positive podosomes and their colocalization with actin and cortactin. Maximal-intensity projection of a confocal stack. Arrows, podosomes. (B–G) Wide-field fluorescence microscopy of actin (phalloidin, B–D) and cortactin (E–G) in A7r5 cells. Multiple podosomes are spread throughout a cell after 40 minutes of PDBu treatment (C,F) in contrast to untreated cells (B,E) or cells pre-treated with nocodazole for 2 hours before PDBu application (D,G). Arrows, podosomes. (H) Podosome numbers based on cortactin staining (similar to E–G). Data show the mean+s.e.m. ($N=40\pm10$); $^{*}P<1\times10^{-6}$ (Student's unpaired two-tailed *t*-test). (I) KIF1C (red) accumulates at the cell edge and podosomes (arrows). Phalloidin, green. The boxed region from the overview (upper panel) is enlarged below.

Journal of Cell Science (2014) 127, 5179–5188 doi:10.1242/jcs.149633

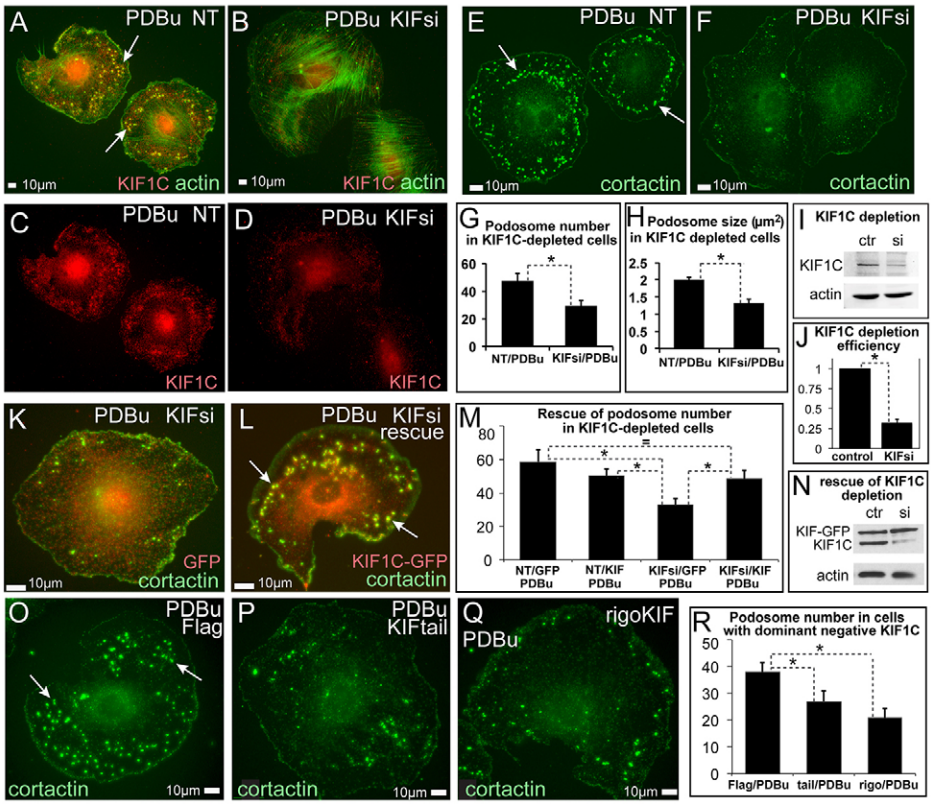

Fig. 2. Podosome formation in A7r5 cells depends on KIF1C. (A–F) Immunofluorescence visualization of podosomes by actin (phalloidin, green, A,B) and cortactin (green, E,F). KIF1C (red) is shown in C,D for cells in A,B. NT, non-targeted control siRNA-treated; KIFsi, KIF1C-depleted. (B,D,F) After KIF1C depletion only few immature podosomes are detected. The remaining KIF1C is detected in the cell center (D). (G) Podosome numbers based on data similar to that shown in E,F. Data show the mean+s.e.m. (N=32); *P<0.01 (Student's unpaired two-tailed t-test). (H) Average of mean podosome area per cell (μm^2) based on data similar to that shown in E,F. Data show the mean+s.e.m. (N=32). *P<1×10^{-6} (Student's unpaired two-tailed t-test). (I) Western blotting indicates significant depletion of KIF1C. Actin is shown as a loading control. Ctr, control; si, KIF1C-depleted. (J) Quantification of KIF1C levels detected by western blotting. Data show the mean+s.e.m. (N=3); *P<0.001 (Student's unpaired two-tailed t-test). (K,L) Re-expression of KIF1C–GFP (red) in KIF1C-depleted cells (L) rescues podosome formation as compared with that of GFP-expressing KIF1C-depleted cells (K). GFP is pseudo-colored red. Cortactin, green. (M) Podosome numbers in KIF1C-depleted and rescued cells. Data show the mean+s.e.m. (N=45); *P<0.05 (Student's unpaired two-tailed t-test). (N) Western blotting indicates KIF1C–GFP expression in control and KIF1C-depleted cells. Actin is shown as a loading control. (O–Q) Expression of dominant-negative FLAG-tagged KIF1C cargo-binding domain (P) or rigor motor mutant (Q) suppresses podosome formation as compared with that of controls (O). Cortactin, green. All arrows indicate podosomes. (R) Podosome numbers in cells expressing dominant-negative constructs. Data show the mean+s.e.m. (N=45); *P<0.05 (Student's unpaired two-tailed t-test).

transport is regulated by podosome-inducing signals and is therefore an essential step in the signaling cascade leading to ECM remodeling.

KIF1C moves along CLASP-associated MTs and can be recruited by CLASPs

In agreement with a prior finding of Kopp and colleagues in macrophages (Kopp et al., 2006), we found that, in VSMCs, KIF1C puncta undergo movements predominantly when associated with the plus ends of polymerizing MTs (supplementary material Fig. S1F,G; Movies 3, 4). This suggests that KIF1C translocates along MTs in close association with the MT plus-end tracking protein (+TIP) complex. Because deposition of KIF1C at the cell periphery was dramatically increased by PDBu treatment, we tested whether cellular localization of major +TIPs was influenced by PDBu. We were looking for a protein that would localize more strongly to MTs during PDBu treatment than in controls and, therefore, could be a positive regulator of KIF1C transport. Among the proteins tested, certain proteins responded to PDBu treatment by decreased MT-plus-end association, including EB1 (not shown), which was recently detected as an important podosome regulator (Biosse Duplan et al., 2014); other proteins did not change significantly (e.g. CLIP170, not shown). Importantly, we found a striking change in localization of +TIPs called CLIP-associated proteins (CLASPs, CLASP1 and CLASP2), which are known to facilitate MT polymerization and stability (Galjart, 2005; Al-Bassam and Chang, 2011). Although immunofluorescent staining for CLASPs normally highlighted short MT plus-end-tracking comets throughout the whole cell, in PDBu-treated cells, CLASPs were arranged in extended patterns only at the cell periphery (Fig. 4A,B); this indicated that CLASP binding to peripheral MT lattice was specifically enhanced by PDBu. We hypothesized that the relocation of CLASPs in response to PKC might be involved in the PDBu-stimulated activation of KIF1C transport to podosomes and, thus, we concentrated on this protein in this study.

Interestingly, CLASP-associated MTs were located in the podosome-rich regions of the cell and were frequently found in close contact with podosomes (Fig. 4B) and peripheral accumulations of KIF1C (Fig. 4C). Live-cell imaging indicated that KIF1C at the cell periphery moved predominantly in association with CLASP-rich peripheral MTs and accumulated

Journal of Cell Science (2014) 127, 5179–5188 doi:10.1242/jcs.149633

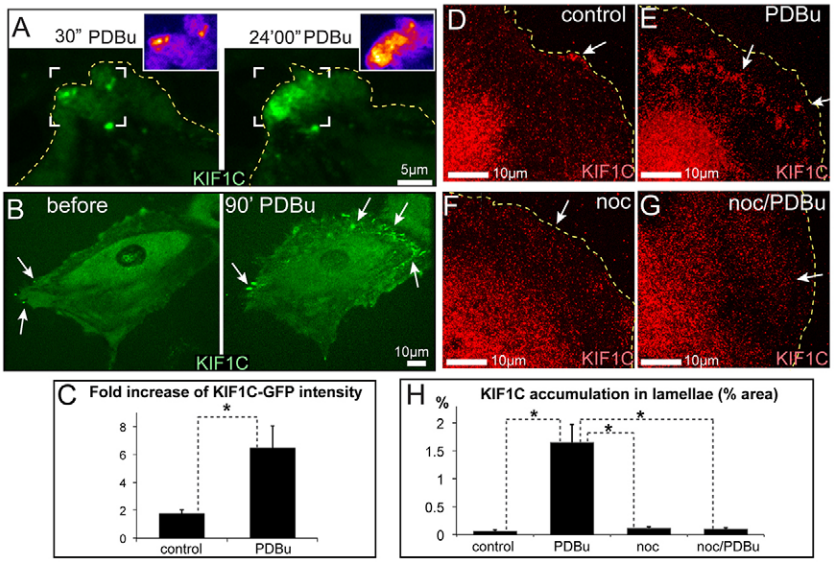

Fig. 3. Podosome induction signaling facilitates MT-dependent KIF1C deposition in lamellae. (A) PDBu facilitates the accumulation of KIF1C–GFP (green) in the cell periphery. Frames from a single-plane confocal image sequence at 30 seconds (left) and 24 minutes (right) of PDBu treatment. Pseudo-colored maps of KIF1C intensity [purple (low) to white (high)] at the indicated areas (white brackets) are shown to the upper right. See supplementary material Movie 1. (B) Deposition of KIF1C–GFP (green) in cell lamellae before (left) and after (right) a 90-minute PDBu treatment. See supplementary material Movie 2. (C) Fold increase in KIF1C–GFP intensity in cell lamellae in live cells with or without PDBu treatment, based on data as shown in B. Data show the mean+s.e.m. (N=6–12); *P<0.01 (Student's unpaired two-tailed t-test). (D–G) Immunostained KIF1C (red, arrows) at the cell periphery. KIF1C modestly localizes to the lamellae of untreated cells (D), and accumulates in cell lamellae after a 40-minute PDBu treatment (E). No KIF1C accumulations are found in nocodazole (noc)-treated (F) and nocodazole-pretreated plus PDBu-treated (G) cells. The images show maximal intensity projections of confocal stacks. Arrows show KIF1C accumulations; dashed lines indicate cell outlines. (H) The percentage of the area in cell lamellae taken up by KIF1C accumulation, based on data as shown in D–G. Data show the mean+s.e.m. (N=10); *P<0.001 (Student's unpaired two-tailed t-test).

in the vicinity of their ends (Fig. 4C,D; supplementary material Fig. S1D; Movies 5, 6).

Thus, it is possible that CLASPs promote KIF1C transport; for example, by stimulating KIF1C recruitment to MTs. In agreement with this hypothesis, when a chimeric protein, in which CLASP2 was combined with the mitochondrial component TOM20 [mito-CLASP, (Efimov et al., 2007)], was expressed in cells, a significant fraction of KIF1C–GFP accumulated at the mitochondria, indicating that KIF1C–GFP followed the CLASP chimera (Fig. 4E–H; supplementary material Fig. S2A,B). This recruitment is likely mediated by the tail domain of KIF1C, because the tail domain (Fig. 4E,F,I,J; supplementary material Fig. S2C,D) but not the KIF1C motor domain (not shown) was significantly recruited to mitochondria by mito-CLASP. Interestingly, full-length KIF1C that was recruited to mitochondria by mito-CLASP was likely functional and responsive to PKC activation; this was evident from relocation of mitochondria towards the cell periphery in transfected cells (Fig. 4K–M; supplementary material Fig. S2E,F). These data indicate that in cells CLASPs interact with a subset of KIF1C molecules through the KIF1C tail domain.

CLASPs are necessary for KIF1C trafficking and deposition at the cell periphery

The evidence that KIF1C transiently associates with CLASPs suggests that CLASPs might be important for KIF1C transport to the sites of podosome formation. Thus, we tested whether CLASPs modulate KIF1C targeting to the cell periphery. Strikingly, CLASP depletion, by two alternative siRNA combinations (Fig. 5A; supplementary material Fig. S3), completely abolished KIF1C accumulation at the cell edge and at podosome formation sites (Fig. 5B–E; supplementary material Fig. S4A–C). In CLASP-depleted cells, KIF1C-positive puncta were diffuse throughout the cell body; however, KIF1C protein levels were not affected by CLASP depletion (supplementary material Fig. S3D). Distribution of KIF1C in CLASP-depleted cells was similar to that observed in nocodazole-treated cells lacking MTs (Fig. 3G,H; supplementary material Fig. S1B), suggesting that without CLASP, MTs cannot support KIF1C transport to the cell periphery. Decreased translocation of KIF1C to the cell periphery might, in principle, be explained by the low MT number in CLASP-depleted cells (Mimori-Kiyosue et al., 2005; Efimov et al., 2007). To test this possibility, we addressed whether KIF1C accumulations could be found at MT plus ends in CLASP-depleted cells. We found that, in sharp contrast to the control cells, no KIF1C accumulation could be detected in association with MTs under these conditions (Fig. 5C,D; supplementary material Fig. S4B,C); this indicates that deficient KIF1C distribution at the cell periphery did not result from the decrease in MT number in CLASP-depleted cells. Rather, our data suggest that translocation of this motor along MTs is blocked without CLASPs.

To test this hypothesis directly, we followed KIF1C–GFP motility in CLASP-depleted and control cells by live-cell imaging. In control cells, KIF1C–GFP puncta and tubes often underwent fast directional translocations typical of MT-dependent membrane trafficking (Fig. 5F,G; supplementary material Movie 7, left). Interestingly, in the absence of CLASPs, these movements were largely abolished (Fig. 5H–J; supplementary material Fig. S4D,E; Movie 7, right), indicating that CLASPs are required for KIF1C transport along MTs.

CLASPs are necessary for podosome formation

Because the podosome-stimulating kinesin KIF1C cannot translocate to the cell periphery in CLASP-depleted cells, one

Journal of Cell Science (2014) 127, 5179–5188 doi:10.1242/jcs.149633

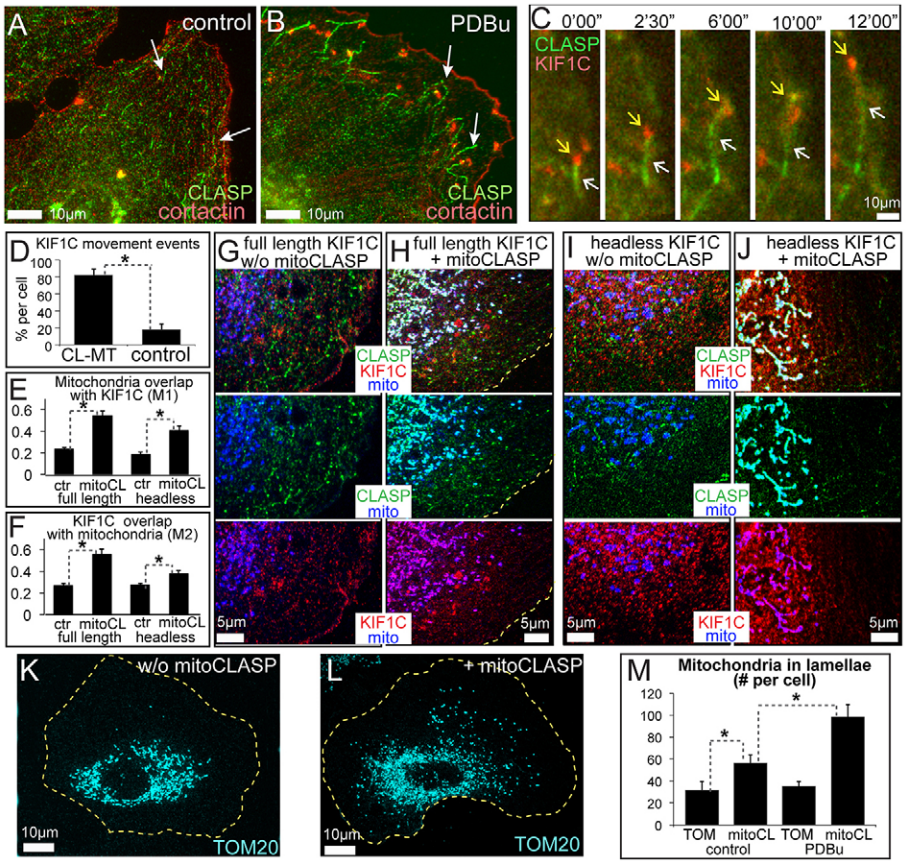

Fig. 4. KIF1C associates with CLASP-rich MTs. (A,B) CLASPs (green, white arrows) mark MT plus ends in a non-treated cell (A), but upon PDBu treatment (B), CLASPs accumulate at the lattice of MTs in close contact with podosomes (cortactin, red). Data show wide-field fluorescence analysis of immunostaining. (C) KIF1C–mCherry (red, yellow arrows) moves with the end of a GFP–CLASP2-associated MT (green, white arrows) in a PDBu-treated cell. Data show frames from a video sequence and are enlarged from the box in supplementary material Fig. S1F. See also supplementary material Movies 5, 6. (D) KIF1C (red) relocation events occurring at the ends of MTs associated with CLASP2 (CL-MT), as compared to the same events superimposed on a spatially shifted RFP–CLASP2 video sequence, based on data as in supplementary material Movies 5, 6. Data show the mean+s.e.m. (N=4 cells, 14–19 events/cell); *P<0.001 (Student's t-test). (E,F) Colocalization of ectopically expressed KIF1C with mitochondria in cells with (mitoCL) or without (ctr) mito-CLASP expression. Mander's coefficients M1 (E) and M2 (F) for thresholded images are shown. Both full-length (left) and (right) and tail domain constructs are recruited to mitochondria by CLASP. Data show the mean+s.e.m. (N=5); *P<0.01 (Student's t-test). (G,H) KIF1C–GFP (red) colocalizes with CLASP (green, immunostained) and mitochondria (mCherry–TOM20, blue) in cells with (H) but not without (w/o, G) mito-CLASP. (I,J) FLAG-tagged KIF1C tail (red) colocalizes with CLASP (green, immunostained) and Mitotracker (blue) in cells with (J) but not without (I) mito-CLASP. See also supplementary material Fig. S2A–D. (K,L) Mitochondria in cells transfected with mCherry–TOM20 alone (K) or mCherry–TOM20 and mito-CLASP (L). See also supplementary material Fig. S2F,G. Yellow dotted lines indicate cell borders. (M) The number of mitochondria in lamellae in cells transfected with mCherry–TOM20 or mito-CLASP, based on the data as shown in K,L. Data show the mean+s.e.m. (N=28–36); *P<0.01 (Student's unpaired two-tailed t-test).

would predict that CLASPs are required for podosome formation. PDBu treatment of cells depleted of CLASPs by two alternative siRNA combinations indicated that podosome numbers, detected by cortactin staining, were dramatically reduced as compared with those of cells treated with non-targeted control siRNA (Fig. 6A–F,K). Podosome numbers in CLASP-depleted cells were efficiently rescued by ectopic expression of CLASP2–RFP, which cannot be silenced by siRNA combination 2 (Fig. 6G–K). Depletion of CLASP1 or CLASP2 separately led to partial podosome suppression (not shown). Thus, it is likely that both CLASPs act redundantly as essential effectors in the podosome induction pathway downstream of PKC.

DISCUSSION

Based on our data, we propose a model in which CLASPs act as essential players in the regulation of podosome formation, because only CLASP-decorated MTs are capable of supporting KIF1C translocation to putative podosome sites at the cell periphery (Fig. 7A). CLASP enrichment at MTs has been shown previously to result from GSK3β inactivation at the cell periphery, which leads to enhanced MT binding of dephosphorylated CLASPs (Wittmann and Waterman-Storer, 2005; Kumar et al., 2009). In our system, this change in MT binding is likely to be caused by PKC-dependent GSK3β inactivation triggered by PDBu treatment (Goode et al., 1992). In organisms, this pathway might be triggered through extracellular factors that induce podosomes, such as PDGF signaling (Quintavalle et al., 2010).

Our data implicate CLASPs as important regulatory factors for the trafficking function of KIF1C. It is also noteworthy that the effects of KIF1C depletion or inactivation are less striking than the effects of CLASP depletion, suggesting that additional factors facilitate podosome formation in a CLASP-dependent manner. It is plausible to suggest that certain molecular motors sharing similarities with KIF1C (e.g. other kinesin-3 family members KIF1B and KIF1A) are involved. However, the nature

Journal of Cell Science (2014) 127, 5179–5188 doi:10.1242/jcs.149633

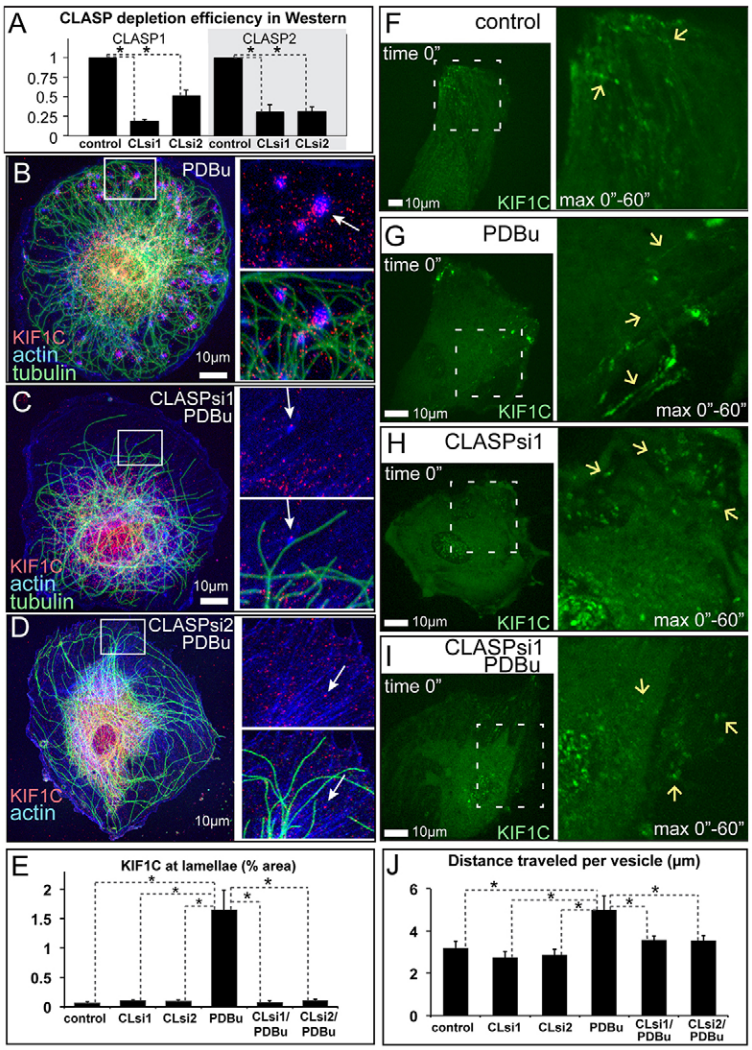

Fig. 5. MT-dependent transport of KIF1C to podosomes requires CLASPs. (A) CLASP1 and CLASP2 depletion levels were investigated by using western blotting in cells depleted of CLASPs by siRNA combinations 1 and 2 (CLsi1, CLsi2). Data show the mean+s.e.m. ($N=3$); *$P<0.01$ (Student's unpaired two-tailed *t*-test). (B–D) KIF1C (red, arrows) accumulates around podosomes in the lamellae of PDBu-treated non-targeted control cells (B), but is missing from the lamellae of CLASP-depleted cells (C,D). Boxed areas on the left are enlarged on the right. Phalloidin, blue; tubulin, green (immunostaining). Images show maximal intensity projections of confocal stacks. (E) The percentage of the area in cell lamellae taken up by KIF1C accumulation, based on data as shown in B–D. The control populations are the same as those shown in Fig. 2C,D. Data show the mean+s.e.m. ($N=10$); *$P<0.001$ (Student's unpaired two-tailed *t*-test). (F–I) KIF1C–GFP (green) trafficking as visualized by a single-plane confocal image sequence. Single-frame cell overviews are shown on the left. Video sequences from the boxed regions are shown on the right as enlarged maximal intensity projections over time. Arrows indicate the tracks of KIF1C particle movement in non-targeted control cells (F,G) and the lack of directional movement in CLASP-depleted cells (H,I), in PDBu-treated (G,I) or untreated (F,H) cells. See supplementary material Movie 7. (J) Directional movement of KIF1C puncta is enhanced by PDBu in control but not CLASP-depleted cells. The graph is based on data as shown in F–I and supplementary material Fig. S4D,E. Data show the mean+s.e.m. ($N=10$–17 cells); *$P<0.05$ (Student's unpaired two-tailed *t*-test).

of additional CLASP-dependent factors is yet unclear; this study is the first direct evidence that CLASPs regulate molecular motor function, which has been previously suggested based on the essential role of CLASPs in specific cellular processes. For example, CLASP-coated Golgi-derived MTs have especially strong capacity for transportation and assembly of Golgi stacks (Miller et al., 2009). Also, CLASP is essential for the transport or positioning of mitochondria in *Schizosaccharomyces pombe* (Chiron et al., 2008), which could be interpreted as a result of CLASP-dependent kinesin regulation in that system.

Because CLASP2 can recruit KIF1C to mitochondria, we propose that MT-bound CLASPs directly stabilize the association of KIF1C with MTs, similar to the recently discovered function of doublecortin–KIF1A cooperation in neurons (Liu et al., 2012) or EB1–KIF17 cooperation in polarizing epithelia (Jaulin and Kreitzer, 2010). A less likely possibility is that CLASPs activate KIF1C in an MT-independent manner, similar to kinesin-1 activation by the MT-associated protein ensconsin (Barlan et al., 2013). In principle, another possible mechanism could involve the indirect effect of a CLASP-dependent increase in MT lifetime and stability (Akhmanova et al., 2001; Mimori-Kiyosue et al., 2005; Drabek et al., 2006; Lansbergen et al., 2006), which has been shown to facilitate transport by specific kinesins (Reed et al., 2006; Cai et al., 2009; Hammond et al., 2010). Stable MTs are indeed important for podosome regulation in osteoclasts (Destaing et al., 2005; Purev et al., 2009). However, KIF1C (similar to another kinesin-3 family member KIF1A; Cai et al., 2009) moves with growing MT plus ends and thus prefers dynamic MT tracks rather than stable ones. Moreover, MT acetylation, typical for stable MTs, suppresses movement of vesicles associated with KIF1C (Bhuwania et al., 2014). Accordingly, we suggest that dynamic CLASP-associated MTs normally serve as preferred tracks for KIF1C transport, and that relocation of CLASPs to peripheral MTs upon PDBu treatment facilitates KIF1C translocation to the lamella and, subsequently, triggers podosome formation (Fig. 7A). This is already the second reported mechanism whereby dynamic, rather than stable, MTs regulate podosome formation and dynamics. It has been shown recently that EB1, a +TIP MT protein that associates only with polymerizing dynamic MT ends, facilitates podosome formation in osteoclasts through an interaction with cortactin (Biosse Duplan et al., 2014). This and our present findings indicate that targeting of podosomes by dynamic MT ends is crucial for regulation of these adhesive structures, a mechanism resembling MT-mediated regulation of focal adhesions (Kaverina et al., 1999). Overall, our data establish CLASPs and KIF1C as sequential molecular players in the signaling cascade downstream

Journal of Cell Science (2014) 127, 5179–5188 doi:10.1242/jcs.149633

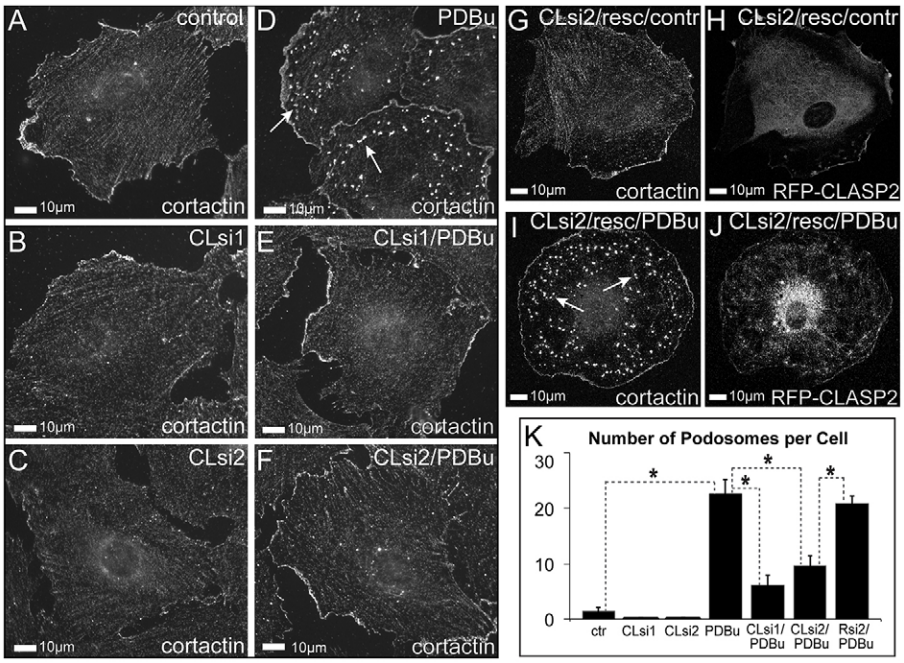

Fig. 6. Podosome formation in A7r5 cells requires CLASPs. (A–F) Cortactin immunostaining of vehicle-treated (A–C) and PDBu-treated (D–F) cells. Arrows, podosomes. Cells were transfected with non-targeted control siRNA (A,D), CLASP-specific siRNA combination 1 (CLsi1; B,E) or CLASP-specific siRNA combination 2 (CLsi2; C,F). Podosomes are formed in controls (D, arrows), but not in CLASP-depleted cells (E,F). Images were acquired by using wide-field fluorescence microscopy. (G–J) In cells treated with CLASP-specific siRNA combination 2, podosome formation in PDBu (I) is rescued by expression of siRNA2-insensitive RFP–CLASP2 (H,J). Cortactin immunostaining is shown in G,I. Arrows show podosomes. (K) Podosome numbers were quantified, based on data similar to that shown in A–J. Data show the mean+s.e.m. (N=45±15); *$P<1\times10^{-5}$ (Student's unpaired two-tailed t-test).

of PKC (Fig. 7B) and as crucial components of the podosome induction pathway.

MATERIALS AND METHODS

Cells

A7r5 rat smooth muscle cells (ATCC) were grown in low-glucose (1000 mg/l) Dulbecco's modified Eagle's medium (DMEM) without Phenol Red, supplemented with 10% fetal bovine serum at 37℃ and 5% CO_2. Cells were plated on glass coverslips or glass-bottomed dishes (MatTek) coated with 10 µg/ml fibronectin 24 hours prior to experiments. In live-cell experiments, cells were maintained on the microscope stage at 37℃ under mineral oil for medium equilibrium maintenance.

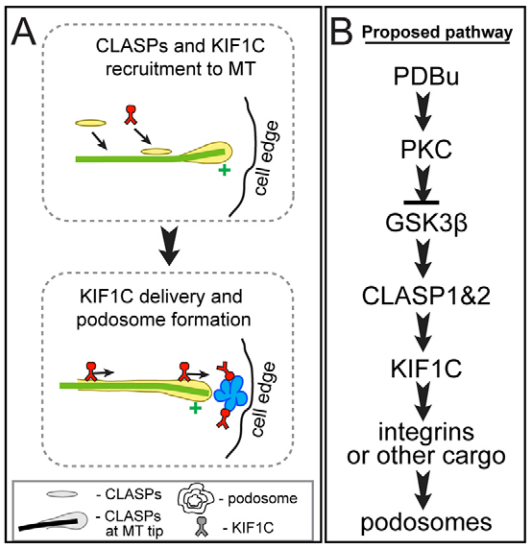

Fig. 7. Models of the roles of CLASPs and KIF1C in podosome formation. (A) A model of podosome regulation by CLASP-dependent KIF1C transportation. Upon PDBu treatment, CLASP is recruited to MTs and stimulates KIF1C binding to MTs. This leads to KIF1C-dependent transport of essential factors to podosome formation sites. (B) A schematic representation of the proposed signaling cascade triggered by PDBu treatment.

Microscopy

Wide-field fluorescence imaging was performed using a Nikon 80I microscope with a CFI APO 60× oil lens, NA 1.4 and CoolSnap ES CCD camera (Photometrics). Single-plane confocal live-cell video sequences (except for Fig. 2A) were taken using a Yokogawa QLC-100/CSU-10 spinning-disk head (Visitec assembled by Vashaw) attached to a Nikon TE2000E microscope with a Perfect Focus System using a CFI PLAN APO VC 100× oil lens NA 1.4 and a back-illuminated EM-CCD camera Cascade 512B (Photometrics) driven by IPLab software (Scanalytics). The video sequence presented in Fig. 2A was acquired at Nikon Sweptfield Confocal with an Andor Ultra 897 camera, attached to a fully motorized Ti-E with Perfect Focus and Tokai Hit incubation chamber using the 100× 1.45 Lambda objective, and driven by NIS-Elements AR.

A Leica TCS SP5 confocal laser-scanning microscope with an HCX PL APO 100× oil lens NA 1.47 was used for taking confocal stacks of fixed cells. DeltaVision Elite with Alexa Fluor 488, Alexa Fluor 594 and Alexa Fluor 647 filter sets (Chroma) and a Coolsnap HQ CCD camera under control of SoftWorx (Applied Precision LLP) was used for acquisition and deconvolution of stacks of fixed cells.

Image acquisition and editing

For Fig. 1B–G, Fig. 2A–F, Fig. 4A,B, Fig. 6A–F and supplementary material Fig. S1A–D, Fig. S3A–C and Fig. S4A–C, wide-field fluorescence microscopy was used and data were acquired as 12-bit images. For Fig. 3B, Fig. 4C, Fig. 5F–I and supplementary material Fig. S1F–J and Fig. S4D,E, single-plane spinning-disk confocal microscopy was performed and data were acquired as 16-bit images. Two-color images were taken in near-simultaneous mode. Single timeframes or maximum intensity projections over time are shown, as indicated in figure legends. For Fig. 3A, single-plane swept-field confocal microscopy was used, and data were acquired as 16 bit. Single time frames are shown. For Fig. 1I, Fig. 3D–G, Fig. 4G–L, Fig. 5B–D, Fig. 6G–J and supplementary material Fig. S2, laser-scanning confocal microscopy was used and data were acquired as 8-bit images. All channels were acquired in sequential mode to avoid cross-talk. Single slices or maximum intensity projections are shown, as indicated in figure

Journal of Cell Science (2014) 127, 5179–5188 doi:10.1242/jcs.149633

legends. For Fig. 1A and Fig. 2K,L,O–Q, wide-field deconvolution microscopy was performed, with images acquired as 16 bit. Maximum intensity projections of deconvolved image stacks are shown. For all multi-color images, single channels were contrasted independently; gamma-adjustment was used to visualize minor details. The kymograph (supplementary material Fig. S1I) was built along a freehand line using the ImageJ 'reslice' function.

Treatments

For MT depolymerization, nocodazole (2.5 µg/ml) was added to the culture medium for 2 hours. For stimulation of podosome formation, phorbol 12,13-dibutyrate (PDBu) (Sigma) was used at a final concentration of 5 µM for 40 minutes in fixed-cell experiments or was added to the medium during live-cell imaging.

siRNA and expression constructs

Two different combinations of mixed siRNA oligonucleotides against CLASP1 and CLASP2 were used. Combination 1 (Mimori-Kiyosue et al., 2005) included the CLASP1-targeted siRNA sequence 5′-CCUACUAAAUGUUCUGACC-3′ and the CLASP2-targeted siRNA sequence 5′-CUGUAUGUACCCAGAAUCU-3′. Combination 2 (custom design, Sigma) included the CLASP1-targeted siRNA sequence 5′-CGGGAUUGCAUCUUUGAAA-3′ and the CLASP2-targeted siRNA sequence 5′- CUGAUAGUGUCUGUUGGUU-3′. The KIF1C-targeted siRNA sequence was 5′- GUGAGCUAUAUGGAGAUCU-3′. Non-targeting siRNA (Dharmacon) was used for controls.

The following plasmid constructs were used: RFP–cortactin (a gift from Marko Kaksonen, EMBL, Heidelberg, Germany), KIF1C–GFP and KIF1C–mCherry (Theisen et al., 2012), EB3–mCherry lentiviral construct (a gift from Al Reynolds, Vanderbilt University, TN), mCherry–dTOM20 (Drosophila outer mitochondrial protein; a gift from Ethan Lee, Vanderbilt University, TN), Tks5–GFP (Oikawa et al., 2008; a gift from Tsukasa Oikawa, Kobe University, Japan), GFP–CLASP2 and RFP–CLASP2 (gifts from Anna Akhmanova, Utrecht University, the Netherlands). Mito-CLASP (dTOM20 fused with the N-terminal end of CLASP2a in a pCS2 vector) was used for CLASP mislocalization to mitochondria (Efimov et al., 2007).

Cloning of the dominant-negative mutations was based on the FLAG-tagged rescue construct of human KIF1C p4×FLAG-KIF1C^{RIP1}, which has been described previously (Theisen et al., 2012). The motor and neck domain (amino acids 1–359) was deleted by amplifying the KIF1C tail using PCR with the primers 5′-ATGAATTCTATGGCCCGGCTGATTA-GAGAGC-3′ and 5′-GTGGATCCACAGCTGCCCCACTCTC-3′ and digestion with *Eco*RI and *Bam*HI. The G102E rigor mutation was introduced into the KIF1C motor domain using a three-step mutagenesis PCR with upstream primer 5′-GGAATTCTGGAGCTATGGCTGGTG-3′, downstream primer 5′-ACTGACCTTCTCCGAGTCC-3′ and mutagenesis primer 5′-TGGTATAGGATTTCTCAGCCC-3′. A fragment comprising the N-terminal half of the motor domain containing the mutation was replaced in p4×FLAG-KIF1C^{RIP1} using *Eco*RI and *Bsi*WI.

The KIF1C rescue plasmid that was used in this study to produce KIF1C that was protected against the KIF1C siRNA was generated on the basis of pKIF1C-eGFP described previously (Theisen et al., 2012). Five silent point mutations were introduced in the RNAi target site using a three-step PCR with upstream and downstream primers as for G102E rigor and the mutagenesis primer 5′-CTGTGGAGGTGTCTTACAT-GGAAATCTACTGTGAGCG-3′. The fragment containing the mutation was exchanged with *Eco*RI and *Bsi*WI to generate pKIF1C^{RIP2}-eGFP. Deletion of the KIF1C tail beyond the first two coiled-coil domains was performed by introducing a *Bam*HI restriction site after amino acid position V490 in KIF1C using the primers 5′-GGAATTCTGGAGCT-ATGGCTGGTG-3′ and 5′-GAAGGGATCCACAGTTCCCCCATC-CTC-3′, and replacing the *Bsi*WI–*Bam*HI fragment in pKIF1C^{RIP2}-eGFP with the truncated fragment to create pKIF1C^{RIP2}(1–490)-eGFP.

Transfection, infection and stable lines

For transient transfection of plasmid DNA, Fugene6 (Roche) or Amaxa nucleofection (Lonza) (X-001 program) were used according to the manufacturer's protocols. Experiments were conducted 18–24 hours after transfection. For siRNA oligonucleotide transfection, HiPerFect (Qiagen) was used according to the manufacturer's protocol. Experiments were conducted 72 hours after transfection, as at this time minimal protein levels were detected. For viral infection, supernatant containing lentiviral particles was collected from HEK293T cells transfected with the lentiviral expression vectors and second-generation packaging constructs (Invitrogen). A7r5 cells were infected with supernatant containing lentiviral particles in the presence of 8 µg/ml polybrene overnight.

The EB3–mCherry A7r5 stable line was generated using lentiviral constructs and maintained under the same conditions as A7r5. The KIF1C–GFP stable A7r5 cell line was produced by G418 antibiotic selection (500 µg/ml). HEK293T cells were cultured in high-glucose DMEM supplemented with 10% fetal bovine serum.

Antibodies and immunofluorescence

The following antibodies were used: rabbit polyclonal anti-CLASP2 VU-83 (Efimov et al., 2007), rabbit polyclonal anti-CLASP1 (Epitomics), rat monoclonal anti-CLASP2 KT69 (Fitzgerald), mouse monoclonal anti-α-tubulin DM1a (Sigma), rabbit polyclonal anti-tubulin (Abcam), rabbit polyclonal anti-KIF1C (Cytoskeleton), mouse monoclonal (Upstate), rabbit polyclonal (Cell Signaling Technology) anti-cortactin and mouse monoclonal anti-FLAG® M2 (Sigma) antibodies. Highly cross-absorbed goat anti-mouse-IgG and anti-rabbit-IgG antibodies conjugated to Alexa Fluor 350, Alexa Fluor 488 and Alexa Fluor 568 (Invitrogen, Molecular Probes) were used as secondary antibodies. The actin cytoskeleton was visualized by using phalloidin conjugated to Alexa Fluor 350, 488, 568 or 647 (Invitrogen, Molecular Probes). For immunofluorescence microscopy, cells on coverslips were fixed in 4% paraformaldehyde plus 0.3% Triton X-100 in cytoskeleton buffer (10 mM MES, 150 mM NaCl, 5 mM EGTA, 5 mM glucose and 5 mM $MgCl_2$, pH 6.1) for 10 minutes at room temperature, or in 4% paraformaldehyde plus 0.1% glutaraldehyde and 0.3% Triton X-100 in cytoskeleton buffer for 10 minutes at room temperature, or for 5 minutes in methanol (for anti-CLASP2 staining) at −20℃. Fixed cells were soaked in PBS for ≥1 hour. Then, non-specificity was blocked with blocking solution (1% horse serum, 0.1% BSA in PBS) for 30 minutes. Incubation with the primary antibodies was performed for 1 hour, and samples were then incubated for 40 minutes with the secondary antibodies. All antibodies were diluted in blocking solution prior to use. Immunostaining was performed at room temperature. After washing, samples were mounted into ProLong® Gold Antifade Reagent (Invitrogen, Molecular Probes) on glass slides and stored at −20℃.

Western blot analysis

Western blotting was performed with the Protein Electrophoresis and Western Blotting System (Bio-Rad). Briefly, cells collected from a 10-cm dish were pelleted and resuspended in Laemmli Sample Buffer (Bio-Rad). We applied 30 µg of total protein samples to a 10% polyacrylamide gel and processed for electrophoresis. Nitrocellulose membrane (0.45 µM) was used for protein blotting. The membrane was incubated with primary and then secondary (LI-COR, IRDye™ 800 or 700) antibodies diluted in Odyssey Blocking Buffer. To reduce the background, 0.2% Tween-20 was added. Odyssey Infrared Imaging System (LI-COR) was used for membrane scanning.

Quantitative analyses

Podosome number per cell (Fig. 1H; Fig. 2G,M,R; Fig. 6K) and average podosome size (Fig. 2H) were quantified using ImageJ particle analysis or ImagePro Analyzer (Media Cybernetics) on thresholded images of cortactin staining visualized by wide-field or deconvolved (DeltaVision) fluorescence microscopy. Objects were verified by comparing with actin staining, and wrongly merged objects were split manually.

To measure the fold increase of KIF1C–GFP intensity at the cell edge (Fig. 3C), 6 µm (20 pixels) around the cell edge was quantified using single-plane spinning-disk confocal movies of KIF1C–GFP-expressing cells. For the first and last frames of a movie, a cell outline was drawn

and a band of 6-µm (20 pixels) width was taken for quantification. After background subtraction, the summarized fluorescence intensity within these bands was measured and the ratio between the last and the first frames was taken as the fold increase.

The accumulation of KIF1C in lamellae (Fig. 3H) was quantified using maximal intensity projections of confocal stacks of immunostained KIF1C. A cell outline was drawn and a band of ~20-µm (150 pixels) width was taken as the cell lamella. The area of lamella and area of KIF1C accumulations were quantified using the ImageJ particle analysis tool, and the percentage of area that contained KIF1C was quantified.

The number of KIF1C movement events that colocalized with MT plus ends was determined using spinning-disk confocal sequences (5 seconds/frame) of KIF1C–GFP and EB3–mCherry-expressing cells. First, all events of directional KIF1C displacement for 4 pixels or more were marked in the GFP channel. Then, moving KIF1C particles were superimposed on the mCherry channel in the 'real' or 'flipped' (control) orientation. The number of KIF1C particles moving together with EB3 comets was detected, and the percentage of colocalized movements out of the overall movement events was quantified. The number of KIF1C movement events that colocalized with CLASP-coated MTs was quantified similarly, with RFP−CLASP2 in the red channel. A flipped red channel was used as a control. The number of KIF1C particles moving along CLASP-rich MTs was detected, and the percentage of colocalized movements out of the overall movement events was quantified.

KIF1C trafficking (Fig. 3J) was determined using spinning-disk confocal sequences (5 seconds/frame) of KIF1C–GFP-expressing cells. KIF1C puncta were manually tracked using the MTrackJ plugin of ImageJ. Particle displacements >0.2 µm (microscope resolution) were isolated. Trajectories were summed and divided by the total number of particles analyzed per cell; this calculation gives the distance travelled per particle. This analysis is modified from an approach used previously (Barlan et al., 2013).

The colocalization of KIF1C and mitochondria (Fig. 4E,F) was quantified as Manders coefficients using the JACoP plugin of ImageJ. Mitochondria images were thresholded automatically and KIF1C images were thresholded for the equal number of pixels above background.

The mitochondria in lamella (Fig. 4M) were quantified using ImageJ particle analysis on thresholded images of mCherry–TOM20 visualized by wide-field fluorescence microscopy, after exclusion of a 20-µm-wide area of compacted mitochondria around the nucleus.

Acknowledgements

We thank Alissa Weaver (Vanderbilt University, Nashville, TN) for helpful suggestions and critical reading of the manuscript, Ulrike Theisen (University of Warwick, Coventry, UK), Kevin Mink (Vanderbilt University, Nashville, TN) and Dmitry Yampolsky (Vanderbilt University, Nashville, TN) for technical support, and Cumberland Dugan (Nikon) for the demo of the Sweptfield microscope.

Competing interests

The authors declare no competing interests.

Author contributions

I.K. conceived of the project, designed the experiments and wrote the paper. A.S. designed and supervised experiments with KIF1C mutants and Tks5 and edited the manuscript. N.E. performed the majority of the experiments. A.G. performed multiple experiments, including mitochondrial targeting, western blotting and siRNA-mediated depletions. A.B. performed experiments with KIF1C mutants and Tks5. K.F. performed live-cell imaging of coexpressed CLASP2 and KIF1C. X.Z. and A.F. developed and performed a part of quantitative analysis. All authors provided intellectual input, vetted and approved the final manuscript.

Funding

This work was supported by the National Institutes of Health [grant number R01-GM078373]; and by an American Heart Association grant-in-aid [grant number 10GRNT4230026] to I.K. A.D.G was supported by an American Heart Association predoctoral fellowship [grant number 12PRE12040153]. A.B. is supported by a non-clinical PhD studentship from the British Heart Foundation [grant number FS/13/42/30377]. A.S. is a Lister Institute Research Prize Fellow. Deposited in PMC for release after 12 months.

Supplementary material

Supplementary material available online at
http://jcs.biologists.org/lookup/suppl/doi:10.1242/jcs.149633/-/DC1

References

Akhmanova, A., Hoogenraad, C. C., Drabek, K., Stepanova, T., Dortland, B., Verkerk, T., Vermeulen, W., Burgering, B. M., De Zeeuw, C. I., Grosveld, F. et al. (2001). Clasps are CLIP-115 and -170 associating proteins involved in the regional regulation of microtubule dynamics in motile fibroblasts. *Cell* **104**, 923-935.

Al-Bassam, J. and Chang, F. (2011). Regulation of microtubule dynamics by TOG-domain proteins XMAP215/Dis1 and CLASP. *Trends Cell Biol.* **21**, 604-614.

Babb, S. G., Matsudaira, P., Sato, M., Correia, I. and Lim, S. S. (1997). Fimbrin in podosomes of monocyte-derived osteoclasts. *Cell Motil. Cytoskeleton* **37**, 308-325.

Barlan, K., Lu, W. and Gelfand, V. I. (2013). The microtubule-binding protein ensconsin is an essential cofactor of kinesin-1. *Curr. Biol.* **23**, 317-322.

Biosse Duplan, M., Zalli, D., Stephens, S., Zenger, S., Neff, L., Oelkers, J. M., Lai, F. P., Horne, W., Rottner, K. and Baron, R. (2014). Microtubule dynamic instability controls podosome patterning in osteoclasts through EB1, cortactin, and Src. *Mol. Cell. Biol.* **34**, 16-29.

Bhuwania, R., Castr-Castro, A. and Linder, S. I. (2014). Microtubule acetylation regulates dynamics of KIF1C-powered vesicles and contact of microtubule plus ends with podosomes. *Eur. J. Cell Biol.* [Epub ahead of print].

Cai, D., McEwen, D. P., Martens, J. R., Meyhofer, E. and Verhey, K. J. (2009). Single molecule imaging reveals differences in microtubule track selection between Kinesin motors. *PLoS Biol.* **7**, e1000216.

Chambers, T. J. and Fuller, K. (2011). How are osteoclasts induced to resorb bone? *Ann. N. Y. Acad. Sci.* **1240**, 1-6.

Chen, Q., Jin, M., Yang, F., Zhu, J., Xiao, Q. and Zhang, L. (2013). Matrix metalloproteinases: inflammatory regulators of cell behaviors in vascular formation and remodeling. *Mediators Inflamm.* **2013**, 928315.

Chiron, S., Bobkova, A., Zhou, H. and Yaffe, M. P. (2008). CLASP regulates mitochondrial distribution in Schizosaccharomyces pombe. *J. Cell Biol.* **182**, 41-49.

Cornfine, S., Himmel, M., Kopp, P., El Azzouzi, K., Wiesner, C., Krüger, M., Rudel, T. and Linder, S. (2011). The kinesin KIF9 and reggie/flotillin proteins regulate matrix degradation by macrophage podosomes. *Mol. Biol. Cell* **22**, 202-215.

Destaing, O., Saltel, F., Géminard, J. C., Jurdic, P. and Bard, F. (2003). Podosomes display actin turnover and dynamic self-organization in osteoclasts expressing actin-green fluorescent protein. *Mol. Biol. Cell* **14**, 407-416.

Destaing, O., Saltel, F., Gilquin, B., Chabadel, A., Khochbin, S., Ory, S. and Jurdic, P. (2005). A novel Rho-mDia2-HDAC6 pathway controls podosome patterning through microtubule acetylation in osteoclasts. *J. Cell Sci.* **118**, 2901-2911.

Dovas, A. and Cox, D. (2011). Signaling networks regulating leukocyte podosome dynamics and function. *Cell. Signal.* **23**, 1225-1234.

Drabek, K., van Ham, M., Stepanova, T., Draegestein, K., van Horssen, R., Sayas, C. L., Akhmanova, A., Ten Hagen, T., Smits, R., Fodde, R. et al. (2006). Role of CLASP2 in microtubule stabilization and the regulation of persistent motility. *Curr. Biol.* **16**, 2259-2264.

Efimov, A., Kharitonov, A., Efimova, N., Loncarek, J., Miller, P. M., Andreyeva, N., Gleeson, P., Galjart, N., Maia, A. R., McLeod, I. X. et al. (2007). Asymmetric CLASP-dependent nucleation of noncentrosomal microtubules at the trans-Golgi network. *Dev. Cell* **12**, 917-930.

Etienne-Manneville, S. (2013). Microtubules in cell migration. *Annu. Rev. Cell Dev. Biol.* **29**, 471-499.

Evans, J. G., Correia, I., Krasavina, O., Watson, N. and Matsudaira, P. (2003). Macrophage podosomes assemble at the leading lamella by growth and fragmentation. *J. Cell Biol.* **161**, 697-705.

Galjart, N. (2005). CLIPs and CLASPs and cellular dynamics. *Nat. Rev. Mol. Cell Biol.* **6**, 487-498.

Gil-Henn, H., Destaing, O., Sims, N. A., Aoki, K., Alles, N., Neff, L., Sanjay, A., Bruzzaniti, A., De Camilli, P., Baron, R. et al. (2007). Defective microtubule-dependent podosome organization in osteoclasts leads to increased bone density in Pyk2(-/-) mice. *J. Cell Biol.* **178**, 1053-1064.

Gimona, M., Buccione, R., Courtneidge, S. A. and Linder, S. (2008). Assembly and biological role of podosomes and invadopodia. *Curr. Opin. Cell Biol.* **20**, 235-241.

Goode, N., Hughes, K., Woodgett, J. R. and Parker, P. J. (1992). Differential regulation of glycogen synthase kinase-3 beta by protein kinase C isotypes. *J. Biol. Chem.* **267**, 16878-16882.

Hai, C. M., Hahne, P., Harrington, E. O. and Gimona, M. (2002). Conventional protein kinase C mediates phorbol-dibutyrate-induced cytoskeletal remodeling in a7r5 smooth muscle cells. *Exp. Cell Res.* **280**, 64-74.

Hammond, J. W., Huang, C. F., Kaech, S., Jacobson, C., Banker, G. and Verhey, K. J. (2010). Posttranslational modifications of tubulin and the polarized transport of kinesin-1 in neurons. *Mol. Biol. Cell* **21**, 572-583.

Hoogenraad, C. C. and Akhmanova, A. (2010). Dendritic spine plasticity: new regulatory roles of dynamic microtubules. *Neurosci.* **16**, 650-661.

Hoshino, D., Branch, K. M. and Weaver, A. M. (2013). Signaling inputs to invadopodia and podosomes. *J. Cell Sci.* **126**, 2979-2989.

Jaulin, F. and Kreitzer, G. (2010). KIF17 stabilizes microtubules and contributes to epithelial morphogenesis by acting at MT plus ends with EB1 and APC. *J. Cell Biol.* **190**, 443-460.
Jurdic, P., Saltel, F., Chabadel, A. and Destaing, O. (2006). Podosome and sealing zone: specificity of the osteoclast model. *Eur. J. Cell Biol.* **85**, 195-202.
Kaverina, I. and Straube, A. (2011). Regulation of cell migration by dynamic microtubules. *Semin. Cell Dev. Biol.* **22**, 968-974.
Kaverina, I., Krylyshkina, O. and Small, J. V. (1999). Microtubule targeting of substrate contacts promotes their relaxation and dissociation. *J. Cell Biol.* **146**, 1033-1044.
Kaverina, I., Stradal, T. E. and Gimona, M. (2003). Podosome formation in cultured A7r5 vascular smooth muscle cells requires Arp2/3-dependent de-novo actin polymerization at discrete microdomains. *J. Cell Sci.* **116**, 4915-4924.
Kopp, P., Lammers, R., Aepfelbacher, M., Woehlke, G., Rudel, T., Machuy, N., Steffen, W. and Linder, S. (2006). The kinesin KIF1C and microtubule plus ends regulate podosome dynamics in macrophages. *Mol. Biol. Cell* **17**, 2811-2823.
Kumar, P., Lyle, K. S., Gierke, S., Matov, A., Danuser, G. and Wittmann, T. (2009). GSK3beta phosphorylation modulates CLASP-microtubule association and lamella microtubule attachment. *J. Cell Biol.* **184**, 895-908.
Lacolley, P., Regnault, V., Nicoletti, A., Li, Z. and Michel, J. B. (2012). The vascular smooth muscle cell in arterial pathology: a cell that can take on multiple roles. *Cardiovasc. Res.* **95**, 194-204.
Lansbergen, G., Grigoriev, I., Mimori-Kiyosue, Y., Ohtsuka, T., Higa, S., Kitajima, I., Demmers, J., Galjart, N., Houtsmuller, A. B., Grosveld, F. et al. (2006). CLASPs attach microtubule plus ends to the cell cortex through a complex with LL5beta. *Dev. Cell* **11**, 21-32.
Lener, T., Burgstaller, G., Crimaldi, L., Lach, S. and Gimona, M. (2006). Matrix-degrading podosomes in smooth muscle cells. *Eur. J. Cell Biol.* **85**, 183-189.
Linder, S., Hüfner, K., Wintergerst, U. and Aepfelbacher, M. (2000). Microtubule-dependent formation of podosomal adhesion structures in primary human macrophages. *J. Cell Sci.* **113**, 4165-4176.
Linder, S., Wiesner, C. and Himmel, M. (2011). Degrading devices: invadosomes in proteolytic cell invasion. *Annu. Rev. Cell Dev. Biol.* **27**, 185-211.
Liu, J. S., Schubert, C. R., Fu, X., Fourniol, F. J., Jaiswal, J. K., Houdusse, A., Stultz, C. M., Moores, C. A. and Walsh, C. A. (2012). Molecular basis for specific regulation of neuronal kinesin-3 motors by doublecortin family proteins. *Mol. Cell* **47**, 707-721.
McMichael, B. K., Cheney, R. E. and Lee, B. S. (2010). Myosin X regulates sealing zone patterning in osteoclasts through linkage of podosomes and microtubules. *J. Biol. Chem.* **285**, 9506-9515.
Miller, P. M., Folkmann, A. W., Maia, A. R., Efimova, N., Efimov, A. and Kaverina, I. (2009). Golgi-derived CLASP-dependent microtubules control Golgi organization and polarized trafficking in motile cells. *Nat. Cell Biol.* **11**, 1069-1080.
Mimori-Kiyosue, Y., Grigoriev, I., Lansbergen, G., Sasaki, H., Matsui, C., Severin, F., Galjart, N., Grosveld, F., Vorobjev, I., Tsukita, S. et al. (2005). CLASP1 and CLASP2 bind to EB1 and regulate microtubule plus-end dynamics at the cell cortex. *J. Cell Biol.* **168**, 141-153.
Murphy, D. A. and Courtneidge, S. A. (2011). The 'ins' and 'outs' of podosomes and invadopodia: characteristics, formation and function. *Nat. Rev. Mol. Cell Biol.* **12**, 413-426.
Oikawa, T., Itoh, T. and Takenawa, T. (2008). Sequential signals toward podosome formation in NIH-src cells. *J. Cell Biol.* **182**, 157-169.
Proszynski, T. J., Gingras, J., Valdez, G., Krzewski, K. and Sanes, J. R. (2009). Podosomes are present in a postsynaptic apparatus and participate in its maturation. *Proc. Natl. Acad. Sci. USA* **106**, 18373-18378.
Purev, E., Neff, L., Horne, W. C. and Baron, R. (2009). c-Cbl and Cbl-b act redundantly to protect osteoclasts from apoptosis and to displace HDAC6 from beta-tubulin, stabilizing microtubules and podosomes. *Mol. Biol. Cell* **20**, 4021-4030.
Quintavalle, M., Elia, L., Condorelli, G. and Courtneidge, S. A. (2010). MicroRNA control of podosome formation in vascular smooth muscle cells in vivo and in vitro. *J. Cell Biol.* **189**, 13-22.
Quintavalle, M., Elia, L., Price, J. H., Heynen-Genel, S. and Courtneidge, S. A. (2011). A cell-based high-content screening assay reveals activators and inhibitors of cancer cell invasion. *Sci. Signal.* **4**, ra49.
Reed, N. A., Cai, D., Blasius, T. L., Jih, G. T., Meyhofer, E., Gaertig, J. and Verhey, K. J. (2006). Microtubule acetylation promotes kinesin-1 binding and transport. *Curr. Biol.* **16**, 2166-2172.
Rottiers, P., Saltel, F., Daubon, T., Chaigne-Delalande, B., Tridon, V., Billottet, C., Reuzeau, E. and Génot, E. (2009). TGFbeta-induced endothelial podosomes mediate basement membrane collagen degradation in arterial vessels. *J. Cell Sci.* **122**, 4311-4318.
Saltel, F., Daubon, T., Juin, A., Ganuza, I. E., Veillat, V. and Génot, E. (2011). Invadosomes: intriguing structures with promise. *Eur. J. Cell Biol.* **90**, 100-107.
Schoumacher, M., Goldman, R. D., Louvard, D. and Vignjevic, D. M. (2010). Actin, microtubules, and vimentin intermediate filaments cooperate for elongation of invadopodia. *J. Cell Biol.* **189**, 541-556.
Teti, A., Marchisio, P. C. and Zallone, A. Z. (1991). Clear zone in osteoclast function: role of podosomes in regulation of bone-resorbing activity. *Am. J. Physiol.* **261**, C1-C7.
Theisen, U., Straube, E. and Straube, A. (2012). Directional persistence of migrating cells requires Kif1C-mediated stabilization of trailing adhesions. *Dev. Cell* **23**, 1153-1166.
van Helden, S. F. and Hordijk, P. L. (2011). Podosome regulation by Rho GTPases in myeloid cells. *Eur. J. Cell Biol.* **90**, 189-197.
Wiesner, C., Faix, J., Himmel, M., Bentzien, F. and Linder, S. (2010). KIF5B and KIF3A/KIF3B kinesins drive MT1-MMP surface exposure, CD44 shedding, and extracellular matrix degradation in primary macrophages. *Blood* **116**, 1559-1569.
Wittmann, T. and Waterman-Storer, C. M. (2005). Spatial regulation of CLASP affinity for microtubules by Rac1 and GSK3beta in migrating epithelial cells. *J. Cell Biol.* **169**, 929-939.

Kinesins in cell migration

Alice Bachmann* and Anne Straube*[1]
*Centre for Mechanochemical Cell Biology, Warwick Medical School, University of Warwick, Gibbet Hill, Coventry, CV4 7AL, U.K.

Abstract

Human cells express 45 kinesins, microtubule motors that transport a variety of molecules and organelles within the cell. Many kinesins also modulate the tracks they move on by either bundling or sliding or regulating the dynamic assembly and disassembly of the microtubule polymer. In migrating cells, microtubules control the asymmetry between the front and rear of the cell by differentially regulating force generation processes and substrate adhesion. Many of these functions are mediated by kinesins, transporters as well as track modulators. In this review, we summarize the current knowledge on kinesin functions in cell migration.

The kinesin superfamily

The first kinesin to be discovered, kinesin-1, was isolated as the translocator molecule in the squid giant axon [1]. Since then, a superfamily comprising more than 40 kinesins in 14 families has been identified, many of the members of which are microtubule-dependent translocators such as kinesin-1. All kinesins contain a motor domain with ATPase activity and a microtubule-binding interface. The ATP hydrolysis cycle is coupled to changes in the affinity for microtubules and allows the motor to perform work. The tails of kinesins are highly diverse and bind cargo proteins, adapters and regulatory proteins. The motor domain can either be positioned at the N-terminus of the molecule for plus-end-directed motors such as kinesin-1, at the C-terminus in minus-end-directed motors of the kinesin-14 family or in the middle of the molecule such as in kinesin-13s. Many kinesins have adopted additional functions beyond transporting cargo along microtubules (Figure 1). For example, the homotetrameric kinesin-5 walks on two microtubules at the same time to separate the spindle poles at the beginning of mitosis [2], whereas kinesin-13s are specialized microtubule depolymerases that use ATP hydrolysis to induce microtubule disassembly, but can no longer walk along microtubules [3]. This multitude of functions in the transport of cellular cargo along microtubules and the organization and dynamics of the microtubule cytoskeleton makes kinesins central players in many essential biological processes such as cell division, morphogenesis and locomotion.

Cell migration

Cell migration underlies embryonic development, immune responses and wound healing. Cell migration is stimulated by physical signals, such as the loss of cell–cell contacts and by chemical extracellular signalling through chemokine gradients. Directional migration requires the establishment and maintenance of a distinct front and rear of the cell and can be thought of as a cycle of four processes: protrusion at the leading edge, the formation of new adhesions at the leading edge, the release of adhesions at the rear of the cell and retraction of the cell rear (Figure 2). Cell migration is largely driven by the polymerization of actin filaments at the cell cortex and the myosin-mediated contraction of actin bundles [4,5]. Adhesion is mediated by integrin-rich adhesion structures that link extracellular fibres to the actin cytoskeleton [6]. Microtubules are emerging as important regulators of the cell migration machinery, controlling force generation, substrate adhesion and signalling pathways [7,8]. Many of these functions are mediated or modulated by kinesins (Figure 3) and will be discussed in detail in the following sections.

Organization of the microtubule network in migrating cells

Many cells depend on the microtubule cytoskeleton to maintain the polarity of the migrating cell and for the asymmetric regulation of force generation and adhesion at the front and rear of the cell. The microtubule cytoskeleton itself needs to be asymmetric to control polarity. Most notable are the position of the centrosome in front of the nucleus and the majority of microtubules pointing with their plus-ends towards the leading edge of the cell. The minus-end-directed microtubule motor dynein is implicated in the positioning of the centrosome by exerting pulling forces on microtubules reaching the cell edge. The front-bias is achieved partly by the nucleation of front-directed microtubules from the *trans*-Golgi network [9] and partly by the differential regulation of microtubule dynamics in the front and rear of the cell. This not only regulates the microtubule number, but also the accumulation of post-translational modifications in front-directed microtubules. A number of kinesins preferentially transport cargo along microtubules

Key words: cell adhesion, cell migration, force generation, intracellular transport, kinesin, microtubules.

Abbreviations: APC, adenomatosis polyposis coli; Arp, actin-related protein; MMP, matrix metallopeptidase; VEGF, vascular endothelial growth factor.

[1]**To whom correspondence should be addressed (email anne@mechanochemistry.org).**

Figure 1 | Kinesin functions

Kinesins function as walking machines to transport cargo along microtubules (green), as dynamases to change the balance of microtubule assembly and disassembly to either stabilize or destabilize microtubules and as cross-linkers to bundle microtubules in specific orientations or to slide microtubules relative to one another.

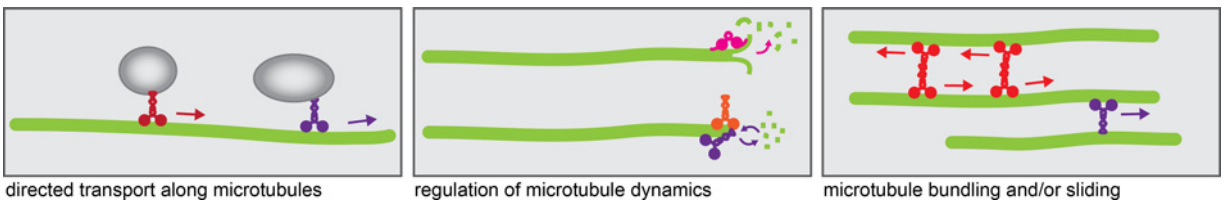

Figure 2 | Simplified model of cell migration

Cell migration requires the polarization of the cell with a morphologically and biochemically different front and rear. The migration process involves the cyclic protrusion and adhesion at the front and retraction of the cell rear to allow forwards movement.

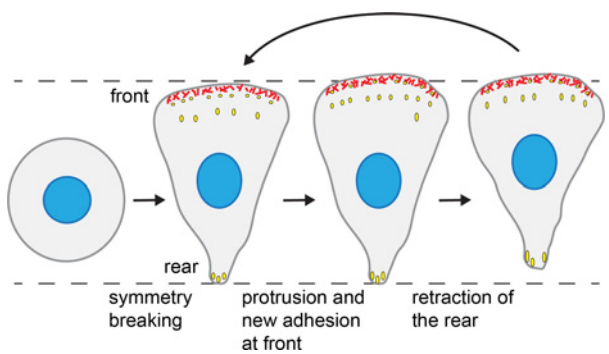

carrying certain modifications [10–12]. This mechanism adds further front-directed bias to the microtubule network in migrating cells, thereby facilitating the efficient delivery of vesicles and molecular cargoes to the leading edge. Kinesins not only transport these cargoes, but also contribute to the organization of the microtubule network itself. For example, the kinesin-13 KIF2C/MCAK (mitotic centromere-associated kinesin) reduces the lifetimes of microtubules in the rear of the cell [13], whereas the kinesin-4 KIF4 stabilizes microtubules at the leading edge [14]. Both these kinesins, thus, contribute to the differences in dynamics between front- and rear-facing microtubules. The kinesin-2 KIF3A regulates the orientation and dynamicity of front-directed microtubules [15]. The inhibition of either of these kinesins results in decreased cell migration, which has been attributed to mis-regulation of microtubule organization and dynamics. Indeed, the suppression of dynamic growth and shrinkage excursions of microtubule ends using low doses of microtubule targeting agents impairs cell migration [16,17]. Thus kinesins are important regulators of microtubule dynamics whose activities serve to maintain a front-biased microtubule network.

Contribution to force-generation processes

As mentioned above, the actin cytoskeleton is usually credited with providing the driving forces for cell protrusion and contractility. However, microtubules are approximately 200 times stiffer than actin filaments [18] and, when laterally reinforced, can bear very high compressive loads [19]. Application of microtubule depolymerizers to polarized epithelial cells or fibroblasts leads to the contraction of cells [20], suggesting that microtubules are important as a load-bearing element in cells. Furthermore, the sliding of microtubules in bundles by kinesin-1 motors generates pushing forces that drive the protrusion of neurites early in neuronal differentiation [21]. Likewise, kinesin-5 KIF11/Eg5 has been implicated in cross-linking microtubules to prevent their penetration into parts of the neuronal growth cone. This process is important to relay the signal of path-finding cues to changing the direction of growth cone advance [22].

More indirectly, kinesins transport mRNAs encoding actin and components of the actin assembly-promoting machinery, as well as actin regulators themselves, to the leading edge. The accumulation of mRNA for actin, profilin and actin-related protein (Arp)2/3, the main nucleator of branched actin-filaments in lamellipodia at the leading edge, requires microtubule-based transport [23–25]. Localized translation of these mRNAs is required for efficient directionally-persistent cell migration as it determines the sites of actin nucleation [23]. The kinesin-2 family members KIF3A and KIF17 bind to adenomatosis polyposis coli (APC) [26,27]. APC accumulates at the leading edge of the cell and stabilizes microtubules, but is also a potent actin nucleator itself and acts in synergy with formins to form long, unbranched actin filaments [28]. The inhibition of kinesin-1 results in reduced lamellipodial protrusion [29]. One potential cargo of kinesin-1 mediating this function is WAVE2, which depends on KIF5B for its localization to the leading edge of migrating MDA-MB-231 cells [30]. WAVE2 promotes actin nucleation and branching by Arp2/3, with both processes being required for lamellipodia formation and protrusion [31]. The identification of a kinesin-1 interaction motif has led to the discovery of more than 400 potential cargoes of kinesin-1 [32]. It is, therefore, likely that kinesin-1 mediated transport stimulates cell protrusion through the delivery of a number of factors to the leading edge.

Figure 3 | Kinesins transport cargo to the leading and trailing edge of the cell

This transport is required for force generation, cell adhesion and matrix remodelling. Kinesins modulate microtubule dynamics spatially distinct at front and rear of the cell, setting up the polarity of the microtubule cytoskeleton, required for microtubules' function in signalling, force generation and adhesion control.

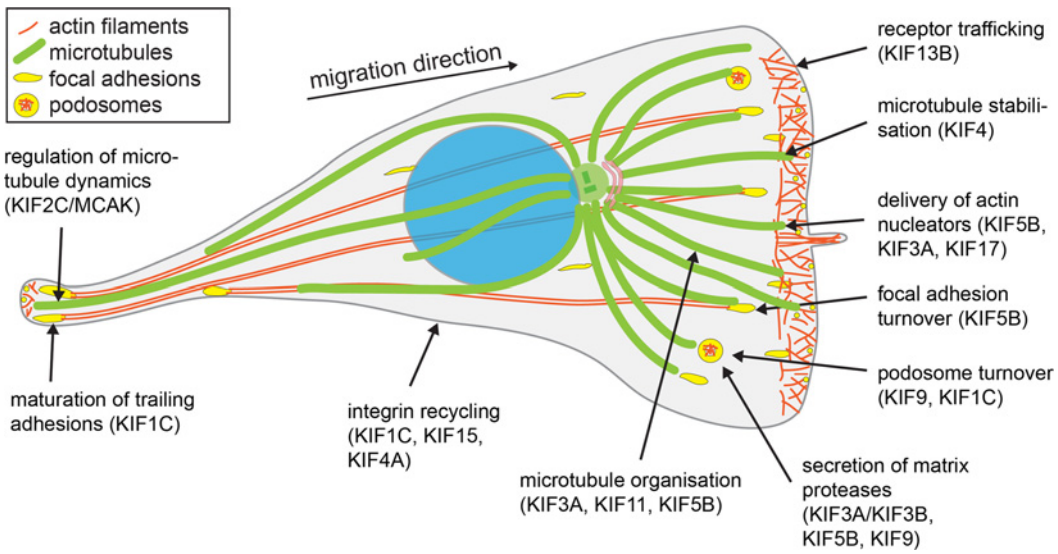

Regulation of cell adhesion

The importance of microtubules and kinesins in the regulation of cellular adhesion to the extracellular substrate has been known for over a decade. Microtubule ends repeatedly target focal adhesion sites and cause their dissolution [33]. The depolymerization of microtubules or the inhibition of kinesin-1 leads to an increase in focal adhesion size [34,35]. Although clathrin-mediated endocytosis has been implicated in mediating the microtubule-dependent destabilization of focal adhesions, it is still unclear which cargoes are delivered by which kinesin to mediate these functions [36,37]. One possible mechanism is the release of adhesions from the extracellular matrix using secreted proteases. KIF5B and KIF3B transport the matrix metallopeptidase 9 (MMP-9) to the cell periphery where it is released to the extracellular environment and subsequently activated to allow the degradation of collagen and elastins, an activity essential for macrophage migration during the inflammatory response [38]. KIF5B and KIF3A/KIF3B are involved in the surface exposure of the transmembranous MT1 (membrane type 1)-MMP [39], a collagenase responsible for the activation of other MMPs [40] as well as the degradation of the matrix components in close contact with the cell. Using *in situ* zymography, the kinesin-9 KIF9 has also been shown to be involved in matrix degradation [41], but which protease KIF9 transports remains to be identified.

Other kinesins promote cellular adhesion by contributing to the recycling of integrins, the major receptors of extracellular matrix proteins. The kinesin-3 KIF1C is involved in both focal adhesion maturation and formation of protruding adhesion structures called podosomes [42–44]. KIF1C participates in the maturation of trailing focal adhesions through its $\alpha5\beta1$-integrin transport activity [44]. $\alpha5\beta1$-integrin is the main fibronectin receptor [45]. When KIF1C transport is impaired, migrating retinal pigment epithelium cells fail to form mature focal adhesions at the rear, reducing their ability to maintain the directionality of migration [44]. Recently, the kinesins KIF4A and KIF15 have also been implicated in integrin recycling: KIF15, a kinesin-12, is required for the internalization of $\alpha2\beta1$-integrin, one of the most important collagen receptors [46], whereas kinesin-4 KIF4A transports $\alpha5\beta1$-integrin into developing axons [47]. Integrin recycling involves routes through different compartments and complex sorting mechanisms to fine-tune the set of displayed cell-surface receptors [48]. It is very likely that kinesins play an important part in cargo sorting and directional transport for spatial exocytosis with the potential to differentially regulate substrate adhesion in different regions of the cell.

Besides integrins, other adhesion molecules are transported along microtubules. The kinesin-3 KIF14 transports adhesion proteins such as cadherin 11 (CDH11) and melanoma cell adhesion molecule (MCAM) to the cell surface, thereby decreasing the ability of cells to migrate and invade tissues [49]. Consistent with this, KIF14 is a prognostic marker for the metastatic potential of cancer: lung adenocarcinoma expressing high levels of KIF14 develop fewer metastases than those expressing low levels of KIF14 [49]. KIF14 over-expression also impairs integrin activation, leading to mis-regulated cell adhesion and cell migration [50].

Furthermore, kinesins have been implicated in the control of specialized matrix-remodelling adhesion structures called podosomes or invadosomes. Podosomes are protruding adhesion structures formed at the ventral side of some

migratory and invasive cells that allows their trans-migration of the basement membrane. KIF1C and KIF9 are required for the formation as well as the turn-over of podosomes [41–43]. Depletion of either of these kinesins leads to a dramatic reduction in the number of podosomes formed by cells. KIF1C and KIF9 have been observed to decorate the plus-ends of a subset of microtubules targeting podosomes. When podosomes are contacted by microtubule ends, they adopt a dynamic behaviour, which results in the fusion or the fission of targeted podosomes [43].

Signalling pathways regulating cell migration

Recent studies highlighted the involvement of kinesins in the control of signalling pathways regulating cell migration. KIF3A over-expression in prostate cancer cells induces activation of the Wnt/β-catenin pathway [51] leading to an increase in cell proliferation as well as cell migration ability of these cells. This function could be mediated by APC, which controls the activity of β-catenin and binds to KIF3A [27].

Signalling is also promoted by kinesin-mediated receptor trafficking. In vascular smooth muscle cells, in response to vascular endothelial growth factor (VEGF) stimulation, the kinesin-3 KIF13B transports vesicles containing newly synthesized VEGF receptor 2 (VEGFR2) from the Golgi to the plasma membrane. The exposure of the receptor at the endothelial cell surface is required for VEGF-induced endothelial cell migration [52].

The kinesin-3 KIF14 negatively regulates integrin inside-out signalling [50]. KIF14 interacts with Radil, an effector of Rap1. Rap1 is a small GTPase that mediates integrin activation and clustering in its activated GTP-bound form [53]. KIF14 recruits Radil to microtubules and, thereby, controls the amount of Radil available for binding to Rap1-GTP at the plasma membrane [50]. Thus KIF14 fine-tunes the balance between cell adhesion and cell migration.

Kinesins also bind to a number of signalling modules, scaffold proteins with important roles in signalling processes, which also mediate activation and cargo-loading of kinesins [54]. It will be interesting to see to which extent these signalling proteins affect the activity of kinesin cargoes and modulate the signalling state at microtubule ends where cargo and motors tend to accumulate.

Conclusion

Kinesins are involved in most steps of cell migration, from force-generating processes that allow protrusion, to regulating adhesion and matrix degrading capabilities and the modulation of signalling pathways controlling migration. Until now, studies have tended to focus on one kinesin's involvement in one aspect of cell migration. How several kinesins work together and how the different cargoes of each kinesin contribute to its function in regulating cell migration is a key challenge for the future. Important requirements to successfully address this challenge will be the identification of the cargoes being transported by each kinesin and the microtubule sub-populations that serve as preferential tracks for their transport. Recent developments, including assays that facilitate kinesin-cargo identification [55] and attempts to crack the tubulin code [12,56], promise significant progress in this area in the coming years.

Acknowledgements

We thank Rob Cross for critical reading of the paper.

Funding

A.S. is a Lister Institute Research Prize Fellow. This work was supported by a British Heart Foundation non-clinical Ph.D. studentship [grant number FS/13/42/30377].

References

1 Vale, R.D., Reese, T.S. and Sheetz, M.P. (1985) Identification of a novel force-generating protein, kinesin, involved in microtubule-based motility. Cell **42**, 39–50 CrossRef PubMed
2 Kashina, A.S., Baskin, R.J., Cole, D.G., Wedaman, K.P., Saxton, W.M. and Scholey, J.M. (1996) A bipolar kinesin. Nature **379**, 270–272 CrossRef PubMed
3 Hunter, A.W., Caplow, M., Coy, D.L., Hancock, W.O., Diez, S., Wordeman, L. and Howard, J. (2003) The kinesin-related protein MCAK is a microtubule depolymerase that forms an ATP-hydrolyzing complex at microtubule ends. Mol. Cell **11**, 445–457 CrossRef PubMed
4 Pollard, T.D. and Borisy, G.G. (2003) Cellular motility driven by assembly and disassembly of actin filaments. Cell **112**, 453–465 CrossRef PubMed
5 Charras, G.T., Yarrow, J.C., Horton, M.A., Mahadevan, L. and Mitchison, T.J. (2005) Non-equilibration of hydrostatic pressure in blebbing cells. Nature **435**, 365–369 CrossRef PubMed
6 Wehrle-Haller, B. and Imhof, B. (2002) The inner lives of focal adhesions. Trends Cell Biol. **12**, 382–389 CrossRef PubMed
7 Kaverina, I. and Straube, A. (2011) Regulation of cell migration by dynamic microtubules. Semin. Cell Dev. Biol. **22**, 968–974 CrossRef PubMed
8 Etienne-Manneville, S. (2013) Microtubules in cell migration. Annu. Rev. Cell Dev. Biol. **29**, 471–499 CrossRef PubMed
9 Miller, P.M., Folkmann, A.W., Maia, A.R., Efimova, N., Efimov, A. and Kaverina, I. (2009) Golgi-derived CLASP-dependent microtubules control Golgi organization and polarized trafficking in motile cells. Nat. Cell Biol. **11**, 1069–1080 CrossRef PubMed
10 Cai, D., McEwen, D.P., Martens, J.R., Meyhofer, E. and Verhey, K.J. (2009) Single molecule imaging reveals differences in microtubule track selection between kinesin motors. PLoS Biol. **7**, e1000216 CrossRef PubMed
11 Reed, N.A., Cai, D., Blasius, T.L., Jih, G.T., Meyhofer, E., Gaertig, J. and Verhey, K.J. (2006) Microtubule acetylation promotes kinesin-1 binding and transport. Curr. Biol. **16**, 2166–2172 CrossRef PubMed
12 Sirajuddin, M., Rice, L.M. and Vale, R.D. (2014) Regulation of microtubule motors by tubulin isotypes and post-translational modifications. Nat. Cell Biol. **16**, 335–344 CrossRef PubMed
13 Braun, A., Dang, K., Buslig, F., Baird, M.A., Davidson, M.W., Waterman, C.M. and Myers, K.A. (2014) Rac1 and Aurora A regulate MCAK to polarize microtubule growth in migrating endothelial cells. J. Cell Biol. **206**, 97–112 CrossRef PubMed
14 Morris, E.J., Nader, G.P., Ramalingam, N., Bartolini, F. and Gundersen, G.G. (2014) Kif4 interacts with EB1 and stabilizes microtubules downstream of Rho–mDia in migrating fibroblasts. PLoS ONE **9**, e91568 CrossRef PubMed
15 Boehlke, C., Kotsis, F., Buchholz, B., Powelske, C., Eckardt, K.U., Walz, G., Nitschke, R. and Kuehn, E.W. (2013) Kif3a guides microtubular dynamics, migration and lumen formation of MDCK cells. PLoS ONE **8**, e62165 CrossRef PubMed

16 Liao, G., Nagasaki, T. and Gundersen, G.G. (1995) Low concentrations of nocodazole interfere with fibroblast locomotion without significantly affecting microtubule level: implications for the role of dynamic microtubules in cell locomotion. J. Cell Sci. **108**, 3473–3483 PubMed
17 Pourroy, B., Honoré, S., Pasquier, E., Bourgarel-Rey, V., Kruczynski, A., Briand, C. and Braguer, D. (2006) Antiangiogenic concentrations of vinflunine increase the interphase microtubule dynamics and decrease the motility of endothelial cells. Cancer Res. **66**, 3256–3263 CrossRef PubMed
18 Gittes, F., Mickey, B., Nettleton, J. and Howard, J. (1993) Flexural rigidity of microtubules and actin filaments measured from thermal fluctuations in shape. J. Cell Biol. **120**, 923–934 CrossRef PubMed
19 Brangwynne, C.P., MacKintosh, F.C., Kumar, S., Geisse, N.A., Talbot, J., Mahadevan, L., Parker, K.K., Ingber, D.E. and Weitz, D.A. (2006) Microtubules can bear enhanced compressive loads in living cells because of lateral reinforcement. J. Cell Biol. **173**, 733–741 CrossRef PubMed
20 Vasiliev, J.M., Gelfand, I.M., Domnina, L.V., Ivanova, O.Y., Komm, S.G. and Olshevskaja, L.V. (1970) Effect of colcemid on the locomotory behaviour of fibroblasts. J. Embryol. Exp. Morphol. **24**, 625–640 PubMed
21 Lu, W., Fox, P., Lakonishok, M., Davidson, M.W. and Gelfand, V.I. (2013) Initial neurite outgrowth in *Drosophila* neurons is driven by kinesin-powered microtubule sliding. Curr. Biol. **23**, 1018–1023 CrossRef PubMed
22 Nadar, V.C., Ketschek, A., Myers, K.A., Gallo, G. and Baas, P.W. (2008) Kinesin-5 is essential for growth-cone turning. Curr. Biol. **18**, 1972–1977 CrossRef PubMed
23 Condeelis, J. and Singer, R.H. (2005) How and why does β-actin mRNA target? Biol. Cell **97**, 97–110 CrossRef PubMed
24 Johnsson, A.K. and Karlsson, R. (2010) Microtubule-dependent localization of profilin I mRNA to actin polymerization sites in serum-stimulated cells. Eur. J. Cell Biol. **89**, 394–401 CrossRef PubMed
25 Mingle, L.A., Okuhama, N.N., Shi, J., Singer, R.H., Condeelis, J. and Liu, G. (2005) Localization of all seven messenger RNAs for the actin-polymerization nucleator Arp2/3 complex in the protrusions of fibroblasts. J. Cell Sci. **118**, 2425–2433 CrossRef PubMed
26 Jaulin, F. and Kreitzer, G. (2010) KIF17 stabilizes microtubules and contributes to epithelial morphogenesis by acting at MT plus ends with EB1 and APC. J. Cell Biol. **190**, 443–460 CrossRef PubMed
27 Jimbo, T., Kawasaki, Y., Koyama, R., Sato, R., Takada, S., Haraguchi, K. and Akiyama, T. (2002) Identification of a link between the tumour suppressor APC and the kinesin superfamily. Nat. Cell Biol. **4**, 323–327 CrossRef PubMed
28 Okada, K., Bartolini, F., Deaconescu, A.M., Moseley, J.B., Dogic, Z., Grigorieff, N., Gundersen, G.G. and Goode, B.L. (2010) Adenomatous polyposis coli protein nucleates actin assembly and synergizes with the formin mDia1. J. Cell Biol. **189**, 1087–1096 CrossRef PubMed
29 Rodionov, V.I., Gyoeva, F.K., Tanaka, E., Bershadsky, A.D., Vasiliev, J.M. and Gelfand, V.I. (1993) Microtubule-dependent control of cell shape and pseudopodial activity is inhibited by the antibody to kinesin motor domain. J. Cell Biol. **123**, 1811–1820 CrossRef PubMed
30 Takahashi, K. and Suzuki, K. (2008) Requirement of kinesin-mediated membrane transport of WAVE2 along microtubules for lamellipodia formation promoted by hepatocyte growth factor. Exp. Cell Res. **314**, 2313–2322 CrossRef PubMed
31 Mendoza, M.C., Er, E.E., Zhang, W., Ballif, B.A., Elliott, H.L., Danuser, G. and Blenis, J. (2011) ERK–MAPK drives lamellipodia protrusion by activating the WAVE2 regulatory complex. Mol. Cell **41**, 661–671 CrossRef PubMed
32 Dodding, M.P., Mitter, R., Humphries, A.C. and Way, M. (2011) A kinesin-1 binding motif in vaccinia virus that is widespread throughout the human genome. EMBO J. **30**, 4523–4538 CrossRef PubMed
33 Kaverina, I., Krylyshkina, O. and Small, J.V. (1999) Microtubule targeting of substrate contacts promotes their relaxation and dissociation. J. Cell Biol. **146**, 1033–1044 CrossRef PubMed
34 Kaverina, I.N., Minin, A.A., Gyoeva, F.K. and Vasiliev, J.M. (1997) Kinesin-associated transport is involved in the regulation of cell adhesion. Cell Biol. Int. **21**, 229–236 CrossRef PubMed
35 Krylyshkina, O., Kaverina, I., Kranewitter, W., Steffen, W., Alonso, M.C., Cross, R.A. and Small, J.V. (2002) Modulation of substrate adhesion dynamics via microtubule targeting requires kinesin-1. J. Cell Biol. **156**, 349–359 CrossRef PubMed
36 Ezratty, E.J., Bertaux, C., Marcantonio, E.E. and Gundersen, G.G. (2009) Clathrin mediates integrin endocytosis for focal adhesion disassembly in migrating cells. J. Cell Biol. **187**, 733–747 CrossRef PubMed
37 Stehbens, S. and Wittmann, T. (2012) Targeting and transport: how microtubules control focal adhesion dynamics. J. Cell Biol. **198**, 481–489 CrossRef PubMed
38 Hanania, R., Sun, H.S., Xu, K., Pustylnik, S., Jeganathan, S. and Harrison, R.E. (2012) Classically activated macrophages use stable microtubules for matrix metalloproteinase-9 (MMP-9) secretion. J. Biol. Chem. **287**, 8468–8483 CrossRef PubMed
39 Wiesner, C., Faix, J., Himmel, M., Bentzien, F. and Linder, S. (2010) KIF5B and KIF3A/KIF3B kinesins drive MT1-MMP surface exposure, CD44 shedding, and extracellular matrix degradation in primary macrophages. Blood **116**, 1559–1569 CrossRef PubMed
40 Strongin, A.Y., Collier, I., Bannikov, G., Marmer, B.L., Grant, G.A. and Goldberg, G.I. (1995) Mechanism of cell surface activation of 72-kDa type IV collagenase: isolation of the activated form of the membrane metalloprotease. J. Biol. Chem. **270**, 5331–5338 CrossRef PubMed
41 Cornfine, S., Himmel, M., Kopp, P., El Azzouzi, K., Wiesner, C., Krüger, M., Rudel, T. and Linder, S. (2011) The kinesin KIF9 and reggie/flotillin proteins regulate matrix degradation by macrophage podosomes. Mol. Biol. Cell **22**, 202–215 CrossRef PubMed
42 Efimova, N., Grimaldi, A., Bachmann, A., Frye, K., Zhu, X., Feoktistov, A., Straube, A. and Kaverina, I. (2014) Podosome-regulating kinesin KIF1C is delivered to the cell periphery in CLASP-dependent manner. J. Cell Sci., doi:10.1242/jcs.149633 PubMed
43 Kopp, P., Lammers, R., Aepfelbacher, M., Woehlke, G., Rudel, T., Machuy, N., Steffen, W. and Linder, S. (2006) The kinesin KIF1C and microtubule plus ends regulate podosome dynamics in macrophages. Mol. Biol. Cell **17**, 2811–2823 CrossRef PubMed
44 Theisen, U., Straube, E. and Straube, A. (2012) Directional persistence of migrating cells requires kif1c-mediated stabilization of trailing adhesions. Dev. Cell **23**, 1153–1166 CrossRef PubMed
45 Hynes, R.O. (2002) Integrins: bidirectional, allosteric signaling machines. Cell **110**, 673–687 CrossRef PubMed
46 Eskova, A., Knapp, B., Matelska, D., Reusing, S., Arjonen, A., Lisauskas, T., Pepperkok, R., Russell, R., Eils, R., Ivaska, J. et al. (2014) An RNAi screen identifies KIF15 as a novel regulator of the endocytic trafficking of integrin. J. Cell Sci. **127**, 2433–2447 CrossRef PubMed
47 Heintz, T.G., Heller, J., Zhao, R., Caceres, A., Eva, R. and Fawcett, J.W. (2014) Kinesin KIF4A transports integrin β1 in developing axons of cortical neurons. Mol. Cell Neurosci. **63**, 60–71 CrossRef
48 Caswell, P.T. and Norman, J.C. (2006) Integrin trafficking and the control of cell migration. Traffic **7**, 14–21 CrossRef PubMed
49 Hung, P.F., Hong, T.M., Hsu, Y.C., Chen, H.Y., Chang, Y.L., Wu, C.T., Chang, G.C., Jou, Y.S., Pan, S.H. and Yang, P.C. (2013) The motor protein KIF14 inhibits tumor growth and cancer metastasis in lung adenocarcinoma. PLoS ONE **8**, e61664 CrossRef PubMed
50 Ahmed, S.M., Thériault, B.L., Uppalapati, M., Chiu, C.W., Gallie, B.L., Sidhu, S.S. and Angers, S. (2012) KIF14 negatively regulates Rap1a–Radil signaling during breast cancer progression. J. Cell Biol. **199**, 951–967 CrossRef PubMed
51 Liu, Z., Rebowe, R.E., Wang, Z., Li, Y., Wang, Z., DePaolo, J.S., Guo, J., Qian, C. and Liu, W. (2014) KIF3a promotes proliferation and invasion via Wnt signaling in advanced prostate cancer. Mol. Cancer Res. **12**, 491–503 CrossRef PubMed
52 Yamada, K.H., Nakajima, Y., Geyer, M., Wary, K.K., Ushio-Fukai, M., Komarova, Y. and Malik, A.B. (2014) KIF13B regulates angiogenesis through Golgi–plasma membrane trafficking of VEGFR2. J. Cell Sci. **127**, 4518–4530 CrossRef PubMed
53 Kim, C., Ye, F. and Ginsberg, M.H. (2011) Regulation of integrin activation. Annu. Rev. Cell Dev. Biol. **27**, 321–345 CrossRef PubMed
54 Schnapp, B.J. (2003) Trafficking of signaling modules by kinesin motors. J. Cell Sci. **116**, 2125–2135 CrossRef PubMed
55 Jenkins, B., Decker, H., Bentley, M., Luisi, J. and Banker, G. (2012) A novel split kinesin assay identifies motor proteins that interact with distinct vesicle populations. J. Cell Biol. **198**, 749–761 CrossRef PubMed
56 Janke, C. and Bulinski, J.C. (2011) Post-translational regulation of the microtubule cytoskeleton: mechanisms and functions. Nat. Rev. Mol. Cell Biol. **12**, 773–786 CrossRef PubMed

Received 16 October 2014
doi:10.1042/BST20140280